19 January 2007 | S10

Science

AAAS

What if staying up to date with the latest technology published in journals and patents were as easy as pushing a button?

It is.

With the "Keep Me Posted" alerting feature, SciFinder sends you automatic updates on areas you—and your competitors—are interested in.

You can monitor specific research topics, companies, authors, substances, or sequences, and choose how frequently you receive notifications: daily, monthly, or weekly.

The service isn't just convenient, it's incredibly current. Journal article records often appear in SciFinder before they're even in print. New references, substances, and sequences are added daily. Patents from all the major offices are added within two days of issuance.

As with all SciFinder features, Keep Me Posted is integrated with your workflow. At any point in a search (including the beginning), simply click on the Keep Me Posted button. SciFinder tracks your steps and will generate the appropriate alert—even for complex topics. When you receive a notification, you can follow each reference as you would in a search: find citing or cited articles (with links to the electronic full text), and follow referenced substances and reactions for further information.

Comprehensive, intuitive, seamless—SciFinder doesn't just alert you, it's part of the process. To find out more, call us at 800-753-4227 (North America) or 614-447-3700 (worldwide) or visit www.cas.org/SCIFINDER.

SciFinder®

Part of the process.™

Systems that set the standard, software that's a step ahead.

Lead the way with a Stratagene personal QPCR system featuring enhanced MxPro™ QPCR Software.

Our Mx3000P® and Mx3005P™ personal quantitative PCR (QPCR) Systems combine an advanced optical system with powerful data analysis to give you complete flexibility at an affordable price. Our open platform design supports traditional and advanced applications as well as newly emerging QPCR chemistries. In addition, our MxPro™ QPCR Software combines leading edge data analysis algorithms with intuitive organization designed for ultimate ease-of-use.

- **Four- or five-color systems to best fit your research needs**
- **96-well thermal block with temperature uniformity of +/-0.25°C**
- **New MxPro™ QPCR Software with optional features for 21 CFR Part 11 compatibility**

Need More Information? Give Us A Call:

Stratagene US and Canada
Order: 800-424-5444 x3
Technical Service: 800-894-1304 x2

Stratagene Japan K.K.
Order: 3-5821-8077
Technical Service: 3-5821-8076

Stratagene Europe
Order: 00800-7000-7000
Technical Service: 00800-7400-7400

www.stratagene.com

STRATAGENE

GE Healthcare

ÄKTA™

100,000 scientists working with proteins believe in ÄKTA, UNICORN and wizards.

To 100,000 scientists worldwide, ÄKTA™ sets the standard in protein purification. All systems in the ÄKTAdesign™ family work with intelligent UNICORN™ software, which makes it easy to control every stage of your purification process. But we're never content to stand still. The result is products like ÄKTAxpress™, which can solve low expression and double-tagged protein purification challenges, and ÄKTApurifier™, a time-saving automated protein purification system that can be configured to suit your personal application and workflow needs.

By continually developing technology that can turn your scientific ideas into reality, we're bringing science to life and helping transform healthcare.

We call it Protein Separations Re-imagined.

Discover the legendary purification power of UNICORN and ÄKTA, visit www.gehealthcare.com/akta

imagination at work

GE09-06

Volume 315, Issue 5810

COVER

A motor neuron from the spinal cord of a turtle, stained with horseradish peroxidase. The elongated soma with an extended dendritic tree (>1 mm) receives unexpectedly balanced input from large groups of both inhibitory and excitatory interneurons. See page 390.

Image: J. Hounsgaard and R. W. Berg

DEPARTMENTS

EDITORIAL

NEWS OF THE WEEK

NEWS FOCUS

Astrobiology

LETTERS

BOOKS *ET AL.*

POLICY FORUM

333

PERSPECTIVES

CONTENTS continued >>

Automated solutions by QIAGEN

Free up your time

- Largest portfolio of purification protocols
- Plug-and-play spin-column automation with QIAcube
- Low- to high-throughput automation
- Molecular diagnostics systems*
- Consultative Application Service and Instrument Care

Contact QIAGEN today or visit www.qiagen.com/goto/Automated .

* artus PCR assays are not cleared for clinical use in USA and Canada.

AUTOFlyer0610751WW

QIAGEN®

Sample & Assay Technologies

SCIENCE EXPRESS

www.sciencexpress.org

MICROBIOLOGY

Staphylococcus aureus Panton Valentine Leukocidin Causes Necrotizing Pneumonia

M. Labandeira-Rey et al.

A virulent form of drug-resistant bacterium not only carries genes for a potent toxin but also makes more of an inflammatory factor, exacerbating the resulting pneumonia.

10.1126/science.1137165

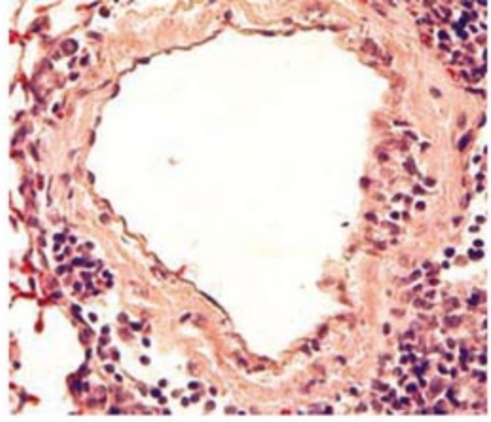

CELL SIGNALING

Integration of TGF-β and Ras/MAPK Signaling Through p53 Phosphorylation

M. Cordenonsi et al.

Two prominent signaling pathways important for cell growth and development intersect at a common tumor suppressor, p53.

10.1126/science.1135961

CHEMISTRY

A Molecule Carrier

K. L. Wong et al.

In a molecular conveyor, CO_2 can be carried across a copper surface on anthroquinone molecules (which diffuse linearly, not isotropically) and then can be unloaded at the end.

10.1126/science.1135302

TECHNICAL COMMENT ABSTRACTS

MATHEMATICS

Comment on "The Geometry of Musical Chords" 330

D. Headlam and M. Brown

full text at www.sciencemag.org/cgi/content/full/315/5810/330b

Response to Comment on "The Geometry of Musical Chords"

D. Tymoczko

full text at www.sciencemag.org/cgi/content/full/315/5810/330c

REVIEW

SCIENCE POLICY

Enabling Europe to Innovate 344

A. Dearing

BREVIA

MATERIALS SCIENCE

Brilliant Whiteness in Ultrathin Beetle Scales 348

P. Vukusic, B. Hallam, J. Noyes

Although only 5 micrometers thick, the scales of a beetle appear brilliantly white because they contain a sparse, random network of cuticular filaments that efficiently scatter light.

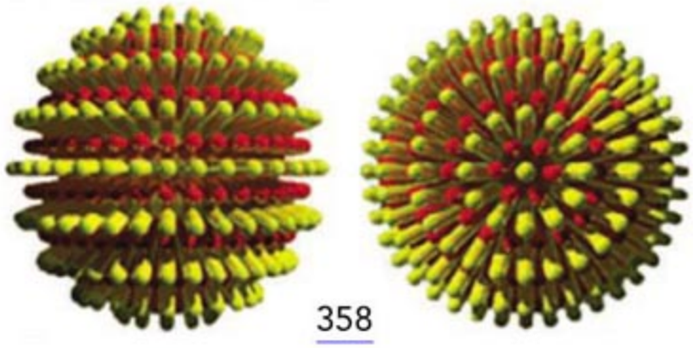

358

REPORTS

PHYSICS

Electric Field–Induced Modification of Magnetism in Thin-Film Ferromagnets 349

M. Weisheit et al.

A weak applied electric field can reversibly modulate the magnetic properties of a thin iron-palladium film immersed in an electrolyte.

MATERIALS SCIENCE

Ultralow Thermal Conductivity in Disordered, Layered WSe_2 Crystals 351

C. Chiritescu et al.

Randomly stacking the layers in tungsten selenide produces a dense solid having a remarkably low thermal conductivity at room temperature that is only twice that of air.

>> *Perspective p. 342*

CHEMISTRY

Organic Glasses with Exceptional Thermodynamic and Kinetic Stability 353

S. F. Swallen et al.

Organic molecules can form stable glasses when deposited from a vapor onto a substrate cooled only 50 kelvin below their usual glass transition temperature.

CHEMISTRY

Unexpected Stability of Al_4H_6: A Borane Analog? 356

X. Li et al.

A pulsed arc discharge yields stable aluminum-hydride clusters, a new compound which has a high heat of combustion and in bulk could potentially be used for hydrogen storage.

CHEMISTRY

Divalent Metal Nanoparticles 358

G. A. DeVries et al.

Different molecules can be placed at opposite positions in the molecular coating of metal nanoparticles to form chemical handles, allowing assembly of the particles into chains or films.

CONTENTS continued >>

EXIQON

Services also available

microRNA expression profiling
- using miRCURY™ LNA Arrays

Dear Researcher, we are happy to announce the launch of miRCURY™ LNA prespotted microarray slides and ready-to-spot probe sets for microRNA profiling for all organisms (vertebrates/invertebrates/plants/viruses) in miRBase 8.1. We have at least 92% coverage in miRBase 9.0.

Stay ahead of the field
- Most comprehensive probe set that contain proprietary miRPlus sequences not yet in miRBase

Increased discovery potential
- Cross species profile comparison possible
- Almost 1500 unique capture probes

Use less sample
- Works on 1 ug total RNA
- Highly sensitive LNA™ capture probes

Get reliable results
- Spike-In control probes for easy and improved normalizationprocedure and assessment of data quality and reproducibility
- Excellent discrimination of let-7 family members
- Tm normalized capture probes

Save time
- No miRNA enrichment required
- Fast 90 minutes miRNA labeling protocol

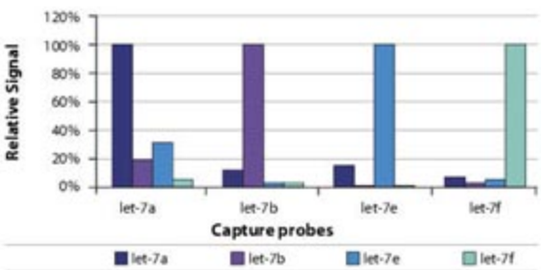

Discrimination of closely related miRNAs.

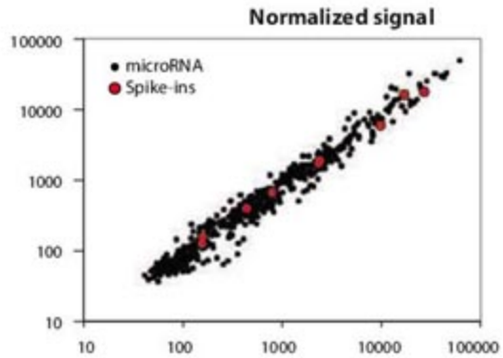

Spike-In capture probes allow assessment of reproducibility.

www.exiqon.com

Visit
www.exiqon.com/array
to learn more....

...or contact us for more info:

Phone:
US: 781 376 4150 / 888 miRCURY (EST)
Rest of world: +45 45 65 09 29 (GMT+1)

Email: support@exiqon.com

REPORTS *CONTINUED...*

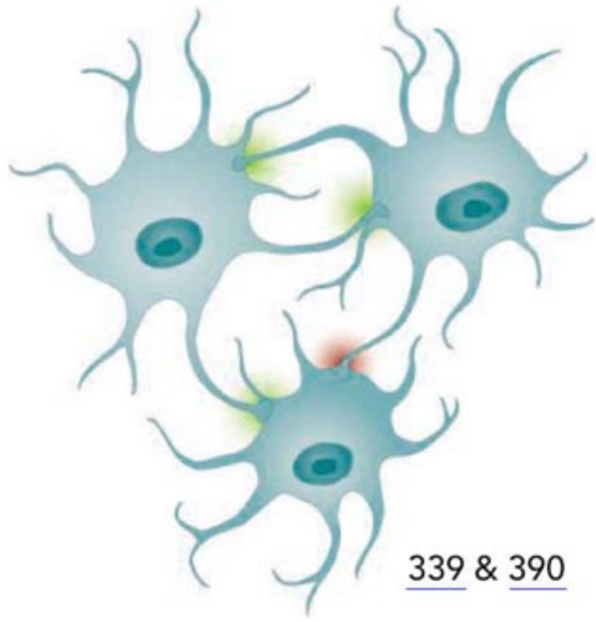

339 & 390

AAAS

ADVANCING SCIENCE, SERVING SOCIETY

SCIENCE (ISSN 0036-8075) is published weekly on Friday, except the last week in December, by the American Association for the Advancement of Science, 1200 New York Avenue, NW, Washington, DC 20005. Periodicals Mail postage (publication No. 484460) paid at Washington, DC, and additional mailing offices. Domestic individual membership and subscription (51 issues): $142 ($74 allocated to subscription). Domestic institutional subscription (51 issues): $710; Foreign postage extra: Mexico, Caribbean (surface mail) $55; other countries (air assist delivery) $85. First class, airmail, student, and emeritus rates on request. Canadian rates with GST available upon request, GST #1254 88122. Publications Mail Agreement Number 1069624. **Printed in the U.S.A.**

Change of address: Allow 4 weeks, giving old and new addresses and 8-digit account number. **Postmaster:** Send change of address to AAAS, P.O. Box 96178, Washington, DC 20090–6178. **Single-copy sales:** $10.00 current issue, $15.00 back issue prepaid includes surface postage; bulk rates on request. **Authorization to photocopy** material for internal or personal use under circumstances not falling within the fair use provisions of the Copyright Act is granted by AAAS to libraries and other users registered with the Copyright Clearance Center (CCC) Transactional Reporting Service, provided that $18.00 per article is paid directly to CCC, 222 Rosewood Drive, Danvers, MA 01923. The identification code for *Science* is 0036-8075. *Science* is indexed in the *Reader's Guide to Periodical Literature* and in several specialized indexes.

CONTENTS continued >>

Now sold as Thermo Scientific

PIERCE

The Protein People™

High-Performance Dialysis

Dialysis tube VS. cassette

SLIPPERY WHEN WET. Flat tubing is difficult to handle and fill when wet.	SAMPLE HANDLING	Easy to hold on to frame and inject sample.
SLIPPERY WHEN WET. Sample can easily be lost when tubing leaks or clamps slip off.	SAMPLE RECOVERY	>95% sample recovery.
SLIPPERY WHEN WET. Leaking into dialysate can compromise sample.	SAMPLE INTEGRITY	Sample remains intact with no contamination from surrounding dialysate.
SLIPPERY WHEN WET. Typically dialyze overnight. Difficult to recover sample from wet tubing.	SPEED	High surface area/sample volume ratio will dialyze twice as fast as conventional tubing.

No more leaking! Avoid sample loss with Pierce Slide-A-Lyzer® Dialysis Cassettes.

The Pierce Slide-A-Lyzer® Dialysis Cassettes have a silicone-like gasket that prevents them from leaking. The new color-coded transparent frames allow you to instantly know the MWCO of the membrane and to see the sample being injected. No knots, caps, lids or clamps to loosen, fall off or leak. Obtain >95% sample recovery with a rigid frame that permits smooth and complete withdrawal of samples.

FREE picture frame offer!*

Buy any package of Slide-A-Lyzer® Dialysis Cassettes before 3/30/07 and receive a free magnetic picture frame that looks just like our Cassettes!

How does the Cassette dialyze?

1. Inject sample into the Cassette through one of the guide ports on top of the gasket. Draw up on the syringe to remove air.
2. For Cassettes other than the 12-30 ml unit, attach a flotation buoy and dialyze. Forget about having to hassle with dialysis bag suspension!
3. After dialysis, inject the Cassette chamber with air, and withdraw your dialyzed sample from the Cassette.

www.piercenet.com

PIERCE

20 K MWCO

Slide-A-Lyzer® Cassettes are available in 2, 3.5, 7, 10 and now 20 K MWCO. See our website for the full line that best serves your dialysis needs.

Tel: 815-968-0747 or 800-874-3723 • Fax: 815-968-7316
Customer Assistance E-mail: CS@piercenet.com

For distributors outside the U.S. and Europe, visit www.piercenet.com

For European offices and distributors, visit www.perbio.com

Junk on a journey.

SCIENCE**NOW**

www.sciencenow.org DAILY NEWS COVERAGE

Modeling the Ocean's Motion
Researchers chart the course of a current as it ferries junk across the Pacific.

A Huff Equals a Puff
Abused inhalants trigger the same brain response as cocaine and nicotine.

Big Melt Threatens India's Water
Himalayan glaciers have declined one-fifth in the past 4 decades, according to new report.

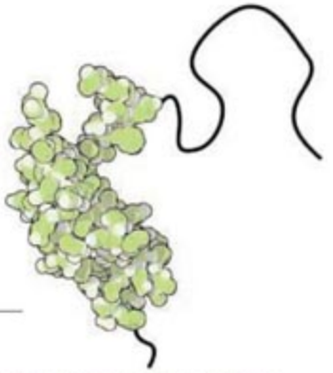

RGS2: A structured RGS domain and unstructured N terminus.

SCIENCE'S **STKE**

www.stke.org SIGNAL TRANSDUCTION KNOWLEDGE ENVIRONMENT

PERSPECTIVE: RGS Proteins—Swiss Army Knives in Seven-Transmembrane Domain Receptor Signaling Networks
S. P. Heximer and K. J. Blumer
An unstructured domain allows RGS2 to regulate more than just G proteins.

PERSPECTIVE: Propping Up Our Knowledge of G Protein Signaling Pathways—Diverse Functions of Putative Noncanonical Gβ Subunits in Fungi
C. S. Hoffman
Proteins that adopt a conformation like that of Gβ serve various functions in G protein signaling.

FORUM
Join the ongoing discussion of redox regulation through cysteine modulation of GPCRs in the "Open Forum on Cell Signaling."

Resisting the temptation to cheat.

SCIENCE **CAREERS**

www.sciencecareers.org CAREER RESOURCES FOR SCIENTISTS

US: Dealing With Deception
B. Benderly
As scientific cheating increases, researchers must protect their own careers and the integrity of science.

US: Tooling Up—Resumé Rocket Science, 2007
D. Jensen
Good CVs and resumés share some common threads.

EUROPE: Mastering Your Ph.D.—Group Dynamics
B. Noordam and P. Gosling
Your Ph.D. experience will depend, in part, on what type of research group you end up in.

CREDIT (SCIENCE NOW): DAVE INGRAHAM

Separate individual or institutional subscriptions to these products may be required for full-text access.

NEW ENGLAND BIOLABS

Phusion™ High-Fidelity DNA Polymerase from New England Biolabs

EXTREME PRECISION WITH UNPARALLELED SPEED AND ROBUSTNESS

With Phusion High-Fidelity DNA Polymerase, there is no need to compromise any aspect of your PCR performance. A superior choice for cloning, this recombinant polymerase has an error rate 50-fold lower than *Taq* DNA Polymerase, making it the most accurate thermostable polymerase available. Phusion DNA Polymerase is supplied in a variety of formats, or with a hot start modification for increased specificity.

Advantages:

- Extreme Fidelity – Highest of any thermostable polymerase
- High Speed – Extension times are dramatically reduced
- Robustness – Reduce reaction failures with minimal optimization
- High Yield – Increase product yields with minimal enzyme amounts
- Specificity – Hot start modification reduces non-specific amplification

Phusion High-Fidelity DNA Polymerase RE	**F-530S/L**
Phusion Hot Start High-Fidelity DNA Polymerase RE	**F-540S/L**
Phusion High-Fidelity PCR Master Mix RE	
with HF Buffer	**F-531S/L**
with GC Buffer	**F-532S/L**
Phusion High-Fidelity PCR Kit RE	**F-553S/L**

RE = Recombinant

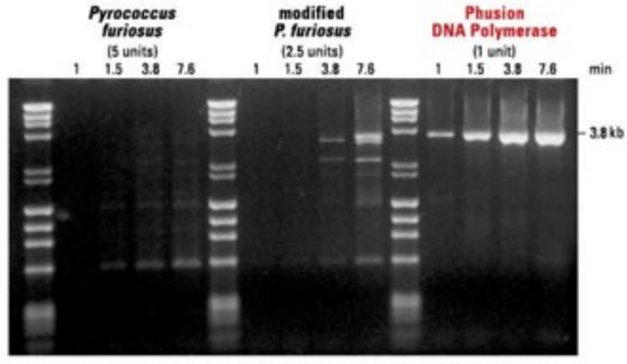

Experience extreme speed and yield with Phusion High-Fidelity DNA Polymerase. A 3.8 kb fragment from human beta globin gene was amplified according to suppliers' recommendations using varying extension times. Phusion DNA Polymerase was able to amplify the fragment with a combined annealing and extension step of only 1 minute. Also, a single unit of Phusion DNA Polymerase produced higher yields than 2.5 or 5 units of *Pyrococcus furiosus* DNA Polymerases.

Phusion™ is a trademark of Finnzymes Oy

For more information please visit www.neb.com

- **New England Biolabs Inc.** 1-800-NEB-LABS Tel. (978) 927-5054 Fax (978) 921-1350 info@neb.com
- **Canada** Tel. (800) 387-1095 info@ca.neb.com
- **Germany** Tel. 0800/246 5227 info@de.neb.com
- **UK** Tel. (0800) 318486 info@uk.neb.com
- **China** Tel. 010-82378266 beijing@neb-china.com

Produced by

FINNZYMES
TOOLS FOR MOLECULAR BIOLOGY

Distributed by

NEW ENGLAND BioLabs® Inc.
the leader in enzyme technology

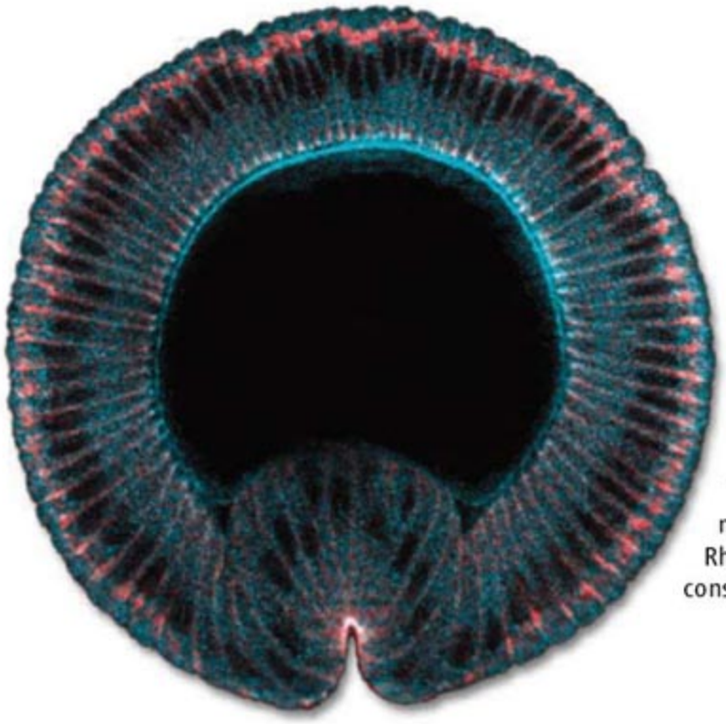

Cellular Morphogenesis with a Twist

Cellular morphogenesis is important throughout much of early development in multilcellular animals. During *Drosophila* gastrulation, epithelial cells on the ventral side of the embryo display apical constrictions that cause the invagination of the mesoderm and formation of a ventral furrow. **Kölsch *et al.*** (p. 384) now identify a target of the transcriptional activator Twist. This transmembrane protein, T48, coordinates with signaling factors Fog and Cta to localize the cytoskeletal modulator RhoGEF2 to the apical side of ventral cells in order to direct apical constriction and ventral furrow formation.

Enabling Innovation

In open innovation, different actors work together in a flexible manner so that they can develop products and services more efficiently than they could on their own. **Dearing** (p. 344) relates ways companies think about innovation within the policies that European governments are putting in place to foster productive innovation. Qualities that define effective ecosystems for innovation include the potential for market growth, straightforward and effective regulations, and the availability of skilled resources.

Aluminum Pyramid

The tendency of boron to compensate for its electron deficiency by forming elaborate polyhedral hydride clusters has long intrigued chemists and given rise to a detailed series of bonding rules that rationalize cage geometries based on electronic structure. In contrast, aluminum has not evinced a comparably rich hydride cluster chemistry, despite sharing boron's valence structure. However, photoelectron spectroscopy studies by **Li *et al.*** (p. 356) indicate that the neutral Al_4H_6 cluster is actually quite stable. Density functional theory supports a distorted tetrahedral aluminum arrangement. The stability of this molecule suggests the potential for synthesizing a broad range of $(AlH)_n$ structures.

Random Stacking Beats the Heat

Materials with low thermal conductivity are not only useful as thermal barriers but thermoelectric energy conversion. **Chiritescu *et al.*** (p. 351, published online 14 December; see the Perspective by **Goodson**) find that when tungsten selenide, a layered material similar to graphite in the weakness of attraction between its layers, is grown from alternating thin films of W and Se, the sheets stack in a random manner. This disordering, coupled with the high in-plane ordering of the layers, leads to an extremely low cross-plane thermal conductivity for a fully solid film—as low as 0.05 watts per meter per kelvin at room temperature, or 30 times less than the *c*-axis thermal conductivity of single-crystal WSe_2. Disruption of the in-plane ordering by ion bombardment actually increased the thermal conductivity of the material.

Electric-Field–Modulated Magnetism

The ability to modulate the magnetic properties of a material with an applied electric field offers the potential of low-power consumption and fast memory devices. **Weisheit *et al.*** (p. 349) report on the fabrication of a tri-layer junction of metallic ferromagnetic thin films immersed in a dry propylene carbonate electrolyte. The ferromagnetic magnetization in the layer in contact with the electrolyte, a 2-nanometer-thick FePd film, could be modified considerably by applying a voltage across this barrier with a Pt counter electrode.

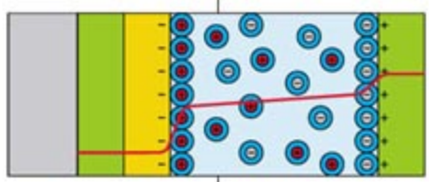

The Ends Enable the Means

During their synthesis, nanoparticles are often coated with a capping layer of rodlike molecules to prevent their further growth or agglomeration. Such a layer might be assumed to be isotropic, so that further derivatization or attempts to connect nanoparticles would be nonselective in terms of bonding directions. However, when rodlike molecules pack on a spherical object, at least two defect areas must form at opposite poles (much in the same way that hair on a person's head must adopt a whirl pattern). **DeVries *et al.*** (p. 358) exploit this phenomenon to selectively bond two different types of ligands to metal nanoparticles, such that they can be further reacted at the poles to give them directional bonding. The nanoparticles could then be formed into free-standing films.

Water Marks the Asthenosphere

Plate tectonics assumes that rigid plates float and move over the weaker asthenosphere, which extends from about 60 to 220 kilometers below the oceans and 150 kilometers below continents. The softness of the asthenosphere may be caused by pockets of hydrous melt. **Mierdel *et al.*** (p. 364; see the Perspective by **Bolfan-Casanova**) have performed experiments which show that the asthenosphere could coincide with a zone that marks a minimum in the solubility of water in mantle minerals. A sharp drop occurs in water solubility in aluminous orthopyroxene with pressure, or equivalently depth, whereas the water solubility in olivine continuously increases. The limits of

Continued on page 299

CREDITS (TOP TO BOTTOM): VERENA KÖLSCH AND MARIA LEPTIN; WEISHEIT *ET AL.*

Continued from page 297

the asthenosphere would be the regions where water comes out of solution and forms pockets of hydrous silicate melt.

Modeling the Cytoskeleton

The cytoskeleton, the mechanical framework of cells, represents a nonequilibrium active machinery that can adapt its mechanics to perform tasks such as cell locomotion. **Mizuno *et al.*** (p. 370) show that in a reconstituted model system comprising actin filaments, a cross-linker and a motor protein (myosin II), the motor activity controls the mechanical properties of the actin network. Adenosine triphosphate could promote near 100-fold increase in stiffness and change the viscoelastic response of the network. A quantitative model connects the large-scale properties of the gel to molecular force generation.

Sideways with a Twist

The family of ABC membrane transporters uses the energy from adenosine triphosphate, hydrolyzed by the nucleotide-binding domain (NBD), to power transport of substances into or out of the cell via the transmembrane domain (TMD). **Pinkett *et al.*** (p. 373, published online 7 December) report the NBD-TMD structure of an inward-facing conformation of a bacterial metal chelate importer and compare it to the outward-facing structure of another ABC family member, the vitamin B_{12} importer. Small shifts in the relative orientations of the membrane-spanning helices in the TMD suffice to switch the accessibility of the central cavity from periplasmic to cytoplasmic. Furthermore, these shifts are associated with, and perhaps driven by, twisting and translational conformational changes in the NBDs.

Making (and Breaking) the Switch

B cells produce different classes of antibodies by combining the highly variable antigen-binding front-end with one of a selection of functional rear-ends through class switch recombination, in which somatic gene rearrangement brings together intronic switch region sequences that flank the constant region segments. After generation of double-strand breaks by the cytidine deaminase AID and subsequent end-joining, intervening DNA is deleted and the upstream variable sequence meets its selected constant-region partner. To look more closely at the role AID and the switch regions themselves play in this process, **Zarrin *et al.*** (p. 377, published online 14 December; see the Perspective by **Chaudhuri and Jasin**) replaced the switch sequences with endonuclease sites from yeast, which allows the production of independent double-strand breaks. Surprisingly, class-switch recombination still took place with a measurable frequency and was independent of AID.

Dance, Turtle, Dance

The basic spinal network mechanisms underlying limb movements are still not fully understood. Investigating spinal cord preparations from adult turtles, **Berg *et al.*** (p. 390; see the cover and the Perspective by **Kristan**) describe how spinal networks operate during motor pattern generation. Balanced increases in synaptic excitation and inhibition operate in spinal motoneurons to produce rhythmic bursts of action potentials that are stochastic in nature. This activity contrasts strongly with the classical notion that antiphasic inhibition and excitation produces rhythmic activity in oscillatory spinal networks.

Daydream Believer

Despite the preponderance of daydreaming during everyday life, little is known about its neurocognitive underpinnings. How does the brain spontaneously produce the images, voices, thoughts, and feelings that constitute stimulus-independent thought? By analyzing functional magnetic resonance imaging signals associated with a cognitive task that was shown to induce a high frequency of mind-wandering, **Mason *et al.*** (p. 393) show that between periods of instrumental thought and goal-directed behavior, the mind exhibits tonic activity in a network of cortical regions. This so-called default network contributes to the production of stimulus-independent thought and the subjective experience of mind-wandering.

CREDIT: PINKETT ET AL.

www.roche-applied-science.com

Introducing Our Second Generation Genome Sequencing System

Genome Sequencer FLX

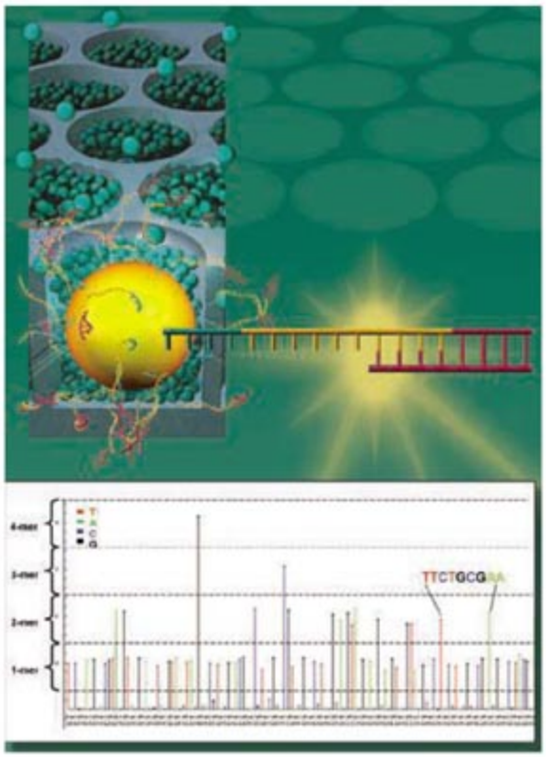

Be First to the Finish with...

- Increased read lengths averaging 200 to 300 bases per read
- Throughput of more than 400,000 reads per run
- High single-read accuracy greater than 99.5% over 200 bases
- Consensus-read accuracy greater than 99.99%

...more Flexibility and more Applications.

Visit ***www.genome-sequencing.com*** to learn about the expanding number of peer-reviewed publications appearing weekly.

454 LIFE SCIENCES

Roche Diagnostics

Roche Diagnostics GmbH
Roche Applied Science
68298 Mannheim
Germany

Donald Kennedy is the Editor-in-Chief of *Science*.

Source It Out

THESE DAYS, OUTSOURCING IS ALL THE RAGE IN THE UNITED STATES; ONE CAN FOLLOW IT ALL the way from the campus to the national park system, then to Iraq, and finally to our domestic political infrastructure. Beginning with the first: It used to be that faculty members at Generic State U. could be sure that the campus bookstore and food service were home-grown enterprises, staffed by people they got to know. Now those enterprises are likely to be connected to Borders or a multinational food service company. These arrangements, a prominent feature of the outsourcing epidemic, are popularly called public-private partnerships. The term lends a sense of comfort, but it also hides some nagging problems.

The U.S. government is getting into outsourcing through public-private partnerships, big time. In the Bay Area, military base closures have created an appetite for putting private ventures on public lands. San Francisco's most desirable piece of public land, the Presidio, was transferred to the National Park Service after its base closed. Congress then created a special agency called the Presidio Trust, with a management plan demanding self-sufficiency by 2015. Originally, it required occupancy by nonprofits, but given the tough target date, it's hardly surprising that somehow the trustees accommodated Lucasfilm Ltd. Meanwhile, at the old Moffett Field, the National Aeronautics and Space Administration is looking around for new partners. How about Google?

Moving on: The public-partnership responsible for the Iraq mess includes a huge array of private organizations holding outsourced roles. Some are contractors, such as Bechtel and Halliburton, whose high overhead may be justified by the challenge of restoring (or not) infrastructure while being shot at. The other commercial partners are, to put the matter bluntly, mercenaries: well-armed contract employees (think Blackstone) playing roles that are at least paramilitary if not more. This high-water mark in outsourcing for war has put some of the legal risks of public-partnerships on display: The *New York Times* reports that of 20 accusations against contract employees of criminal abuses against Iraqi and American detainees, none have been acted on. If part of the partnership deal entails immunity, the deal may not be all that wonderful.

When functions vital to a democratic society are partially outsourced to private interests, legal problems arise and social costs are likely to result. To be sure, there are some benefits. Much of U.S. domestic infrastructure has been put into the hands of private commercial entities for sensible reasons. Privately run toll roads are worked into the highway system, and the Internet is a valuable utility that operates well as a public-private partnership. But although voter confidence in the system by which we choose our government representatives is essential, in many places private vendors have provided the electronic touch-screen machines that count the votes. This public-private partnership has produced both technical doubts (how can the voter be sure that the vote gets counted?) and legal ones (can the state know and reveal what's inside the machines?).

A major supplier of such machines, Diebold, is a central player in the debate, partly because its CEO, also the chair of the Republican Party in Ohio, unwisely declared his hope to secure his state's 2004 vote for Bush. The next year, North Carolina asked for bids for machines, with the requirement that bidders reveal the computer codes and other details about how the machines would work. Diebold appeared to get the bid but refused to meet this stipulation, claiming that the information was a trade secret. The state Elections Commission then decided to disregard its own requirement on the basis that no bidder could be expected to meet it. The stalemate broke when, after a court test in which the state's provision was upheld, Diebold withdrew. Meanwhile, another bidder acceded, showing that the requirement could be met despite the commission's earlier conclusion.

Diebold's withdrawal was fortunate, but they are selling machines elsewhere. The lesson from these adventures with public-to-private oursourcing is that if you're going to hire others to do your work, better make them as accountable as you are. Otherwise you've bought yourself a fig leaf.

– Donald Kennedy

10.1126/science.1139569

CREDIT: PAT LEWIS

EDITED BY GILBERT CHIN AND JAKE YESTON

GENETICS

Generating Varieties

Paralogs are the result of a gene duplication event arising after speciation. By examining expressed sequence tags (ESTs) in the B73 strain of maize, Emrich *et al.* identified gene copies with 98% or more similarity, which they have labeled as nearly identical paralogs (NIPs). Approximately 1% of all genes in maize (*Zea mays* L.) have a NIP, a significantly higher rate than found in *Arabidopsis*. Many of these NIPs demonstrate linkage, suggesting that they originated via tandem gene duplication. Among NIP families it was found that both gene copies were often expressed (~80%) and that the expression of an individual gene often differed from that of its paralog. These data suggest that paralogs may be a means by which organisms generate variation and, in the case of maize, may have been important in providing varieties for selection and domestication by humans. — LMZ

Genetics 10.1534/genetics.106.064006 (2006).

PSYCHOLOGY

Morality on the Web

Inconsistencies—for instance, between what is observed and what is reported—can be fecund ground for researchers to till, and a topic of current interest is the incongruence between the moral judgments that people make and the reasons that people proffer as a basis for those judgments. At one side are the proponents of conscious or deliberative thought as the means for making choices when confronted with moral dilemmas, whereas another view favors intuitions arrived at via automatic or inaccessible processes as the motivation for their responses.

Cushman *et al.* have elicited "ought versus ought not" judgments and postjudgment rationales from more than 500 people by using a Web-based script. Participants read carefully constructed scenarios and registered their judgments; they were then presented with their choices in pairs of the scenarios that differed in only one of three dimensions and asked for a justification. In situations where action (or inaction) was involved, participants were consistent in their judgments and generally had no difficulty in articulating a reasoned argument for how they had decided which behavior was morally better. In contrast, when intentional (or unintentional) harm was the issue, the pattern of judgment was just as clear as in the action scenarios, but most participants could not explain why they had chosen as they did. Hence, there may be more than one way to reach a decision on morality. — GJC

Psychol. Sci. **17**, 1082 (2006).

CHEMISTRY

From Soup to Nuts

The promise of microfluidic systems, in which very small volumes of liquids are manipulated, processed, and interrogated, is that it may be possible to develop low-cost diagnostic systems, particularly for use under challenging field conditions. Although there has been tremendous progress in developing microfluidic components, creating an integrated system that can analyze an unpurified sample has remained a goal.

Easley *et al.* describe a microfluidic system with three distinct functional domains. The first two are for sample preparation, consisting of solid-phase extraction (SPE) to pull out sample DNA from a crude specimen and for subsequent PCR amplification. After this, the amplified products are then injected along with a DNA standard into an electrophoretic detection domain. One key aspect of the device (3 x 6 cm) is a series of valves that are used to isolate each unit, thus keeping SPE reagents from reaching the PCR domain; these valves are also used in a diaphragm-like fashion to pump the amplified DNA into the analytical chamber. The authors demonstrate the detection of *Bacillus anthracis* in 750 nl of whole blood taken from infected but asymptomatic mice, and they also are able to measure *Bordetella pertussis* in 1 μl of nasal aspirate taken from a patient suspected of having whooping cough. — MSL

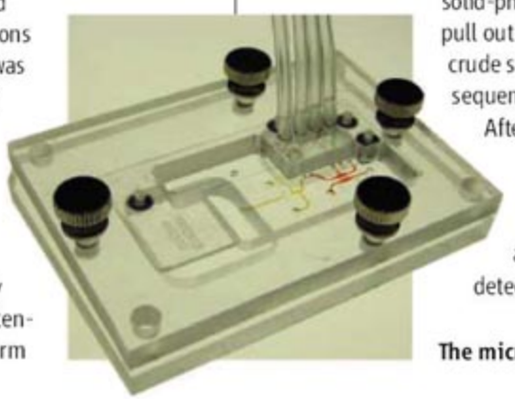

The microfluidic lab bench.

Proc. Natl. Acad. Sci. U.S.A. **103**, 19272 (2006).

IMMUNOLOGY

A Loss of Intestinal Fortitude

The large-scale and rapid depletion of CD4+ T cells in the weeks after HIV infection occurs predominantly in the gastrointestinal tract. Accompanying this loss is a sustained whole-scale activation of the immune system, which corresponds directly with the eventual progression to AIDS.

Brenchley *et al.* propose that the two processes are tightly coupled, with impaired intestinal integrity leading to the translocation of gut microbes, or some of their constituent components, which overstimulate the immune system. Circulating levels of bacterial lipopolysaccharide (LPS), which was used as a marker for microbial translocation, were markedly elevated in the sera of chronically infected HIV individuals and in macaques experimentally infected with the simian immunodeficiency virus (SIV). This increase corresponded directly with footprints of immune acti-

CREDITS (TOP TO BOTTOM): MISSOURI BOTANICAL GARDEN/HTTP://WWW.BOTANICUS.ORG; EASLEY *ET AL.*, *PROC. NATL. ACAD. SCI. U.S.A.* **103**, 19272 (2006)

vation, including circulating cytokines, antibodies to LPS, and immune-cell turnover. In HIV patients undergoing highly active antiretroviral therapy, LPS levels were decreased, with a corresponding rebound in CD4+ T cell numbers. Furthermore, in the absence of pathology—as typified in the infection of natural primate hosts for SIV—signs of substantial microbial translocation or immune activation were not apparent. The link between HIV infection, integrity of the mucosal immune system, and chronic peripheral immune activation may prove important to consider in future therapies for HIV infection. — SJS

Nat. Med. **12**, 1365 (2006).

APPLIED PHYSICS

Eavesdropping Foiled by Decoys

Secure communication between a sender and a receiver generally requires the message to be encrypted, with the sender and recipient sharing a secret key that encodes and deciphers the message. Ideally, the key should be changed often, and so for practical reasons the key should be distributable over normal communication channels. However, the possibility of the interception of the key by an eavesdropper would compromise security. There is, therefore, a need for a method to distribute the key to the recipient securely so that any attack on the communication channel by a potential eavesdropper can be detected and appropriate action taken.

Yuan *et al.* use a combination of signal and decoy optical pulses sent over a 25-km optic fiber to demonstrate unconditionally secure quantum-key distribution to a recipient. Because the decoy pulses are weaker than the signal pulses, interception by an eavesdropper considerably reduces their transmission rate to the receiver, thereby revealing the existence of an eavesdropper. Although the use of decoy pulses does provide for secure communication, it also places stringent requirements on the calibration of the sources and the detectors so that artifacts do not compromise security. — ISO

Appl. Phys. Lett. **90**, 011118 (2007).

CHEMISTRY

Stabilizing Porphyrin Stacks

Expanded porphyrins are larger versions of the familiar tetrapyrrole compounds. These extended aromatic frameworks could potentially form discotic, liquid-crystalline phases, but the floppiness of the electron-rich structure disrupts stacking.

Stępień *et al.* have prepared cyclo[8]pyrrole cations bearing phenylalkyl side chains and a central sulfate counter-ion. They find that electron-acceptor molecules such as trinitrobenzene (TNB) form 1:1 adducts with the expanded porphyrins, which leads to changes in color and can produce columnar stacking and the formation of discotic mesophases. This approach, if successfully applied to related explosives such as TNT (trinitrotoluene), might provide a simple visual method for detection or sensing. — PDS

Liquid crystal structure (gray, side chains; green, pyrrole cores; red, TNB; yellow, sulfate).

Angew. Chem. Int. Ed. 10.1002/anie.200603893 (2006).

CREDIT: STĘPIEŃ *ET AL., ANGEW. CHEM. INT. ED.* 10.1002/ANIE.200603893 (2006)

Science stke AAAS

www.stke.org

<< A Balance Between Life and Death

Cancerous cells often exhibit not only a capacity for excessive proliferation but also a resistance to apoptosis. For example, the oncoprotein c-MYC, an important contributor to many human tumors, activates the transcription of some genes and represses that of others and thus influences many target genes that might contribute to the regulation of apoptosis. Patel and McMahon have extended earlier studies that showed that the binding of c-Myc to the transcription factor MIZ-1 and the inhibition of MIZ-1–dependent transcription were important for promoting apoptosis. In human fibroblasts, a form of c-MYC (c-MYCV394D) that does not interact with MIZ-1 was defective in inducing apoptosis. Furthermore, when the level of MIZ-1 was reduced in these cells, the apoptotic effect of c-MYCV394D was restored. MIZ-1 activates the transcription of several hundred genes, and a search of target genes in microarrays yielded a promising candidate: the gene encoding the antiapoptotic protein BCL2. Indeed, expression of BCL2 was decreased by c-MYC but not by c-MYCV394D, and inhibiting BCL2 expression rescued the ability of c-MYCV394D to promote apoptosis. Previous studies of mouse models and of human tumor cells have shown that BCL2 and c-MYC appear to work together in promoting cancer, and these results indicate that transcription of the *BCL2* gene is regulated through c-MYC and MIZ-1. — LBR

J. Biol. Chem. **282**, 5 (2007).

you've got **better** things to do...

better consistency

better purification

better results

Introducing
Personal Automation™

Meet Maxwell

Maxwell® 16 gives you consistent purification results — processing up to 16 samples in 30 minutes. It's Personal Automation™, right at your lab bench. DNA, RNA or protein purification, your choice. Finally reagents, instrumentation, service and support from one reliable source. You'd better visit: **www.MeetMaxwell.com**

Promega

www.sciencemag.org

Science

1200 New York Avenue, NW
Washington, DC 20005
Editorial: 202-326-6550, FAX 202-289-7562
News: 202-326-6500, FAX 202-371-9227

Bateman House, 82-88 Hills Road
Cambridge, UK CB2 1LQ
+44 (0) 1223 326500, FAX +44 (0) 1223 326501

Subscription Services For change of address, missing issues, new orders and renewals, and payment questions: 866-434-AAAS (2227) or 202-326-6417, FAX 202-842-1065. Mailing addresses: AAAS, P.O. Box 96178, Washington, DC 20090-6178 or AAAS Member Services, 1200 New York Avenue, NW, Washington, DC 20005

Institutional Site Licenses please call 202-326-6755 for any questions or information

Reprints: Author Inquiries 800-635-7181
Commercial Inquiries 803-359-4578
Corrections 202-326-6501

Permissions 202-326-7074, FAX 202-682-0816

Member Benefits Bookstore: AAAS/BarnesandNoble.com bookstore www.aaas.org/bn; Car purchase discount: Subaru VIP Program 202-326-6417; Credit Card: MBNA 800-847-7378; Car Rentals: Hertz 800-654-2200 CDP#343457, Dollar 800-800-4000 #AA1115; AAAS Travels: Betchart Expeditions 800-252-4910; Life Insurance: Seabury & Smith 800-424-9883; Other Benefits: AAAS Member Services 202-326-6417 or www.aaasmember.org.

science_editors@aaas.org	(for general editorial queries)
science_letters@aaas.org	(for queries about letters)
science_reviews@aaas.org	(for returning manuscript reviews)
science_bookrevs@aaas.org	(for book review queries)

Published by the American Association for the Advancement of Science (AAAS), *Science* serves its readers as a forum for the presentation and discussion of important issues related to the advancement of science, including the presentation of minority or conflicting points of view, rather than by publishing only material on which a consensus has been reached. Accordingly, all articles published in *Science*—including editorials, news and comment, and book reviews—are signed and reflect the individual views of the authors and not official points of view adopted by the AAAS or the institutions with which the authors are affiliated.

AAAS was founded in 1848 and incorporated in 1874. Its mission is to advance science and innovation throughout the world for the benefit of all people. The goals of the association are to: foster communication among scientists, engineers and the public; enhance international cooperation in science and its applications; promote the responsible conduct and use of science and technology; foster education in science and technology for everyone; enhance the science and technology workforce and infrastructure; increase public understanding and appreciation of science and technology; and strengthen support for the science and technology enterprise.

Information for Authors

See pages 120 and 121 of the 5 January 2007 issue or access www.sciencemag.org/feature/contribinfo/home.shtml

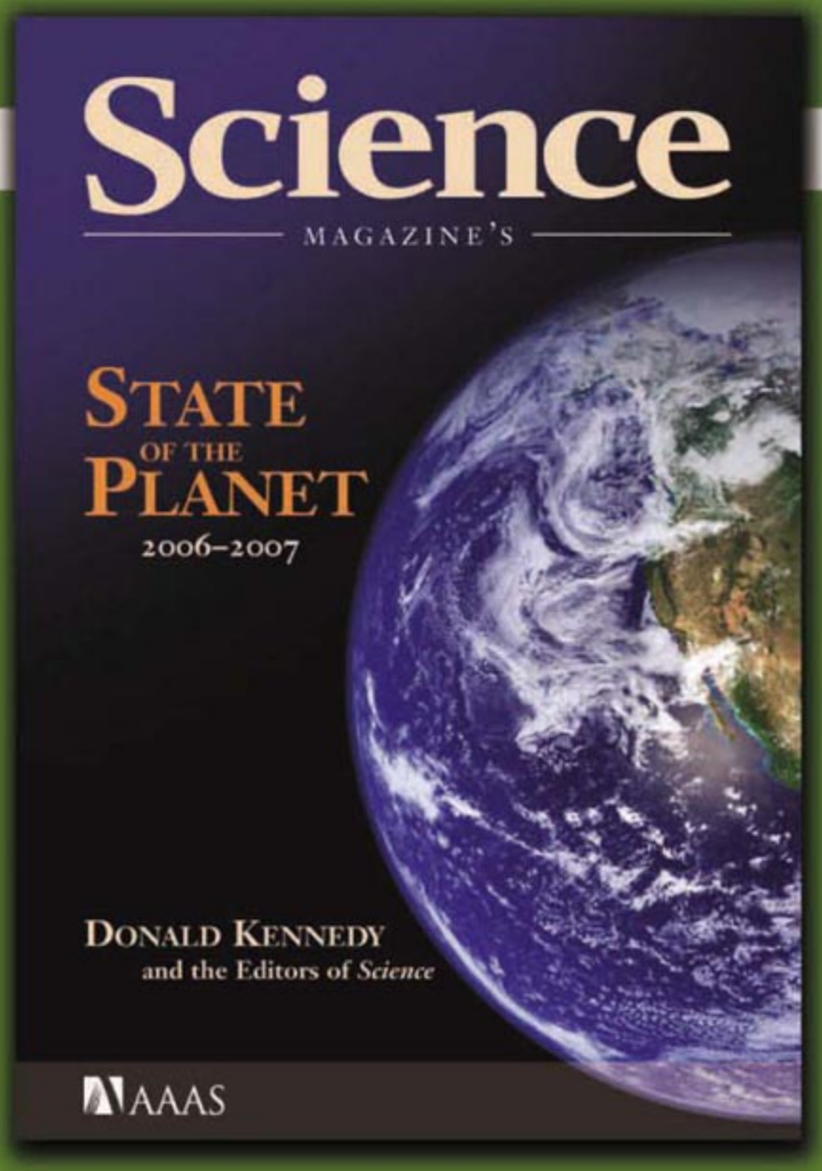

Science Magazine's

State of the Planet 2006-2007

Donald Kennedy, Editor-in-Chief, and the Editors of *Science*

The American Association for the Advancement of Science

The most authoritative voice in science, *Science* magazine, brings you current knowledge on the most pressing environmental challenges, from population growth to biodiversity loss.

COMPREHENSIVE • CLEAR • ACCESSIBLE

ISLANDPRESS

Science
AAAS

islandpress.org

Telltale Stripes

NET WATCH

Devotees of DNA bar-coding, a method of differentiating species using short, standard DNA sequences, hope to speed the description of new kinds of organisms and make it easier for nontaxonomists to identify tricky specimens such as this tachinid fly (*Adejeania vexatrix*; left).

Keeping track of the latest developments in the field is Mark Stoeckle, a physician who teaches in the Program for the Human Environment at Rockefeller University in New York City. Last March, Stoeckle launched the Barcode of Life Blog, which provides weekly news updates, analyses of papers, and other information. Recent posts, for example, discuss the technique's success in distinguishing hard-to-separate species of red algae and why the mitochondrial DNA sequences often used as bar codes differ more between species than within them.

>> phe.rockefeller.edu/barcode/blog

Outwitting the Grim Reaper

The bigger your brain is relative to your body, the smarter you are, increasing your chances of staying alive in a dangerous world. That's the idea explaining the evolution of brain size, and it's indirectly supported by evidence that big-brained animals are better problem solvers and socially more complex. But there are few data directly connecting bigger brains with survival.

Now, evolutionary biologist Daniel Sol of the Autonomous University of Barcelona in Spain and colleagues in the United Kingdom, Hungary, and Canada have used birds to fill in this gap. The team analyzed mortality rates in 300 natural populations of 220 species in environments from tropical to polar regions. They found that relative to body size, birds with larger brains, such as parrots and crows, live longer than do smaller-brained species such as grouses or pigeons. The average tropical parrot, for example, has a 6% to 12% chance of dying in any given year, whereas the odds of survival for a morning dove are less than 50–50.

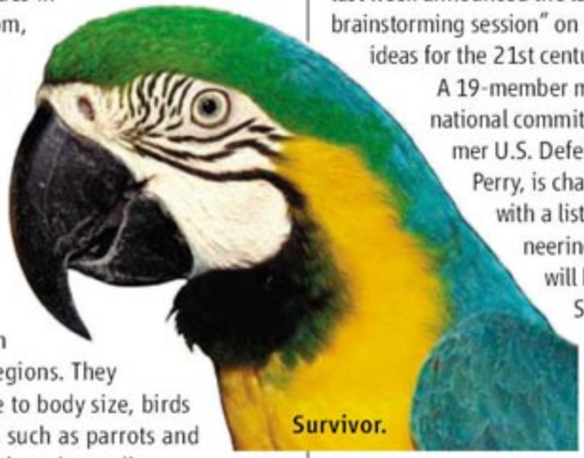

Survivor.

The correlation remained significant even after accounting for other factors such as migration casualties and the life-shortening effects of caring for young, the scientists reported online on 4 January in the *Proceedings of the Royal Society B*. Evolutionary psychologist Robert Deaner of Grand Valley State University in Allendale, Michigan, says the findings are not unexpected, but they supply the "first real evidence" for the idea that "large-brained species have a low probability of dying" within a given period.

Let's Brainstorm

The U.S. National Academy of Engineering (NAE) last week announced the launch of a "worldwide brainstorming session" on great engineering ideas for the 21st century.

A 19-member multidisciplinary international committee, headed by former U.S. Defense Secretary William Perry, is charged with coming up with a list of about 20 engineering challenges, which will be announced in September.

The public is invited to chime in at www.engineeringchallenges.org, where engineer and former President Jimmy Carter has a lead-off essay on his favorite challenge, "the growing chasm between the rich and poor."

NAE spokesperson Randy Atkins says this exercise is a natural follow-up to NAE's list of "greatest engineering achievements of the 20th century."

Scientist surveys wall of detached ice shelf.

ARCTIC BREAKUP

Canada used to have six ice shelves; now it only has five, after the astonishingly rapid and total collapse of the Ayles shelf off Ellesmere Island near northern Greenland. The Canadian Ice Service noted the breakup on satellite images shortly after it occurred on 13 August 2005, but it got no public notice until last week.

In a striking example of fallout from climate change, 87.1 square kilometers of ice calved off in less than an hour, according to a team led by University of Ottawa glaciologist Luke Copland. In a paper now under review at *Geophysical Research Letters*, the scientists say a long crack appeared in the 4500-year-old shelf when pack ice normally pinning it in place melted away. The shelf ice moved rapidly offshore in several pieces, causing the disappearance of a rare freshwater lake ecosystem that had been dammed behind it.

Ice shelves "are endangered landscape features," says Warwick Vincent, a polar scientist at Laval University in Quebec. Ellesmere's have shrunk 90% since 1900, and summer ice cover on its lakes has thinned by nearly two-thirds since the 1990s. The largest chunk of Ayles ice shelf—now Ayles ice island—is now frozen into sea ice about 50 kilometers from its origin. But this winter, normally solid ice has been fractured by high winds and temperatures 7°C above normal. If the island breaks loose, Copland says, it could gyre on currents into the lower-Arctic Beaufort Sea, where it may menace ships and oil rigs.

CREDITS (TOP TO BOTTOM): JONATHAN STOECKLE; WARWICK VINCENT; PHOTOS.COM

Q AAAS

Who's helping bring the gift of science to everyone?

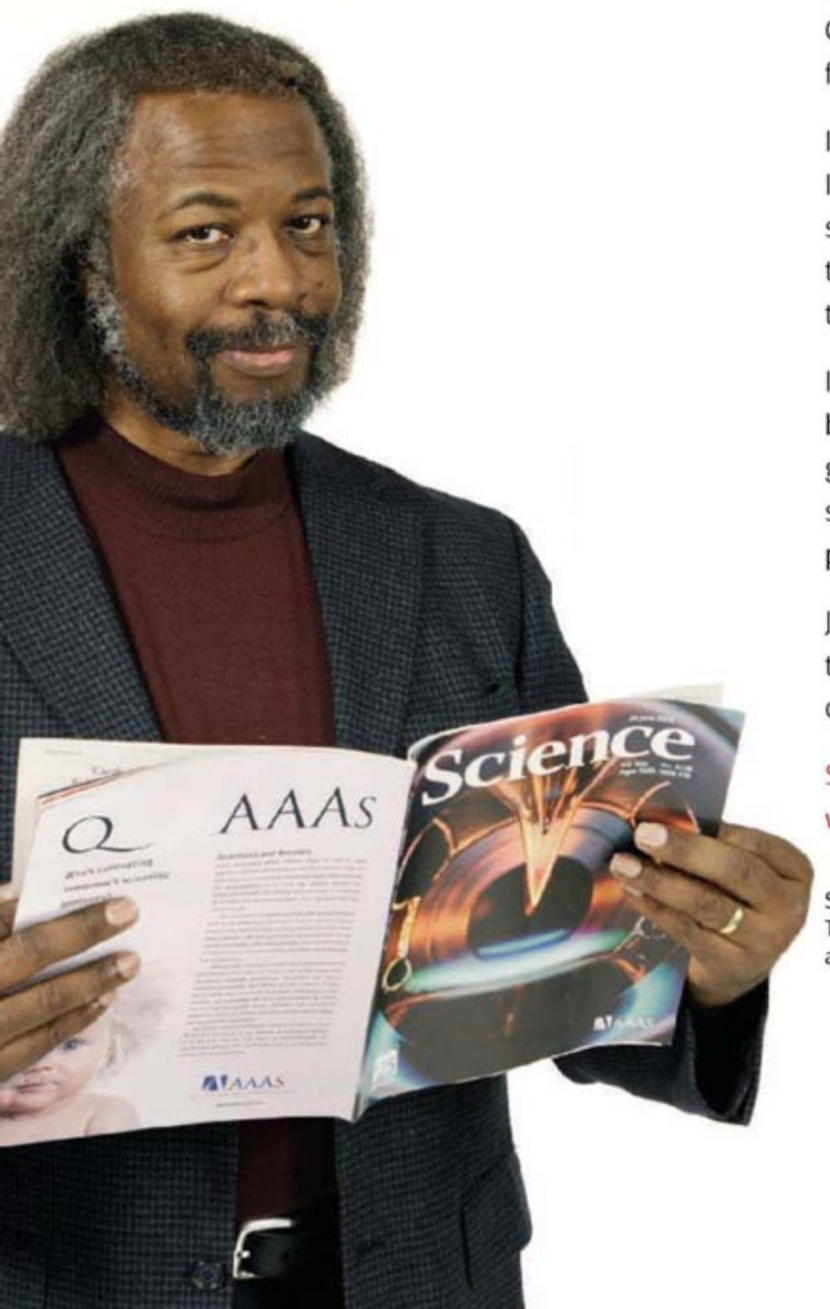

"As a child I got very interested in space travel. When I was six my father gave me some books on rockets and stars. And my universe suddenly exploded in size because I realized those lights in the sky I was looking at were actually places.

I wanted to go there. And I discovered that science and technology was a gift that made this possible. The thrill of most Christmas presents can quickly wear off. But I've found that physics is a gift that is ALWAYS exciting.

I've been a member of AAAS for a number of years. I think it's important to join because AAAS represents scientists in government, to the corporate sector, and to the public. This is very vital because so much of today's science is not widely understood.

I also appreciate getting *Science* because of the breadth of topics it covers. It gives me a great grounding for many activities in my professional life, such as advising government agencies and private corporations."

Jim Gates is a theoretical physicist and professor at the University of Maryland. He's also a member of AAAS.

See video clips of this story and others at www.aaas.org/stories

S. James Gates Jr., Ph.D.
Theoretical physicist
and AAAS member

AAAS
ADVANCING SCIENCE, SERVING SOCIETY

EDITED BY KELLI WHITLOCK BURTON

Movers

PATENTED FINISH. Raghunath Anant Mashelkar (above, left), director general of the Council of Scientific and Industrial Research (CSIR) in New Delhi, India, retired last month after an 11-year tenure. Mashelkar's emphasis on new technology paid off, as the number of U.S. patents owned by CSIR rose from 41 to more than 800. In a rare gesture, Indian Prime Minister Manmohan Singh (above, right) gave a farewell speech praising Mashelkar and noting that "perhaps the best is yet to come." Mashelkar, a polymer engineer, plans to do research at the National Chemical Laboratory in Pune, India.

TRIPLE PLAYER. Last fall, the University of Chicago, long the steward of Argonne National Laboratory, took managerial responsibility for another U.S. Department of Energy lab: the famed Fermi National Accelerator Laboratory (Fermilab) in Batavia, Illinois. This month, Donald Levy, a physical chemist, was given the job of managing science at all three institutions.

Levy, 67, wants to strengthen ties between Fermilab and the university's particle astrophysicists as well as between the two labs. Levy says he's reluctant to give up his research on jet cooling and molecular structure to take on the new challenge, which includes having the proposed International Linear Collider built at Fermilab. "Had this job come along 20 years ago, I wouldn't have even considered it for that reason."

Got a tip for this page? E-mail people@aaas.org

CREDITS (TOP TO BOTTOM): P. BAGLA/SCIENCE; GEORGE MASON UNIVERSITY; UNIVERSITY OF CHICAGO; THE SCIENCE AND TECHNOLOGY FOUNDATION OF JAPAN

DEATHS

DEMOCRACY PIONEER. Seymour Martin Lipset, a sociologist and political scientist renowned for his studies of American democracy, died 31 December at age 84. The only person to be president of both the American Sociological Association and the American Political Science Association, Lipset taught at Harvard University, the University of California, Berkeley, and George Mason University in Fairfax, Virginia, and was most recently a senior fellow at Stanford University's Hoover Institution.

Lipset traced the peculiarities of American institutions back to the nation's revolutionary roots and the strict Protestant religious codes of its founders. This contradictory heritage has made Americans "disobedient" and "more lawless" than citizens of many other countries while at the same time "much more moralistic," he told an interviewer in 1996.

Earl Raab, director emeritus of the Nathan Perlmutter Institute for Jewish Advocacy at Brandeis University in Waltham, Massachusetts, and co-author of three books with Lipset, called him "a great intellect and an excellent communicator."

Awards >>

ENGINEERING HONORS. Advances in information technology, biomechanics, and engineering education earned five scientists top honors from the U.S. National Academy of Engineering.

Tim Berners-Lee of the Massachusetts Institute of Technology and the University of Southampton will receive the Charles Stark Draper Prize, a $500,000 annual award. Berners-Lee designed many of the most fundamental features of the World Wide Web. The Fritz J. and Dolores H. Russ Prize, a $500,000 biennial award, will go to Yuan-Cheng "Bert" Fung, a professor emeritus at the University of California, San Diego. Fung is known as the "father of modern biomechanics" for theories explaining such things as blood microcirculation and soft tissue response to trauma. And Harold S. Goldberg, Jerome E. Levy, and Arthur W. Winston of Tufts University will share the $500,000 annual Bernard M. Gordon prize for educational innovation for developing a multidisciplinary graduate program for "engineering leaders."

The prizes will be presented on 20 February.

JAPAN PRIZES. This year's Japan Prizes go to a forest conservationist and creators of technology essential for personal computers, video recorders, and portable music players. The Science and Technology Foundation of Japan, which sponsors the prizes, each year creates two new categories in basic research for the $435,000 awards.

Albert Fert (above, left) of the University of Paris-South and Peter Grünberg (above, center) of Germany's Research Center of Solid State Physics in Jülich share the prize for Innovative Devices Inspired by Basic Research. In 1988, the pair independently described giant magnetoresistance (GMR), in which the electrical resistance of certain materials drops when a magnetic field is applied. GMR is used in devices requiring large-capacity hard disk drives, such as personal computers.

Peter Shaw Ashton (above, right), professor emeritus of forestry at Harvard University, will receive the prize for Science and Technology of Harmonious Co-Existence for his work on tropical forest conservation and the development of modern forest classification systems. The awards will be presented in April.

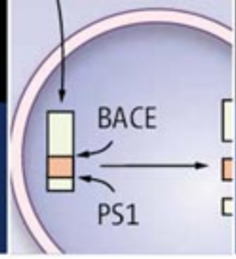

Gene linked to late Alzheimer's
314

Another round on stem cells
315

NEUROBIOLOGY

A Surprising Connection Between Memory and Imagination

People with amnesia struggle to remember their past. They may also struggle to envision their future, according to a new study. Researchers have found that people with amnesia caused by damage to the hippocampus, a brain region intimately tied to memory, have difficulty envisioning commonplace scenarios they might reasonably expect to encounter in the future.

The findings challenge long-held views about the function of the hippocampus and the nature of memory, says Lynn Nadel, a cognitive neuroscientist at the University of Arizona in Tucson. "The claim here is that the same system we use to remember the past we also use to construct possible futures," says Nadel.

In the new study, published online this week by the *Proceedings of the National Academy of Sciences*, cognitive neuroscientist Eleanor Maguire of University College London and colleagues examined five amnesic patients. All of them had severe memory deficits caused by damage to the hippocampus; they had great difficulty forming new memories and recalling events that happened after their injuries. Ten healthy individuals who matched the patients' ages and education levels participated in the study as controls.

Maguire's team asked each subject to imagine and describe several ordinary experiences, such as meeting a friend or visiting a beach, a pub, or a market. The healthy subjects provided rich descriptions, remarking for example on the curve of a beach, the sound of waves hitting the shore, and the feel of burning hot sand. The amnesic patients were able to follow the researchers' instructions, but their descriptions were far less vivid. They described fewer objects, fewer sensory details such as sounds and smells, and fewer thoughts or emotions that might be evoked in the imagined scenario. The patients' responses on a questionnaire indicated that what they saw in their mind's eye were fragmented collections of images rather than coherent scenes.

The work suggests that the hippocampus may have a broader role in cognition than many researchers have thought, says Morris Moscovitch, a cognitive neuroscientist at the University of Toronto in Canada. The textbook view is that the main function of the hippocampus is to encode new memories, creating an initial memory trace that is eventually filed away to the cortex for long-term storage. In this view, the hippocampus is not needed to maintain or retrieve memories once they've been stored in the cortex. If this view were correct, Maguire says, the patients in her study, who did not have substantial damage to the cortex, should have been able to construct imaginary experiences by drawing on memories formed before their injuries. But their inability to integrate those memories into a coherent imagined scene suggests that the hippocampus does more than simply record current events.

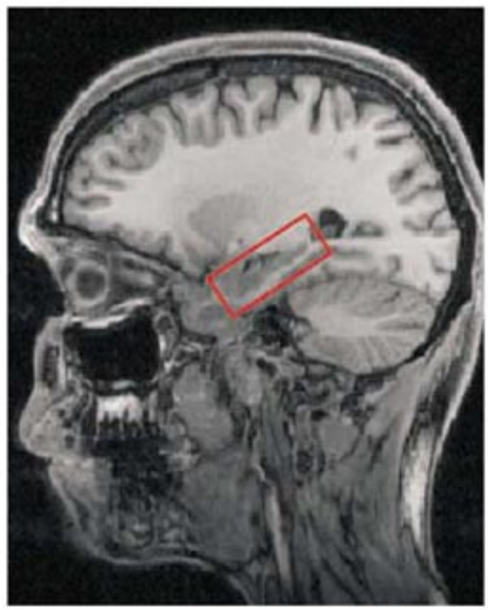

The Janus center? The hippocampus (red box) may be as important for imagining the future as it is for remembering the past.

Nadel, Moscovitch, and others have argued in recent years that the traditional view of the hippocampus's role is too narrow. Work from Moscovitch and colleagues, for example, suggests that the hippocampus binds together elements of remembered scenes to create vivid and coherent memories. Maguire's findings point to a similar role in constructing imagined scenes, Moscovitch says. "In order to have vivid constructions of the past, the future, or of imaginary events, you always need the hippocampus," he says.

The idea that thinking about the past has much in common with thinking about the future has ancient roots, says Yadin Dudai, a neuroscientist at the Weizmann Institute of Science in Rehovot, Israel: "In prescientific times, many people thought that the role of memory is not necessarily to remember the past but to enable you to imagine the future." In modern times, Dudai says, the notion was resurrected by the memory researcher Endel Tulving, who speculated that the ability to predict the future was a major driving force in the evolution of memory. Even so, Dudai says, only very recently have studies like Maguire's begun to provide experimental evidence that memory and imagination may share neural circuitry.

More evidence comes from a functional magnetic resonance imaging study now in press at *Neuropsychologia*. Cognitive neuroscientist Donna Addis and psychologist Daniel Schacter of Harvard University scanned the brains of healthy volunteers who had been asked either to recall a vivid memory or to envision a future experience. Both situations activated a similar network of brain regions, including the hippocampus, the researchers found.

If the hippocampus does turn out to be as important for imagination as it is for memory, that could have interesting implications for aging, Addis says. The hippocampus is one of the first brain regions to show signs of deterioration as we get older, and Addis has recently found evidence that the ability to envision future experiences declines in parallel with memory as people age. Meanwhile, Moscovitch is examining the work of famous artists and novelists to see whether the detail of their work declined in their later years. The picture of the hippocampus that's emerging suggests yet another compromise facing us in old age, he suggests: "Age will contribute wisdom because you can draw on a lot of past experience, but that experience may not be quite as rich as it used to be."

–GREG MILLER

CREDIT: ELEANOR MAGUIRE

SCIENTIFIC PUBLISHING

Fossil Dealers Launch Research Journal

One of the biggest taboos in paleontology is publishing papers about fossils owned by private collectors. The problem is that these fossils are traded, and analyses can't be vetted if a new owner slams the door shut. Last week, a trade association of commercial fossil dealers launched an online journal to provide assurances of access to and documentation of the fossils. Predictably, the announcement has sent ripples through the academic community.

"This self-publishing of fossils in private hands will further undermine our science," says Mark Goodwin of the University of California, Berkeley, one of many scientists who oppose the new venture. But other scientists are hoping that their collaboration will bring important skeletons out of the closet and raise the standards of commercial dealers.

Out of the box. Commercial fossil dealers hope their association's new journal will encourage the study of privately owned specimens, such as this *Tyrannosaurus rex*.

The crux of the issue is access to specimens. All researchers agree that important, rare fossils must be available for study in perpetuity. A fossil in a private collection may end up lost to science if it deteriorates or is sold to a secretive buyer. Many academics also dislike commercial collecting because sloppy fieldwork can damage fossils and omit important contextual information.

For those reasons, the editorial policy of the Society of Vertebrate Paleontology (SVP) commits members to publishing only on fossils that are cataloged in public institutions. Nevertheless, researchers sometime find themselves casting a furtive eye over important but privately owned specimens. "We know about this stuff, but we can't say anything," say Thomas Holtz of the University of Maryland, College Park, one of several academics who studied a *Tyrannosaurus rex* skull owned by a British millionaire while it was temporarily at the Carnegie Museum of Natural History in Pittsburgh, Pennsylvania.

The founders of the new publication, the *Journal of Paleontological Sciences* (*JPS*), say they want to help bring these fossils into the daylight. "It's a shame to ignore a fossil just because it is not in a public repository," says commercial collector Mike Triebold, president of the Association of Applied Paleontological Sciences (AAPS), the trade group that is publishing *JPS*. Some specialized journals, mostly in Europe, already publish analyses of privately held specimens, but AAPS has laid down explicit guidelines to address the concerns of the scientific community and to encourage more responsible behavior among dealers and collectors. "They really are trying hard to do it right," says Kenneth Carpenter of the Denver Museum of Nature and Science in Colorado, one of two academics on the nine-member editorial board.

The free journal will be published online quarterly, with plans to sell an annual print edition. Editorial board member Walter Stein, a dealer in Belle Fourche, South Dakota, says the goal is a self-sustaining journal with advertisements—but none for fossils. A pool of 20 academics will review submissions in which the owner has agreed to make the fossil freely available to researchers. The exact location of the excavation site must be registered with the journal, although that information will remain a trade secret for 25 years. Other documentation, such as photographs and replicas, must also be supplied.

Opponents say that's not good enough. The pledge of access by the current owner is no guarantee of future availability, says Goodwin: "The fact remains that the owner retains all rights and controls access to the specimen." Photographs are no substitute, because they can't be measured accurately and can be faked, notes Hans-Dieter Sues of the National Museum of Natural History in Washington, D.C. "If you can't look at [a fossil] yourself, it might as well not exist."

Some scientists worry that publishing research on privately owned specimens could remove the incentive for collectors to donate their fossils in return for having them studied and named after the discoverers. "In the worst case, the journal might be just a free propaganda platform for private specimens … and thus for raising their price," says Reinhold Leinfelder, director of the Berlin Museum of Natural History. High prices lead to more thefts and illegal collecting, says Goodwin, adding that any involvement in the journal by academics "undermines the science of paleontology and borders on unethical conduct."

Carpenter and others disagree, saying that the benefits of collaboration outweigh the risks. "Better to try to work with people and help guide them toward doing the right thing for science rather than shove them away and say, 'We won't work with you unless you do everything we want,'" Holtz says. "That hasn't worked."

SVP isn't likely to budge on permanent, guaranteed access, says society vice president Blaire Van Valkenburgh of the University of California, Los Angeles. "You have to stick tightly to your guns when you're doing science."

–ERIK STOKSTAD

CREDITS: CARNEGIE MUSEUM OF NATURAL HISTORY, PHOTOGRAPHY BY MELINDA MCNAUGHER; (INSET) AAPS

MOLECULAR BIOLOGY

Trafficking Protein Suspected in Alzheimer's Disease

Traffic control is every bit as important for our cells as it is for our cities. A protein that ends up in the wrong cellular location can cause as much trouble as, say, a car crash in midtown Manhattan. Indeed, growing evidence suggests that improper protein trafficking contributes to the development of Alzheimer's disease (AD) by fostering the production of abnormal amyloid deposits, a key pathological feature of the mind-robbing disease. A new genetic study now gives a boost to the idea that misdirected protein transport contributes to the development of AD, particularly in older people.

In a *Nature Genetics* paper published online on 14 January, a multi-institutional team linked a gene called *SORL1* to the late-onset form of AD. "This gene is robustly associated with an increased risk of Alzheimer's disease in several groups," the group's co-leader Peter St. George-Hyslop of the University of Toronto in Canada said at a press conference last week. (The other co-leaders are Lindsay Farrer of Boston University School of Medicine, Richard Mayeux of Columbia University's College of Physicians and Surgeons in New York City, and Steven Younkin of the Mayo Clinic in Jacksonville, Florida.)

The protein made by the gene, also known as *SORLA* or *LR11*, is thought to be involved in regulating protein movements through the cell. The *Nature Genetics* results, combined with recent findings from other groups, suggest that mutations in *SORL1* lead to a decrease in its protein product, which in turn increases the risk of developing the disorder. When the SORL1 protein is lacking, St. George-Hyslop says, the so-called amyloid precursor protein (APP) is trafficked off to compartments in the cell that contain enzymes that snip out and release the small and highly toxic protein fragment known as β amyloid. Accumulation of this protein is thought to underlie brain neuron degeneration. If confirmed, the new findings should clarify the causes of AD and point to better ways of identifying—and possibly treating—people at risk of developing the disease.

Other genes have been linked to AD. Mutations in three of these, *APP* itself and *presenilin 1* and *-2*, cause the early-onset form of the disease that strikes people in their 40s, 50s, and 60s. Most AD cases occur later in life, after age 70, however, and getting a handle on the genes that contribute to these late-onset cases has been difficult. Although there are many candidate genes, only one has been firmly established, the epsilon 4 variant of the *APOE* gene, involved in perhaps 30% of the cases.

To try to find other genes for late-onset AD, about 4 years ago, St. George-Hyslop, Mayeux, Farrer, Younkin, and their colleagues embarked on a large collaborative study involving some 41 co-authors located at 14 institutions. Because most β amyloid is produced in endosomes, membrane-bound vacuoles that transport proteins from the outer cell membrane where APP is normally located into the cell interior, the researchers decided to focus on seven genes, including *SORL1*, involved in protein shuttling in the endosomes.

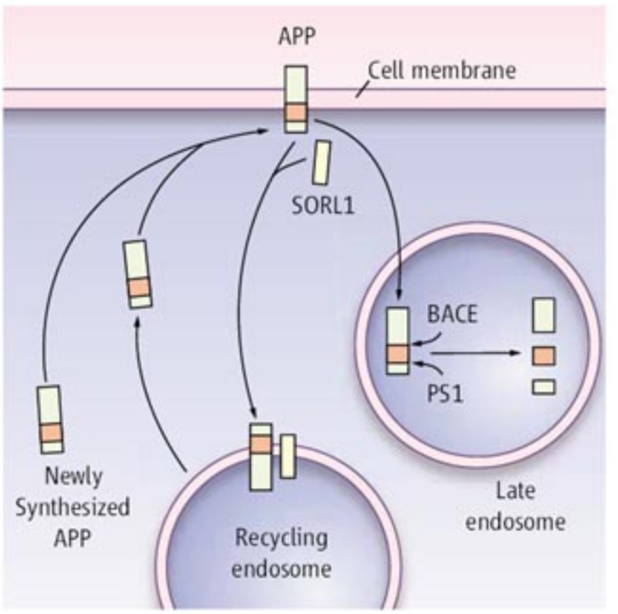

Bad move. The SORL1 protein directs APP into recycling endosomes, which shuttle it to the cell membrane. But when SORL1 is absent, APP goes instead to the late endosomes, where the enzymes BACE and PS1 snip out neurotoxic β amyloid.

They looked for associations between AD and gene variations called single-nucleotide polymorphisms (SNPs) in people of varying ethnic backgrounds—about 6800 total, divided between AD patients and unaffected controls. Only SNPs in *SORL1* associated with the disease. These are only markers, however. The true disease-causing mutations have not yet been identified. Until they are, Mayeux says, the researchers can't get a good fix on how much they contribute to AD, but he estimates they may be involved in 10% to 20% of the cases.

Researchers do have some good ideas, however, about how *SORL1* alterations could lead to AD. About 2 years ago, James Lah and colleagues at Emory University in Atlanta, Georgia, found that brain tissue from AD patients contains less SORL1 protein than do brains of unaffected individuals. Since then, the Emory team and also that of Thomas Willnow at the Max Delbrück Center for Molecular Medicine in Berlin, Germany, have been building a case that SORL1 protects against AD by directing APP away from the late endosomes, where it will be clipped into β amyloid.

They've found, for example, that increasing SORL1 expression in neurons decreases β-amyloid production, but decreasing the gene's expression increases β-amyloid production. The *SORL1* genetics group reports similar findings in their *Nature Genetics* paper. "The biology is pretty compelling" in favor of the idea that a SORL1 deficiency can increase AD susceptibility, says AD geneticist Rudolph Tanzi of Harvard's Massachusetts General Hospital in Boston.

A genetic linkage between the SORL1 pathway and AD would nail down those findings. "That would definitely implicate the pathway," says another AD researcher, Sam Sisodia of the University of Chicago in Illinois. Still, he and others, including St. George-Hyslop and the other team members, say that the results need to be confirmed. In unpublished work described at meetings, Tanzi and his colleagues found a weak link between SORL1 and early-onset AD but no link to the late-onset form.

Such discrepancies are common in attempts to find genes linked to diseases that have multiple causes. But as Farrer pointed out at the press conference, finding the linkage in four distinct ethnic groups—persons of European descent, African Americans, Caribbean Hispanics, and Israeli Arabs—gives them confidence. That, Farrer says, "was unexpected and highly unlikely to be due to chance." Tanzi, too, is optimistic that the result will hold up. "When everything is said and done," he predicts, "I think [*SORL1*] will be added to the list" of AD genes. **–JEAN MARX**

ILLUSTRATION: C. BICKEL/SCIENCE

Replay. Senate stem cell boosters (*left to right*) Orrin Hatch (R–UT), Arlen Specter (R–PA), Tom Harkin (D–IA), and Dianne Feinstein (D–CA).

CREDIT: JONATHAN ERNST/REUTERS

STEM CELL DEBATE

Scientists Protest 'Misrepresentation' As Senate Vote Looms

Several leading scientists are charging that the White House has misrepresented their research in an attempt to influence the ongoing stem cell debate in Congress.

On 11 January, the U.S. House of Representatives voted overwhelmingly to expand the number of human embryonic stem (ES) cell lines available to federally funded researchers. The bill, designated H.R. 3 and considered a top priority in the new Democrat-controlled Congress, passed 253 to 174—a significant jump in support from May 2005 when the same bill passed by 238 to 194. But it still falls more than 30 votes short of the two-thirds needed to override a presidential veto.

With the Senate expected to vote on the same measure next month, the stage is set for a replay of the veto dealt by President George W. Bush last July. The White House has rebuffed attempts by the bill's sponsors to meet with the president, and it's fighting hard to cast the debate in its own terms.

As part of that effort, the White House Domestic Policy Council issued a new report on 10 January to promote methods of getting stem cells that don't harm embryos. The report, *Advancing Stem Cell Science Without Destroying Human Life*, suggests that a variety of "non-embryo-destructive" approaches may prove capable of creating cell lines with all the potential of ES cell lines. It repeatedly mentions a new study by scientists at Wake Forest University in Winston-Salem, North Carolina, who reported in the January issue of *Nature Biotechnology* that stem cells found in human amniotic fluid have many of the same qualities as ES cells (*Science*, 12 January, p. 170). The White House report also touts adult stem cells, saying some "may be pluripotent," and suggests that these could be adequate to treat Parkinson's disease and other conditions for which ES cells have been held up as the great hope. Also put forth are potential alternative sources for pluripotent ES-like cells, advanced in the past by the President's Council on Bioethics, which include the possibility of getting viable cells from dead embryos or through somatic cell "de-differentiation."

Scientists have already reacted strongly to some of the material in the report. Three Harvard stem cell researchers—Kevin Eggan, Chad Cowan, and Douglas Melton—wrote to the sponsors of H.R. 3 complaining of the "clear misrepresentation of our work" in the document, which heavily cites Eggan and Cowan. "We are surprised to see our work on reprogramming adult stem cells used to support arguments that research involving human embryonic stem cells is unnecessary," they wrote. "Our work directly involves the use of human embryonic stem cells … [and] is precisely the type of research that is currently being harmed by" the president's policy.

Anthony Atala, lead author of the amniotic cell paper, also feels that his work is ▶

Wall Stall

Construction of a portion of Israel's defense barrier is on hold. Amid several lawsuits as well as pressure from environmental activists and prominent ecologists, Israeli Defense Minister Amir Peretz announced last week that he will hold up work on the 300-km separation fence into the southeastern Judean Desert. Work on this section, which includes ecologically sensitive territory, began in December.

Tel Aviv University zoologist Yoram Yom-Tov wants the government to build a chainlink fence that would allow small animals to pass through what in most places is an 8-meter-high cement barrier. He also says a well-considered route could protect the movement of ibex, wolves, and other animals in the area.

–ELI KINTISCH

Three's a Crowd Pleaser

Researchers stand to benefit from a new cooperative agreement signed last week by the science ministries of China, Japan, and South Korea. Scientists in the three countries have long shared personal connections, but officials hope the new agreement will foster joint work on the environment, epidemic disease, disaster prevention, Oriental medicine, and new sources of energy. In March, experts will gather in Tokyo to discuss environmental and energy research. The initiative is part of efforts by Japanese Prime Minister Shinzo Abe to improve relations with regional neighbors.

–DENNIS NORMILE

Saving Superfreaks

The Zoological Society of London announced a $975,000 conservation campaign this week to focus on endangered mammals that are evolutionarily distinct. Researchers have come up with a priority list both by analyzing the status of endangered animals and by creating a "supertree" of evolutionary relationships, to be published shortly in *Nature*.

Topping the list of 100 species is the Yangtze River dolphin, which is near extinction (*Science*, 22 December 2006, p. 1860), followed by the long-beaked echidna. Lead scientist Jonathan Bailie says there were also some surprises: Number three is a riverine rabbit of South Africa's Karoo Desert. In addition to expanded efforts to study and protect animals and habitat, the society plans to sponsor 10 research fellows in countries where the endangered mammals live.

–ERIK STOKSTAD

being misinterpreted. Opponents of H.R. 3 have seized upon the report, which appeared on the eve of the House debate, and are citing it as further evidence that noncontroversial cell types can substitute for ES cells. Atala wrote a letter to the bill's sponsors emphasizing that that is not the case.

More friction may be in store: According to *The Wall Street Journal*, presidential aides are drafting a possible executive order favoring alternative sources, although a White House spokesperson says they have nothing to announce at present.

The focus of the debate now turns to the Senate, which passed the same bill (now labeled S. 5) in the last Congress by a vote of 63 to 37. Many estimates put the count at 66 in favor—one vote short of a veto override. But the bill's advocates think there might be a chance of avoiding a veto, because Senate rules will allow for amendments. Certain changes could make the bill more palatable to the president—such as adding provisions for more ethical oversight; a program to promote embryo adoption; or even a new, later deadline for cells that are eligible for federal funding. (Currently, cells have to have been derived by 9 August 2001 to qualify.)

Still, many see another veto as the likely outcome. But stem cell advocates are convinced that public opinion is increasingly on their side. "This is an issue that will not go away," says one of the bill's sponsors, Representative Diana DeGette (D–CO). Until it becomes law, "we intend to introduce it over and over." **–CONSTANCE HOLDEN**

REGULATORY SCIENCE

Panel Pans Proposed Change in U.S. Risk Assessment

Government regulators and toxicologists with private industry are assessing the impact of an unusual rebuke last week by an expert panel of a White House proposal to change how the U.S. government practices risk assessment. The expert panel, which called the proposal "fundamentally flawed," urged the White House to focus on "goals and general principles" and to leave the details of risk assessment to agencies with more expertise.

The proposal, issued in January 2006 by the White House Office of Management and Budget (OMB), laid out technical guidelines for estimating risks posed by anything from toxic chemicals to large engineering projects. Among other things, the guidelines called on agencies to calculate and disclose the uncertainties surrounding their risk estimates. Agencies shouldn't just create a "worst-case" estimate, it said, but also prepare a "central or expected estimate."

That approach is often unrealistic, says a panel of the National Academies' National Research Council (NRC) asked to review the proposed guidelines. A major reason it's not feasible, say public health officials, is because the data required to calculate such values may not exist. "The OMB is looking for a Cadillac of risk assessment," says Gary Ginsberg, a toxicologist with the Connecticut Department of Public Health. "A lot of the time, we're lucky if we have something that moves."

The dispute highlights one of the most difficult issues in risk assessment: what to do when there are no data showing, for instance, how many people became ill after exposure to a particular chemical. "For a few chemicals, you can do this," says Joseph Rodricks, a former U.S. Food and Drug Administration official now with the consulting firm ENVIRON International Corp. in Arlington, Virginia. "But most of the time, you can't."

More than a drop. Billions of dollars are at stake in setting limits for exposure to chemicals, such as perchlorate in drinking water.

CREDIT: PETER CADE/GETTY IMAGES

Rodricks points to the example of acrylamide, a chemical used to manufacture dyes. Animals exposed to this chemical have developed cancer, but studies of workers at factories where acrylamide is used haven't found similar effects. With no solid data from humans to go on, the Environmental Protection Agency (EPA) assumes that animal studies do reflect human biology and, as a result, regulates acrylamide as a substance that can cause cancer.

Such assumptions play a critical role in risk assessment, says Rodricks, a member of the NRC review panel. "You have to do something rather than nothing," he says. The OMB's proposed guidelines, however, didn't provide any guidance to agencies on how to cope with an absence of data.

Many critics, including industry groups, have faulted EPA for sometimes relying on worst-case assumptions in reviewing substances such as perchlorate, a chemical used in rocket fuel that's been found in drinking water supplies. "I think the OMB was trying to push agencies in the direction of being perhaps less conservative, or more realistic, about risks," says Rodricks.

But the actual result of implementing OMB's demand for more and better data, according to some critics of the proposal, would be regulatory paralysis. "It would give industry lots of tools for slowing down the process," says Renee Sharp, an analyst in the Oakland, California, office of the Environmental Working Group.

In response to the NRC's report, the White House announced last week that it will reconsider its proposal. "We will not finalize it in its current form," said Steven Aitken, acting administrator of the OMB office that issued the guidelines.

In the future, many hope that new scientific advances will begin to fill in the data gaps about effects on human health. Among the new techniques are detailed studies of the biology of human cells, or examination of chemical effects on arrays of DNA. NRC has convened another expert panel to evaluate how these and other techniques might improve EPA's risk analysis.

Such new approaches can raise as many questions as they answer, Rodricks admits. "You can find all kinds of effects to chemical exposures" once you start looking for them, he says. The hard part is translating these observations into useful guidance on the chemical's potential harm to humans.

–DANIEL CHARLES

Daniel Charles is a freelance writer in Washington, D.C.

SCIENTIFIC MISCONDUCT

Former Hwang Colleague Faked Monkey Data, U.S. Says

Another Korean cloning repercussion sounded last week: A former member of Woo Suk Hwang's research team has been sanctioned by the Office of Research Integrity (ORI) of the U.S. Public Health Service for faking figures in a paper on monkey cloning being prepared at the University of Pittsburgh in Pennsylvania.

Jong Hyuk Park, who was a postdoc in the lab of Pittsburgh researcher Gerald Schatten, has been barred for 3 years from any relationships with U.S. agencies. The university began investigating the monkey work in January 2006, after Schatten alerted officials to possible irregularities, and the paper was never submitted.

Schatten has not talked to the press for more than a year, but university spokesperson Lisa Rossi says that, despite the fraud, the research team is confident that it succeeded in cloning rhesus monkey embryos and generating pluripotent embryonic stem (ES) cell lines from them. The team is repeating the experiments before submitting the paper. Don Wolf of the Oregon National Primate Research Center in Beaverton says he has "little doubt that it is possible" that Schatten has derived ES cells from cloned monkey embryos, as Schatten reported at a meeting in Toronto last March, but says he will "withhold judgment."

Facing the music. Jong Hyuk Park arriving in Seoul last year.

CREDIT: YONHAP NEWS AGENCY

Park was a postdoc at Magee-Women's Research Institute in Pittsburgh from August 2004 to February 2006. The university concluded last April that he had committed misconduct and referred the case to ORI, which published its finding in the *Federal Register* on 9 January. According to the ORI notice, Park "repeatedly misrepresented" the accuracy of one of the figures in the paper to the Pittsburgh investigative panel, "presented false figures as true," and "falsified the record of revisions of the figures by deleting all prior versions from the laboratory server." ORI says the research, funded by the National Institutes of Health, was to be submitted to *Nature* in a paper entitled "Rhesus Embryonic Stem Cells Established by Nuclear Transfer: Tetraploid ESCs Differ from Fertilized Ones."

John Dahlberg, director of ORI's Division of Investigative Oversight, says the Pittsburgh investigation verified that three pluripotent lines of rhesus ES cells were in fact generated. But Park used photographs from one of them as representing all three. "This is not a huge case of misconduct, to be honest; much of the damage was in the cover-up," says Dahlberg.

Park, before coming to Pittsburgh, was on Hwang's team in Seoul, where he was a co-author of two papers, published in *Science* in 2004 and 2005, that were later retracted. A 9 January statement from Pittsburgh says "other papers co-authored by Dr. Park also have been retracted," but no information was available on what they were.

The episode is another blow to Schatten, whose collaboration with Hwang led to his being found guilty of "research misbehavior" by his university in February 2006. Although the panel found no evidence that Schatten falsified data or was aware of any fraud, it said he failed to exercise "a sufficiently critical perspective" in ensuring that the 2005 *Science* paper was sound (*Science*, 17 February 2006, p. 928).

Although Korean prosecutors said Park was involved in fabrication of data for the 2004 Hwang paper, he was not one of the six researchers indicted on misconduct charges last May in Seoul. ORI does not know the current whereabouts of Park, who returned to Seoul to talk to prosecutors last February. **–CONSTANCE HOLDEN**

The Demise of the Eyes In the Skies

The U.S. satellite sensors monitoring a rapidly changing planet Earth will inevitably shut down in coming years as orbits and equipment decline. But neither NASA nor the National Oceanic and Atmospheric Administration has plans to replace enough of them to avoid a collapse of the U.S. observing system, warned a committee of the National Academies' National Research Council this week.

"Things have gone downhill" since a 2005 interim report that issued a similar warning, says committee co-chair Berrien Moore of the University of New Hampshire, Durham, citing the government's recent decision to remove climate sensors from the National Polar-Orbiting Operational Environmental Satellite System (NPOESS) mission. A NPOESS test satellite is scheduled for launch in 2009.

The committee's solution to the federal belt-tightening is 17 missions between 2010 and 2020, at a cost of $3 billion per year. "These are affordable numbers" in line with 1990s annual budgets for Earth observation, says co-chair Richard Anthes of the University Corporation for Atmospheric Research in Boulder, Colorado. The White House told *The New York Times* that space observations remain a top priority. **–RICHARD A. KERR**

U.K. Takes Eggstra Time

The U.K.'s Human Fertilisation and Embryology Authority (HFEA) will hold a public "consultation" before deciding whether to license scientists who want to create research embryos by putting human DNA into cow eggs.

Several scientists have applied to use the procedure to generate new lines of human embryonic stem cells, but in December, a government report advised banning such research, at least until new regulatory legislation is passed (*Science*, 12 January, p. 173). Stem cell scientists were worried that HFEA would decide against the applications. But HFEA chief Angela McNab says "we have a duty to judge this work under the current law." She says the applications will be taken up in the fall.

"The very encouraging thing is the HFEA didn't kowtow to government pressure," says Stephen Minger of King's College London, one of those who has applied to do the cow-egg research. But "we're obviously disappointed" at the delay, he adds.

–CONSTANCE HOLDEN

Astrobiology Fights for Its Life

A decade after NASA pledged to create a robust program to find and understand life in the universe, researchers face a debilitating budget crunch and skepticism within their own agency

THESE SHOULD BE HEADY TIMES FOR astrobiologists. Reports of recent liquid water on Mars and organic matter in the far reaches of the solar system signal that the fledgling discipline, which seeks to understand the nature of life in the universe, is coming of age. Add an expanding roster of newly discovered extrasolar planets and examples of life flourishing in extreme environments on Earth—amid the high ultraviolet of the Andes, in Australian radioactive springs, and in granite formations deep underground—and the research challenges seem boundless. "The field is not only promising," says Steven D'Hondt, an oceanographer at the University of Rhode Island, Kingston, who studies microbial life deep in ocean sediment. "It is productive and extremely successful."

But don't ask D'Hondt how astrobiology is faring in his lab. He is turning away prospective graduate students because his support from NASA has dried up. D'Hondt's colleagues have similar tales to tell. They are scrambling to find funds from other sources to cope with a 50% cut over the past 2 years in NASA's support for astrobiology.

"We're in dark times now for astrobiology," says Michael Meyer, a former senior scientist for astrobiology and now NASA's lead scientist on Mars exploration. Researchers are afraid that the field may go the way of the agency's life and materials science effort, a once-robust $1 billion program now virtually extinct as more pressing needs in the human space flight program have siphoned off funds. Those fears grew stronger last summer when NASA Administrator Michael Griffin told the Mars Society that astrobiology is marginal to the agency's mission. The fiscal downturn has meant staff cuts at the program's centerpiece, the decade-old NASA Astrobiology Institute (NAI) at NASA's Ames Research Center, on the edge of Silicon Valley in Mountain View, California, and less money for the outside scientists it supports.

New, politically savvy leaders in place at Ames, NAI, and NASA headquarters have high hopes that they can make a better case for astrobiology within the space agency and outside. And the new Congress, which includes a more powerful California delegation, is expected to go to bat for the field in upcoming budget battles with the White House. "We're going to emerge from this in an even stronger position," insists Carl Pilcher, the new NAI director. But others aren't so sanguine. "I feel a pang in my stomach," says Kenneth Nealson, a biologist at the University of Wisconsin, Madison. "Survival is going to be tough."

Astrobionauts. Scott Hubbard (*left*) helped recruit Baruch Blumberg to beef up NAI's research program.

Life mission

NASA has spent a half-century looking for life beyond Earth. For most of that time, however, the exercise was an afterthought to the agency's main focus on space exploration. That modest effort underwent a dramatic change in the mid-1990s, the same time NASA's sprawling Ames center—founded on the eve of World War II to promote aeronautical research—appeared to be on the verge of closure. A team of senior NASA officials proposed a makeover for Ames that would draw upon its existing small programs in exobiology, the life sciences, and computing to focus on two core missions: computing and what was termed astrobiology. The idea wowed then–NASA chief Daniel Goldin,

who was eager to link up with the exploding biological revolution.

The makeover got a boost when scientists announced in 1996 that they had detected evidence of fossilized life in a martian meteorite found in Antarctica. With the backing of then–Vice President Al Gore, Goldin folded NAI and astrobiology funding as a whole into a larger package that included several ambitious Mars missions. He forecast a $100-million-a-year budget line for astrobiology that would help biologists, astronomers, geologists, chemists, and other researchers probe the nature of life on Earth and throughout the universe. His vision had its critics—particularly among biologists—who groused that NASA was using the hype over the martian meteorite to jump on the biology bandwagon. But those concerns were given little credence by a White House, Congress, and NASA leadership intent on pursuing a field that had captured the public's imagination.

Befitting its nontraditional subject, the new NAI was designed to be a nontraditional institute. Its research, done by collaborative teams from universities outside the institute, would focus on the existence of habitable planets and moons within the solar system, the origins of life on early Earth, the limits of terrestrial life, and signatures of life on extrasolar planets. Instead of having a large staff housed in one location, NAI would function as a "virtual" institute, employing a few civil servants who would grow a cadre of experienced scientists working arm in arm with NASA engineers to plan future missions. "We knew that if we didn't keep a connection to missions, this thing would look like NSF [the National Science Foundation], and someone would challenge its existence," says physicist G. Scott Hubbard, NAI's founding director and later chief of Ames itself. He and others envisioned NAI pursuing basic research while also taking a lead role in proposing astrobiology instruments that could fly on spacecraft.

In 1998, after a stiff competition, NAI picked 11 university teams to receive approximately $1 million annually for 5 years. The next year, Hubbard was replaced by Baruch Blumberg, a Nobelist in medicine from Fox Chase Cancer Center in Philadelphia, Pennsylvania, who played a critical role in developing a vaccine for hepatitis B. The appointment satisfied Goldin's demand to Hubbard to find "a King Kong biologist" who would provide NAI with instant biological gravitas.

But that gravitas came at a price: Blumberg had no experience with NASA or space projects. "My understanding was that this was to be a basic science institute, and the teams were selected and funded on that

Astrobiology's Roller-Coaster Budget

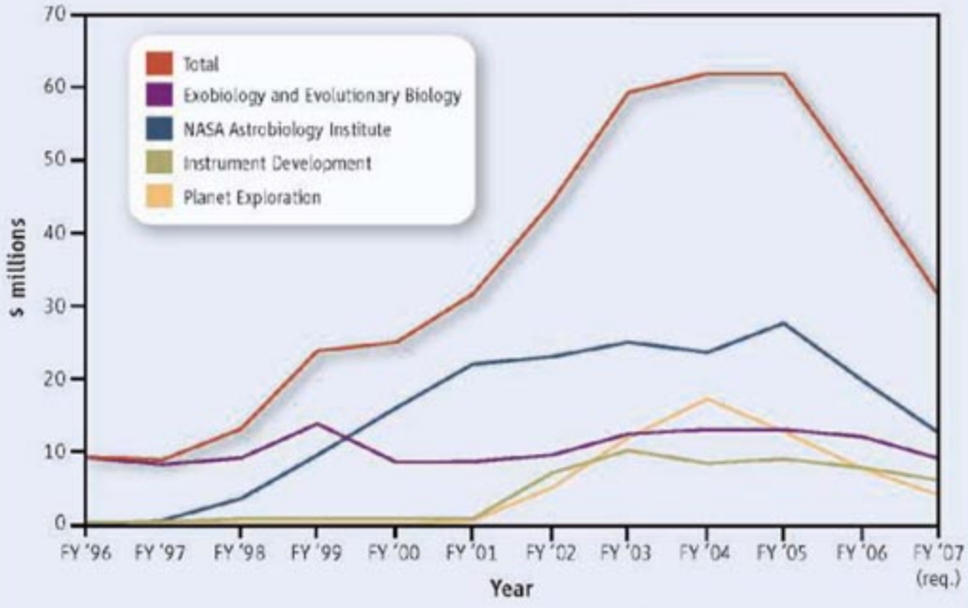

Downward spiral. NASA's increased focus on human exploration has meant less money for astrobiology within an already tight science budget.

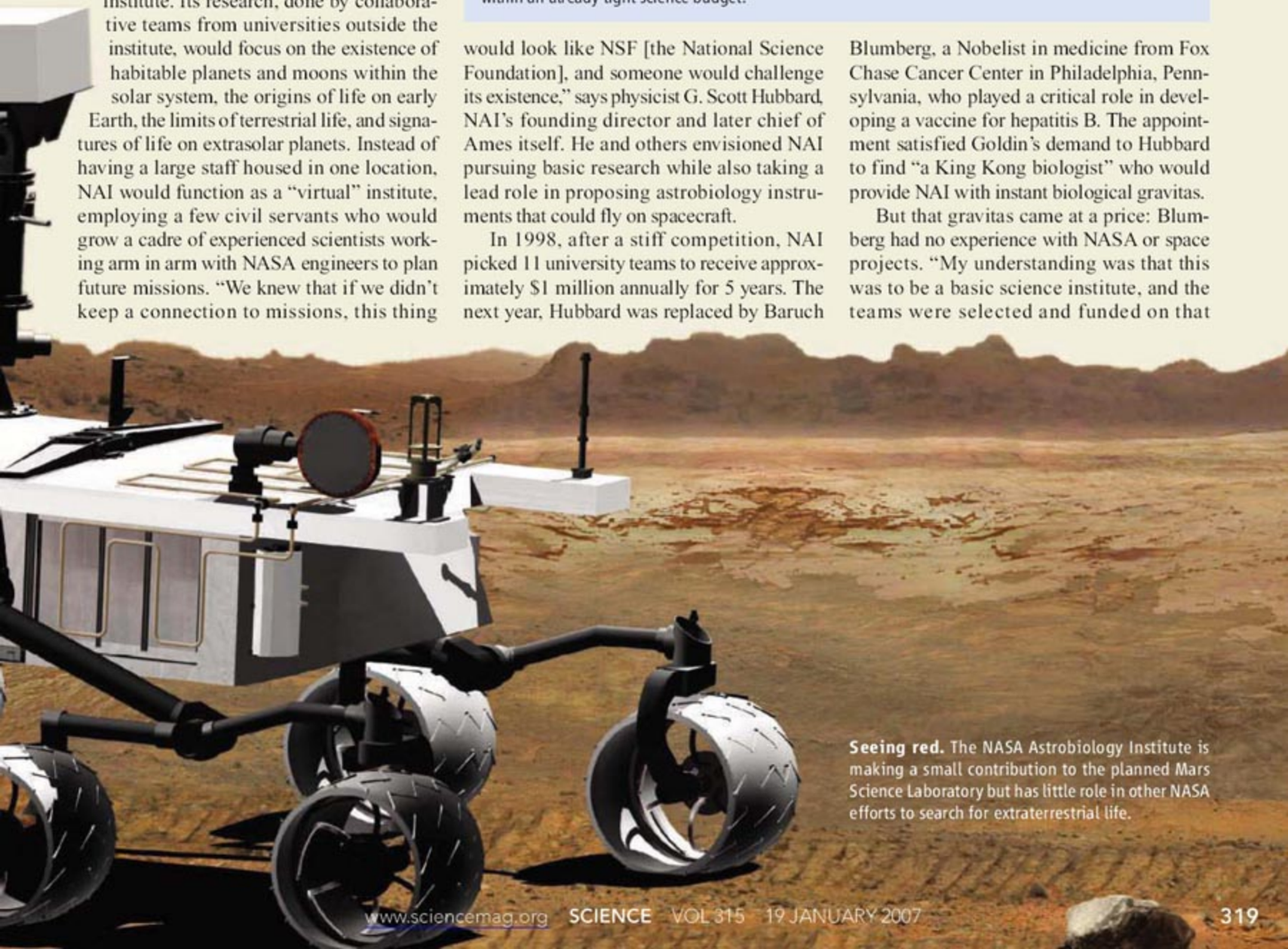

Seeing red. The NASA Astrobiology Institute is making a small contribution to the planned Mars Science Laboratory but has little role in other NASA efforts to search for extraterrestrial life.

basis," Blumberg recalls. "Scientists were given broad direction" to pursue a host of topics. And so they did, with projects on everything from chemical evolution in the interstellar medium to biosynthetic pathways in living cells. The work was intended to lay the foundation for seeking signatures of life, says Blumberg, an approach that he calls "very mission-oriented."

When Blumberg returned to Fox Chase in 2002, astrobiology at NASA appeared to be thriving. The institute's original $4 million annual budget had grown to $25 million, the number of NAI teams stood at 16, and some 15% of the 150 senior scientists on those teams were members of the U.S. National Academy of Sciences. NASA was also spending considerable sums on technologies to monitor life on other planets and for traditional exobiology, which focuses on prebiotic conditions for life in the universe.

But astrobiology's apparent good health proved illusory. The gulf between NAI and the engineers who traditionally run NASA began to widen as the institute's work diverged from the agency's mission pipeline. "Engineers know what they're going to build, while basic scientists don't know what they are going to find," acknowledges Blumberg. Although many scientists associated with the institute worked on missions to Mars and other astrobiology-related flight projects, NAI and its team members did not have a seat at the table when the relevant instruments were chosen. Without their participation, NAI had little direct impact on planning missions. And missions are at the heart of NASA's reason for being. Several university scientists and NASA insiders give Blumberg credit for establishing an excellent research program, but they believe that his failure to pursue a solid role in future missions became the institute's Achilles' heel.

Distance learning. Ames biologist Lynn Rothschild hunts for extremophiles in an Australian pond.

Others note that Blumberg and his successor labored under tough constraints. Spacecraft projects can take a decade or two to complete, and the cost and technology needed to build specific instruments far exceed the means of a $60-million-a-year institute. Such instruments typically require the technical and scientific muscle of a NASA center, aerospace corporation, or large research university. Having its roster of scientists on competitive, 5-year grants hampers long-range planning. And government regulations preclude the teams from bidding on new NASA projects because they are already collaborating with the agency. Their diversity would also make it virtually impossible to settle on a single instrument, notes Bruce Runnegar, a University of California, Los Angeles, paleontologist who served as a team member and then succeeded Blumberg.

Over time, NAI's portfolio veered noticeably toward the study of extremophiles. That unintended shift—driven perhaps by the high quality of proposals it received in that area, say scientists—was a boon to researchers, who canvassed the globe to examine life that could live off radioactivity from rocks in deep mines, metabolize in subzero temperatures, or thrive in highly alkaline or highly acidic environments. "If you are looking for life on Mars, Europa, or the outer planets, you have to look at other kinds of energy sources," says Andrew Knoll, a Harvard University paleobiologist who led one of the teams whose work was not renewed. That makes work on organisms in mines on Earth relevant to the search for subsurface life on Mars, he notes.

But the emphasis on extremophiles also widened the gap between the institute and NASA's core mission. NASA continued to develop, launch, and gather data on missions to Mars, asteroids, Jupiter, and Saturn that provided exciting data on the existence of

A strong foundation. Spain's astrobiology center has steady funding.

It Rains in Spain and Wilts in Australia

In a gleaming steel-and-glass building in Madrid surrounded by manicured lawns, dozens of Spanish researchers are probing the hows, wheres, and whys of life in the universe. With an annual budget approaching $3 million, Spain's Centro de Astrobiologia is thriving. Interdisciplinary teams of scientists, engineers, and lab technicians are working on a sophisticated laser that could sample elements in martian soil as early as 2013, developing a drill system for detecting organisms under the Red Planet's surface later in that decade, and simulating in their labs Earth's early conditions. Each project includes European or American researchers from a host of institutions.

The center's happy buzz of activity stands in stark contrast to the angst felt by its U.S. cousin, the NASA Astrobiology Institute (NAI) (see main text). Ironically, the creation of NAI spurred Spanish researchers to start their own institute in 1999. Construction grants from the European Union and the Spanish government provided a $20 million showcase for astrobiology, and the defense and education and science ministries—along with the regional government of Madrid—supply a steady stream of operating funds. "We are independent and have sufficient funds," says Director Juan-Pérez Mercader, ticking off a long list of ongoing projects. Although its budget and staff are a fraction of the size of NAI and its university teams, the Madrid center is linked both to basic research in the lab and to specific European Space Agency missions, such as the ExoMars orbiter and rover planned for launch in 2013.

The same cannot be said for the 4-year-old Australian Centre for Astrobiology at Macquarie University in Sydney. The Australian institute also was a beneficiary of the U.S. decision to develop the field. "We had a lot of encouragement from NAI and [its director] Baruch Blumberg," says Director Malcolm Walter. With five scientists, 10 graduate students, and an annual budget of $1 million, the Australian center focuses primarily on extremophile research. But a proposed 40% cut in government funding, which Walter sees as a direct result of the NASA cuts, is likely to mean layoffs. "When the U.S. sneezes, we get a cold," he says.

Some U.S. scientists worry that the Europeans are moving into astrobiology's driver seat. "The center of gravity will shift to Europe, and we'll lose leadership," predicts Lynn Rothschild, a biologist at NASA Ames Research Center in Mountain View, California. Indeed, younger researchers may want to book a flight to Madrid. Spain's center has just announced plans for a graduate student program, and as Mercader makes clear, "it is open to anyone who wants to come." **–A.L.**

PREVIOUS PAGE: NASA/JPL-CALTECH; NASA/AMES/TOM TROWER; SOURCE: NASA; CREDITS (TOP TO BOTTOM): CENTRO DE ASTROBIOLOGÍA; NASA

water and other conditions that might be favorable to life elsewhere. At the same time, astronomers using both space-based and ground-based telescopes detected extrasolar planets with increasing frequency.

However, none of these missions—most of which were well under way when the institute was formed—include specific instruments designed to test for life. That makes it hard to judge NAI's impact over the past decade. "What credit can the NAI take? I don't have a good quantitative answer," says Bruce Jakosky, a planetary scientist at the University of Colorado, Boulder, and longtime advocate of the field. And with the exception of a contribution to the future Mars Science Laboratory slated for a 2009 launch, the NASA astrobiology effort is not directly involved in upcoming missions. The Terrestrial Planet Finder, a good candidate for picking up biological signals from extrasolar planets, has been put on indefinite hold, as has a proposed Astrobiology Field Lab to Mars that could probe beneath the planet's surface for hidden microbes.

Its ambiguous contributions make astrobiology tremendously vulnerable as NASA attempts to finish the space station, build a new launcher, and set up a base for humans on the moon—all without significant budget increases. Whereas space and earth sciences have formidable political allies, astrobiology so far has proved too small, too scattered, and too new to fight off budget threats. Griffin has proposed cutting astrobiology funding in 2007 to half of its 2005 level, and NAI has repeatedly delayed its next team competition. Without a new round of winners, there will be no teams left by 2008.

That decline runs counter to the conclusions of a May report from the National Academies' National Research Council that called astrobiology "an outstanding example of the development of a successful new interdisciplinary area" and recommended continued robust funding. However, Griffin says that it's not his job to nurture a fledgling field that won't help him put humans on the moon. Asked at an August meeting of the Mars Society about the impact of the cuts on astrobiology students, he retorted that "if they want to work for government money, they must look at what the government wants—not what they think it should want."

New life

Despite Griffin's skepticism, some scientists expect astrobiology to survive and prosper. Last fall, John Rummel took over as astrobiology chief at NASA headquarters. A biologist with a strong affinity for the human space program, Rummel is a respected agency insider. At the same time, Pilcher, a longtime NASA headquarters official, took over as the institute's fourth director. And his boss is Simon P. "Pete" Worden (see following story), who has big plans for Ames.

Rummel and Pilcher confront a worried batch of researchers as well as a shrinking pool of graduate students. "Plenty of people are getting fed up with the lack of proposals funded," says Kevin Hand, a graduate student at Stanford University in Palo Alto, California. "People are doing other things ancillary to astrobiology," he notes, while they wait for NASA to pump more money back into the effort. And some researchers such as Nealson are skeptical that the program can be redirected to make it more relevant to exploration-focused NASA.

There is a chance Congress may come to the rescue. Whereas Republican legislators regularly defended U.S. President George W. Bush's push for a new launcher and human exploration of the moon, Democrats have spoken out against raiding the science budget to pay for those projects. And some members of the overwhelmingly Democratic California delegation—including Representative Anna Eshoo (D–CA), who represents the area around Ames and is a close ally of new House Speaker Nancy Pelosi (D–CA)—are aware and concerned about the fate of astrobiology.

In the meantime, scientists soldier on. Thanks to an NSF grant, D'Hondt traveled to the South Pacific last month to study deep-sea microbes. But he is worried that the NASA cuts may inflict long-term damage to the field. "We won't be able to produce the scientists needed for future space missions," he warns.

Not everyone is so pessimistic. Even if the institute becomes a victim of the current budgetary storm, many scientists think that the field will survive. "Given the incredible nature of the questions posed by astrobiology," says Hand, "I'd be doing this if I had to pick up dimes from the street."

–ANDREW LAWLER

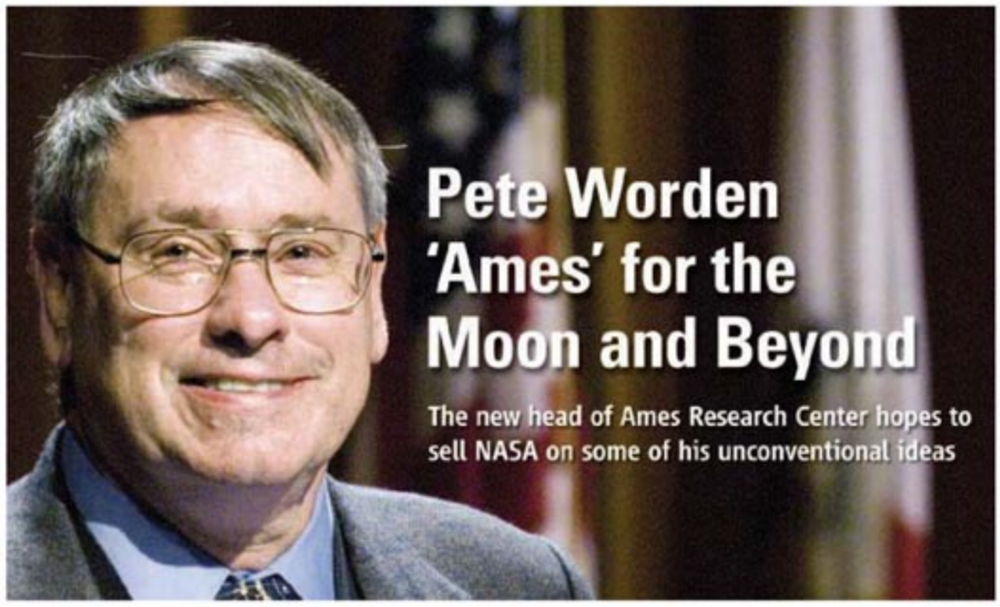

CREDIT: NASA/AMES/TOM TROWER

Pete Worden 'Ames' for the Moon and Beyond

The new head of Ames Research Center hopes to sell NASA on some of his unconventional ideas

To Simon P. "Pete" Worden, NASA's Ames Research Center in Silicon Valley seemed like the perfect beachhead from which to launch a retrograde campaign for a new generation of smaller, cheaper, faster scientific spacecraft. But the maverick astronomer and retired U.S. Air Force general had barely arrived as the center's director last May when he encountered unexpected fire.

The first blow was the transfer of responsibility for developing lunar robotic orbiters and landers—the center's key piece in U.S. President George W. Bush's human exploration effort announced 3 years ago—from Ames to Marshall Space Flight Center in Huntsville, Alabama. Weeks later, Ames lost another project when NASA headquarters decided that the rival Dryden Flight Center in southern California was better able to hold down the cost of readying the Stratospheric Observatory for Infrared Astronomy for flight later this decade. By the end of the summer, Worden's superiors shot down his bold proposal to incorporate smaller and cheaper probes into the fleet set to explore the lunar surface early in the next decade.

Those three early setbacks haven't deterred Worden, a self-proclaimed NASA basher who jokes that the agency's initials stand for "Never a Straight Answer." Instead,

Worden remains bent on radical changes for the troubled lab. Ames and its famous neighbor, Google, last month agreed to an innovative technology-sharing deal that will make NASA's enormous archives of Earth and space data accessible to the public. The deal could pave the way for Google Moon to join Google Earth and Google Mars. And Worden hasn't given up on smaller, faster, and cheaper: He has wrangled $10 million from his bosses to begin thinking about small spacecraft that could journey to asteroids and the outer solar system as well as the moon. He hopes to scale up the program once there's more money for such activities. In the meantime, he's pursuing contracts from other federal agencies to help the center's 2500-strong workforce weather the current NASA budget crisis.

True mavericks are rare among the government's colorless cadres of generals and civilian bureaucrats. But the 57-year-old Worden, who earned an astronomy doctorate from the University of Arizona, Tucson, has a history of bucking conventional wisdom regardless of its effect on his career. In the 1980s, he was an early advocate of President Ronald Reagan's Strategic Defense Initiative, an unpopular stance that earned him the sobriquet of Darth Vader in space circles. As a White House staffer under Reagan's successor, President George H. W. Bush, Worden helped engineer the ouster of NASA chief Richard Truly and his replacement by Daniel Goldin, who touted the smaller, faster, cheaper approach. He then led a tight-knit group of Defense Department officials that applied the philosophy to the successful 1994 Clementine mission to the moon, finding hints of ice at the lunar poles and thoroughly embarrassing NASA and its fleet of large, costly spacecraft.

After the 9/11 terrorist attacks, Worden did a brief and controversial stint as chief of the Pentagon's Office of Strategic Influence, set up to place stories favorable to the United States in foreign media and on the Internet. But then–Defense Secretary Donald Rumsfeld shut it down after the office came to be seen as simply a propaganda vehicle for the Bush Administration.

Worden's unconventional ideas often make his superiors nervous—he served for more than a decade as a full colonel before winning his first star. The debacle with Rumsfeld squashed further chances for promotions, so after working briefly for Senator Sam Brownback (R–KS), Worden left the military in 2004 to join the University of Arizona as a research professor. He lost out to his less-controversial civilian friend Michael Griffin when Sean O'Keefe stepped down as NASA administrator. As for the Ames appointment, mutual acquaintances say Griffin is eager for Worden's help in promoting the president's new exploration vision but chose to keep him far outside the fishbowl of Washington politics.

Worden spoke recently with *Science* about his setbacks, plans, and vision for the center.

–ANDREW LAWLER

On budget cuts to life sciences and astrobiology:

The agency has been given certain priorities and missions by Congress and the president. Astrobiology—not that it isn't superb science—has a lower priority. But there is non-NASA funding—the private sector, other government agencies—and we are aggressively pursuing those options. Is it easy? No. It is much like what happens at a university. I spent the last 2 years as research faculty at Arizona. I didn't have a tenured position, and you did the work you needed to do. I'm a scientist. If I were king, I'd double the science budgets. I think scientific exploration of the solar system and the universe is really exciting and a key area of our future. I'd love to spend two-thirds of the defense budget on science if I could get away with it.

On tension between Griffin and the science community:

It's unfortunate there's a perceived problem. There are clearly a lot of incensed people. Mike's position—which I support—is that an agency has a set of customers, first and foremost the Congress and the White House. They set priorities. If they want to change those priorities, they can. There has been a tendency [for astronomers] to regard what NASA does as a sinecure.

On how scientists can help:

I'm an advocate of small, fast missions that could do 80% of the capability for 10% of the cost. What would be useful is for the scientific community to prioritize missions within the budget we've got, so we can get more science, better science, by doing more smaller missions and fewer bigger ones.

On exploration versus science:

We are faced with a crisis in exploration. The vehicle we have is being phased out for a lot of good reasons, and there's an investment to make. Once the shuttle is phased out, I would anticipate scientific opportunities will go up quickly with a much more flexible system.

Robot Seeks New Life—and New Funding—in the Abyss of Zacatón

With missions to other worlds in mind, explorers ready an ambitious robot to plumb a deadly sinkhole, looking for new life—or at least the bottom

Thirteen years ago on a sunny spring morning, two divers prepared to descend into what could be the world's deepest water-filled pit: northeastern Mexico's El Zacatón, a 180-meter-wide limestone sinkhole filled by hydrothermal springs. The water is 30°C, teeming with strange microbes, and pitch-black below the first 30 meters. One diver was Sheck Exley, then holder of the world's scuba depth record; the other was his friend Jim Bowden, a top underwater caver. They wished each other luck, adjusted their masks, and began free-falling down separate safety lines. Ten hours later, Bowden surfaced with a new world record—925 feet (282 meters)—without ever finding the bottom. Exley did not surface. Three days later, his body was pulled out, tangled in the line. No one knows what killed him.

The sinkhole's depth remains unknown; sonars work poorly in narrow spaces, so readings peter out at about 330 meters. But this week another team is preparing to replumb the mysteries of Zacatón—this time, with an audacious new robot made to probe both its geology and biology. The NASA-funded Deep Phreatic Thermal Explorer (DEPTHX) is designed to navigate and map deep underwater tunnels, spot living things, grab them, and bring them back—all without direction from the surface. If it survives its first voyage in March, DEPTHX will be a major advance in robotics and exploration of extreme environments. If it survives NASA budget cuts, it could be a model for probing Jupiter's moon Europa, where Zacatón-like cracks or holes in the icy surface may offer the best chance of finding extraterrestrial life.

Compared to other autonomous underwater vehicles (AUVs), DEPTHX is "well ahead," says Gwyn Griffiths, head of the National Oceanography Centre underwater lab in Southampton, U.K. But like other

NASA-funded astrobiology projects, the robot's future is uncertain. Its funding is about to run out, and a follow-up project may be a long shot as NASA cuts back support for such efforts (see p. 318). "Robotic exploration of our planet and the universe has been wildly successful and cheap," says Dana Yoerger, an AUV guru and cheerleader for DEPTHX at Woods Hole Oceanographic Institution in Massachusetts. "To cut back on stuff like that for manned exploration is going to give the taxpayers very poor value."

The ringleader of DEPTHX is extreme engineer and cave explorer Bill Stone, who in 1989 made it to NASA's semifinal astronaut-selection round but was nixed as being too independent. During the past 3 decades, he has worked on space and military projects for the National Institute of Standards and Technology and on the side explored some of Earth's most dangerous caverns. Traveling a kilometer or more under the surface, he has stayed down for weeks at a time in air-filled caves. Underwater, he has often dived through twisty, silt-choked passages, re-emerging alive to appear in *National Geographic*. Finding standard scuba tanks too bulky, he invented a compact rebreather that recycles gases, now used by divers worldwide. In 1998, he made the first high-resolution maps of an underwater cavern, Florida's Wakulla Spring, by inventing a torpedo-like personal propulsion vehicle studded with sonars—the precursor to DEPTHX. He and colleagues drove the devices through 6.4 kilometers of inky-black passages to create three-dimensional (3D) images of the invisible walls. "Deep cave systems are the last terrestrial frontier; they push the limits of human endeavor, technology, and psychology," says Stone.

They are also dangerous. Stone has lost 16 friends to exploration accidents and has dragged out the bodies of seven himself. Exley was his cave-diving mentor. "I've come to the conclusion that there are places where humans cannot travel safely," says Stone, now 54. "We need a surrogate."

At Zacatón, Stone is working with Marcus Gary, a University of Texas, Austin, Ph.D. student who assisted at the fatal 1994 dive and became obsessed with the sinkhole. In a Geological Society of America paper last year, Gary reported that the system owes its vastness to volcanism that adds heat and gases to water running into the limestone. This hastens chemical dissolution of the rock as well as making things cozy for unusual bacteria. In 2003, Stone and Gary joined with a cast of luminaries in space, robotics, and microbiology to win a $5 million, 3-year grant from NASA's Astrobiology Science and Technology for Exploring Planets (ASTEP) program to use Zacatón as a proving ground for a prototype robot that could explore Europa. A side benefit would be exploring Zacatón itself.

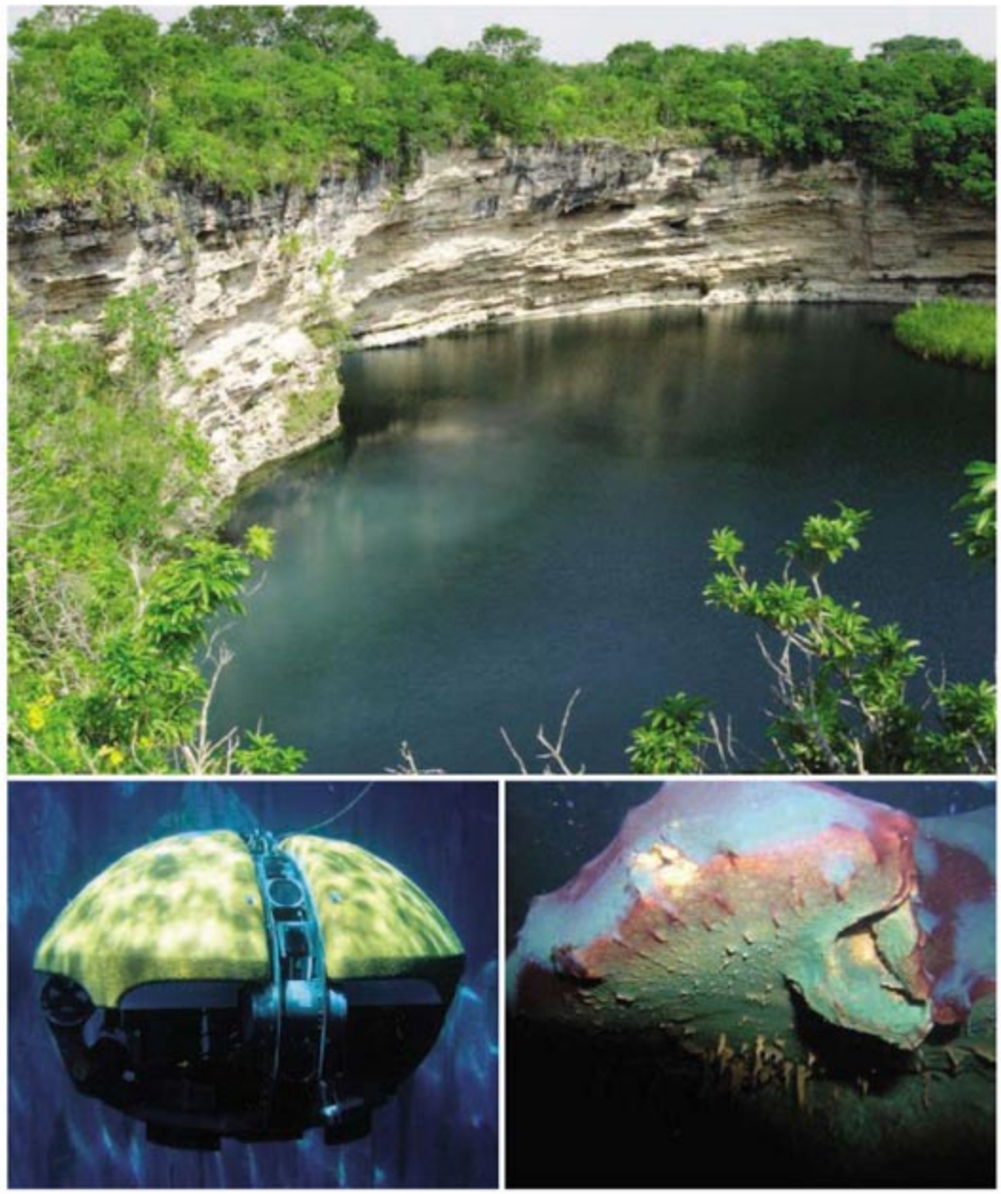

Into deep water. DEPTHX will plunge into Zacatón (*top*) and sample microbial mats (*above, right*).

CREDITS (TOP TO BOTTOM): JOHN R. SPEAR; STONE AEROSPACE; MARCUS GARY

Another team member is Richard Greenberg, a planetary scientist at the University of Arizona in Tucson who helped show that Europa, about the size of Earth's moon, has a hidden ocean covered with an icy crust. Tides crack and puncture the ice from below, creating sinkholelike features on the surface. Like Zacatón, Europa's ocean is also probably heated by volcanism—ideal for the development of life. Many scientists think a robot might have to melt through some 10 kilometers of ice to reach liquid and thus life, but Greenberg says organisms—probably strictly microbes—may also lie in the surficial slushy cracks and holes. "The beauty of this robot is that it would have the smarts to get in there and look itself," he says. (A separate craft would probably melt its way to the bottom of the ice and release one or more DEPTHX-like robots to search the liquid ocean.)

So far, robots have made only baby steps toward this goal. Deep-sea research still depends heavily on remotely operated vehicles powered by tethers from mother ships. Even the Mars rovers receive radioed instructions from Earth and power from the sun. Robots sent under ground or ice can receive neither, because these block radio and light waves, and tethers would become tangled. New AUVs hold promise, but so far most operate in open waters, merely recording temperature, depth, and salinity. "The fully 3D environment and true autonomy are things robotics is only beginning to address," says David Wettergreen, a robotics engineer at Carnegie Mellon University in Pittsburgh, Pennsylvania, and DEPTHX team member.

Early drawings of the 1500-kilogram

DEPTHX robot had it looking like an outboard motor, but in 2005, the team switched to a flattened egg shape to help make it slippery and all-seeing in tight spaces. Wettergreen's team has girdled the surface with 56 transducers that bounce narrow sonar beams in all directions. These hook to a newly elaborated technology called simultaneous localization and mapping (SLAM). As DEPTHX moves—slowly, about 0.1 meters per second—SLAM computers integrate the signals into real-time maps of walls, ceilings, and floors. Theoretically, the craft should hover within less than an arm's length of these features and traverse almost any passage it can fit into. As it travels, it will store the maps and look both forward and back; it is supposed to recognize where it is, and, when it is time to go home, follow the maps back.

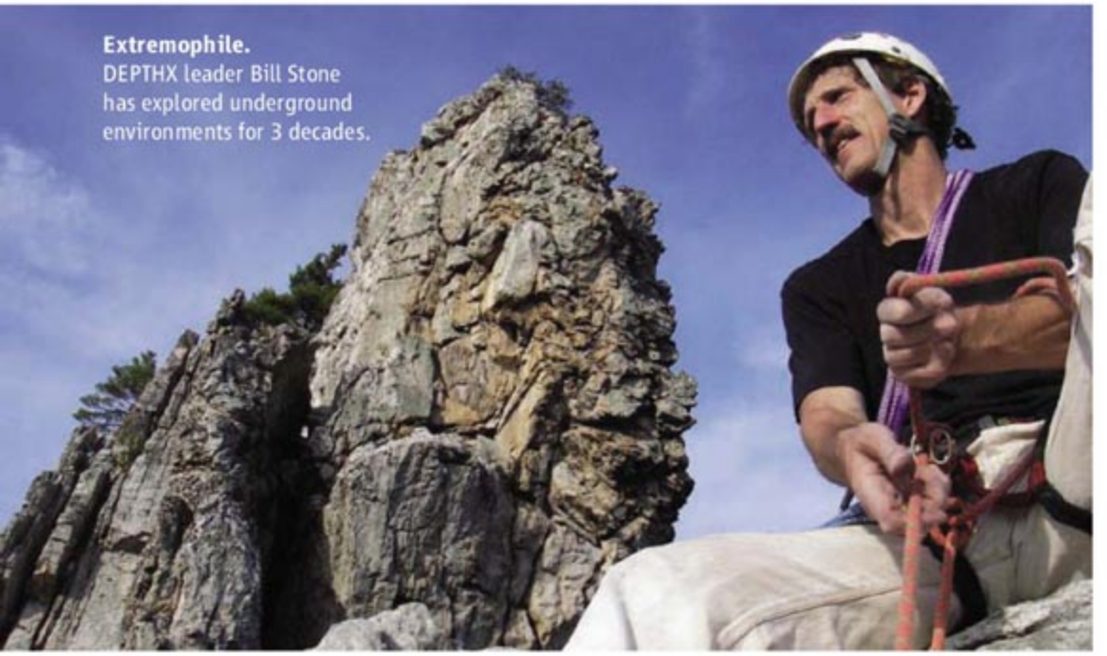

Extremophile. DEPTHX leader Bill Stone has explored underground environments for 3 decades.

In spring 2005, the team lowered a stripped-down version of the sonar array into Zacatón and retrieved exquisite 3D images of the sinkhole down to 290 meters, the first even partial glimpse of its shape. Below its wide, circular top, it narrows into something like a tornado spout. Gary says the bottom could lie as deep as a kilometer—the probable limit of water-soluble limestone—and labyrinths of horizontal tunnels could run many kilometers, possibly connecting to other sinkholes nearby.

As for navigation, the team is still working out bugs. During a shakedown cruise at a water-filled quarry in Austin, Texas, last month, the robot smacked the muddy bottom, then surfaced unexpectedly under the team's rowboat, smashing a $5000 Wi-Fi antenna and rattling researchers. "The risk of losing this vehicle down there is non-negligible," admits Carnegie Mellon roboticist George Kantor.

The greatest challenge at Zacatón may be finding and sampling organisms. It's no problem on top: Along with little fish, water moccasins and other snakes up to 2.7 meters long cut the surface faster than humans can swim. But below about half a meter, the hot, chemical-laced water lacks both oxygen and conventional aquatic life. Divers have found a shallow tunnel connecting Zacatón to a nearby river that holds the bones of countless turtles; like Exley, they may have dived too far or too long. On the other hand, hydrogen sulfide and other volcanic gases feed thriving communities of extremophile microbes. Each morning the water is clear, but by noon it turns milky gray, probably from elemental sulfur precipitated out by photosynthetic sulfide-eating bacteria. Further down, the walls are lined with spongy red and purple microbe mats, says the team's microbiologist, John Spear of the Colorado School of Mines in Golden. In the first 82 meters—as far as human divers dare sample—Spear has spotted 27 divisions of bacteria, including six that may be new, along with archaea and planktonic diatoms. "The diversity is astounding. I think that if we get down further, there will be even more," he says. He expects only microbes but does not rule out bigger life forms. "We could run into tubeworms, or crabs, or something else. We really have no idea."

To search for such life, DEPTHX is equipped with sensors and software that will allow it to follow plumes of heat, sulfide, nitrates, or turbidity—likely emanations of the volcanic vents that almost certainly lie below and potential hot spots for life. "It's the old 'getting hot, getting cold' game, built into a robotic brain," says co-investigator Daniel Durda, a planetary scientist and cave diver at Southwest Research Institute (SwRI) in Boulder, Colorado (*Science*, 6 September 2002, p. 1640). The robot also continually sips water through a microscope designed to pick out living cells by spotting motion. If cell numbers spike, the robot may follow that trail and suck in a water sample to carry back. Once the robot reaches a likely spot, cameras are programmed to look for changes in colors, textures, or shapes that could set bacterial mats apart from bare rock or open water. "We're not quite sure what we're looking for yet—just something different," says SwRI engineer Ernest Franke, head of the science-package team. DEPTHX has an arm with a coring device primed to stick itself into a prospective life form and pluck out a sample about the size of one's thumb-end, Little Jack Horner–style.

Skeptics may think all this unlikely, but from 2002 to 2005, a NASA-funded robot that Wettergreen worked on crisscrossed Chile's near-lifeless Atacama Desert seeking patches of photosynthetic algae by its telltale fluorescence. The robot successfully scooped up samples and applied dyes to detect amino acids and lipids—the stuff of life.

However, NASA has slashed exobiology budgets, and this could prematurely end DEPTHX and related ventures. ASTEP, the main funder of exotic robots, has gone from $15 million in 2005 to a planned $4 million in 2007. DEPTHX's current funding ends after its March deployment. Stone and colleagues had next hoped to develop a smaller, smarter DEPTHX to slip into Antarctic subglacial lakes, and then to design a robot to land on Europa by 2020. Already, another cutting-edge DEPTHX-like AUV slated to sample volcanic vents under the ice-covered Arctic Ocean this summer has run over budget, and ASTEP has not rescued it. But John Rummell, NASA's senior scientist for astrobiology, notes that there is still some money in 2007. "It is my fervent hope that we'll be able to fund the next stage of DEPTHX," he says.

This month, the team will test the robot in the shallower sinkholes near Zacatón. Electrical-resistivity tests around several suggest that their bottoms may be false floors of travertine hiding much deeper watery voids below. These may be sealed environments like the Antarctic subglacial lakes or like Europa's hidden ocean. Then, DEPTHX will swim down into Zacatón itself and meet whatever might be living there. "Whether we actually get that far, we'll see," says Stone. "No guts, no glory, right?"

–KEVIN KRAJICK

Kevin Krajick is a writer in New York City.

CREDIT: YVONNE DROMS

Tread lightly. The zebra-tailed lizard's toes may explain why this species can outrun ghost crabs (*below*) on soft sand.

BIOMECHANICS

Crab's Downfall Reveals a Hole in Biomechanics Studies

The melding of materials and movement to better understand locomotion gets a boost from physicists studying the properties of granular materials

PHOENIX, ARIZONA—When it comes to running on sand, the ghost crab is an Olympic champion. With legs that are a blur to the naked eye, *Ocypode quadrata* scoots up to 2 meters per second on hard-packed sand. But soften up the sand a bit, and the gold medal instead goes to the zebra-tailed lizard, an animal that spends little time on the grainy material. This surprising observation, reported earlier this month here at the annual meeting of the Society for Integrative and Comparative Biology, comes courtesy of physicist Daniel Goldman of the Georgia Institute of Technology in Atlanta.

Goldman has jumped into the field of biomechanics by employing a device physicists have long used to examine granular materials. That's allowed him to study how animals move over different kinds of surfaces, an approach that Goldman and others feel has been neglected to a large extent. "It's nice to see practical and theoretical applications of granular physics applied to an organismal biomechanics problem," says Andrew Biewener, a biomechanicist at Harvard University. "It creates an entirely new field of investigation," which will advance both basic biology and robot engineering.

Until now, most researchers have studied how animals walk, run, trot, and otherwise move using hard, nonskid platforms. "When we studied forces, the last thing we wanted was to have slippery surfaces," says Catherine Loudon, a biomechanicist at the University of California, Irvine. And this approach has proved useful, as researchers have made progress analyzing how muscles and tendons make different gaits possible (*Science*, 21 January 2005, p. 346).

But in the wild, organisms must contend with mud, gravel, and ground littered with debris. Sand can be particularly challenging, as its grains give way briefly underfoot, transforming the surface from a solid to a virtual liquid. Goldman wants to understand how organisms deal with this complexity. "We can't predict how animals will move until we understand the substrate," he says.

At the University of California, Berkeley, Goldman and Wyatt Korff, now at the California Institute of Technology in Pasadena, built a "fluidized" bed, a box of glass beads that were stand-ins for sand. The bed's underside has a porous membrane, and by pumping air at different speeds up through the membrane, Goldman can change how tightly packed the beads are, thereby controlling the properties of the "sand." More air results in looser packing and, eventually, a surface much like quicksand. Aerated enough, the bed turns into a fluid. The method is "extremely brilliant," says Frank Fish, a biomechanicist at West Chester University in Pennsylvania.

Goldman and his colleagues chased ghost crabs, geckos, and various lizard species down a sand-filled track and across the bed, filming the animals as they traversed hard, soft, and "liquid" sand. In addition, he and Korff dropped wires attached to rods into the sand to determine the mechanical requirements for locomotion in sand of different consistencies.

As expected, the ghost crab zoomed across the hard-packed sand. But in soft sand, its eight legs sank in, and the crab trudged along at about 40 centimeters per second. That's about the speed of the gecko, which is adapted for living in trees, not on beaches. "We didn't think there would be such a big difference," Goldman says. The Mohave fringe-toed lizard, another sand dweller, also got bogged down: Its speed dropped by 10%. "Being specialized for sand doesn't necessarily mean better performance" on all forms of sand, Goldman reported.

The big winner on the softer sands was the zebra-tailed lizard. It left the ghost crab in the dust, maintaining at least a 1.5-meter-per-second pace, even in quicksand. This species lives in a varied environment, traveling through brush and on rocks, gravel, and, occasionally, sand; therefore, Goldman expected that it would lack any special adaptation that would enable it to excel on any one surface. But the zebra-tailed lizard didn't sink, and "it seems to use feet as a buffer against the substrate," Goldman said. The lizard has extremely long, gangly toes, and Goldman discovered that it spreads the toes wide as they hit the sand and then curls them up as it lifts the foot. He suspects that sand caught between the toes causes the sand to stop flowing such that it supports the lizard's weight and allows the animal to push off into the next step.

Fish is not convinced that long toes are the secret to this lizard's success. "I don't think they understand enough about the dimensions of the feet and how they interact with the sandy environment," he says.

Goldman is addressing those interactions. He and Korff have designed an artificial "foot": a rod with crossed wires attached perpendicularly at the end. They vary the angle between the wires and drop the "foot" into the sand, measuring how far it sinks. "The penetration depth depends on the angle" between the individual wires, Goldman reported. "It shows geometry can be important in your foot."

Understanding the differences between how the ghost crab and zebra-tailed lizard move could help engineers make better robots, which for the most part stop dead in sand. "You want to have robots that can run around on all surfaces," says Loudon. For that reason, "it's of great importance to understand how animals can [handle] such different surfaces."

–ELIZABETH PENNISI

CREDITS (TOP TO BOTTOM): MADALYN BERNS; CHEN LI

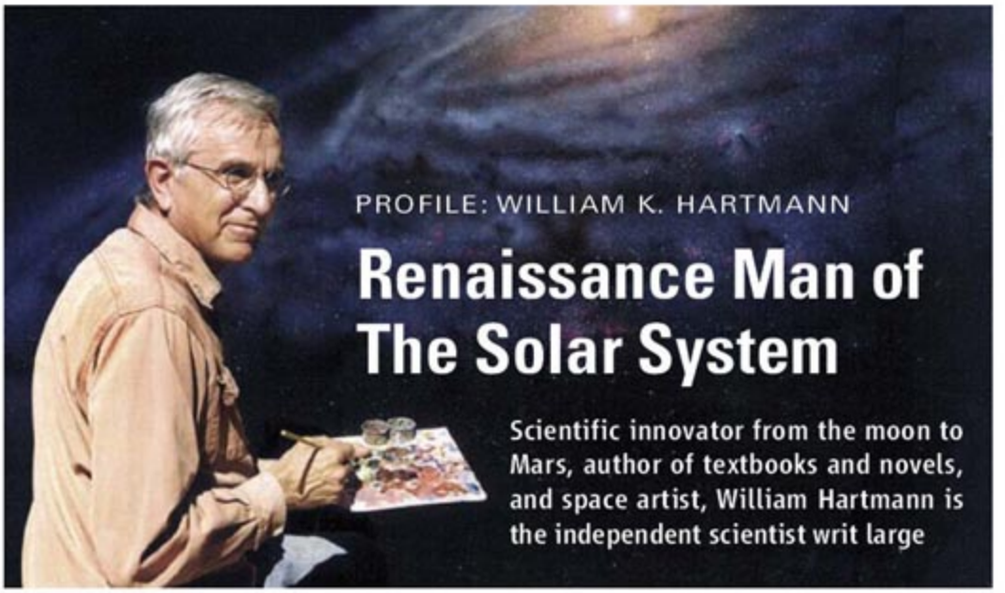

PROFILE: WILLIAM K. HARTMANN

Renaissance Man of The Solar System

Scientific innovator from the moon to Mars, author of textbooks and novels, and space artist, William Hartmann is the independent scientist writ large

TUCSON, ARIZONA—Whether it's his office, studio, or home, William Hartmann packs the pictures in. Everywhere the walls are covered with paintings. And they are paintings of everywhere: an abstract of Paris by writer Henry Miller; Carmel Beach, California, by Hartmann's space-artist hero, the late Chesley Bonestell; his own depiction of a European café; a Swiss landscape by his grandfather.

And then there are the chockablock paintings of the Great Out There from Hartmann's 35-year career as a space artist. The one still on the easel in his backyard studio depicts icy geysering on Saturn's moon Enceladus. Another shows how a giant impact 4.5 billion years ago could have splashed the makings of the moon off Earth, an offbeat hypothesis he co-originated, which is now the scientific consensus on how the moon formed. Hartmann's imagined views of space blend with his words in his fifth-edition planetary science textbook, his half-dozen popular books, and even his first novel.

"He's one of the most productive, innovative scientists in the field," even while pursuing his painting and writing, says planetary geologist Ross Irwin of the National Air and Space Museum in Washington, D.C. "He's made as many discoveries as anyone could hope to."

And he's done it without tenure, without an academic position or even a salaried one the past 36 years. He did help found the Planetary Science Institute in Tucson, where he—like all other PSI staffers—has done his science on nothing but soft money. A nonprofit, PSI has lately been a model for a growing number of planetary scientists looking for workplaces "run by scientists for the benefit of science," as PSI's founders put it.

A backyard start

Hartmann, 67, approached planetary science at an auspicious moment asking the right question. "What are the planets like?" he wondered as a 14-year-old. Through the telescope that he built with the help of his engineer father, he could make out the cratered lunar surface well enough, but from his home in suburban Pittsburgh, mysterious Mars was a tiny disk of shifting smudges.

At the time, professional astronomers couldn't do much better. As a graduate student at the University of Arizona (UA) at the dawn of the space age, the early 1960s, Hartmann found himself studying existing images of the moon taken from Earth. But his adviser Gerard Kuiper, a founding father of planetary science, showed him a new way to look at the moon, one that would shape much of his scientific career.

From Earth, astronomers could see only the near side of the moon. Around the edges, they could see it only at terrain-distorting low angles. So Hartmann projected telescopic photographs of the moon on a plain white 1-meter sphere and photographed this lunar globe from the side, simulating an overhead perspective not available until the Apollo missions. His darkroom experience would eventually involve him in a major UFO study for the U.S. Air Force and image analysis for the U.S. House of Representatives Select Committee on Assassinations. The scientific payoff, however, was the discovery of the Orientale basin, a huge impact scar on the extreme west limb of the moon, the first of its kind to be recognized.

Orientale's discovery would typify much of Hartmann's science. "A lot of my career has been the big-picture stuff," he says. While most of his contemporaries worked to become the world's expert on the topics of their dissertations and to turn out data to five significant figures, Hartmann headed the other way. "The first-order things linking different planets has always appealed to me," he says.

In that spirit, he next used impact craters on the moon and on Earth to gauge the age of the great lunar lava plains that shape the man in the moon. Assuming impactors steadily rain in from the asteroid belt like sand through an hourglass, the number of craters on a surface measure the age of that surface. Comparing lunar crater counts and craters on dated surfaces on Earth, Hartmann calculated the age of the lunar lava plains to be about 3.6 billion years. The late Eugene Shoemaker, the leading cratering expert of the time, put the age at 0.1 billion years. Five years later, lab dating of Apollo rocks proved that Hartmann's estimate was right on.

In the early 1970s, after serving on the science team for Mariner 9—the first artificial satellite of Mars—Hartmann applied his crater-counting idea to the Red Planet. Mars may have looked geologically decrepit, but he found some lava plains whose low crater counts implied that they could be a mere 100 million years old, born last year if Mars were an octogenarian. In the 1980s, dating of meteorites from Mars confirmed the youthfulness of at least some martian lavas. By the late 1990s, Hartmann had co-authored the gold-standard cratering chronology for the inner solar system.

Playful. PSI researchers of the 1970s worked on a computer model that made solar systems.

Freelancers unite

So in the late 1960s, Hartmann was at the start of a roll. He even had an assistant professor's position at UA. But by 1970, Kuiper—concerned that Hartmann develop some professional independence—was nudging him out of the nest when there were still few places to go in planetary science. As it happened, Hartmann had company. In 1968, UA graduate Alan

CREDITS (TOP TO BOTTOM): GAYLE HARRISON HARTMANN; PLANETARY SCIENCE INSTITUTE

Binder had talked his Chicago-based employer into opening a Tucson office. By 1971, the office included not only Hartmann but also UA Ph.D. Donald Davis and UA student and Massachusetts Institute of Technology Ph.D. Clark Chapman, now at the Southwest Research Institute in Boulder, Colorado.

From the start, the Tucson group was on a mission of its own. It would pass through a half-dozen leased offices and work its way through three parent organizations, always searching for a free hand and a lower overhead. It was a nonprofit division before going independent in the late 1990s, but the philosophy remained the same. "We tried to design PSI to be good for the individual researcher," says Hartmann. "We designed it around how people wanted to live and work. We didn't have faculty meetings or deans, but we didn't have assured money either."

That meant gathering a few young researchers less interested in teaching than in doing hands-on science in overlapping fields, and then bringing them up to speed on the fine art of winning NASA grants. By the mid-1970s, PSI was a group of five researchers with all the expertise necessary to tease out the secrets of how a disk of dust and gas had clumped into balls of ice and rock that banged into each other to form planets, moons, asteroids, and comets. Hartmann briefly served as manager of the group until, as a short history of PSI by Davis, Hartmann, and a colleague puts it, "his natural inabilities were recognized."

PSI has ballooned in the past 5 years, as have several other nonprofit planetary institutes. It has gone from a staff of 13 and annual revenue of three-quarters of a million dollars to a staff of 55 (half of them women, with only four or five administrators) and an annual revenue of $3.5 million. Many were attracted not just by the organizational simplicity but also by the geographical flexibility to work where they wish or where their spouses work. The result is a "virtual institute."

The PSI synergy soon led Hartmann to the biggest find of his career. From his own cratering work, Russian theoretical studies, and lab experiments, he and PSI colleagues realized that bodies violently colliding in the still-forming solar system came in a range of sizes. There were far more small ones than large ones. The object that hit the moon to form the Orientale basin was about 150 kilometers across. What was the biggest body that could have hit the nascent Earth? wondered Hartmann.

If the biggest impact were big enough to blast some of Earth's iron-poor mantle into orbit to form the moon, "it seemed to me that would explain a lot," says Hartmann. Apollo astronauts had just brought back lunar rocks for geochemists to analyze. "I was in awe of the geochemists because they worked at such high levels of accuracy," he says. Yet they couldn't explain even the grossest of the moon's properties, such as its dearth of iron.

So Hartmann teamed with Davis—a dynamicist—to develop the giant-impact theory of the moon's origin. Pretty much ignored after its 1975 publication, it became the surprise leading contender at a workshop in 1984 and has been pulling away ever since. The success of the giant-impact hypothesis gave Hartmann renewed faith in making inferences from a few fundamental properties rather than a welter of data. Hartmann has missed the misspelling of his own name on papers, Chapman says, but "he sees things in a subjective way that can be more effective" than fighting through all the details.

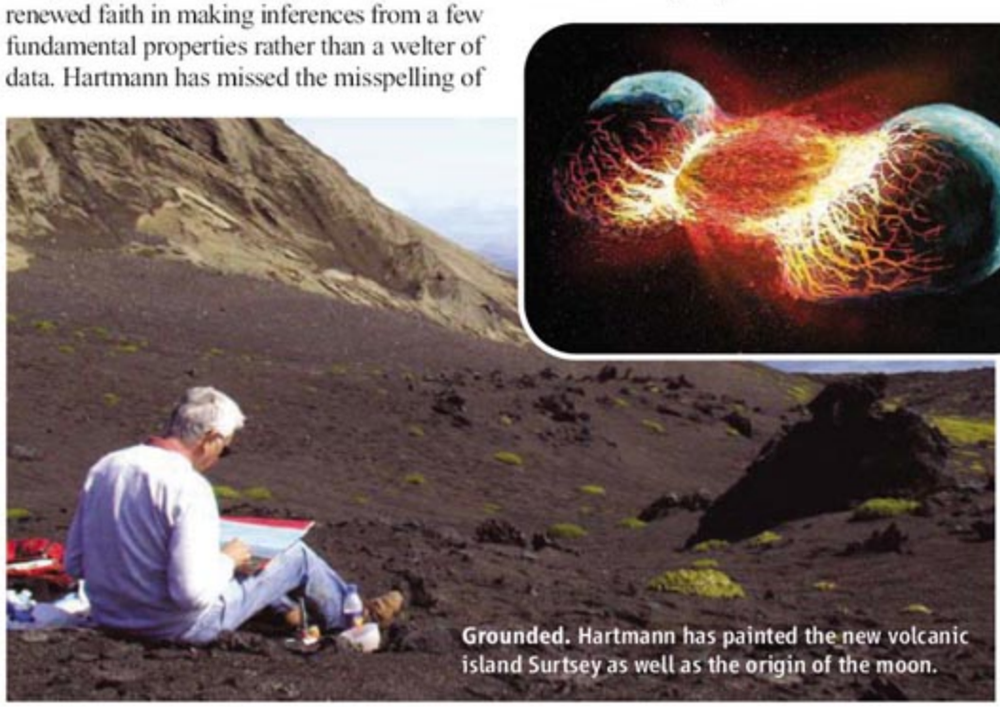

Grounded. Hartmann has painted the new volcanic island Surtsey as well as the origin of the moon.

CREDITS (TOP TO BOTTOM): W. K. HARTMANN, COLLECTION LARRY MCGLYNN; KAREN MEECH

Another side of science

At least part of Hartmann's more intuitive approach was nearly left behind with the trappings of amateur astronomy. He had grown up with a sketchbook in his hand and his grandfather's paintings all over the walls of his home. But by grad school, he had absorbed the message that he'd need physics, not graphics, to understand the planets. That changed in 1970 when a publisher asked him to write an introductory textbook for planetary science. The prospects for illustrating solar system bodies other than the moon and Mars were bleak. So he solicited paintings from his growing contacts in the space-art community and took up his own acrylics and brush.

Hartmann sees a productive interaction between "the painter's eye versus the scientist's eye." For instance, sometimes he understands planetary photometry—the interaction of light and surface—"experientially" by noting how the color of a terrestrial dune he's painting changes with changing sun angle. And trying to paint an alien scene not yet visited by a lander "forces you to ask what we actually know."

As a young scientist, says Hartmann, he was considered something of a dilettante because of his painting. But other scientists eventually saw the rewards of someone translating their data into a form accessible to the public. In 1997, Hartmann even won the first Carl Sagan Medal for communication of science to the public from the American Astronomical Society, in part for his art.

The other part of his public communication has been writing, starting with a textbook and a half-dozen popular science books. Since the Sagan award, he has also published two novels. *Mars Underground* combines science fiction and mystery on a scientifically realistic Mars, while *Cities of Gold* switches back and forth between 1989 Tucson and the early days of Spanish incursion there. "I like having a dialogue with interesting people who take you to different places or times," says Hartmann. "Novelists can be the scientists of the human psyche. You can talk about everything."

Eyeing retirement, Hartmann has been cutting back his science in recent years to favor painting and writing, although he still feels an obligation to contribute to PSI and its effort to groom new planetary scientists. Whether PSI is primed to produce another renaissance man, or woman, is hard to tell. "A lot of the questions I wanted answered at 14 have been answered," says Hartmann. And gigabytes of those pesky details he tended to avoid have been returned from spacecraft, with terabytes more to come.

–RICHARD A. KERR

LETTERS

edited by Etta Kavanagh

Treating Diseases with Adult Stem Cells

IN THEIR LETTER "ADULT STEM CELL TREATMENTS FOR DISEASES?" (28 JULY 2006, P. 439), S. Smith *et al.* claim that we misrepresent a list of adult stem cell treatments benefiting patients (*1*). But it is the Letter's authors who misrepresent our statements and the published literature, dismissing as irrelevant the many scientists and patients who have shown the benefits of adult stem cells.

We have stated that adult stem cell applications have "helped," "benefited," and "improved" patient conditions. Smith *et al.*'s Supporting Online Material (*2*) repeatedly notes patient improvement from these cells (*3*). We have never stated that these treatments are "generally available," "cures," or "fully tested in all required phases of clinical trials and approved by the U.S. Food and Drug Administration (FDA)." Some studies do not require prior FDA approval (*4*), and even the nine supposedly "fully approved" treatments acknowledged by Smith *et al.* would not be considered "cures" or "generally available" to the public at this stage of research.

The insistence that no benefit is real until after FDA approval is misplaced. Such approval is not a medical standard to evaluate patient benefit, but an agency determination that benefits outweigh risks in a broad class of patients. Physicians and patients use an evidentiary standard. Our list of 72 applications, compiled from peer-reviewed articles, documents observable and measurable benefit to patients, a necessary step toward formal FDA approval and what is expected of new, cutting-edge medical applications.

Smith *et al.* also mislead regarding citations for testicular cancer and non-Hodgkin's lymphoma, referring to "[t]he reference Prentice cites…," as though only one reference existed in each case, and not mentioning four other references that, according to their own SOM, show "improved long-term survival" of patients receiving adult stem cells. There are currently 1238 FDA-approved clinical trials related to adult stem cells, including at least 5 trials regarding testicular cancer and over 24 trials with non-Hodgkin's lymphoma (*5*). They also disregard studies showing successful stimulation of endogenous cells for Parkinson's.

"The ethical and political controversy surrounding embryonic stem cell research makes scientific claims especially **prone to exaggeration or distortion.** All such claims should receive careful scrutiny…."

—Prentice and Tarne

The ethical and political controversy surrounding embryonic stem cell research makes scientific claims especially prone to exaggeration or distortion. All such claims should receive careful scrutiny, as recently acknowledged by the editors of this journal after two articles claiming human "therapeutic cloning" success were revealed to be fraudulent. This scrutiny should be directed equally to all sides. We note that two of our critics, Neaves and Teitelbaum, are founding members of a political group whose Web site lists over 70 conditions that "could someday be treated or cured" using embryonic stem cells (*6*). High on this list is Alzheimer's disease, acknowledged by experts as a "very unlikely" candidate for stem cell treatments, with one NIH expert describing such a scenario as a "fairy tale" (*7*). The entire list, in fact, is based on no evidence of benefit in any human patient from embryonic stem cells and little evidence for its claims in animal models. No one should promote the falsehood that embryonic stem cell cures are imminent, for this cruelly deceives patients and the public (*8*).

DAVID A. PRENTICE[1,2]* AND GENE TARNE[2]

[1]Family Research Council, 801 G Street, NW, Washington, DC 20001, USA. [2]Do No Harm: The Coalition of Americans for Research Ethics, 1100 H Street, NW, Suite 700, Washington, DC 20005, USA.

*To whom correspondence should be addressed. E-mail: dap@frc.org

References and Notes

1. Posted at the web site of Do No Harm: The Coalition of Americans for Research Ethics: www.stemcellresearch.org.
2. Available at www.sciencemag.org/cgi/content/full/1129987/DC1.
3. See Table S1 in the Supporting Online Material on *Science* Online at www.sciencemag.org/cgi/content/full/315/5810/328b/DC1; seven applications were not analyzed in the editorial update of 12 July 2006.
4. E.g., for studies done outside the United States. FDA approval is irrelevant; also see, e.g., 21 CFR 1271.10, 21 CFR 1271.15, 21 CFR 1271.3.
5. See www.clinicaltrials.gov/ct/search?term=stem+cell (accessed 13 October 2006); initial search shows clinical trials recruiting patients; click box in upper left to show all trials, including those no longer recruiting patients.
6. Missouri Coalition for Lifesaving Cures; www.missouricures.com/diseases.php (accessed 9 Aug. 2006).
7. R. Weiss, "Stem cells an unlikely therapy for Alzheimer's," *Wash. Post*, 10 June 2004, p. A3.
8. M. Enserink, *Science* **313**, 160 (2006).

Moving Toward Decarbonization

CONCENTRATED SOLAR THERMAL (CST) ENERGY, such as that used at the SEGS solar energy plants, is not new. What appears to be new is R. Shinnar and F. Citro's suggestion that oil at a temperature of >800°F can be stored for hours or days before being used to generate steam ("A road map to U.S. decarbonization," Policy Forum, 1 Sept. 2006, p. 1243).

Tucson, Arizona, at 32°N latitude has average daily solar insolation of 2,000 Btu/feet^2. This is the highest level in the United States and occurs only in the southern half of Arizona and a small part of New Mexico. During the peak summer periods, the rate of solar energy falling on a given land area is more than five times the rate in winter. Further, about 60% of the solar energy comes between 10 a.m. and 2 p.m.

Consequently much of the oil would be heated to >800°F during midday in summer and stored for use in the winter. The amount of hot oil storage required to provide 50% of U.S. energy consumption is enormous and impractical.

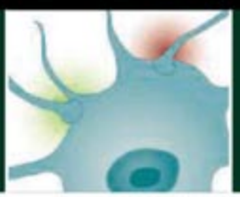

Neuronal circuits balance signals

319

Biodiversity and agriculture

314

Howard Hayden describes part of the SEGS operation as follows (*1*): "The optical efficiency varies from 71% (units I and II) to 80% (units VIII and IX). That is, between 71% and 80% of the sunlight that strikes the mirrors is actually reflected to the pipes containing the therminol. They achieve this high efficiency by washing the mirrors every five or so days, and with a high pressure wash every ten-to-twenty days. Let's repeat that: they wash the several million square meters of mirror – much more than the 2.3 million m^2 of aperture – about 25 times a year!"

The storage and cleaning problems render this CST project nonviable. A third problem is that of finding 15,000 square miles of land suitable for SEGS systems that can be made available.

H. DOUGLAS LIGHTFOOT

Global Environmental and Climate Change Centre, McGill University, Montreal, QC H9X 3C2, Canada. E-mail: dlightfo@aei.ca

Reference

1. H. Hayden, *The Solar Fraud—Why Solar Energy Won't Run The World* (Vales Lake Publishing, Pueblo West, CO, 2005), p. 189.

MOVING TOWARD A DECARBONIZED ENERGY system is an essential element of any strategy to mitigate climate change. In their Policy Forum "A road map to U.S. decarbonization" (1 Sept. 2006, p. 1243), R. Shinnar and F. Citro have outlined one possible technological road map to achieve U.S. decarbonization, in large part by using extensive concentrated solar thermal technology for large-scale, carbon-free electricity generation. Although we fully support studies that explore the potential of technology to "solve the climate problem" (*1*), we are of the opinion that strong policy analysis is needed to reinforce the findings of such work and that policy research in support of this or other technological futures should adhere to common research standards (*2*). Policies—or lack thereof—are probably the most profound barrier to successful implementation of technological climate change mitigation measures.

Shinnar and Citro have used an engineering cost-effectiveness calculation to estimate that the investment in carbon-free energy technology would cost $45 to $50 per ton of CO_2 reduced. They state that this figure is the appropriate value for a CO_2 tax, but cite no previous policy research or new analyses to support this. Rather than a single policy solving the climate mitigation problem, a policy analysis might reveal that a portfolio of policies, implemented at different levels of government, introduced over different time scales, and aimed at different parts of the energy system, will be required to make decarbonization a reality. In addition to pollution taxes (a price instrument), there are many other empirically validated policy approaches (*3*, *4*), such as "cap and trade" quantity limits, financial incentives or subsidies, and emission standards. A full consideration of all options through rigorous policy research is critical to overcome the "political hurdles" mentioned at the end of the Policy Forum.

CONOR REYNOLDS AND ERIC MAZZI

Institute for Resources, Environment and Sustainability, University of British Columbia, Vancouver, BC V6T 1Z4, Canada.

References

1. S. Pacala, R. Socolow, *Science* **305**, 968 (2004).
2. M. G. Morgan, M. Henrion, *Uncertainty: A Guide to Dealing with Uncertainty in Quantitative Risk and Policy Analysis* (Cambridge Univ. Press, Cambridge, 1990).
3. R. W. Hann, R. N. Stavins, *Am. Econ. Rev.* **82**, 464 (1992).
4. W. Pizer, D. Burtraw, W. Harrington, R. Newell, J. Sanchirico, "Modeling economywide versus sectoral climate policies using combined aggregate-sectoral models" (Discussion Paper 05-08, Resources for the Future, Washington, DC, 2005) (available at www.rff.org/Documents/RFF-DP-05-08.pdf).

Response

LIGHTFOOT SEEMS TO CONFUSE SOLAR CELLS with concentrating solar power (CSP). CSP plants constructed by Luz have been operating in the Mojave Desert for 20 years (*1*, *2*). The interval required for cleaning the collectors is not considered to be an impediment to their operation (*1*, *3*). The storage capability of these plants was an important technical breakthrough that, if properly designed, can allow solar energy to become a major source of electric power in countries with large desert areas.

Lightfoot is not correct when he says that the use of a high-temperature heat transfer fluid for energy storage is "new." It was an essential part in the initial Luz design that provided storage for two hours. This capability, which is not feasible for solar cells, is the critical concept that makes large-scale use of solar energy via CSP possible. Our Policy Forum also shows that, with simple design changes, CSP with storage can provide a load-following capability that can stabilize the grid and increase the usefulness of solar cells.

One of Lightfoot's main arguments is the assertion that the solar irradiance ratio in Tucson, Arizona, between summer and winter is larger than 5. Figure S1 (*4*) shows that the measured monthly solar irradiance ratio, averaged over a period of 30 years, for Tucson and two other places is less that 1.8 (1.7 for Tucson), and that the difference from the average is less than 30%.

As rainy or cloudy days do occur even in the desert (less than 25 days a year), the ability to store energy and to use fossil fuel as backup gives CSP a critical edge over any other renewable energy with variable output. In our plan, the excess electricity generated will be used to obtain the hydrogen to produce hydrocarbons as well as storable fuels for backup.

Regarding Lightfoot's concern about available space, extensive studies by the U.S. Department of Energy have identified four Southwest states (Arizona, California, Nevada, and New Mexico) with deserts large enough to generate 4000 GW (*5*), more than twice the output needed for our plan. Larger deserts with stronger and more even solar irradiance are available in nearby Mexico.

We fully agree with Reynolds and Mazzi that dealing with the decarbonization of the economy requires a complete systems analysis. Political problems, costs, and the economic constraints on implementation must be taken into account, as well as time factors and competing priorities. But the methodology they recommend requires quantitative data on risks, penalties, and costs that cannot be clearly defined. When guesses replace hard numbers, the results can be highly misleading. The only sensible response when faced with a calamitous risk is to do everything feasible and affordable to prevent it.

Our Policy Forum did not deal with a complete systems analysis. We accepted the conclusions of previous analysts that the risk of any of the three problems—peaking of oil and gas reserves, energy independence, and global warming—we discussed is unacceptable (*6*). Instead, we identified the technological options available and focused solely on proven technology that we can start to implement now. We demonstrated that a totally decarbonized economy can be realized with existing technology at an affordable cost. Furthermore, as each of the problems mentioned has unbearable consequences, we showed that it is cheaper and more effective to treat them simultaneously, which

our plan tries to achieve. We estimated a cost of $200 billion a year, but this is the total investment required; the cost to society would be significantly less, probably reduced by one-third, by the income realized from the investment. The reduction of imported oil and gas alone would free up between $200 and $300 billion a year.

We agree with Reynolds and Mazzi that there can be many ways to help implement our plan and that a CO_2 tax is only one possible example. But no risk analysis can lead to positive results unless we acknowledge that the problems we face are ominous and that no foreseeable research will provide a "silver bullet" that will make the solution pain-free.

REUEL SHINNAR AND FRANCESCO CITRO

The Clean Fuels Institute, City College of New York, New York, NY 10031, USA.

References

1. R. Shinnar, *ChemTech* **23**, 50 (1993).
2. *Assessment of Parabolic Trough and Power Tower Solar Technology Cost and Performance Forecasts* (Sargent & Lundy Consulting Group, Chicago, for the National Renewable Energy Laboratory, Golden, CO, 2003) (www.nrel.gov/docs/fy04osti/34440.pdf).
3. Private communications between authors and operating plants.
4. See Supporting Online Material on *Science* Online at www.sciencemag.org/cgi/content/full/315/5810/328c/DC1.
5. See www.solargenix.com/pdf/Southwest.pdf.
6. D. Goodstein, *Out of Gas. The End of the Age of Oil* (W. W. Norton, New York, 2004).

Letters to the Editor

Letters (~300 words) discuss material published in *Science* in the previous 6 months or issues of general interest. They can be submitted through the Web (www.submit2science.org) or by regular mail (1200 New York Ave., NW, Washington, DC 20005, USA). Letters are not acknowledged upon receipt, nor are authors generally consulted before publication. Whether published in full or in part, letters are subject to editing for clarity and space.

CORRECTIONS AND CLARIFICATIONS

News of the Week: "U.S. weighs protection for polar bears" by E. Pennisi (5 Jan., p. 25). The article incorrectly referred to the Natural Resources Defense Council as the National Resources Defense Council.

Table of Contents: (24 Nov. 2006, p. 1209). The one-sentence summary for the Report "Two Dobzhansky-Muller genes interact to cause hybrid lethality in *Drosophila*" by N. J. Brideau *et al.* was incorrect. It should read, "Lethality in the hybrid offspring of two fruit fly species is caused by a pair of interacting genes, both of which have been positively selected."

TECHNICAL COMMENT ABSTRACTS

COMMENT ON "The Geometry of Musical Chords"

Dave Headlam and Matthew Brown

Tymoczko (Reports, 7 July 2006, p. 72) proposed that the familiar sonorities of Western tonal music cluster around the center of a multidimensional orbifold. However, this is not true for all tonal progressions. When prototypical three-voice cadential progressions by Bach converge on the tonic, the chords migrate from the center to the edge of the orbifold.

Full text at www.sciencemag.org/cgi/content/full/315/5810/330b

RESPONSE TO COMMENT ON "The Geometry of Musical Chords"

Dmitri Tymoczko

The basic sonorities of traditional Western tonality divide the octave nearly evenly and are found near the center of the orbifolds $\mathbb{T}^3/S_3$ and $\mathbb{T}^4/S_4$. Many common musical patterns exploit this fact, which permits efficient voice leading between structurally similar chords. In actual music, these patterns sometimes appear incompletely or are accompanied by additional notes. Using orbifolds in musical analysis therefore requires interpretive skills.

Full text at www.sciencemag.org/cgi/content/full/315/5810/330c

SCIENCE AND THE MEDIA

Breaking the Embargo

Richard Horton

"Can we expect a few broken fingers?" asked one news agency journalist. "The embargo break caused me serious embarrassment," wrote the science editor for a leading international broadsheet newspaper. "There should be consequences for this sort of behavior," remarked another reporter.

Embargoed Science

by Vincent Kiernan

University of Illinois Press, Urbana, 2006. 190 pp. $30. ISBN 9780252030970.

These were just a few of the many angry reactions I received from journalists when three U.S. newspapers—the *New York Times*, *Washington Post*, and *Wall Street Journal*—broke *The Lancet*'s news embargo on the recent Johns Hopkins survey of mortality in Iraq.

Admittedly, the story was hot. Could it be true that increased death rates after the U.S.-led invasion of Iraq in March 2003 have claimed an additional 650,000 lives? We planned to publish the research paper online. Following our standard practice (one shared with many journals), we had issued a press release and advance copy of the article to journalists a few days before the day of publication. But a dispute over who had rights to disseminate the research led journalists at those three newspapers to believe they were free to ignore our usual embargo rules. We felt stamped upon by this embargo violation. In retaliation, and at the urging of other journalists, we temporarily removed the three newspapers from our press lists (thus depriving them of advance access to papers we were about to publish).

Vincent Kiernan might, I think, be quite pleased with this outcome. In *Embargoed Science*, his compelling critique of the self-aggrandizing embargo system that currently rules scientist-editor-reporter relations, he stresses that journalists should not break embargoes. But he also believes that, as he bluntly puts it, "The embargo should go." What happened to *The Lancet* shows that the system does fracture under pressure. Welcome news, perhaps.

In practice, an embargo means that the content of a journal is sent to journalists on the understanding that they will not write about the work until a prespecified date and time. Editors use the journal embargo as a marketing tool to extract the maximum possible publicity for their publications. We do so in the belief (or, at least, hope) that we have something useful to say. Kiernan claims that embargoes create and sustain an elite cadre of journals, a cabal of titles that exerts an ever-widening and unjustified authority over journalists.

He goes on to argue that the control of information through the embargo creates an "impression of immediacy." But it is a misleading impression. The governing idea behind the journal embargo is a bad one: it is a mechanism to restrict, not promote, the communication of science to the press and public. The editors of scientific and medical journals have somehow assumed the power to decide which journalists will and will not have privileged access to information. Kiernan concludes that this system is manifestly against the public interest.

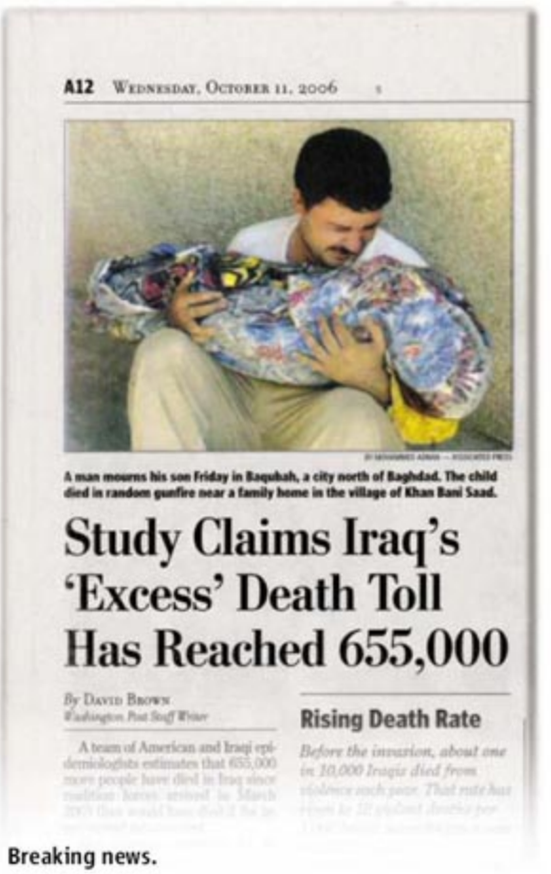

A12 WEDNESDAY, OCTOBER 11, 2006

A man mourns his son Friday in Baqubah, a city north of Baghdad. The child died in random gunfire near a family home in the village of Khan Bani Saad.

Study Claims Iraq's 'Excess' Death Toll Has Reached 655,000

By David Brown
Washington Post Staff Writer

Rising Death Rate

Before the invasion, about one in 10,000 Iraqis died from violence each year. That rate has

Breaking news.

My fellow editors and I usually deploy a well-rehearsed series of defenses at this point. The embargo creates a level playing field for journalists. No one journalist gets an advantage over any other, we say. But who says journalism is about fairness? Kiernan invites readers to view the "primary purpose" of journalism as providing information that citizens need to be "free and self-governing." A level playing field has no part to play in this noble cause.

The embargo gives time for journalists to research a story properly, we retort. Insulting, suggests Kiernan (himself a senior writer at the *Chronicle of Higher Education*). Journalists react to complex breaking news all the time. Why should science and medicine be any different? But what is good for science (the production and publication of excellent research) is surely good for society, we bluster. Maybe. Maybe not. That is a value judgment, one that journalists are not paid to make. Their allegiance is to something far higher, a cause independent of any one interest.

But journalists like embargoes, we editors cry. It is not us who impose embargoes on news reporters. Kiernan shows that this is true, historically as well as currently. The embargo was born because journalists "demanded advance access" to scientific research. But the publishers of science soon realized what a powerful stranglehold over the press they had been given. They have exploited that power ever since.

Kiernan wins the argument about embargoes cleanly and comprehensively. Embargoes do create deference among journalists to the scientific and medical establishment. They are artificial, perpetuating the work of less-skilled journalists and giving attention to often weak and dubious science. They turn journalists away from investigating science as they would any other institution in society.

The constant stream of embargoed news releases distracts journalists from what they should be doing—namely, taking a more critical approach to their beat. The existence of this embargo-driven "pack journalism" should be antithetical to a group that usually resists any authority trying to influence what it does. It is strange that journalists acquiesce to the will of such powerful publishing organizations.

If the "tyranny" of the embargo was to disappear, and the "gentility" of science and medical journalism were to end, what would happen? Would the world self-destruct?

The reviewer is the editor of *The Lancet*, 32 Jamestown Road, London NW1 7BY, UK. E-mail: richard.horton@lancet.com

CREDIT: WASHINGTON POST, 11 OCTOBER 2006, P. A12; PHOTO BY MOHAMMED ADNAN/ASSOCIATED PRESS

Much second-rate research would likely not get reported. Poor science journalists would move into less-specialized fields. Good journalists would flourish and work faster.

Nobody would mourn the embargo. It's a wonder we editors still defend it. But which medical or science journal will move to erase the embargo first? Ah, there lies the rub.

10.1126/science.1135374

LINGUISTICS

Language Learning Through Selection

Jeffrey Lidz and Lisa Pearl

Everyone knows that language acquisition is a protracted process. It takes a child a minimum of 3 to 5 years to be able to talk, for the most part, the way everyone else does. The commonsense understanding of language learning is that children start knowing nothing about their language and gradually build up a system of knowledge that enables them to communicate.

The orthodoxy of generative linguistics, however, could not be more different from this commonsense view. Rather than building up a language from scratch, children bring innate knowledge of the space of possible languages to the learning task. Language learning, from this perspective, involves mapping experience from the language the child is exposed to onto this hypothesis space so that one language emerges. This perspective derives from two interrelated considerations. First, the range of variation found among the world's languages is surprisingly restricted. Viewed from a certain level of abstraction, languages vary along a finite set of parameters, each with a narrowly restricted range of values (typically two or three). Second, children's linguistic behavior appears to be restricted along these same dimensions. Although children obviously make many errors in the course of language learning, many of these errors mimic the variation found across the world's languages. Together, these considerations lead to the conclusion that the learning task consists primarily of selecting the set of parameter values that best fits the language the child hears.

What has been missing from the parameter-setting perspective on language learning is a theory of how learners use the input to identify the correct parameter values. In *The Infinite Gift: How Children Learn and Unlearn the Languages of the World*, Charles Yang offers a popularization of his ideas about how this is done.

The Infinite Gift
How Children Learn and Unlearn the Languages of the World
by Charles D. Yang
Scribner (Simon and Schuster), New York, 2006. 285 pp. $25, C$34.50. ISBN 9780743237567.

Yang's central thesis borrows from population biology, where variation within a population is a fundamental feature. The insight underlying his approach is that a population does not need to be a population of organisms in order for the principles of natural selection to apply. Instead, Yang (a computational linguist at the University of Pennsylvania) argues that the mechanisms of natural selection can apply to a population of languages within the mind of a language learner, where a "language" is viewed as a set of parameter values.

To understand the application to languages, it is first necessary to remember some basic principles of Darwinian evolution. Population biology provides a formal basis for describing how variation within a population both exists and changes over time. Natural selection provides the driving mechanisms via quantified notions of reward, punishment, and competition. The key is Darwin's variational principle: individual members of the population differ from each other in some specified traits, and the population system as a whole evolves by changes in the proportions of the different members in the population. The proportions map directly onto the probability of finding an organism with a certain trait in the population at any given time. Over evolutionary time, these probabilities shift.

Yang applies the variational principle directly to the population of languages within the mind of the learner. Just as populations of organisms evolve by changing the probabilities of organisms over evolutionary time, so does the learner change the probabilities of languages over ontogenetic time. These probabilities shift in direct response to the useful data in the linguistic environment. The more successful a language is at analyzing data from the linguistic environment, the more it is rewarded; the less successful it is, the more it is punished. These languages are competing against each other, and the winner is ideally the one that provides the best fit to the language spoken around the child.

The book represents the first popularization of ideas coming from a new wave of research in cognitive science. That field has traditionally been divided between the representationalists, who propose that the mind is essentially a symbol-processing device, and the associationists, who propose that all behavior is driven by probabilities of distributed neural activity. The difference here lies in the existence of symbols as distinct mental objects. The new wave recognizes that there is no inconsistency between symbolic computation and probabilistic computation. Yang's ideas illustrate how these two styles of computation can coexist in the same organism.

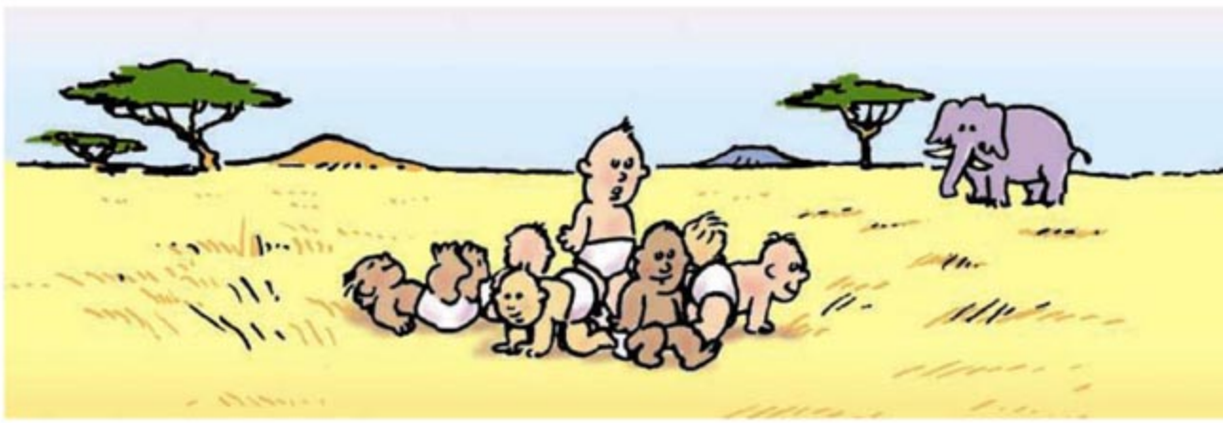

CREDIT: JOE SUTLIFF

Much of *The Infinite Gift* is spent running through a set of standard arguments about the complexity of language learning, but the last two chapters represent the real strength of the book. In them, Yang provides an easy-to-read and insightful distillation of how acquisition of a symbolic system can take advantage of the tools of probability theory and natural selection.

10.1126/science.1135673

The reviewers are at the Department of Linguistics, 1401 Marie Mount Hall, University of Maryland, College Park, MD 20742, USA. E-mail: jlidz@umd.edu; llsp@umd.edu

SCIENCE FOR DEVELOPMENT

Poverty Reduction Through Animal Health

The global community needs to give greater thought and investment to building scientific capacity in animal health research within developing countries.

Brian Perry[1]* and Keith Sones[2]

Livestock contribute to the livelihoods of roughly 70% of the world's poor (*1*), supporting farmers, consumers, traders, and laborers throughout the developing world (*2*). Furthermore, there is an increasing demand for livestock products for the growing and more affluent populations of many developing countries, particularly in Asia (*3*, *4*), which offers new market opportunities for poor farmers. Animal diseases severely constrain livestock enterprises in developing countries but are not being given the attention they deserve by the global community.

The global animal health product market was worth $15 billion (U.S. dollars) in 2005, of which Western Europe, North America, East Asia, Latin America, and Eastern Europe held 97% of market, leaving ~3% to Africa and South Asia (*5*). Of this market, 40% was targeted toward companion animals, and this proportion is growing (*6*). The global veterinary pharmaceutical industry puts ~10% back annually into research and development (~$1.5 billion) (*6*). Public-sector contributions to animal health research come mainly from wealthy economies, and target principally their domestic priorities, such as bovine spongiform encephalopathies (BSEs). For BSEs, the research budget in the United Kingdom for the financial year 2005–06 was roughly $25.7 million (*7*). Compare these figures with the estimated $20 million allocated over 10 years by the Animal Health Programme of the U.K.'s Department for International Development (DFID) to research targeted at developing countries (*8*).

Animal diseases can be divided into three categories (*9*): those that (i) influence the vulnerability and assets of smallholder livestock keepers, (ii) constrain increases in productivity, and (iii) constrain market access. Reducing vulnerability and improving market access are themes that appear in frameworks developed by the DFID to evaluate strategies for poverty reduction (*10*). Diseases affecting vulnerability are those causing high levels of mortality in key livestock species important to the poor (such as the seasonal epidemics of hemorrhagic septicemia of cattle and buffalo in South Asia and the epidemic waves of Newcastle disease of poultry in Africa and Asia) and those causing illness in their owners and keepers (such as brucellosis of cattle, small ruminants, and pigs in many regions). Diseases constraining productivity include those that are more pathogenic in nonindigenous breeds of livestock that are increasingly used to improve performance [such as the tick-borne disease East Coast fever (ECF) of cattle in eastern and southern Africa]. Diseases constraining market access include those in which human disease can be caused by consumption of meat or milk products (such as cysticercosis of pigs in Africa, Asia, and Latin America) and those spread by movement of animals or livestock products, such as foot-and-mouth disease (FMD) of ruminants and pigs.

CREDIT: BRIAN PERRY

A need for sustained vaccination programs. Under the auspices of a project in Mozambique funded by the Australian Agency for International Development, a community animal health worker is seen vaccinating a village chicken against Newcastle disease. Unfortunately, the funding for that program ended in 2005.

Many developing countries are stuck in a time-warp of outdated service delivery systems that are incompatible with the needs of their poorer clients and are compromised by inadequate funding. The conditions imposed by the International Monetary Fund and World Bank two decades ago on loan agreements with borrowing nations precipitated attempts to privatize state-owned enterprises. This, in turn, resulted in dramatic cuts in social service programs, which have never recovered, particularly in parts of Africa (*11*).

What can science offer to this situation? New, more cost-effective approaches to delivery of animal health services are critical to poverty reduction processes, with greater incorporation of demand-led features that consider accessibility, acceptability, and sustainability as well (*12*). An essential component will be the growing set of participatory approaches used for disease surveillance, priority setting, and interventions (*11*–*15*), as well as the growing understanding of how innovation systems can help tools reach the poorer sectors of society (*16*). Quantitative epidemiological sciences, in combination with economics tools, can aid in prioritization and in identifying the most cost-effective intervention strategies (*17*). In addition, there are the more high-tech tools of complex systems science modeling that show considerable promise (*18*), although these are data-hungry animals in a data-barren environment.

Vaccines are critical technologies for the prevention of infectious diseases (*19*), and here science has a major role to play. Vaccines are available for some diseases, but for many they are rudimentary, inadequate, or lacking. Many animal diseases prevalent in the developing world do not occur in the developed world. Of particular importance are the tsetse-transmitted trypanosomiases and the tick-borne ECF in Africa, for which safe and effective vaccines do not exist. These are complicated infections, but because their distributions are restricted to developing countries and the risk of their spreading beyond Africa is minimal, the research investment they have attracted has been relatively small. Encouragingly, the genome for *Theileria parva*, the cause of ECF, has been sequenced (*20*), providing new tools to approach an ECF vaccine, should funding become available. But even diseases that have shown potential to spread to the developed world, such as African swine fever (ASF) and African horse sickness (AHS), have not attracted the funding they arguably deserve. There is still no safe and effective vaccine against ASF, and there is

[1]International Livestock Research Institute (ILRI), Post Office Box 30709, Nairobi 00100, Kenya. [2]Keith Sones Associates, Post Office Box 24720, Karen 00502, Nairobi, Kenya.

*Author for correspondence. E-mail: b.perry@cgiar.org

little incentive outside Africa to develop one. Should ASF reemerge in Europe, countries would likely eradicate through slaughter and compensation, a policy that is not an option in most developing countries. There is a vaccine against AHS, but it was developed 40 years ago and does not meet the demands for more effective control in rural African communities, in which equines are economically important for farm work and transportation (*21*).

Even with diseases that clearly pose a global risk, such as FMD, the investment in new vaccines has focused primarily on products that respond to the needs of the West, rather than tackling the control of the disease at its source. FMD-free countries require vaccines that induce immunity rapidly in the face of an outbreak (to minimize further spread), with the induction of a long-lasting immunity unimportant (because many vaccinated animals will subsequently be slaughtered in order to allow the rapid resumption of FMD-free meat and animal exports). Neither are FMD-free countries interested in the thermostability of the vaccine (as refrigeration facilities are ubiquitous) or even the vaccine's price (relatively speaking). In contrast, developing countries require vaccines that protect for longer (so that herd immunity can be established and maintained in the face of weak veterinary services), are less reliant on a chain of cold facilities, and are affordable.

But there is some hope. The Wellcome Trust and the European Union (EU) have recently led the funding of an initiative to focus on the research needs of endemic FMD settings (*22*). Two years ago, the Wellcome Trust launched "Animal health in the developing world," which now funds 12 projects (*23*), including one on African swine fever. Within this, there is a "Livestock for Life" scheme that supports smaller projects to strengthen links between stakeholders working in animal health. Both these initiatives contributed a total of $32 million to animal health research targeted at developing countries, which is impressive, but small when compared with the amount of money the United Kingdom is spending annually on BSE alone. In quite a different style, but with the same target audience, is the public-private partnership in the international animal health–pharmaceutical sector called GALVmed (*24*), with initial financial backing from the U.K.'s DFID. This organization was established to respond to market failures in development and delivery of animal health technologies targeted at developing countries. Although not a research organization per se, it is expected to fund adaptive research that promotes the tailoring of technologies to developing country settings.

There is growing concern in the developed world about changing disease distributions, including potential expansion of vector-borne diseases as a result of global warming (*25*–*28*). This reflects an increasing awareness of the internationality of disease spread and the responsibility for leadership by those who can afford it, exemplified by the Foresight Programme of the U.K. government (*29*), and by the European Technology Platform in Global Animal Health (*30*). The latter aims to guide research in the EU over the next 10 years and will "take into account the globalized setting in which important diseases occur," but will concentrate on animal diseases of priority to Europe.

Such initiatives will undoubtedly bring benefits to some developing countries, but they will be the result of "spill-over" effects. The focus of these initiatives is primarily on developing "new technologies for shared problems," which, if we judge by history, will still need substantial tailoring for use in developing country environments, even if affordable. It is likely that many animal diseases of high significance to the assets and vulnerability of poor rural communities, to market access, or to the aspirations for improved productivity will not qualify for such global attention, given the low direct risk they pose to the developed world.

The capacity to develop and refine vaccines and other tools in research institutes of developing countries must be enhanced. One encouraging initiative is the creation of Biosciences for East and Central Africa (BecA) with funding from Canada (*31*). BecA has a hub located on the campus of the International Livestock Research Institute (ILRI) in Nairobi, Kenya, that will provide a biosciences research platform, research-related services, and capacity building. A great idea— but current funding is for infrastructure development, meaning that much work is yet to be done to secure operational resources and to build effective research partnerships. Another promising model is the South African Chairs Initiative (SARChI) of the South African National Research Foundation, designed to help reverse the systemic decline in research outputs and capacity at national science councils and research institutions (*32*). SARChI aims to create 210 new research chairs in South Africa by 2010.

Despite some encouraging new initiatives, we conclude that sectors of the affluent world are still basing their science contributions to poverty reduction on self-interest, relying on the spillovers from investments designed primarily to protect themselves. At the moment, only the crumbs go to the poor.

References and Notes

1. Livestock in Development, *Livestock in Poverty-Focused Development* (Livestock in Development, Crewkerne, UK, 1999), 95 pp.
2. P. K. Thornton *et al.*, Mapping *Poverty and Livestock in the Developing World* (ILRI), Nairobi, Kenya, 2002.
3. C. Delgado, *J. Nutr.* **133** (suppl. 2, Animal Source Foods), 3907 (2003).
4. A. Gulati, N. Minot, C. Delgado, S. Bora, paper presented at the symposium "Towards high-value agriculture and vertical coordination: Implications for agri-business and smallholders," New Delhi, India, 7 March 2005 (National Agricultural Science Center, Pusa, New Delhi, India, 2005).
5. *The Animal Health Industry 2005, Annual Report of the International Federation for Animal Health (IFAH)* (Wood Mackenzie, Ltd., London 2005), www.ifahsec.org/annual_report/RA_IFAH_2005_global%20final.pdf.
6. Peter Jones, IFAH, personal communication.
7. U.K. Department for Environment, Food, and Rural Affairs; www.defra.gov.uk/animalh/bse/science-research/research-quanda.html.
8. Department for International Development (DFID), Animal Health Programme; www.dfid-ahp.org.uk/downloads/Annual_Report_2005-06.pdf.
9. B. D. Perry, T. F. Randolph, J. J. McDermott, K. R. Sones, P. K. Thornton, *Investing in Animal Health Research to Alleviate Poverty* (ILRI, Nairobi, Kenya, 2002), 140 pp. plus CD-ROM.
10. DFID, "How to accelerate pro-poor growth: A basic framework for policy analysis" (DFID Pro-Poor Growth Briefing Note 2, DFID, London, 2004), 6 pp.
11. Animal Production and Health Programme, U.N. Food and Agriculture Organization (FAO), Rome, Italy; www.fao.org/AG/againfo/resources/en/publications/agapubs/Saps3_e.pdf.
12. A. McLeod, A. J. Wilsmore, in (*8*), Appendix 11.
13. J. Mariner, P. Roeder, *Vet. Rec.* **152**, 641 (2003).
14. A. Catley, *Prev. Vet. Med.* **65**, 17 (2004).
15. J. Weaver, "Participatory disease surveillance and response in Indonesia" (FAO, U.N. Development Group, Geneva, 2006); www.undg.org.
16. A. J. Hall, V. R. Sulaiman, N. G. Clark, M. V. K. Sivamohan, B. Yoganand, in *Agricultural Research Policy in an Era of Privatization: Experiences from the Developing World*, D. Byerlee and R. G. Echeverria (Eds.) (CABI, Wallingford, 2002), pp. 155–176.
17. S. Eubank *et al.*, *Nature* **429**, 180 (2004).
18. B. D. Perry, J. J. McDermott, T. F. Randolph, *Prev. Vet. Med.* **48**, 231 (2001).
19. R. M. Anderson, R. M. May, *Infectious Diseases of Humans* (Oxford Scientific Press, Oxford, 1991), 757 pp.
20. M. J. Gardner *et al.* *Science* **309**, 134 (2005).
21. "Impact of African horse sickness in South Africa," report of a stakeholder workshop to plan an impact assessment study, University of Pretoria, South Africa, 27 September 2006 (Equine Research Centre, Faculty of Veterinary Science, University of Pretoria, 2006), 25 pp.
22. Global roadmap for improved control of FMD in endemic settings, http://endemicfmdroadmap.net.
23. Wellcome Trust Funding Initiative; www.wellcome.ac.uk/node2144.html.
24. Global Alliance for Livestock Vaccines, Edinburgh, UK; www.galvmed.org.
25. D. J. Rogers, S. E. Randolph, *Science* **289**, 1763 (2000).
26. C. D. Harvell *et al.*, *Science* **296**, 2158 (2002).
27. M. Baylis, A. K. Githeko, "The effects of climate change on infectious diseases of animals" (U.K. Foresight Programme, London, 2006), 35 pp.; www.foresight.gov.uk.
28. C. Calvete *et al.*, *Vet. Rec.* **158**, 130 (2006).
29. *Infectious diseases: Preparing for the future, Final reports, P1: Action Plan* (U.K. Foresight Programme, London, 2006); www.foresight.gov.uk/Previous_Projects/Detection_and_Identification_of_Infectious_Diseases/Index.htm.
30. A European technology platform for global animal health; www.ifahsec.org/europe/EUPlatform/Platform.htm.
31. Biosciences Africa; www.biosciencesafrica.org.
32. South African Research Chairs Initiative of the S. A. National Science Foundation; www.nrf.ac.za/sarchi.

10.1126/science.1138614

IMMUNOLOGY

Antibodies Get a Break

The process by which a lymphocyte specifies antibody production may have evolved by exploiting existing cellular DNA repairing mechanisms.

Jayanta Chaudhuri and Maria Jasin

Antibodies [or immunoglobulins (Igs)] are produced by B lymphocytes of our immune system against almost any foreign substance. Antigenic substances are captured by a variable region at the amino terminus of an antibody but trigger different responses depending on which of the invariant (constant) regions are present at the antibody's carboxyl terminus. The IgM isotype is the first antibody made in an immune response, but upon encountering antigen, mature IgM-producing B cells switch to express secondary isotypes (IgG, IgE, or IgA) with different effector functions. This switch in antibody class requires recombination of specific DNA segments in the Ig locus called switch (S) regions, but many aspects of the mechanisms of DNA breakage and joining are unclear. On page 377 of this issue, Zarrin *et al.* (*1*) challenge the notion that S regions and a specific DNA deaminating enzyme have roles in class switch recombination beyond the initial introduction of DNA breaks, and argue that once DNA breaks are formed, they are processed by the cell's general DNA repair pathways that promote joining of widely separated DNA breaks within a chromosome.

The production of antibodies initially encompasses the Cμ constant region to generate IgM. B cells switch Cμ for one of the downstream constant regions (Cγ, Cα, or Cε), to express IgG, IgA, or IgE, respectively. This class switch recombination occurs within the intronic S regions, which in the mouse range from ~1 to 12 kb in length and can be as far apart as 200 kb. A major breakthrough in understanding the mechanism of class switch recombination came about with the discovery of the role of activation-induced cytidine deaminase (AID) (*2*). This enzyme targets deoxycytidines in S regions, leading to an as yet unclear mechanism of DNA breakage and repair to join Sμ to one of six downstream S regions (see the figure) (*3*). Through a series of elegant in vivo genetic manipulations in the mouse, Zarrin *et al.* (*1*) show that the requirement for both S regions and AID can be circumvented by artificially generating double-strand DNA breaks upstream of the switching

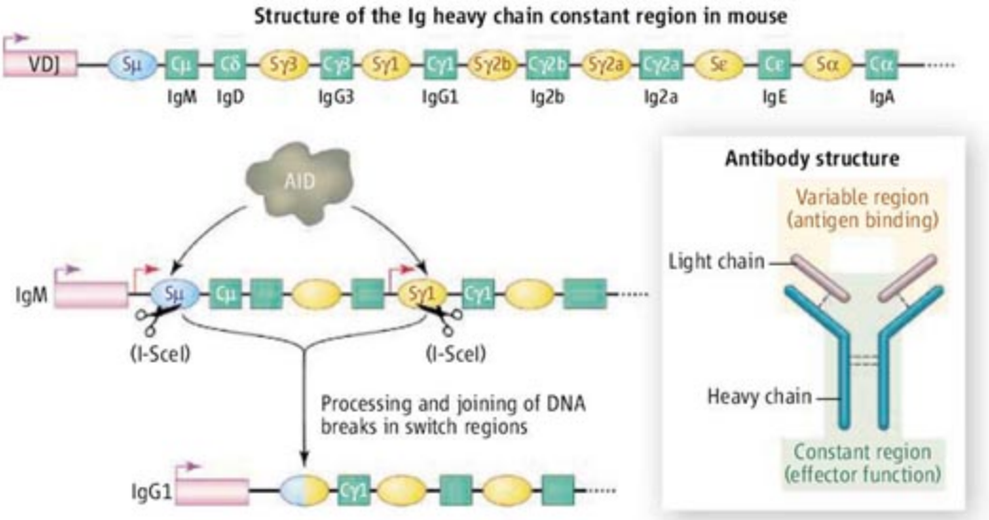

Switching class. (**Top**) Mouse immunoglobulin heavy chain (IgH) locus before class switch recombination. (**Bottom**) Activation-induced deaminase (AID) targets deoxycytidines within the transcribed S regions (red arrows at Sμ and Sγ1). The deaminations lead to the generation of double-strand breaks in DNA (scissors). The breaks are processed and joined, leading to a switch in antibody production, from IgM to IgG1. If S regions are replaced by endonuclease cleavage sites (I-SceI), the requirement for AID in antibody class switching is bypassed when the endonuclease is expressed.

constant regions. These results provide strong evidence that S regions have evolved to provide substrates for deaminase activity en route to generating double-stranded DNA breaks. The study also challenges the notion that AID and S regions have roles in class switch recombination downstream of DNA break formation (*4*, *5*).

Since the discovery of DNA recombination as the basis for Ig isotype switching (*6*), our understanding of the mechanism of class switch recombination has been constantly evolving. It is now generally accepted that transcription through S regions generates structures in which the template DNA strand is stably associated with nascent RNA while the nontemplate DNA strand, which is rich with deoxyguanosine (dG), is "looped out." AID acts primarily on the nontemplate DNA strand, altering dC to dU. The mismatch between the generated dU and dG on the template DNA strand is then processed by components of the cell's base excision and DNA mismatch repair pathways to generate double-strand DNA breaks in the S regions (*7*). Double-strand breaks between the two S regions are brought together, or synapsed, and then ligated, possibly by components of the cellular machinery that joins the ends of nonhomologous DNA (*3*). During this joining process, S regions can also undergo intra–S region deletions, probably reflecting AID activity on an S region that is not synapsed with another S region. Several proteins of the double-strand break response pathway have been implicated in Ig class switch recombination, including the phosphorylated histone H2AX (γH2AX), ataxia telangiectasia mutated (ATM), and 53BP1 (*8*). Deficiencies in these proteins impair class switch recombination without affecting intra-S deletions, suggesting that the recombination defect might be due to a defect in synapsis. Notably, specific mutations in AID severely impair class switch recombination without altering intra-S deletions, indicating that AID itself might participate in synapsis (*4*).

To address the potential roles of AID and S regions in synapsis, Zarrin *et al.* took advantage of the yeast endonuclease I-SceI (*9*), which has no known cleavage sites in the mouse genome and which has been widely used to study double-strand break repair in mammalian cells (*10*). Manipulations in the S regions were done in mouse embryonic stem cells that contain two distinguishable immunoglobulin heavy chain (IgH) alleles (a cell has two alleles for each gene, one from each parent), IgH^a and IgH^b. All mutations in

J. Chaudhuri is in the Immunology Program and M. Jasin is in the Developmental Biology Program, Memorial Sloan-Kettering Cancer Center, New York, NY 10021, USA. E-mail: chaudhuj@mskcc.org, m-jasin@ski.mskcc.org

the S regions were incorporated into the IgH^a allele. This allowed assessment of class switching of the mutated IgH^a allele relative to that of the wild-type IgH^b allele after the generation of mature B cells. Zarrin *et al.* generated mutations in which one (Sγ1) or both (Sμ and Sγ1) S regions were each replaced by two nearby I-SceI endonuclease cleavage sites. When mouse splenic B cells or B cell hybridomas (B cells engineered to grow indefinitely) expressed the I-SceI endonuclease, IgG1^a production was observed at ~10 to 20% the level observed in cells with wild-type S regions. Because B cell hybridomas do not express detectable AID, Zarrin *et al.* could bypass the requirement for both the deaminase and S regions by artificially generating DNA double-strand breaks.

Two other notable results were obtained. Although deletions between two nearby I-SceI cleavage sites—reminiscent of intra–S region recombination—occurred more frequently than class switching involving distant cleavage sites, the frequency of these short-range deletions (up to ~0.5 kb) was only ~10 times that of the long-range deletions (~100 kb) that occurred during class switching. Moreover, S-region transcription could be dispensed with.

These striking results raise several interesting questions about the role of both S regions and AID in class switch recombination. The frequency of class switching in the Zarrin *et al.* system is much higher than has been seen for joining two double-strand DNA breaks on heterologous chromosomes (*11*). Does some unknown component of the IgH locus provide sites for synapsis that promote DNA joining during recombination, or is the joining of two distant breaks on a single chromosome more frequent than might have been expected? If the latter, perhaps joining is promoted by components of the double-strand break response pathway such as 53BP1 and γH2AX, which may spread a megabase from the break sites (*12*). Although the requirement for S-region transcription is bypassed in the system used by Zarrin *et al.* (at least at Sγ1), is class switching still dependent on activation of other B cell–specific elements involved in gene expression?

B cells orchestrate a complex series of events for class switch recombination, rather than simply providing site-specific endonucleases (like I-SceI) to cleave DNA that lies upstream of constant regions. It may be that involving a specific deaminase and controlling its access to DNA by transcription provide the necessary level of regulation for choosing which of six downstream possible S regions to use. Moreover, cleavage by the yeast endonuclease did not result in normal levels of class switching. Perhaps the multiple DNA lesions throughout the long S regions provide the necessary amount of damage to promote normal levels of class switch recombination. Finally, it may be that AID and/or S regions do have a role in synapsis in the context of normal class switch recombination, and that in the absence of these agents, a high proportion of double-strand breaks are channeled into DNA translocations. The approach designed by Zarrin *et al.* will now allow these questions to be addressed.

References

1. A. A. Zarrin *et al.*, *Science* **315**, 377 (2007); published online 14 December 2006 (10.1126/science.1136386).
2. M. Muramatsu *et al.*, *Cell* **102**, 553 (2000).
3. J. Chaudhuri, F. W. Alt, *Nat. Rev. Immunol.* **4**, 541 (2004).
4. V. Barreto, B. Reina-San-Martin, A. R. Ramiro, K. M. McBride, M. C. Nussenzweig, *Mol. Cell* **12**, 501 (2003).
5. E. D. Larson, M. L. Duquette, W. J. Cummings, R. J. Streiff, N. Maizels, *Curr. Biol.* **15**, 470 (2005).
6. T. Honjo, T. Kataoka, *Proc. Natl. Acad. Sci. U.S.A.* **75**, 2140 (1978).
7. S. K. Petersen-Mahrt, R. S. Harris, M. S. Neuberger, *Nature* **418**, 99 (2002).
8. S. Franco, F. W. Alt, J. P. Manis, *DNA Repair (Amst)* **5**, 1030 (2006).
9. L. Colleaux, L. D'Auriol, F. Galibert, B. Dujon, *Proc. Natl. Acad. Sci. U.S.A.* **85**, 6022 (1988).
10. P. Rouet, F. Smih, M. Jasin, *Proc. Natl. Acad. Sci. U.S.A.* **91**, 6064 (1994).
11. D. M. Weinstock, B. Elliott, M. Jasin, *Blood* **107**, 777 (2006).
12. E. P. Rogakou, C. Boon, C. Redon, W. M. Bonner, *J. Cell Biol.* **146**, 905 (1999).

Published online 14 December 2006;
10.1126/science.1138091
Include this information when citing this paper.

NEUROSCIENCE

Is More Neurogenesis Always Better?

The clinical relevance of increasing neurogenesis in the adult mammalian brain is being questioned as increasing the number of new neurons has positive effects on some brain functions but not others.

Helen E. Scharfman and Rene Hen

For decades, it was believed that the adult mammalian brain could not generate new neurons, but during the 1990s, that concept changed. Evidence of the birth of new neurons in adult mammals, including humans, raised expectations for improved treatment for patients with central nervous system injury or illness. But this enthusiasm has been tempered since then, as more recent studies indicate that excess adult neurogenesis can be as detrimental as a deficit. In some cases, the clinical relevance of increasing neurogenesis may need to be reconsidered.

Neurogenesis in the normal adult mammalian brain is primarily limited to three areas: the subventricular zone, hippocampal dentate gyrus, and olfactory bulb (*1*). The identification that this is true in humans, at least in the hippocampus (*2*), together with the findings that neurogenesis can be increased in laboratory animals by learning, exercise, and antidepressants and decreased by stress and aging (*1*), reinforced the expectation that neurogenesis might be clinically beneficial. Moreover, additional sites in the adult brain—the cortex and hypothalamus—demonstrate ongoing neurogenesis (*3*, *4*), although this remains controversial (*5*). However, we now know that neurogenesis in the adult brain occurs at a very low rate after maturity, and many of the new neurons do not survive for long (*6*). Thus, new neurons born in the adult brain may support plasticity on an acute time scale because of their increased excitability (*7*) but have limited long-term restorative ability. Such transient existence of new neurons should not necessarily dampen therapeutic potential. Survival of new neurons increases with benign interventions such as learning and enriching the environment (*1*). Dormant stem cells may also exist throughout the brain (*8*). These cells could potentially be stimulated to mature in pathological situations or

H. E. Scharfman is in the Departments of Pharmacology and Neurology, Columbia University, and Center for Neural Recovery and Rehabilitation Research, Helen Hayes Hospital, West Haverstraw, NY 10993–1195, USA. R. Hen is in the Departments of Pharmacology and Psychiatry and the Center for Neurobiology and Behavior, Columbia University, New York, NY 10032, USA. E-mail: scharfmanh@helenhayeshosp.org

after pharmacological interventions. Indeed, a possible reason for the beneficial effects of rehabilitation or psychotherapy may be that treatment increases survival of new neurons.

But an increase in neurogenesis may not always result in improved function. Recent studies show surprising limitations in the ways new neurons in the adult brain can improve function. For example, dentate gyrus neurogenesis influences some hippocampal-dependent behaviors in laboratory animals, but not others. Specifically, there are positive effects on trace and contextual fear conditioning, but not on spatial learning (*9*–*11*). Animals without new neurons also perform better in certain working memory paradigms (*12*). Specifically, mice that are devoid of neurogenesis due to irradiation or genetic ablation display improved memory in a radial maze, but only when repetitive information is presented. Therefore, manipulations that increase neurogenesis may have positive effects on some behaviors but negative effects on others. In addition, improved function may not always be caused by increased neurogenesis. For example, some of the behavioral effects of enriched environment and antidepressants are independent of their influence on hippocampal neurogenesis (*13*). So despite increasing experimental support for an influence of neurogenesis on specific behaviors, it is not yet clear how these effects may translate into clinical benefits.

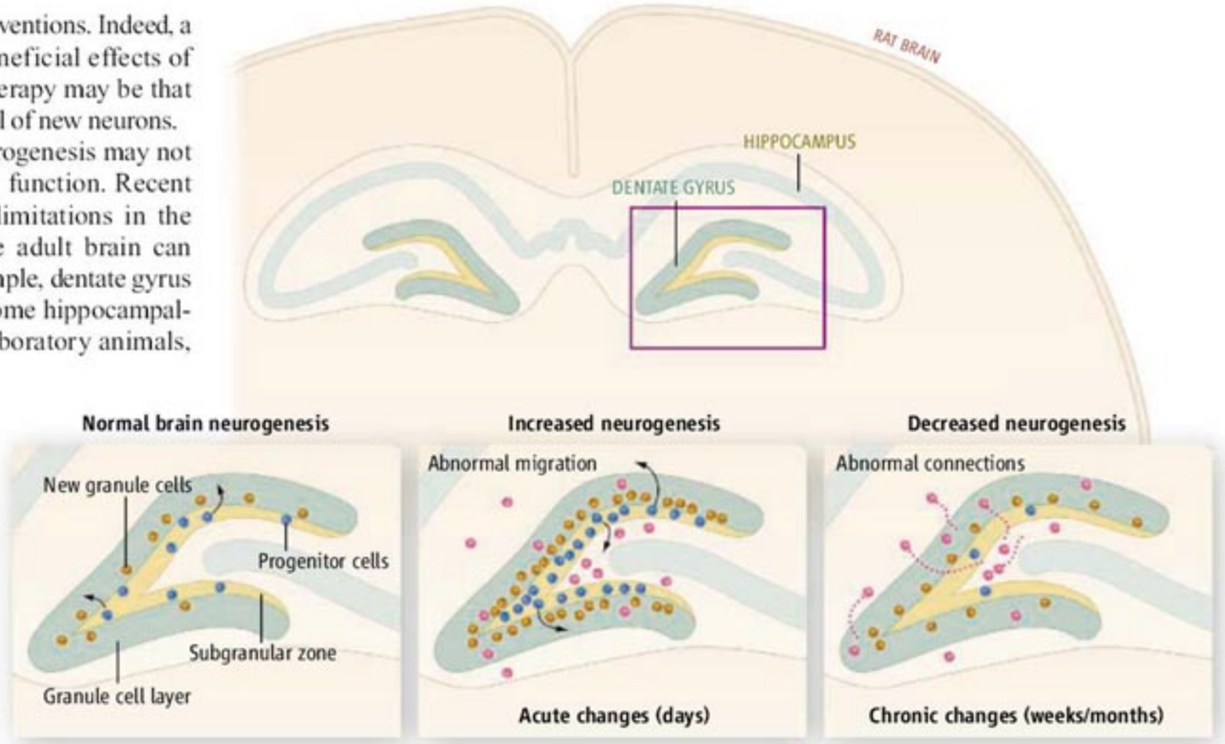

Adult hippocampal neurogenesis. Acute and chronic changes in rat brain neurogenesis after severe seizures parallel changes observed in temporal lobe epilepsy. (**Left**) Most progenitor cells typically become granule cells that migrate to the granule cell layer. (**Center**) Seizures rapidly and transiently increase the rate of neurogenesis and expression of growth factors that influence neurogenesis. (**Right**) Ectopic migration of new neurons may result in abnormal neuronal connections. Neurogenesis in laboratory animals and humans may decline at later times, but some of the neurons that were born in the acute period persist. Reduced neurogenesis and growth factor levels, together with abnormal new circuitry, may contribute to the chronic condition.

Neurogenesis under pathological conditions also indicates limits to the utility of new neurons in improving brain function. A common theme is that neurogenesis increases after injury to the central nervous system (*14*). This could be considered restorative, and findings such as the migration of new neurons to the site of damage, at least in animal models of stroke (*15*, *16*), support this view. Because pathological conditions also increase the production of factors that promote neurogenesis (brain-derived neurotrophic factor, vascular endothelial growth factor, insulin-like growth factor, fibroblast growth factor 2, and neuropeptide Y), there may be a rapid response of the brain to damage that reflects a recapitulation of developmental programs. However, the acute increase in neurogenesis and associated growth-related changes are often transient, limiting their influence. Indeed, after an acute increase in neurogenesis, there may be a protracted decline in the rate of neurogenesis (see the figure), and this could contribute to what is often an intractable clinical condition.

Drugs that increase hippocampal neurogenesis
Antidepressants (*19*, *20*, *22*)
Tricyclic antidepressants
Selective serotonin reuptake inhibitors
Mood stabilizers (*22*)
Lithium
Valproic acid
Cognitive enhancers (*23*)
Galantamine
Memantine
Anesthetics (*24*)
Ketamine
Steroids (*1*, *22*)
Estradiol
Dehydroepiandrosterone
Other (*22*)
Rolipram
Statins
Sildenafil (Viagra)

Increasing neurogenesis may not always be beneficial in the context of pathology. New neurons may not develop, migrate, or integrate correctly, as in animal models of temporal lobe epilepsy. In such models, severe prolonged seizures (status epilepticus) are followed not only by robust increases in numbers of new granule neurons in the dentate gyrus, but also by inappropriate migration, differentiation, and integration of many of these new neurons (see the figure) (*17*). This may contribute to persistent seizures in animals, and a similar process may occur in some patients with intractable temporal lobe epilepsy (*18*).

Some commonly prescribed drugs have robust effects on neurogenesis. These include antidepressants and mood stabilizers (see the Table). Indeed, some of these treatments may ameliorate symptoms because of their effects on neurogenesis, as suggested by studies in animal models (*19*, *20*). Specifically, the behavioral effects of selective serotonin reuptake inhibitors and tricyclic antidepressants were blocked in two rodent models of anxiety/depression by radiological and genetic ablation of neurogenesis in the dentate gyrus (*19*). How do changes in hippocampal function, presumably caused by neurogenesis, affect mood or anxiety? Although the answer to this question is not clear, ablation of the ventral hippocampus can alter mood, presumably because of its connectivity with limbic structures such as the amygdala, the prefrontal cortex, and the nucleus accumbens (*21*).

Although neurogenesis occurs throughout life, its clinical potential remains unclear in

some cases. While there is some evidence that strategies to increase neurogenesis may lead to the development of new therapeutics such as antidepressants, decreasing neurogenesis may be beneficial in other cases, such as epilepsy.

References and Notes

1. G. Kempermann, *Adult Neurogenesis: Stem Cells and Neuronal Development in the Adult Brain* (Oxford Univ. Press, New York, 2006).
2. P. S. Eriksson *et al.*, *Nat. Med.* **4**, 1313 (1998).
3. M. V. Kokoeva, H. Yin, J. S. Flier, *Science* **310**, 679 (2005).
4. A. G. Dayer, K. M. Cleaver, T. Abouantoun, H. A. Cameron, *J. Cell. Biol.* **168**, 415 (2005).
5. P. Rakic, *Nat. Rev. Neurosci.* **3**, 65 (2002).
6. A. G. Dayer, A. A. Ford, K. M. Cleaver, M. Yassaee, H. A. Cameron, *J. Comp. Neurol.* **460**, 563 (2003).
7. F. Doetsch, R. Hen, *Curr. Opin. Neurobiol.* **15**, 121 (2005).
8. M. Zhao *et al.*, *Proc. Natl. Acad. Sci. U.S.A.* **100**, 7925 (2003).
9. M. D. Saxe *et al.*, *Proc. Natl. Acad. Sci. U.S.A.* **103**, 17501 (2006).
10. T. J. Shors, D. A. Townsend, M. Zhao, Y. Kozorovitskiy, E. Gould, *Hippocampus* **12**, 578 (2002).
11. G. Winocur, J. M. Wojtowicz, M. Sekeres, J. S. Snyder, S. Wang, *Hippocampus* **16**, 296 (2006).
12. M. Saxe *et al.*, *Society for Neuroscience 2006, Online*, Program No. 266.6, 14 to 18 October 2006, Atlanta.
13. D. Meshi *et al.*, *Nat. Neurosci.* **9**, 729 (2006).
14. H. G. Kuhn, T. D. Palmer, E. Fuchs. *Eur. Arch. Psychiatry Clin. Neurosci.* **251**, 152 (2001).
15. A. Arvidsson, T. Collin, D. Kirik, Z. Kokaia, O. Lindvall, *Nat. Med.* **8**, 963 (2002).
16. J. M. Parent, Z. S. Vexler, C. Gong, N. Derugin, D. M. Ferriero, *Ann. Neurol.* **52**, 802 (2002).
17. H. E. Scharfman, *Adv. Med. Exp. Biol.* **548**, 192 (2004).
18. J. M. Parent, R. C. Elliott, S. J. Pleasure, N. M. Barbaro, D. H. Lowenstein, *Ann. Neurol.* **59**, 81 (2006).
19. L. Santarelli *et al.*, *Science* **301**, 805 (2003).
20. J. E. Malberg, A. J. Eisch, E. J. Nestler, R. S. Duman, *J. Neurosci.* **20**, 9104 (2000).
21. D. M. Bannerman *et al.*, *Neurosci. Biobehav. Rev.* **28**, 273 (2004).
22. F. M. Longo, T. Yang, Y. Xie, S. M. Massa, *Curr. Alzheimer Res.* **3**, 5 (2006).
23. K. Jin, L. Xie, X. O. Mao, D. A. Greenberg, *Brain Res.* **1085**, 183 (2006).
24. G. Keilhoff, H. G. Bernstein, A. Becker, G. Grecksch, G. Wolf, *Biol. Psychiatry* **56**, 317 (2004).

25. Supported by the National Institute of Neurological Disorders and Stroke, the National Institute of Mental Health, and the National Alliance for Research on Schizophrenia and Depression.

10.1126/science.1138711

GEOCHEMISTRY

Fuel for Plate Tectonics

Nathalie Bolfan-Casanova

Water storage in Earth's mantle causes seismic waves to slow down when passing through Earth's interior.

Our understanding of plate tectonics relies on the concept of relatively rigid rocky plates moving on a more ductile shallow mantle called the asthenosphere (*1*). The word asthenosphere comes from the Greek "a-sthenos" meaning "without strength." This lack of strength especially affects seismic waves, which slow down when entering the asthenosphere (see the figure). For decades, Earth scientists have tried to understand the reason for this seismic wave deceleration. On page 364 of this issue, Mierdel *et al.* (*2*) report new experimental findings on the maximum amount of water that can be stored by the shallow mantle. These results may solve a number of riddles, including the cause of the seismic slowdown.

Why is water important? Water not only is essential to life but also controls the dynamics of Earth's interior (*3*). Since the 1990s, geologists have recognized with increasing certainty that mantle minerals can hold substantial amounts of water. This implies that the oceans may no longer be the main water reservoir of Earth. But water does not necessarily have to be fluid to be stored in the deep Earth. Rather, it dissolves as hydroxyl (OH^-) in anhydrous minerals (such as olivine, pyroxenes, garnet, and their high-pressure forms) as a result of the association of a proton (H^+) with oxygen of the mineral lattice. This creates a defect in the lattice and thereby speeds up the kinetics of physical properties that depend on the concentration of defects. Even at very low concentrations—lower than 1% by weight—the presence of water has many consequences for mantle properties such as creep and electrical conductivity (*4*, *5*). When present in minerals as a defect, water will enhance the deformation of rocks and make them more ductile. Dissolved as H^+ in minerals, water will also increase the electrical conductivity of the mantle by adding mobile charges. Water also lowers the melting point of mantle rocks and allows melting at greater depths than in the absence of water.

To understand how water affects mantle properties, we need to know how much water can be stored in mantle minerals and how this storage capacity varies with increasing depth. Researchers have firmly established that the solubility of water in minerals increases with pressure and water partial pressure (*6*). The water storage capacity of Earth's upper mantle (extending from the base of the crust down to the transition zone at 410 km depth) was thought to increase monotonically with depth. Moreover, in a mantle consisting of 60% by volume of olivine, this mineral was believed to be the one that dictates the water budget.

The results of Mierdel *et al.* completely change the picture: Water storage capacity in Earth's shallow mantle is controlled by orthopyroxene, a less abundant phase than olivine, because water solubility in this phase is more than two orders of magnitude higher than in olivine. The reason for this is composition. The enhanced affinity of pyroxenes for water is indeed aided by aluminum through the coupled substitution of $2Al^{3+} + 2H^+$ for $2Mg^{2+} + Si^{4+}$, which is a very efficient way to store up to 1 weight % water in $MgSiO_3$ orthopyroxene.

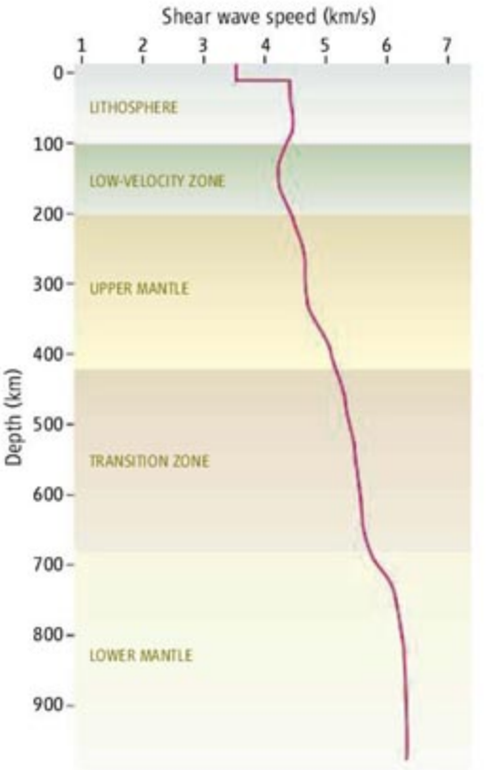

Seismic speed bumps. Schematic shear wave speed profile across Earth's mantle.

Mierdel *et al.* also show that the curve of water saturation versus depth has a pronounced minimum between 100 and 200 km. Indeed, the water storage capacity of pyroxene with substituted aluminum is dependent on the acceptance of the large aluminum cation into the small tetrahedral site of silicon, the

The author is at Laboratoire Magmas et Volcans, Université Blaise Pascal, 63038 Clermont-Ferrand, France. E-mail: n.bolfan@opgc.univ-bpclermont.fr

size of which diminishes as a function of increasing pressure because of atomic compaction. This leads to the drastic change of water solubility in pyroxene at pressures between 3 and 5 GPa, corresponding to depths of 100 to 175 km. Depending on the tectonic environment and the temperature, the minimum in solubility is shallow in the case of the oceanic mantle but deepens in the case of the colder continental mantle.

Still, what are the physical and chemical changes that create the deceleration of seismic waves and the mechanical distinction between brittle lithosphere and ductile asthenosphere? Early models have invoked the presence of molten silicate to explain the reduced shear-wave velocity because these waves do not travel through liquids (*1*). This explanation was abandoned for two reasons: (i) To have an effect on wave propagation, the melt should form films lapping the boundaries between the solid grains, which is not the case; and (ii) the presence of excessive amounts of melts is required to effectively reduce the viscosity of the asthenosphere. The most accepted explanation of mineral physicists has thus been that the asthenosphere is weak because it is hydrous and not because it is partially molten. Because the melt has an affinity for water that is 1000 times that of the minerals, melting does not occur in the asthenosphere as it would dehydrate the mantle (*7*, *8*).

The consequence of this drying out would be that minerals become stiffer and deform less in response to convective flow. Such a model implies that the lithosphere-asthenosphere boundary limits the storage capacity of the mantle; this model would be in agreement with the interpretation of the electrical conductivity of the mantle. The oceanic mantle where the asthenosphere is shallower is more conductive than the adjacent continental lithosphere, which is deeper and less conductive (*9*).

Mierdel *et al.* conclude that melting must occur in the asthenosphere because their minimum in water storage capacity coincides with the depth of the low-velocity zone. This is an additional argument to constrain the water content in Earth's mantle, and yields a minimum of 0.07% weight occurring around 100 km in the oceanic mantle. These conclusions agree with recent observations of the melting depth of a hydrous mantle (*10*) and further imply that melting starts deeper, in the garnet stability field. Thus, these findings show how mantle properties such as viscosity, melting, and differentiation are tied to its water storage capacity.

References

1. D. L. Anderson, *Theory of the Earth* (Blackwell Scientific, Boston, 1989).
2. K. Mierdel, H. Keppler, J. R. Smyth, F. Langenhorst, *Science* **315**, 364 (2007).
3. N. Bolfan-Casanova, *Mineral. Mag.* **69**, 229 (2005).
4. D. L. Kohlstedt *et al.*, in *Physics and Chemistry of Partially Molten Rocks*, N. Bagdassarov, D. Laporte, A. B. Thompson, Eds. (Kluwer Academic, Dordrecht, Netherlands, 2000).
5. D. Wang *et al.*, *Nature* **443**, 977 (2006).
6. Q. Bai, D. L. Kohlstedt, *Nature* **357**, 672 (1992).
7. G. Hirth, D. L. Kohlstedt, *Earth Planet Sci. Lett.* **144**, 93 (1996).
8. S. Karato, H. Jung, *Earth Planet Sci. Lett.* **157**, 193 (1998).
9. G. Hirth, R. L. Evans, A. D. Chave, *Geochem. Geophys. Geosyst.* **8**, 2000GC0000048 (2000).
10. C. Aubaud, E. Hauri, M. Hirschmann, *Geophys. Res. Lett.* **31**, 10.1029/2004GL021341 (2004).

10.1126/science.1137738

NEUROSCIENCE

A Push-Me Pull-You Neural Design

How do spinal neurons control patterned motor output? A balance in simultaneous excitation and inhibition of neuronal circuits produces rhythmic activity that drives motor behavior.

William B. Kristan

Networks of neurons producing behavioral outputs can be both excitatory and inhibitory—that is, they can activate or block the activity of their target neurons. The important interplay between these two opposing effects in the mammalian central nervous system has been recognized for at least 100 years, ever since Nobel laureate Sir Charles Sherrington investigated leg reflexes controlled by spinal cord motor neurons in cats (*1*). We now know that there is continual, intermixed chattering of inhibition and excitation in many parts of the mammalian brain, including the cerebral cortex (*2*, *3*), that maintains a balance between responsiveness and stability (*4*–*6*). On page 390 of this issue (*7*), Berg *et al.* show the very surprising result that the rhythmic input onto motor neurons during scratching behavior in turtles excites and inhibits networks of motor neurons not alternately, as expected, but in phase. This synchronization of simultaneous excitation and inhibition—pushing and pulling at the same time—appears to be counterproductive and wasteful. What possible function might it serve? To understand the possible importance requires a brief excursion into some other functions of neural inhibition.

Sir John Eccles and colleagues recorded the first inhibitory synaptic potential, in a cat spinal motor neuron, in 1952 (*8*). Since then, inhibition—a block to signal transmission through a neuron—has been found all over the central nervous system. For example, stimulating input from neurons to the mammalian cortex produces an initial direct excitation of target neurons followed quickly by strong indirect inhibition (*9*). The auditory systems of many animals have taken advantage of the relative timing difference of the excitation and inhibition elicited by neural signaling pathways from the two ears to determine the location of sound in space (*10*).

In a different network arrangement, a single source of neuronal activity can excite one population of neurons and inhibit another (see the figure) to activate one behavior and turn off others. The nature of the connection pattern found in the turtle scratching reflex circuit, which Berg *et al.* investigated, differs from this behavioral choice connectivity pattern in that the excitation and inhibition onto a neuronal target overlap completely in both space and time (see the figure). In this configuration, the target neuronal network is effectively a comparator: It is active only when the input carried by the excitatory pathway is greater than that from the inhibitory one, and the magnitude, and even the qualitative nature, of its response will vary with the magnitude of the difference.

Berg *et al.* show that the input onto turtle motor neurons during the scratching reflex is oscillatory (from an input neural network that is a central pattern generator for scratching), with excitation being somewhat stronger than inhibition. In this mode, the target spinal motor neurons produce bursts of impulses (spikes) in phase with the synchronous excitatory and inhibitory bursts. At first glance, there would be no practical merit to having nearly equal input from excitatory and inhibitory inputs. The resultant activity of the target neuronal network would be the same if its total input were entirely from a much weaker excitatory input (see the figure). A little reflection shows that this is not accurate.

The author is in the Neurobiology Section, Division of Biological Sciences, University of California, San Diego, La Jolla, CA 92093–0357, USA. E-mail: wkristan@ucsd.edu

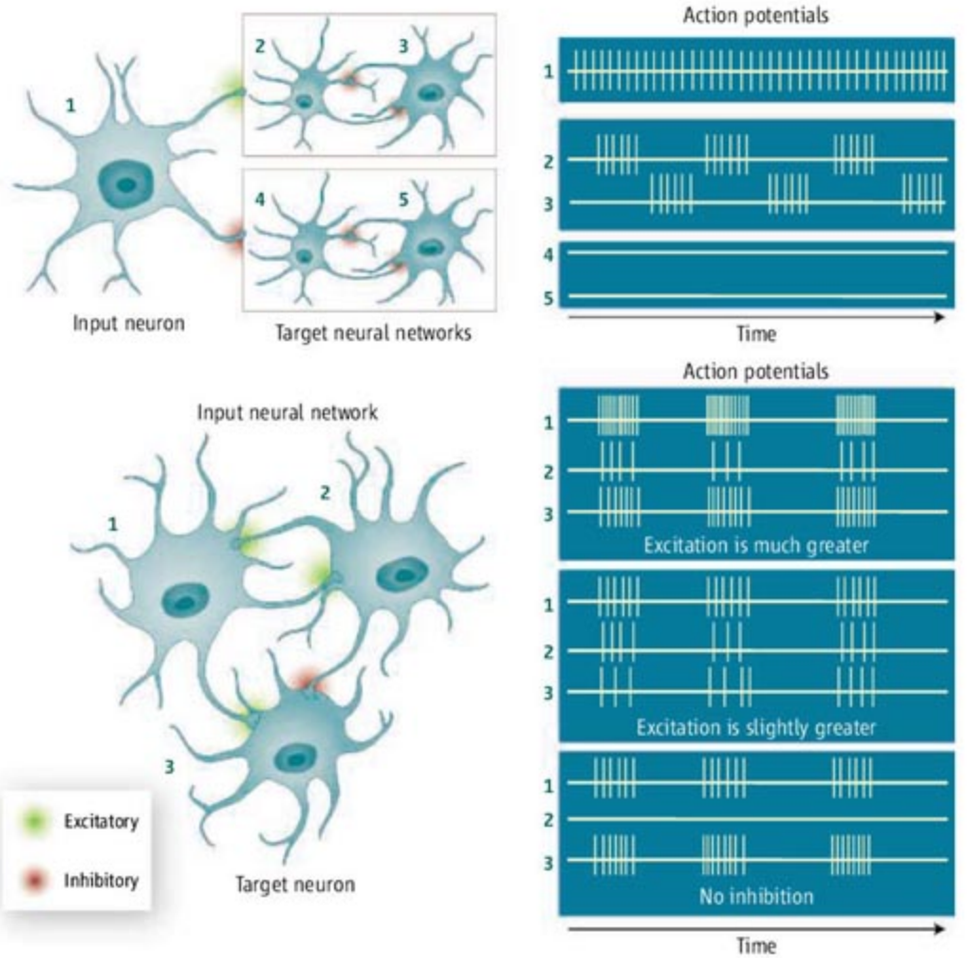

Neural circuit designs. In simulated recordings of neuron activity, time runs left to right and the vertical blips represent action potentials (spikes) within the bursts of activity in the individual neurons. (**Top**) If a single input excites one neural network and inhibits another, it can turn one target network (pattern generator) on, resulting in alternate bursts of activity, and turn the other off. (**Bottom**) If there is excitatory and inhibitory input from a rhythmic pattern-generating circuit (shown is a circuit of two neurons) onto a single target neuron, such as a motor neuron, the magnitude of the target's response depends on the relative strengths of the inputs. When excitation is much stronger than inhibition, the same input from the neural circuit produces more spikes per burst. When the excitation is slightly stronger, the target's response is diminished. When there is no inhibition at all, the target's response increases—the same amount of excitatory input can produce a large output in the target neuron.

Both signaling pathways increase the target neuron's electrical conductance (i.e., it becomes leakier to electric current), and it is therefore in a very different state when excitatory and inhibitory inputs are both active than it would be if the input were exclusively a weaker excitation.

Because the conduction of action potentials along axons and the consequent chemical synaptic transmission are expensive energetically (*11*), there must be a strong benefit gained from simultaneous stimulation by inhibitory and excitatory sources. The reason proposed by Berg *et al.* is to randomize the timing of the spikes produced by different motor neurons to provide the muscles with a smoother excitation, and thus to produce smoother reflex responses. The authors provide several pieces of data in support of this hypothesis. For instance, they show that the intervals between spikes become more regular when inhibition to the motor neurons is blocked pharmacologically.

Although convincing, this mechanism seems to be a long walk for a short drink. One can imagine a number of mechanisms with no involvement of inhibition that would do equally well at smoothing the motor response, including slow decay times in the motor neuronal membrane, asynchrony in the excitatory inputs to the motor neurons, or variability in synaptic transmission. In fact, nervous systems are usually faced with just the opposite problem: how to maintain timing accurately in the face of variability in all the components of a complicated neuronal circuit. Ultimately, the decoder of the motor neuron activity—the contraction of muscles—may not be affected very much by such subtleties as the degree of regularity in the motor neuronal spike bursts.

It may be that competing excitation and inhibition in a network are used for more interactive functions. Studies of seizures emphasize the need for inhibition to avoid the system's "blowing up," because there is a great tendency for neural systems with too much excitation to go into a maximal activity state (*4*, *6*). In general, neuronal circuits with both excitation and inhibition are better able to control their level of activity because they have a broader dynamic range (*5*). They can thus change their gain more effectively than can purely excitatory networks. One consequence of this broader range of control may be that sensory input from a source that is external to the circuit, or parallel input from other behavioral circuits (onto either the excitatory or inhibitory pathways that impinge on the target motor neuron), can be integrated more smoothly into the ongoing activity of the primary circuit. These additional possibilities, however, do not detract from the one model proposed by Berg *et al.* In fact, a major strength of the turtle scratch reflex system is that the whole system—from sensory input through the central pattern generator to motor neuron output (*12*)—is much more tractable than is cortical brain activity, for instance. The turtle system, or other spinal cord locomotory networks, should provide a good test bed for approaching the many possible reasons for having cojoint inhibition and excitation.

The findings of Berg *et al.* are jarring because they provide clear evidence for an unlikely cellular system architecture in a completely unexpected place. This elicits both practical thoughts (Is there something like this in other neural systems?) and theoretical ones (What else can such a mechanism do?), sure signs of a particularly interesting piece of work.

References

1. C. S. Sherrington, *The Integrative Action of the Nervous System* (Scribner, New York, 1906).
2. B. Haider *et al.*, *J. Neurosci.* **26**, 535 (2006).
3. M. J. Higley, D. Contreras, *J. Neurosci.* **26**, 448 (2006).
4. E. Salinas, T. J. Sejnowski, *J. Neurosci.* **20**, 6193 (2000).
5. F. S. Chance, L. F. Abbott, A. D. Reyes, *Neuron* **35**, 602 (2002).
6. V. Litvak, H. Sompolinsky, I. Segev, M. Abeles, *J. Neurosci.* **23**, 3006 (2003).
7. R. W. Berg, A. Alaburda, J. Hounsgaard, *Science* **315**, 390 (2006).
8. L. G. Brock, J. S. Coombs, J. C. Eccles, *J. Physiol.* **117**, 431 (1952).
9. L. Gabernet, S. P. Jadhav, D. E. Feldman, M. Carandini, M. Scanziani, *Neuron* **48**, 315 (2005).
10. C. E. Carr, M. Konishi, *J. Neurosci.* **10**, 3227 (1990).
11. D. Attwell, S. B. Laughlin, *J. Cereb. Blood Flow Metab.* **21**, 1133 (2001).
12. A. Berkowitz, *J. Neurophysiol.* **94**, 4455 (2005).

10.1126/science.1138110

ECOLOGY

Managing Farming's Footprint on Biodiversity

A simple risk-assessment model that predicts the effect of environmental change on farmland biodiversity may be more generally applicable to analyzing the effects of environmental changes on populations.

Tim G. Benton

Managers of both agricultural resources and conservation areas increasingly need to know how environmental change will affect population size. However, the biological mechanisms that link changing environment to changing population size, through changes in an organism's life history and demographic rates, are often highly complex (*1*). Gathering sufficient data to build a detailed model to predict a species' response to environmental change is far from trivial, and we may not have the luxury of spending years collecting biological information or of simply mitigating the change by creating nature reserves (*2*). On page 381 of this issue, Butler *et al.* (*3*) introduce a simple risk-assessment framework that can predict the impact of environmental change on biodiversity. Although the authors applied it to predicting species' responses to agricultural management, it is a general method for risk assessment.

Biodiversity management in an agricultural setting has recently become a focus of conservation biology. About 37% of the globally available land area is agricultural, and a predicted additional 10^9 hectares of land will be required by 2050 to produce the 50% increase in production required (*2*, *4*, *5*). Thus, a substantial proportion of total biodiversity is associated with farming and, given that agricultural intensification has reduced biodiversity (*6*–*9*), it is under considerable threat. Biodiversity on nonagricultural land is also affected by the quality of farmland as it forms the landscape matrix between fragments of suitable habitat. Degradation of the matrix through agricultural intensification can therefore affect species' dispersal between patches and hence the survival of all the local populations in a region (*10*).

During the 1970s and 1980s, a marked decline in the abundance of species that are strongly associated with farmland, especially birds, created considerable alarm (*9*). So great has been the public concern at the potential loss of agricultural biodiversity that governments have begun to channel resources into mitigating the effect of intensive agriculture. The major policy instruments have been to (i) decouple the relation between price support (subsidy) paid on the basis of yield in favor of support based on the area farmed—reducing the incentive for farmers to maximize outputs, and (ii) introduce voluntary schemes in which farmers are reimbursed to undertake practices aimed at benefiting biodiversity—so-called agri-environment schemes such as retiring land from production ("set aside") or leaving field margins uncropped. In total, nearly $5.25 billion is spent annually on agri-environment schemes in Europe and North America (*10*). The importance of positive intervention is indicated by, for example, the UK government's commitment to reverse the population declines of farmland birds by 2020 (see the figure). Given the way agriculture is set to change in the future (by both increasing food production and diversifying into nonfood crops), the impact of agriculture on global biodiversity, and the money now being spent on mitigating agriculture's effects, it is increasingly important to predict biodiversity's response to agricultural change.

Predicting any population's response to an environmental change is difficult, and not simply because of inherently complex biology. A population's response depends also on the web of interactions within its habitat (*11*) and, as we are increasingly recognizing, local biodiversity is also influenced by different factors at different spatial scales (*12*, *13*). Constructing a detailed, mechanistic, cutting-edge population model [e.g.,(*14*)] may take so long that it neither produces an answer to a policy-led question within the policy-makers' required time frame nor produces a sufficiently general answer (*15*). So what is needed is a simple approach to allow risk assessments of the effects of environmental change on populations, an approach

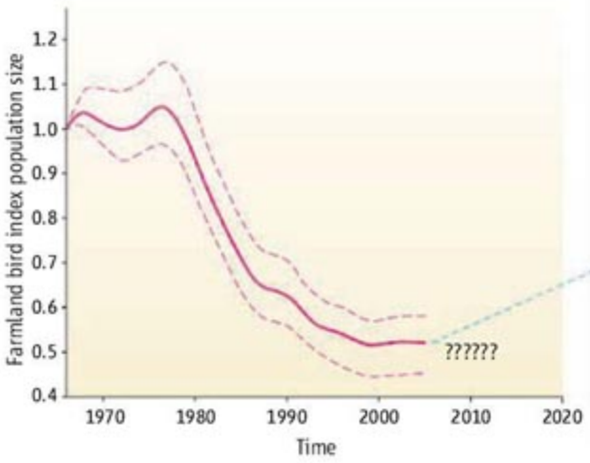

Estimating the risk. Declines in the community of farmland birds in the United Kingdom are described by the Farmland Bird Index (FBI). How can we predict what intervention will fulfill the government's pledge to reverse the decline by 2020? Butler *et al.* outline a very simple method of risk analysis. Conceptually, this involves producing a matrix of basic ecological requirements and estimating a weighted sum of the negative effects an environmental change may have (such as the tabulated example for increasing pesticide usage). This risk score is strongly correlated with the population decline for each species that makes up the FBI, and can be used to predict how it will change with change in management.

Habitat requirements		Summer	Winter
Foraging habitat	Area quality	Negative	Negative
Nesting habitat	Area quality	Negative	

The author is at the Institute of Integrative and Comparative Biology, University of Leeds, Leeds LS2 9JT, UK. E-mail: t.g.benton@leeds.ac.uk

that is quick to implement, not spatially restricted, able to assess the impacts on multiple species, and usable where existing data may be of sufficient quality or quantity. Nirvanas, even modeling ones, are the stuff of fantasy, but are there shortcuts to produce a pragmatically useful, "quick and dirty" risk-assessment approach that produces answers that are good enough? The answer, somewhat surprisingly, seems to be "yes," according to Butler *et al.* (*3*).

Like many good ideas, this approach is elegantly simple: What proportion of an organism's habitat requirements will be affected by any given environmental change? Birds inhabiting farmland require only a few types of resource: somewhere to nest, somewhere to forage in summer and winter, and food to be available in each foraging habitat. Typically, we know enough about a species' biology to estimate whether a given environmental change (e.g., a switch from spring to winter sowing) will have a negative impact on the abundance of dietary items or the amount of foraging or nesting habitats. The species' risk depends not on only the number of negative impacts but also on its specialization on the resources; this is incorporated into the risk score by a simple weighting factor. The risk score in response to six historical agricultural changes was estimated for a sample of 57 United Kingdom bird species found on farmland. This simple score is remarkably well correlated with the rate of population change over the past 40 years (and thus with the species' conservation status) and does as well as, or better than, a range of much more complex formulations.

Having developed the methodology, Butler *et al.* (*3*) illustrate its use with an assessment of how farmland birds may respond to two changes in the farmed environment. First, the widespread introduction of two species of genetically modified herbicide-tolerant crops is predicted to have little effect, a result that may contribute to public acceptance of such crops. Second, a 2005 UK agri-environment scheme offers a wide range of options, but those most commonly taken up affect the management of hedgerows and field margins. The risk assessment identifies within-crop habitat as that whose degradation most strongly affects population size. Birds' reliance on cropped areas is so strong that population declines in half to two-thirds of species will not be reversed by the widespread margin management resulting from farmers' current choices. For the scheme to reverse declines, farmers should be more strongly encouraged to take up options that address the drivers of change.

This framework not only applies to birds but also can be used on any species or groups of species whose habitat and resource requirements are known and for whom the impacts of any environmental change can be estimated. The targets could be species of conservation concern or species that provide ecosystem services (such as biocontrol or pollination), and the environmental change could be a management or a climate change. Predicting population change will always be an inexact science (*16*), but this approach is so simple that it will provide a very useful first approximation. A quick answer that is good enough may be more influential on policy than a better answer supplied years later.

References

1. T. G. Benton, S. J. Plaistow, T. N. Coulson, *Proc. R. Soc. Lond. Ser. B Biol. Sci.* **273**, 1173 (2006).
2. R. E. Green, S. J. Cornell, J. P. W. Scharlemann, A. Balmford, *Science* **307**, 550 (2005).
3. S. J. Butler, J. A. Vickery, K. Norris, *Science* **315**, 381 (2007).
4. D. Tilman *et al.*, *Science* **292**, 281 (2001).
5. United Nations Environment Programme, Global Environmental Outlook-1, www.unep.org/GEO/geo1/ch/toc.htm.
6. D. E. Chamberlain, R. J. Fuller, R. G. H. Bunce, J. C. Duckworth, M. Shrubb, *J. Appl. Ecol.* **37**, 771 (2000).
7. R. A. Robinson, W. J. Sutherland, *J. Appl. Ecol.* **39**, 157 (2002).
8. P. F. Donald, R. E. Green, M. F. Heath, *Proc. R. Soc. Lond. Ser. B Biol. Sci.* **268**, 25 (2001).
9. J. R. Krebs, J. D. Wilson, R. B. Bradbury, G. M. Siriwardena, *Nature* **400**, 611 (1999).
10. P. F. Donald, A. D. Evans, *J. Appl. Ecol.* **43**, 209 (2006).
11. P. Casula, A. Wilby, M. B. Thomas, *Ecol. Lett.* **9**, 995 (2006).
12. J. Bengtsson, J. Ahnstrom, A. C. Weibull, *J. Appl. Ecol.* **42**, 261 (2005).
13. D. Gabriel, I. Roschewitz, T. Tscharntke, C. Thies, *Ecol. Appl.* **16**, 2011 (2006).
14. P. A. Stephens, R. P. Freckleton, A. R. Watkinson, W. J. Sutherland, *J. Appl. Ecol.* **40**, 970 (2003).
15. W. J. Sutherland *et al.*, *J. Appl. Ecol.* **43**, 617 (2006).
16. C. Loehle, *J. Appl. Ecol.* **43**, 957 (2006).

10.1126/science.1137650

MATERIALS SCIENCE

Ordering Up the Minimum Thermal Conductivity of Solids

K. E. Goodson

Disorder usually interferes with heat conduction in most materials, but an exception has been found for insulators made from multiple layers of crystalline tungsten selenide.

Although record-high thermal conductivities in ordered materials such as diamond and carbon nanotubes have captured headlines (*1*, *2*), a few researchers have pursued materials with the minimum thermal conductivity. Although the best thermal insulators are porous (like styrofoam), many applications require electrical and mechanical properties that are only available in fully dense materials. The best nonporous insulators are amorphous dielectrics, which have conductivities as much as four orders of magnitude less than that of diamond (*3*, *4*). On page 351 of this issue, Chiritescu *et al.* (*5*) report a breakthrough value nearly an order of magnitude lower still for WSe_2 films. The material combines the thermal conductivity of a porous insulator with a density near that of copper (see the figure). In addition, the conductivity of the WSe_2 films increases after ion-irradiation damage, undermining the assumption that more disorder is better in the quest for the worst heat conductor. This finding promises improved, dense thermal insulators for gas turbine engines, thermoelectric refrigerators and power generators, and thermal data storage devices.

The highest thermal conductivity in a given material is generally achieved through crystalline order. Many of the best room-temperature heat conductors are crystals with high speeds of sound (like diamond and silicon carbide), in which atomic vibrations (phonons) carry energy hundreds of nanometers before attenuation. Ordered crystals provided early successes for the phenomenological phonon transport theory, which relates the thermal conductivity to the mean free path and heat capacity contributions of phonons [e.g., (*6*)]. Even today, with molecular dynamic simulations capturing the essential physics of conduction, phonon transport theory is helpful for interpreting the impact of localized disorder in crystals.

The minimum thermal conductivity is found in amorphous dielectrics. Atomic-scale disorder in these solids attenuates vibrational waves within a few angstroms. Con-

The author is in the Mechanical Engineering Department, Stanford University, Stanford, CA 94305–3030, USA. E-mail: goodson@stanford.edu

ductivity modeling for amorphous materials has roots in the Einstein heat conduction model, in which atoms behave as oscillators with random phase and the vibrational attenuation length scale is near the interatomic separation. When this approach is recast with the Debye heat capacity and a mechanistic scale equal to the vibrational wavelength, conductivity predictions agree with data for a broad variety of amorphous glasses (*4*). Porosity is another route to low conductivity. Low-density xerogel films, for example, have conductivities well below 0.1 $W\,m^{-1}\,K^{-1}$ (*7*). However, porosity strongly degrades other properties, including mechanical stiffness and electrical conductivity.

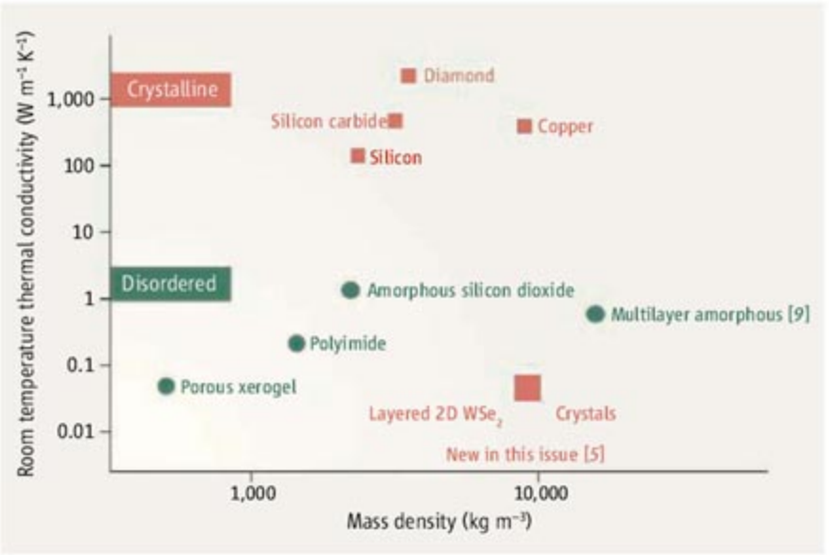

Search for the worst. Room-temperature thermal conductivities of a few representative materials compared with new data for ordered WSe_2 films (*5*). The material sets a record for the lowest thermal conductivity of a fully dense material at 300 K. Remarkably, the ultralow conductivity is achieved through the introduction of crystalline order.

More recently, systematic layering of materials has reduced the conductivity. Material interfaces scatter atomic vibrational waves and can strongly limit the phonon mean free path. Phonon scattering at interfaces reduces the thermal conductivity and improves the thermoelectric properties (*8*). Multilayers of disordered materials lead to further conductivity reductions, with disorder and interfaces working in concert. Costescu *et al.* (*9*) showed that the thermal conductivity of disordered W/Al_2O_3 nanolaminates decreased with increasing interface density to a value of 0.5 $W\,m^{-1}\,K^{-1}$ (see the figure).

Before the work of Chiritescu *et al.*, a natural assumption was that the minimum thermal conductivity in fully dense solids would be achieved in multilayers of disordered materials. However, their results (*5*) demonstrate a dramatic further reduction in room-temperature conductivity, down to 0.05 $W\,m^{-1}\,K^{-1}$, in multilayers of crystalline WSe_2 sheets. The films are fabricated by depositing sequential layers of W and Se on silicon and annealing. X-ray diffraction confirms a precise layering of WSe_2 sheets with spacing of 6.6 Å, in which the crystalline orientation may be random in the direction parallel to the substrate. The thermal conductivity is measured perpendicular to the film with a well-established laser heating and thermometry technique having high sensitivity to the film properties. Although thermal conductivity data are provided only in the cross-plane direction, further research on the in-plane component is likely to capture a very large conductivity anisotropy.

The key to the low thermal conductivity lies in the WSe_2 structure, which features covalent bonding within two-dimensional sheets that are themselves bonded by weaker van der Waals forces. The authors show that the data are consistent with molecular dynamics simulations by using differing interaction energies within and between the WSe_2 sheets. The strong anisotropy of bond strengths may localize vibrational waves attempting to travel normal to the film. To confirm the connection between crystalline order and low conductivity, the authors showed that ion bombardment (and the associated disruption in the ordered *a-b* planes) increased the conductivity by a factor of 5. The conductivity increase with damage is a remarkable finding and indicates that the careful combination of order and disorder can minimize the thermal conductivity in other materials.

There is no shortage of applications for low-conductivity nonporous materials, particularly in the area of energy conversion. The challenge is to provide thermal insulators that retain other attractive mechanical, electrical, and optical properties. Thermoelectric energy conversion (refrigeration or power generation) requires low thermal conductivity, high electrical conductivity, and a high Seebeck coefficient (which relates temperature gradients and electric fields in the material). The new findings will launch research on the correct recipe of in-plane order and cross-plane disorder that impairs heat conduction while promoting electrical transport of charge and energy. Another example is thermal barrier coatings for gas turbine blades, which require thermal insulation from combusting flows (*10*). Achieving mechanical strength, high-temperature stability, and high resistance to radiative transfer will be key challenges for the new class of thermal insulators in this application. Phase change memory technology, which uses electrical current and heating to alter the stored data bits through phase transformations, has a write energy that decreases rapidly with increasing thermal resistance (*11*). The new class of thermal insulators may provide a route to minimizing the energy required for storage.

The minimum thermal conductivity is yet another example where nanostructuring enables us to reach the extreme limit of a basic material property. Because thermal conductivity is rarely the only key property, this finding highlights a challenge for nanotechnology: Nanostructured materials will find the greatest impact if they provide radically new combinations of properties, rather than merely an extreme value of one property. For applications ranging from thermoelectrics to turbine blades, the primary challenge will be to introduce the layered disorder that minimizes the thermal conductivity while maintaining the other targeted properties, including mechanical stability and high electrical conductivity.

References

1. J. R. Olsen, R. O. Pohl, J. W. Vandersande, A. Zoltan, *Phys. Rev. B* **47**, 14850 (1993).
2. P. Kim, L. Shi, A. Majumdar, P. L. McEuen, *Phys. Rev. Lett.* **87**, 215502 (2001).
3. G. A. Slack, *Solid State Phys.* **34**, 1 (1979).
4. D. G. Cahill, S. K. Watson, R. O. Pohl, *Phys. Rev. B* **46**, 6131 (1992).
5. C. Chiritescu *et al.*, *Science* **315**, 351 (2007); published online 14 December 2006 (10.1126/science.1136494).
6. J. M. Ziman, *Electrons and Phonons* (Oxford Univ. Press, New York, 1960).
7. A. Jain *et al.*, *J. Appl. Phys.* **91**, 3275 (2002).
8. R. Vankatasubramanian, E. Silvola, T. Colpitts, B. O'Quinn, *Nature* **413**, 597 (2001).
9. R. M. Costescu, D. G. Cahill, F. H. Fabrequette, Z. A. Sechrist, S. M. George, *Science* **303**, 989 (2004).
10. M. J. Kelly *et al.*, *Int. J. Appl. Ceram. Technol.* **3**, 81 (2006).
11. A. Pirovano, A. L. Lacaita, A. Benvenuti, F. Pellizzer, R. Bez, *IEEE Trans. Electron Dev.* **51**, 452 (2004).

10.1126/science.1138067

Enabling Europe to Innovate

Andrew Dearing

As activities that relate to innovation become increasingly global and open and so draw the private and public sectors into complex networks of partnerships, these activities also tend to concentrate where the ecosystem is most supportive. European public policy, which in recent years has emphasized the importance of research and development (R&D) in achieving competitive knowledge-based societies, is shifting toward approaches that address the broader qualities required of favorable ecosystems for innovation in a global economy, thereby incorporating the roles of market demand, public procurement, and regulation, as well as science, education, and industrial R&D, as part of determining effective innovation policies.

Successful innovation once depended mainly on the controlled qualities of the corporate research and development (R&D) laboratory, but noticeable changes became evident in the 1990s. These changes, at first stimulated by companies' desire to reduce cycle time and to bring technology development more closely under business unit control, have been turned to advantage by those companies that recognized that they could no longer develop all required technology in-house and that "gold plating" of proprietary technologies was counterproductive. Within this environment, small innovative companies have thrived through their ability to test, develop, and supply new methods and approaches more effectively than larger companies.

Coombs and Georghiou (*1*) referred to these changes as a "new industrial ecology" and Chesbrough (*2*) introduced the term "open innovation" to describe approaches that combine in-house and external resources. Organizations succeed by virtue of their ability to gain comparative advantage from the combined activities of competitors, suppliers, and customers; to obtain economic value also from intellectual property (IP) that is not needed for internal business purposes; to treat public research as a strategic resource; to spot and rapidly internalize discoveries from sources outside the company; and thereby to concentrate their own efforts on activities (such as improved service content) that best contribute to value creation and innovation for the company itself.

These trends are playing a major part in shaping corporate approaches to innovation. The March 2006 issue of the *Harvard Business Review* (*3*) describes the "connect-and-develop" approach taken by the global consumer goods company, Procter and Gamble (P&G). P&G reported that this approach now yields more than 35% of the company's innovations and billions of dollars in revenues. The approach was illustrated using an example of a small bakery in Bologna, Italy, run by a university professor who had extended ink-jet technology to print edible images on foodstuffs. By transferring this technology and modifying it to deal with different process conditions, P&G was able to take a new product (Pringle Prints) (Fig. 1) from concept to launch in less than a year, at a fraction of the cost of in-house development.

Open innovation has also been stimulated by the decreasing time frames during which companies can command premium prices from proprietary technologies. Whereas the price of videocassette recorders fell by 50% over a 10-year period, the price of DVD recorders, which came to market 25 years later, fell by this amount in 2 years. Remaining competitive in this situation requires considerable agility from companies, forcing them to concentrate on core skills.

As technological content of products and services grows, this must be packaged in ways that consumers find reliable and easy to use. Philosophies such as ambient intelligence (*4*) emphasize within the corporation that technology has to become a more natural, yet pervasive, part of the environment in which we live. The introduction of advanced consumer products such as luxury coffee machines, which bring the qualities of the professional espresso bar into the home and office, and music and video players like Apple's iPod shows how this goal is starting to be being addressed.

As a result of these combined pressures on innovation, emphasis within companies has shifted toward linking research and development more closely with activities such as design, production, and distribution. Growing technological complexity requires that the company anticipates developments in standards and stimulates the development of shared component platforms and technology roadmaps. Research collaboration among companies and with universities and other public research organizations takes on a more strategic importance. New businesses (*5*) mediated by the Internet facilitate technology exchange among companies and help match scientific skills globally with the problems that companies wish to resolve.

European Industrial Research Management Association, 46 rue Lauriston, 75116 Paris, France. E-mail: adearing@eirma.asso.fr

European Public Policy: Understanding the R&D Numbers

A key task for policy-makers is to address these developments in ways that benefit the home economy. Soon after the summit meeting of European heads of state in Lisbon in March 2000 placed innovation at the heart of the policy agenda, a substantial gap became evident between overall R&D intensities within the European Union (EU) and its main economic competitors, particularly with regard to private-sector investment. Treating this gap initially as both symptom and cause of lack of competitiveness, a subsequent summit projected that levels of R&D investment should rise from 1.9 to 3% of gross domestic product, in effect addressing a gap in competitiveness and innovation performance by means of a "research push." This has become known as "the Barcelona target," for which two-thirds of R&D investment would come from the private sector.

To a large extent, the gap between current levels of R&D investment in Europe and the 3% goal reflects a concentration of large R&D investors in certain industrial sectors. Most in-

dustrial R&D worldwide is financed by a few hundred large companies (*6*). A main factor differentiating the levels of R&D in different regions (Table 1) is the sector concentration that resulted from previous patterns of company growth.

Competing companies tend to invest in a similar fashion in R&D regardless of where they are headquartered. In sectors such as information technology (IT) hardware, computer software, and biotechnology, large amounts of money are committed to R&D per unit of sales. Many larger companies in these sectors are headquartered in the United States, and most grew large in the last 50 years. Many of the larger European players are in sectors such as automotives and chemicals, where absolute R&D investments are high, but R&D intensity per dollar of sales is lower. There are also more specific European strengths in key growth sectors, for example, in the IT systems embedded into products such as cars and telephones.

Because of the dominant part played by the larger companies, aggregate R&D figures fail to reveal the part played by smaller companies. Deeper examination shows that the larger companies now depend on and, in turn, support extensive networks of smaller companies, some of which will become the large companies of the future. It is important to emphasize this interdependency and to understand its consequences.

Here, There, or Somewhere Else?

A second part of the policy equation is to understand and to anticipate where companies will place their new R&D investments. In the pharmaceuticals sector (*7*), for example, from 1990 to 1994, 88 "new molecular entity" pharmaceuticals came to market in Europe and 74 in the USA, and companies' R&D efforts were concentrated accordingly [1990: EU, €8 billion ($10.5 billion U.S. dollars); USA, €6 billion ($7.8 billion)]. These patterns have since reversed (2000–04: 57 new molecular entities in EU, 70 in the USA; estimated in 2004: EU, €21 billion ($27.5 billion) spent on R&D; USA, €27 billion ($35.4 billion). The shifts continue as new markets, trained people, and adequate support structures become available in Asia. In May 2006, the Anglo-Swedish pharmaceutical major, AstraZeneca, followed its Swiss and Danish counterparts, Novartis International, Novo Nordisk, and Roche, in announcing plans for R&D facilities in China.

Two recent studies examining factors driving decisions about the global R&D investments of U.S.- and EU-based companies (*8*, *9*) concluded that the most important features are potential for market growth, availability of environments that foster the development of a high-quality work force, and opportunities for productive collaboration between corporations and universities. There is still a tendency to place work addressing newer technologies and newer markets close to home, but this is by no means an absolute rule. Contrary to some assumptions, research costs have not proved to be the main factor stimulating companies to look toward Asia.

In its 2006 study (*8*) of more than 200 larger European companies, the European Commission found market access to be the most important factor in deciding where to locate R&D, followed by a predictable legal framework for R&D, access to specialized R&D knowledge and results, high availability of researchers, and macroeconomic and political stability. Respondents reported outsourcing an average of 18% of their R&D, around two-thirds going to other companies and one-third to public research organizations. Pharmaceutical and biotechnology companies outsource roughly twice the share of R&D as their counterparts in other sectors. These figures are consistent with other studies, including those by the author's organization, which suggest a U-shaped curve over the past 80 years. The minimum of around 3% outsourcing occurred in the mid-1970s, when the corporate laboratory was the dominant feature of the industrial landscape. Since then, the proportion of R&D performed outside the corporation has increased steadily, in line with the reported adoption of more open approaches.

Respondents distinguished between locations they considered most attractive for new R&D investment and where they expected their companies' R&D activities will grow. Although they often placed their home country first and saw the United States as most attractive outside the EU, they expected to direct most new investment toward China and the United States.

Thursby and Thursby (*9*) studied a similarly sized sample of medium and large U.S.- and European-based corporations and found that 38% reported that they plan to "change substantially" the worldwide distribution of their R&D over the next 3 years, with China and India attracting the greatest increase. For emerging country locations, the most important factors were found to be output growth potential, followed by quality of R&D personnel, supporting sales, IP protection, the ability to own IP, costs, collaborating with universities, and the expertise of university faculty. In developed countries, what matters most is the quality of R&D personnel and IP protection, university collaboration, output market factors, and IP ownership. The study revealed little difference between the views of U.S.- and European-based companies.

From Collaboration to Platforms to a Pact for Innovation

These and other (*10*) surveys confirm that companies prize locations that support business growth and offer high-quality work forces and collaborative partners. How can policy-makers improve the attractiveness of their own region?

In the European Union, a key objective remains to gain full benefit from a large single market. This still requires much work to reconcile the legal and other traditions of 25 member states and to overcome significant barriers, such as those concerning regulatory matters and mobility. There is a widely shared belief in having strong social structures supported by considerable public investment in areas like health care and transport. However, most public funding for these structures and for the dense network of public universities and national research organizations remains at the national level. As an illustration, the current European Research Framework Program (FP6) accounts for only a few percent of Europe's total research expenditure.

In recent years, smaller countries like Finland, Sweden, and Ireland have performed better than their larger, southern neighbors in terms of encouraging innovation-led growth through policies of market reform and effective public-private collaboration (and Finland and Sweden are well ahead of the Barcelona target for R&D), but these economies are now running close to their full capacity. The challenge is to find approaches that benefit the whole EU, improving and gaining more leverage from all the capabilities available within and beyond Europe.

Responding to discussions about innovation-led growth among heads of state in late 2005, a group led by former Finnish Prime Minister Esko Aho has recently reported (*11*) on how this

Table 1. Distribution of the headquarters of the 700 multinational companies that account for some 80% of private sector R&D investment and over 50% of all R&D within Organization for Economic Cooperation and Development member states (*6*).

Type of industry	Headquarters' location			R&D/Sales
	Europe	North America	Rest of the world	
Global 700	192	334	174	4.3%
"High R&D"	72	220	87	
IT hardware	15	93	22	10.1%
Automotive/parts	16	14	17	4.2%
Pharmaceuticals/biotechnology	22	42	18	13.7%
Electronics/electrical	10	14	28	6.0%
Software/services	9	57	2	9.0%
Other sectors	120	144	131	2.0%

might be achieved. The report recommended a combination of approaches, which reflect the trends described in the first part of this review. The group called for simultaneous, synchronous efforts in three areas:

1) To provide an innovation-friendly market for businesses, requiring actions on regulation, standards, public procurement, and IP; fostering a more pro-innovation culture; and creating demand focused on large-scale strategic actions.

2) To increase resources for excellent science, industrial R&D, and the science-industry nexus; to improve R&D productivity; and to shift the use of the so-called "structural funds" (used to underpin economic development in poorer regions) toward R&D.

3) To achieve far greater mobility of people across sectors, of financial resources and knowledge, and in the structures and clusters that frame innovation.

The report calls for a pact for research and innovation from political, business, and social leaders to drive the agenda forward. Its recommendations are strongly market-oriented in philosophy. Areas mentioned as possibilities for large-scale strategic actions include health, pharmaceuticals, energy, environment, transport and logistics, security, and digital content, where opportunities go beyond the capacity of individual economic actors. Although more resources for R&D and innovation are seen as a necessity, the 3% target for R&D becomes an indicator of success rather than an objective in its own right.

The response to these recommendations is currently being worked out and will become evident in the months ahead. Some conclusions can already be drawn from the wide range of programs that are already under way at European and national levels to establish conditions for greater competitiveness through research and innovation. There is growing understanding of the use of direct tax and fiscal measures, and the Dutch approach of relating tax credits to R&D employment through social charges is proving attractive. The revision of rules for State Aid (*12*) is intended to bring these rather arcane rules more in line with the requirements for innovation-led growth and effective use of public R&D grants. One more push may be sufficient to achieve a uniform single patent regime in Europe, even though this has defied all attempts at a solution for 40 years.

Ambitions for the European Framework Program are perhaps the easiest to state. A substantially larger budget, €50.5 billion ($66.3 billion) from 2007 to 2013 (*13*), has been agreed for the new program (FP7), whereas clearer emphasis is placed on excellence and utility. Its success depends on obtaining the best proposals and improving participation by both industrial and public research. An important innovation in FP7 is support for the new European Research Council, charged with fostering the best "frontier research" (a term intended to highlight that the traditional distinction between basic and applied research is no longer appropriate). A first priority for ERC's Scientific Council is the development of independent careers for excellent researchers establishing their first research team.

Improving Links Between Science and Industry

The quality of connections among companies and with universities and other public research organizations is an increasingly important factor that supports open models of innovation and is as important (or perhaps more important) in the long term as the number of university spin-offs and simple technology licensing agreements. Although there is a long tradition of informal joint supervision of Ph.D. projects in some European countries, the well-known difficulties presented by industry-academic collaboration are becoming more apparent as these activities take on more strategic importance. It is necessary to improve management of IP by public research organizations; to take steps to align interests, motivation, and culture; to address ownership of results and exclusivity; to improve project management; to compensate indirect costs; to deal with volatility of relationships; and to ensure equitable share of returns in case of success. These improvements require new professional skills and mind-sets, so that collaborative activities can enhance, not dilute, the distinct missions of public and private-sector research.

One way forward is through the development of standard model agreements and codes of practice for collaborative R&D, steps recently taken, for example, by the U.K. (*14*) and Irish governments (*15*). The 2005 launch of the Responsible Partnering initiative in Europe (*16*) marked renewed efforts to support changes in attitude and approaches to collaboration at the grass-roots level. Its recommendations are very similar to those reached by a similar initiative launched by the U.S. Government-University-Industry Round Table (GUIRR) (*17*). Both initiatives emphasize the need to establish conditions that foster stable, long-term collaboration and trust. This requires developing a better understanding at senior levels within public and private-sector organizations of managing open innovation, then recruiting and developing the new skills needed to handle collaborations effectively, establishing quality of collaboration as a key performance metric.

It is also important to raise standards within public research itself. This will almost certainly entail giving these institutions greater autonomy to set direction and to concentrate on strengths and, thereby, to attract the best talent to come to, and remain in, Europe. In several countries, universities remain subject to extensive national regulatory frameworks and have little control over their resources and priorities. There are close to 2000 universities in the EU, and most conduct research and offer postgraduate degrees across a broad curriculum. By contrast, fewer than 250 U.S. universities award postgraduate degrees and fewer than 100 are recognized as research-intensive.

Educational curriculum reform is under way in more than 40 European countries through what is known as the Bologna process. This aims to establish easily recognizable and comparable degrees based around a two-cycle system of studies, starting with a bachelor's degree and moving on to the master's level. A third cycle aims to ensure that doctoral studies remain relevant to changing career patterns.

Technology Platforms and Shared Strategic Research Agendas

Technology roadmaps have been used for more than a decade as a tool for providing frameworks for discussion between different business functions and for a more conscious integration of all aspects of technology into business strategy. The roadmaps enable decisions to be taken more quickly and to be implemented with greater confidence. They can also be shared within an industry sector and so lead to the adoption of common development platforms and strategic research agendas.

These approaches are being extended, thereby involving more stakeholders in the early stages and subsequent implementation of major research programs. As one example, the Netherlands Genomics Initiative (NGI) (*18*), involving many Dutch companies and university departments, is coming toward the end of its first, €300 million ($393.7 million), phase of a program to build an internationally leading genomics infrastructure that will stimulate excellent research and generate a continuous flow of new economic activity, while remaining firmly linked to the concerns and interests of Dutch society. NGI is set to enter its next phase, when it will seek to couple national resources more closely with international strengths while also concentrating on delivering economic benefits to the Netherlands.

European Technology Platforms (*19*) take the approach a step further. Some 29 of these industry-led initiatives provide frameworks for all stakeholders to define research and development priorities, time frames, and action plans on issues where growth, competitiveness, and sustainability objectives require major medium- to long-term research and technological advances. A number of platforms are now ready to begin implementation. Some funds for work that has a high degree of industrial relevance may come from the Framework Program, although this is not guaranteed. The challenge for the platforms is to fully mobilize resources and public authorities at national and regional levels, as well as from the private sector. In some cases, the scope of an objective and the scale of resources may lead to the setting up of long-term European public-private partnerships, in what are being

termed Joint Technology Initiatives (JTIs). The intention is that JTIs will combine private-sector investment and national and European public funding, including grants from the Framework Program and loan finance from the European Investment Bank.

An example comes in the field of health care. Among ways to respond to the trends in the health-care industry described earlier in this review are to obtain more effective methods for early safety evaluation, to provide better tools for integrated and predictive management of enormous volumes of data, to improve education and training in the use of these techniques, and to reduce barriers to carrying out clinical trials in Europe. These require efforts that go beyond the capabilities and remit of an individual company or public body. The Innovative Medicines Initiative (*20*) began by developing a strategic research agenda by consultation among all stakeholders. The agenda proposes the establishment of a public-private partnership to be operational in 2007, with investments around €440 million ($577.4 million) per year.

Conclusions

The challenge for European governments, companies, and public research institutes is to use the opportunities offered by open innovation to develop strengths and to build greater critical mass within Europe to support sustainable markets from new science. A main lesson from the past is that primarily top-down, centrally planned approaches are rarely effective. There is still much to gain from removing existing barriers to innovation, but policy-makers must now learn how to channel the significant resources and skills available within both public and private sectors to better address market opportunities. The goal will be to encourage innovation in ways that address the desire for strong social systems in Europe without either compromising the global competitiveness of European companies or reverting to old styles of "picking technological winners." A twofold approach is likely to emerge, aimed at encouraging a more market-oriented view of innovation while using direct measures to support more effective industrial and public-sector R&D. The appropriate balance between these elements remains an open question, the answer to which is likely to be determined by how responsibilities are shared between nation states and the European Commission as the Union continues to develop.

References and Notes

1. R. Coombs, L. Georghiou, *Science* **296**, 471 (2002).
2. H. Chesbrough, *Open Innovation: The New Imperative for Creating and Profiting from Technology* (Harvard Business School Press, Cambridge, MA, 2002).
3. L. Huston, N. Sakkab, *Harv. Bus. Rev.* **84**, 58 (2006).
4. Ambient intelligence, espoused by Philips, a large global electronics company, refers to a vision of a world in which technology, in the form of small, but powerful, silicon chips, is integrated pervasively to create an environment sensitive to the presence of people and responsive to their needs; see www.research.philips.com/technologies/syst_softw/ami/background.html.
5. For example, yet2.com, www.yet2.com/appl/about/home, assists companies in realizing value from their IP, including offering a suite of online services for technology evaluation, licensing, and acquisition. Innocentive, www.innocentive.com, offers Web-based communities to match companies' global requirements for R&D to leading scientists willing to carry out this work.
6. Company data can be found at www.innovation.gov.uk/rd_scoreboard.
7. Figures obtained from the relevant industry associations [European Federation of Pharmaceutical Industries and Associations (EFPIA), Pharmaceutical Research and Manufacturers of America (PhRMA), Japan Pharmaceutical Manufacturers Association (JPMA)]. Pharmaceutical R&D investments are compared using constant exchange rates for 2003.
8. European Commission (EC), in *Monitoring Industrial Research: The 2005 EU Survey on R&D Investment Business Trends* (EC, Seville, 2006), pp. 10–14; http://iri.jrc.es/documents.htm.
9. J. Thursby, M. Thursby, *Here or There? A Survey on the Factors in Multinational R&D Location* (Report to the U.S. Government–University-Industry Research Roundtable, National Academies Press, Washington, DC, 2006).
10. T. Goldbrunner, Y. Doz, K. Wilson, S. Veldhoen, *The Well-Designed Global R&D Network* (INSEAD and Booz Allen Hamilton, 2006); www.strategy-business.com/resilience/rr00032.
11. E. Aho, J. Cornu, L. Georghiou, A. Subirá, *Creating an Innovative Europe* (Aho Group Report to the European Commission, EC, Brussels, 2006); http://ec.europa.eu/invest-in-research/action/2006_ahogroup_en.htm.
12. State Aid Rules are designed to limit governments' freedom to distort markets through industrial subsidy; http://ec.europa.eu/comm/competition/state_aid/legislation.
13. Other figures may be seen [e.g., €48 billion to €54.4 billion ($63 billion to $71.5 billion)], depending on whether the budget is expressed in current values or reflects inflation and which items are being considered as part of the Framework Program.
14. Lambert Agreements at the U.K. Department of Trade and Industry, www.innovation.gov.uk/lambertagreements.
15. Irish government Advisory Council for Science, Technology, and Innovation (ACSTI), *National Code of Practice for Managing and Commercialising Intellectual Property from Public-Private Collaborative Research* (ACSTI, Dublin, 2005); www.sciencecouncil.ie/reports/acsti051125/acsti051125_ip_code_of_practice_webopt.pdf.
16. Responsible Partnering is a joint initiative of the European Industrial Research Management Association (EIRMA); public laboratory R&D, the European Association of Research and Technology Organizations (EARTO); universities, the European University Association (EUA); and technology transfer professionals and companies affiliated with universities and other public research organizations (ProTon Europe); www.responsible-partnering.org.
17. *Guiding Principles for University-Industry Endeavors* (National Council of University Research Administrators, Washington, DC, 2006).
18. The Netherlands Genomics Initiative, www.genomics.nl.
19. European Technology Platforms provide an industry-led framework for defining R&D priorities, time frames, and action plans in strategically important issues affecting Europe's future growth, competitiveness, and sustainability objectives; http://cordis.europa.eu/technology-platforms/home_en.html.
20. Innovative Medicines Initiative, FP6; http://ec.europa.eu/research/fp6/index_en.cfm?p=1_innomed.

21. This Review draws on information provided in discussions with representatives of many companies, universities, public research organizations, and governments. The conclusions and any factual errors are the author's responsibility. Funding for this review is drawn from general subscriptions paid by member companies of the European Industrial Research Management Association.

10.1126/science.1131373

Brilliant Whiteness in Ultrathin Beetle Scales

Pete Vukusic,[1]* Benny Hallam,[2] Joe Noyes[1]

The colored appearances of animals are invariably controlled by pigmentation, highly periodic ultrastructure, or a combination of both (*1*, *2*). Whiteness, however, is less common and is generated by neither of these methods, because it requires scattering processes appropriate for all visible wavelengths. We report the identification of whiteness resulting from a three-dimensional (3D) photonic solid in the scales of *Cyphochilus* spp. beetles. Their scales are characterized by their exceptional whiteness, their perceived brightness, and their optical brilliance, but they are only 5 μm thick. This thickness is at least two orders of magnitude thinner than common synthetic systems designed for equivalent-quality whiteness.

Archetypal brilliant whiteness that is not augmented by fluorescence, such as whiteness from snow or milk, is the result of multiwavelength scattering arising from aperiodic and multiply oriented interfaces between low-absorbance media of appropriately different refractive index (*3*). The whiteness of *Cyphochilus* spp. originates from elongated flat white scales that imbricate its body, head, and legs (Fig. 1A). These scales are about 5 μm thick, 250 μm long, and 100 μm wide. Their interiors are composed of a random network of interconnecting cuticular filaments with diameters of about 250 nm (Fig. 1B and fig. S1).

Two-dimensional fast Fourier transforms (FFTs) of electron microscope images of the scales' interior (Fig. 1C) confirmed an absence of well-defined periodicity. Wave vector space maps produced by this transform [Supporting Online Material (SOM) text] were free from any single spatial component of refractive index variation (fig. S2A). Experimentally this was confirmed by recording the diffraction pattern associated with light incident on individual scales. By mounting specific white scales on separate needle tips and directing low-intensity focused laser light exclusively through the center of each scale, we imaged the reflection and transmission diffraction patterns on spherical screens (fig. S2B). The resulting diffraction patterns closely matched the FFT maps of the scales' interior (fig. S2C) and confirmed the cuticular filament network as the origin of the whiteness. The intrascale cuticle volume occupancy is about 70%. This appears to optimize scattering intensity by maximizing the scattering center number density while avoiding substantial unfavorable optical crowding (*4*). Optical crowding occurs when the radiation fields associated with individual scattering centers overlap. It causes the system to adopt characteristics of fewer and larger scattering centers when the distance between individual scatterers becomes too small. The relatively high void fraction in this *Cyphochilus* beetle's scales appears to be a vital part of the system's ability to scatter light. It is this, as well as the system's aperiodicity and index contrast of about 0.56, that create such intense optical whiteness for very limited thickness.

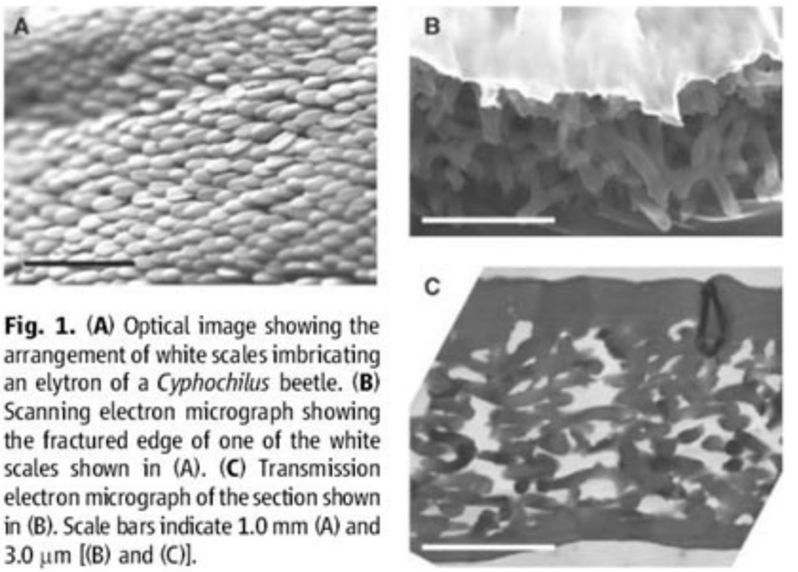

Fig. 1. (**A**) Optical image showing the arrangement of white scales imbricating an elytron of a *Cyphochilus* beetle. (**B**) Scanning electron micrograph showing the fractured edge of one of the white scales shown in (A). (**C**) Transmission electron micrograph of the section shown in (B). Scale bars indicate 1.0 mm (A) and 3.0 μm [(B) and (C)].

The quality of the beetle's whiteness and brightness was quantified according to International Organization for Standardization national standards (SOM text). Its whiteness and brightness values (*5*) were measured to be 60 and 65, respectively, quantitatively indicating remarkable multiwavelength scatter for systems that are only 5 μm thick. In synthetic systems where whiteness is desirable, far more substantial structure is necessary. For example, conventional white uncoated wood-free papers (comprising random networks of bleached cellulose fibers) can be upward of 25 times thicker than these beetle scales but return only an 8% superior brightness. Carbonate or kaolin crystal inclusions and optical brightening agents (blue fluorescing dyes) are added to paper coating formulations to enhance scattering contrast and to improve the perceived appearance of white. However, individual isolated 5-μm-thick calcium carbonate coating layers have a brightness of only 40 to 50, with such poor opacity that its whiteness value is meaningless. Similarly, the whiteness of human teeth is dominated by multiwavelength scattering from packed hydroxyapatite crystals in up to ~2 mm of tooth enamel. Although they are generally considered to be white, their best natural whiteness and brightness are relatively low; typical human milk teeth exhibit a whiteness under 40 and a brightness of about 53, reflecting relatively low index contrast and high absorption at blue wavelengths.

For proportionally insignificant supplementary thickness, the addition of these scales' form of photonic solid would strongly enhance the desirable quality of whiteness in these and many other systems. Additionally, it offers a permeable, flexible, and fault-tolerant ultrathin layer with which to back large-area white light–emitting devices (OLEDs) and control their emission direction.

The phenotypic color of this *Cyphochilus*, credited for cryptism among white fungus, arises from an aperiodic form of structure that might appear to contrast strongly with the highly periodic structure in narrow-band colored weevil scales (*6*). However, they do share several important features: a cuticular filament network with typical filament diameter of the order from 200 to 250 nm, a scale thickness of about 5 μm, and similar extrusion from single epidermal cells into the sealed parcels that comprise each scale. The form of the photonic solid in these white beetle scales confirms that the transition from high-contrast saturated color (SOM text) to optically brilliant whiteness is largely a matter of structural order.

References

1. P. Vukusic, J. R. Sambles, *Nature* **424**, 852 (2003).
2. M. Srinivasarao, *Chem. Rev.* **99**, 1935 (1999).
3. S. Fitzwater, J. W. Hook, *J. Coatings Technol.* **57**, 39 (1985).
4. L. E. McNeil, R. H. French, *Acta Mater.* **48**, 4571 (2000).
5. E. Ganz, *Appl. Opt.* **15**, 2039 (1976).
6. S. Kinoshita, S. Yoshioka, Eds., *Structural Colors in Biological Systems: Principles and Applications* (Osaka Univ. Press, Osaka, 2005).

Supporting Online Material

www.sciencemag.org/cgi/content/full/315/5810/348/DC1
SOM Text
Figs. S1 to S4

5 September 2006; accepted 30 October 2006
10.1126/science.1134666

[1]School of Physics, Exeter University, Exeter EX4 4QL, UK. [2]Imerys Minerals Limited, Par, Cornwall PL24 2SQ, UK.

*To whom correspondence should be addressed. E-mail: P.Vukusic@ex.ac.uk

Electric Field–Induced Modification of Magnetism in Thin-Film Ferromagnets

Martin Weisheit,[1,2]* Sebastian Fähler,[1,2] Alain Marty,[3] Yves Souche,[1] Christiane Poinsignon,[4] Dominique Givord[1]

A large electric field at the surface of a ferromagnetic metal is expected to appreciably change its electron density. In particular, the metal's intrinsic magnetic properties, which are commonly regarded as fixed material constants, will be affected. This requires, however, that the surface has a strong influence on the material's properties, as is the case with ultrathin films. We demonstrated that the magnetocrystalline anisotropy of ordered iron-platinum (FePt) and iron-palladium (FePd) intermetallic compounds can be reversibly modified by an applied electric field when immersed in an electrolyte. A voltage change of −0.6 volts on 2-nanometer-thick films altered the coercivity by −4.5 and +1% in FePt and FePd, respectively. The modification of the magnetic parameters was attributed to a change in the number of unpaired *d* electrons in response to the applied electric field. Our device structure is general and should be applicable for characterization of other thin-film magnetic systems.

Spin electronics has recently emerged as a field of science and technology in which the electron's spin is directly exploited. Giant magnetoresistance and tunnel magnetoresistance sensors, used in read heads of hard disks, are both examples of the application of spin-electronic devices. In contrast, there are very few active (i.e., non-sensor) systems that exploit spin electronics. Such systems are operated through electrical current actuation, which requires much larger energy consumption than electric field (E) actuation used in usual electronic circuits and/or electromechanical systems. E actuation of magnetic properties has been demonstrated in the semiconducting (Ir,Mn)As system, in which the Curie temperature T_C was varied by 1 K under a voltage of 125 V, corresponding to an electric field of approximately 1.6×10^8 V/m (*1*, *2*). However, the possible applications of this phenomenon are limited as a result of the low T_C of magnetic semiconductors (<< room temperature). The recent renewed interest in multiferroic materials in which piezoelectricity and ferromagnetism may coexist is also driven by the same objective of practical application (*3*, *4*). In this case, the deformation of the material's structure under E results in the modification of the magnetic properties and vice versa. Again, this effect is limited to low temperatures in single-phase multiferroics.

Because the T_C values of the 3*d* metals—Fe, Co, and Ni—and of some of their alloys are above room temperature, the possible use of an electric field to modify and control the intrinsic magnetic properties [e.g., magnetization or magnetocrystalline anisotropy (K_U)] of such metallic systems is attractive. However, as a result of screening by the E-induced surface charge, the field does not penetrate the bulk of the material and is confined to a depth on the order of atomic dimensions. It may be expected that substantial E-induced effects may be found in nanosystems where the surface-to-volume ratio is high, with a large E obtained by the application of a high voltage at both sides of an insulating layer (e.g., a thin dielectric deposited on the surface of the metal). However, the preparation of thin and homogeneous dielectric layers free of pinholes is challenging. The immersion of metal particles in an electrolyte was suggested as an elegant approach to overcome this problem (*5*). In a liquid electrolyte, an insulating ionic layer—the electrolytic double layer—forms naturally in front of a conducting surface, and most of the potential drop between the electrodes occurs across this layer (*6*). Subsequently, it was shown (*7*) that a macroscopic strain of 0.15% is created in Pt nanoparticles under a voltage difference of 0.6 V, and this was attributed to the modification in metal bonding resulting from the E-induced change in the surface electron density at the Fermi level E_F.

In metallic systems that show itinerant electron magnetism, the material's intrinsic magnetic properties are primarily determined by unpaired *d* electrons with energies close to E_F. It is expected that these properties will be affected by changing the electron density at E_F under E. We selected $L1_0$-ordered FePt and FePd ultrathin films, because these compounds combine high T_C (750 K), saturation magnetization (1.4 T), and K_U (6.6 MJ/m^3 in FePt and 1.8 MJ/m^3 in FePd) values and exhibit high coercivity. In addition, these compounds are chemically stable.

Epitaxial films of FePt and FePd (2 and 4 nm thick) were grown by means of Pt and Pd buffer layers, respectively, on MgO(001) substrates (*8*). The superstructure lines as seen by x-ray diffraction indicate that the alloy crystallizes in the $L1_0$ phase, with the Fe and Pt (or Fe and Pd) atoms being highly ordered on their two respective crystallographic sites. All films exhibit the magnetic easy axis perpendicular to the layer plane with anisotropy fields in excess of 8 and 2.5 T, as expected for the tetragonal $L1_0$ FePt and FePd compounds, respectively (*8*).

The effect of E on the alloy magnetic properties was observed at room temperature by measurements of the magnitude of the signal and coercive field (H_C) via the polar Kerr effect. For these measurements, the electrolyte propylene carbonate (PC) was chosen to prevent hydrogen formation and its diffusion into the film when a negative potential was applied to the sample. Traces of water in the electrolyte were removed by introducing small Na pieces, which at the same time provided the Na^+ ions necessary for the

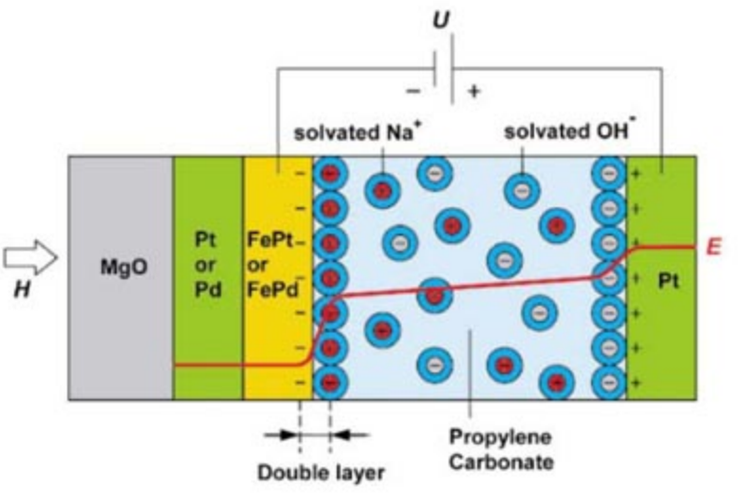

Fig. 1. Schematic of the electrolytic cell containing the FePt or FePd film within an applied magnetic field H. The potential profile E due to the applied potential U is indicated by the red line. The potential drop at the Pt electrode side is much lower (as compared to that of the sample surface) as a result of the Pt electrode's large surface area.

[1]Institut Néel, 25 Avenue des Martyrs, Boite Postale 166, F-38042 Grenoble Cedex 9, France. [2]IFW Dresden, Institute for Metallic Materials, Post Office Box 27 01 16, D-01171 Dresden, Germany. [3]Département de Recherche Fondamentale sur la Matière Condensée, Service de Physique des Matériaux et Microstructures, CEA Grenoble, 17 Avenue des Martyrs, F-38054 Grenoble Cedex 9, France. [4]Laboratoire d'Electrochimie de Physicochimie des Materiaux et des Interfaces, Ecole Nationale Superieure d'Electrochimie et d'Electrometallurgie, 1130 Rue de la Piscine, Boîte Postale 75, F-38402 Saint Martin d'Hères Cedex, France.

*Present address: AMD Saxony LLC and Company KG, Materials Analysis Department, Wilschdorfer Landstrasse 101, D-01109 Dresden, Germany.

†To whom correspondence should be addressed. E-mail: martin.weisheit@amd.com

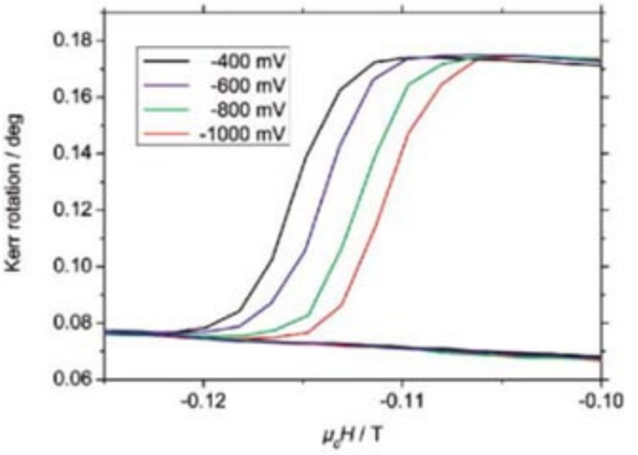

Fig. 2. Magnetization switching of the 2-nm-thick FePt film for different U values between the film and the Pt counter electrode. μ_0, the permeability of vacuum.

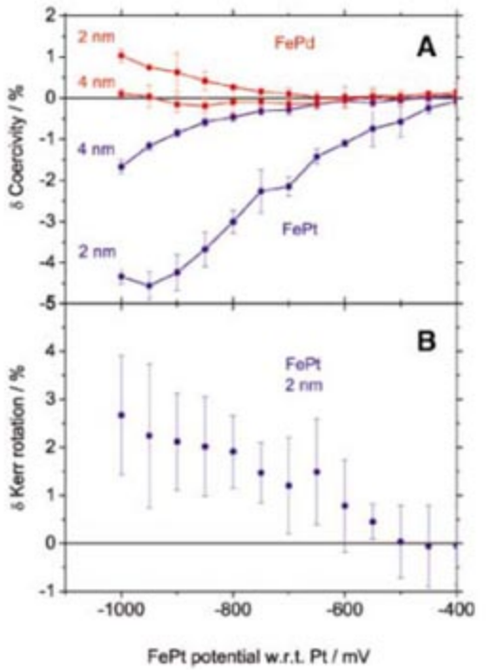

Fig. 3. (**A**) Change of the film coercivity for FePt and FePd with external voltage at given thicknesses and (**B**) change of the Kerr rotation for the 2-nm-thick FePt film with regard to (w.r.t.) the value at −400 mV. Error bars indicate the statistical variation (σ) of the measurements.

formation of the electrolytic double layer at the sample surface. A large sheet of inert Pt was used as the counter electrode (Fig. 1).

The H_C variation as a function of the applied voltage U was derived from the measurements of the easy-axis hysteresis loops (Fig. 2). A sharp switching of the magnetization occurs at H_C. To avoid possible dissolution of Fe from the alloy, we maintained the sample potential at or lower than –400 mV. The potential was also restricted to values above –1 V in order to avoid other electrochemical reactions at the film surface. Small but detectable irreversible film degradation occurred above –400 mV and below –1 V. Figure 3 shows the coercivity change δH_C (relative to the value at –400 mV) versus U for FePt and FePd. A change of voltage $\Delta U = -600$ mV results in a δH_C by –4.5% for FePt and +1% for FePd films with a thickness of 2 nm. The 4-nm-thick films show a lower variation of –1% for FePt and no variation (within experimental resolution) for FePd. The observed change in H_C as a function of U was essentially reversible, and the Kerr signal variation with magnetic field was the same upon increasing E as upon decreasing it. Both results imply that the observed effect is intrinsic and not due to film contamination or degradation that would be associated with the occurrence of irreversible phenomena (*8*). Note that δH_C is stronger than a linear response in all cases.

In addition to the effect of E on the coercivity, an increase in the Kerr rotation by 3% is observed upon changing U from –400 to –1000 mV for the 2-nm-thick FePt film. Within experimental accuracy, no such effect was found in the other samples.

The results reveal that the magnetic properties of itinerant electron magnetic systems can be changed in a controlled way under E. During the measurements, the film microstructure is expected to remain essentially unaltered (to the extent that the very slow irreversible film degradation can be neglected), and, to first-order approximation, the coercivity can be assumed to be directly proportional to the K_U from which it originates. The observed δH_C values were evaluated with respect to K_U energies (MAE) derived from electronic structure calculations (*9*). A capacitance value C per surface area A of $C/A = 30\ \mu F/cm^2$ was used, because this is a typical value for a clean metal surface in an electrolyte such as PC that is characterized by a large dielectric constant $k = 66$ (*10*). Under a voltage U that acts almost exclusively at the FePt/PC interface because of the 30 times larger surface area of the Pt counter electrode as compared to the sample surface, a charge CU accumulates in the whole film volume Ad, where d is the film thickness. Considering that the volume of the $L1_0$ FePt or FePd primitive cell is $V_{cell} = a^2c/2 = 0.027\ nm^3$, where a is 0.385 nm and c is 0.371 nm, the charge variation per unit cell becomes

$$q = \frac{CU}{Ad} V_{cell} \qquad (1)$$

In particular, for $U = 600$ mV and $d = 2$ nm, this amounts to 0.015 electrons per unit cell. From electronic structure calculations (*9*), a decrease of the MAE by 200% per electron is predicted for FePt and an increase of the MAE by 70% per electron is predicted for FePd. This result corresponds to expected changes of –3% and +1% for 2-nm-thick FePt and FePd, respectively. The induced excess charge in such metallic films is concentrated close to the surface and not distributed homogeneously. However, to first-order approximation, the anisotropy variation depends solely on the total film excess charge. This is a direct consequence of the linearity of all operations (i.e., it does not make a difference whether an anisotropy distribution is calculated first and then averaged over the whole film or whether the electron distribution is averaged right away).

The sign and magnitude of δH_C that was measured agree well with the calculations for both alloys. It is quite notable that this simple concept is sufficient to explain the experimental results. Considering that we are dealing with ultrathin films, surface anisotropy should be included in the comparison between the experiment and calculation. However, neither experimental nor calculated data are available on the surface anisotropy of FePt. As a very qualitative argument, it may be argued that surface anisotropy in FePt is not expected to be dominant to the same extent as it is in cubic systems where surface symmetry breaking is the only source for the occurrence of a second-order anisotropy term. It has been shown (*11*) that there is only a weak thickness dependence of the nucleation field in FePt down to 2 nm, which supports this assumption.

The fact that the voltage dependence of the coercivity is stronger than a linear response can be attributed to a change in the thickness of the electrolytic double layer with U: When the charge is increased at the sample surface, the double layer is compressed and, in turn, C and E acting on the sample are increased.

Because the Kerr angle is another intrinsic material property, its variation (detected in FePt only) upon the application of a voltage is another proof of the influence of E on the magnetic properties. However, in the absence of any calculated data, it is not possible to discuss the importance of the observed effect any further.

Our results have shown that the magnetic properties of thin-film ferromagnetic systems can be varied in a controlled way by an applied electric field. It must be stressed that the majority of modern magnetic materials belong to this category of materials. Beyond this proof of principle, this approach could offer an alternative and attractive generic actuation mechanism for electronic and electromechanical systems.

References and Notes

1. H. Ohno *et al.*, *Nature* **408**, 944 (2000).
2. D. Chiba, M. Yamanouch, F. Matsukura, H. Ohno, *Science* **301**, 943 (2003).

3. J. Hemberger *et al.*, *Nature* **434**, 364 (2005).
4. N. Hur *et al.*, *Nature* **429**, 392 (2004).
5. H. Gleiter, J. Weissmüller, O. Wollersheim, R. Würschum, *Acta Mater.* **49**, 737 (2001).
6. See, for example, the special issue on double layer modeling: *Electrochim. Acta* **41**, 2069 (1996).
7. J. Weissmüller *et al.*, *Science* **300**, 312 (2003).
8. Materials and methods are available as supporting material on *Science* Online.
9. G. H. O. Daalderop, P. J. Kelly, M. F. H. Schuurmans, *Phys. Rev. B* **44**, 12054 (1991).
10. Y. Chernyak, *J. Chem. Eng. Data* **51**, 416 (2006).
11. S. Okamoto *et al.*, *Phys. Rev. B* **67**, 094422 (2003).
12. We thank the Joseph Fourier University in Grenoble and the French Ministry of National Education for financial support. Part of this work was also supported by the Deutsche Forschungsgemeinschaft under grant FA 453/1.

Supporting Online Material
www.sciencemag.org/cgi/content/full/315/5810/349/DC1
Materials and Methods
Figs. S1 to S3
References

23 October 2006; accepted 30 November 2006
10.1126/science.1136629

Ultralow Thermal Conductivity in Disordered, Layered WSe_2 Crystals

Catalin Chiritescu,[1] David G. Cahill,[1]* Ngoc Nguyen,[2] David Johnson,[2] Arun Bodapati,[3] Pawel Keblinski,[3] Paul Zschack[4]

The cross-plane thermal conductivity of thin films of WSe_2 grown from alternating W and Se layers is as small as 0.05 watts per meter per degree kelvin at room temperature, 30 times smaller than the *c*-axis thermal conductivity of single-crystal WSe_2 and a factor of 6 smaller than the predicted minimum thermal conductivity for this material. We attribute the ultralow thermal conductivity of these disordered, layered crystals to the localization of lattice vibrations induced by the random stacking of two-dimensional crystalline WSe_2 sheets. Disordering of the layered structure by ion bombardment increases the thermal conductivity.

Materials with the lowest thermal conductivity are typically found among electrically insulating amorphous solids and glasses. In these materials, heat conduction is adequately predicted by a simple phenomenological model, the minimum thermal conductivity, in which heat conduction is described by a random walk of vibrational energy on the time and length scales of atomic vibrations and interatomic spacings (*1*). More sophisticated theories of heat conduction in disordered materials support this description: A majority of the vibrational modes [termed "diffusons" by Allen and Feldman (*2*)] carry heat in this manner, and only a small fraction of the vibrational modes propagate as waves or are localized and therefore unable to contribute to heat conduction. Recently, we (*3*) and others (*4*) have shown that the minimum thermal conductivity can be circumvented in multilayer thin films of metals and oxides. When the spacing between the interfaces is only a few nanometers, the thermal resistance of the interfaces reduces the thermal conductivity far below the thermal conductivity of the homogeneous amorphous oxide.

Here, we demonstrated by both experiment and computer simulation an alternative route for achieving ultralow thermal conductivity in a dense solid. The thermal conductivity of disordered thin films of the layered crystal WSe_2 can be as small as 0.05 W m^{-1} K^{-1}, a factor of 6 smaller than the predicted minimum thermal conductivity and, to the best of our knowledge, the lowest thermal conductivity ever observed in a fully dense solid. Disruption of the layered structure and the crystallinity of the WSe_2 sheets by ion irradiation actually produces a marked increase in the thermal conductivity of the thin film. Thus, the lowest thermal conductivities are not found in the fully amorphous form of WSe_2; rather, ultralow thermal conductivity is achieved by controlling both order and disorder, and hence the thermal pathways, in this anisotropic material.

We synthesized WSe_2 thin films by the modulated elemental reactants method (*5*, *6*). Sequential bilayers of W and Se were deposited in an ultrahigh vacuum chamber onto unheated Si (100) wafers with a stoichiometry of 1:2 and then annealed for 1 hour at elevated temperatures in N_2 atmosphere to form the desired layered structures (*6*). The microstructure of the films was stable at room temperature. In the WSe_2 structure, a hexagonal plane of W atoms is bonded to two Se layers by strong covalent-ionic bonds, and each two-dimensional (2D) WSe_2 sheet is bonded to adjacent sheets by weaker van der Waals forces (*7*, *8*). We purchased a single crystal of WSe_2 from Nanoscience Instruments to provide a baseline for comparisons. Thermal conductivity was measured by time-domain thermoreflectance (TDTR) (*6*, *9*–*12*). In our implementation of TDTR, we determine the thermal conductivity by comparing the time dependence of the ratio of the in-phase V_{in} and out-of-phase V_{out} signals from the radio-frequency lock-in amplifier to calculations made with the use of a thermal model (*11*). The thermal model has several parameters, but the thermal conductivity of the WSe_2 sample is the only important unknown.

We used synchrotron x-ray diffraction to characterize the microstructure of a typical WSe_2 film (Fig. 1). Data for (0 0 L) reflections (*6*) showed that the layering of the 2D WSe_2 sheets was very precise; the surface normal to each sheet (hexagonal *c* axis) was well aligned with the surface normal of the substrate, and the spacing between the centers of WSe_2 sheets was highly uniform at 0.66 nm. These highly textured films had completely random crystalline orientation in the *a*-*b* plane. We examined the crystalline structure of the film by scanning the diffraction intensity through reciprocal space where the (1 0 3) reflection intersected the Ewald sphere. The relatively narrow line width (0.06 in reciprocal lattice units) in the direction parallel to the surface, [h 0 3], gave a lateral coherence length of 23 nm (Fig. 1C). Scans through the

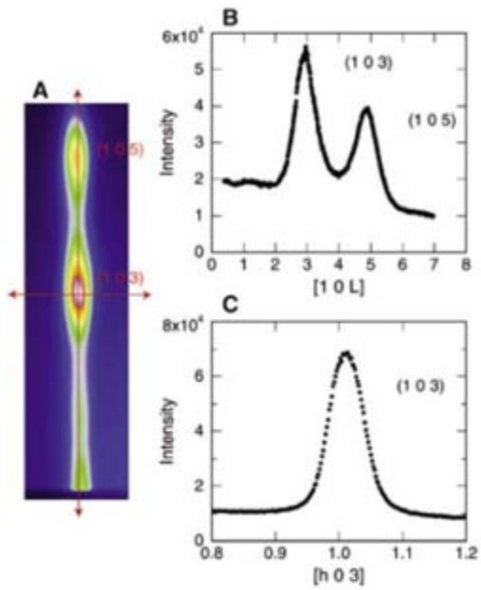

Fig. 1. X-ray diffraction data for a 32.5-nm-thick WSe_2 film collected at the 33–bending magnet beamline of the Advanced Photon Source with the use of 18.5-keV photons. After deposition, the WSe_2 film was annealed for 1 hour at 650°C in a N_2 atmosphere. (**A**) False-color depiction of the x-ray diffraction intensities collected by the area detector in the vicinity of the (1 0 3) and (1 0 5) reflections. The vertical direction is normal to the sample surface and the horizontal direction is in the plane of the sample. (**B**) Scan of the x-ray diffraction intensities along the surface normal. The scan direction is shown as the vertical red line in (A). (**C**) Scan of the x-ray diffraction in the in-plane direction. The scan direction is shown as the horizontal red line in (A).

[1]Department of Materials Science and Engineering, Frederick Seitz Materials Research Laboratory, University of Illinois, Urbana, IL 61801, USA. [2]Department of Chemistry, University of Oregon, Eugene, OR 97403, USA. [3]Department of Materials Science and Engineering, Rensselaer Polytechnic Institute, Troy, NY 12180, USA. [4]Advanced Photon Source, Argonne National Laboratory, Argonne, IL 60439, USA.

*To whom correspondence should be addressed. E-mail: d-cahill@uiuc.edu

intersection of (1 0 L) reflections with the Ewald sphere probed the coherence of the crystal structure along the direction normal to the WSe_2 sheets. The large line widths (Fig. 1B) indicated that crystallographic ordering in the stacking of the WSe_2 sheets was limited to <2 nm.

We next compared the thermal conductivity of annealed WSe_2 films to the conductivity of a single crystal of WSe_2 and the predicted minimum thermal conductivity (Fig. 2). The thermal conductivity of single-crystal WSe_2 was approximately proportional to $1/T$ (the reciprocal of absolute temperature), as expected for a dielectric or semiconductor in which heat transport is dominated by phonons with mean-free paths limited by anharmonicity. Calculations of the minimum thermal conductivity require knowledge of the number density of atoms and the speed of sound (*1*). We used picosecond acoustics to measure the longitudinal speed of sound in the cross-plane direction of nominal 360-nm-thick films and found that $v_L = 1.6$ nm ps^{-1} (*13*, *14*). This measurement is in good agreement with an independent measurement of the same film ($v_L = 1.7$ nm ps^{-1}) with the use of picosecond interferometry (*15*) and an index of refraction at the laser wavelength of 800 nm of $n = 4.13$. If we use the average of these values, $v_L = 1.65$ nm ps^{-1}, and a mass density of $\rho = 9.2$ g cm^{-3}, we obtain an elastic constant $C_{33} = 25$ GPa, which is approximately a factor of 2 smaller than C_{33} for single crystals of $NbSe_2$ and $TaSe_2$ measured by neutron scattering (*16*) and single-crystal WSe_2 measured by picosecond interferometry. The transverse speed of sound v_T is not accessible to the standard methods of picosecond acoustics; instead, we estimated $v_T = 1.15$ based on our measurement of v_L and the ratio C_{44}/C_{33} previously measured for $NbSe_2$ and $TaSe_2$ (*16*).

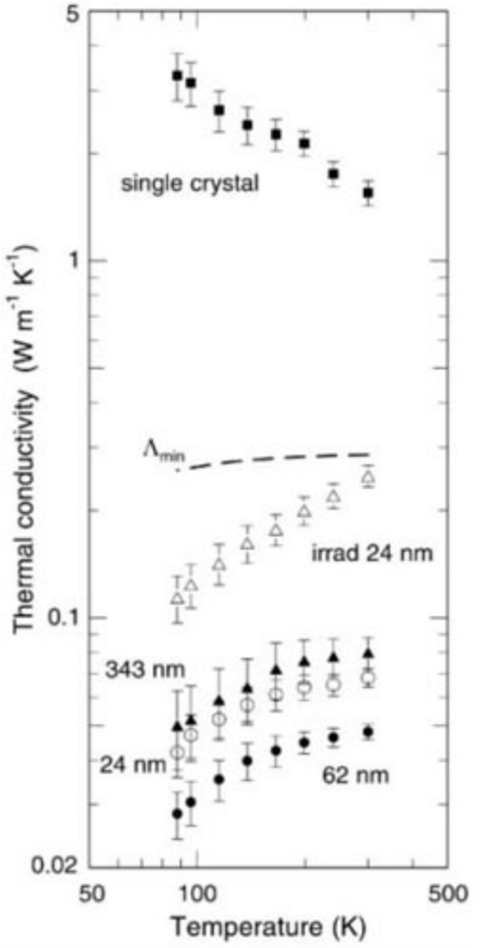

Fig. 2. Summary of measured thermal conductivities of WSe_2 films as a function of the measurement temperature. Each curve is labeled by the film thickness. Data for a bulk single crystal are included for comparison. Error bars are the uncertainties propagated from the various experimental parameters used to analyze the data (*6*). The ion-irradiated sample (irrad) was subjected to a 1-MeV Kr^+ ion dose of 3×10^{15} cm^{-2}. The dashed line marked Λ_{min} is the calculated minimum thermal conductivity for WSe_2 films in the cross-plane direction.

The lowest thermal conductivity, Λ, measured at 300 K is $\Lambda = 0.048$ W m^{-1} K^{-1} for a 62-nm-thick WSe_2 film, 30 times smaller than the cross-plane thermal conductivity of a single-crystal sample of WSe_2 (Fig. 2) and a factor of 6 smaller than the predicted minimum thermal conductivity. This degree of deviation from the predicted minimum thermal conductivity in a homogeneous material is unprecedented (*17*). Notably, the conductivity of the 62-nm-thick film is smaller than the conductivity of a thinner film (24 nm) or a thicker film (343 nm). The reasons for these differences are not understood in detail, but we speculate that variations in the degree of crystallographic ordering along the thickness of the films are playing an important role.

The data shown in Figs. 1 and 2 lead us to conclude that the ultralow thermal conductivities are produced by random stacking of well-crystallized WSe_2 sheets. To test this idea, we used irradiation by energetic heavy ions to disrupt the crystalline order in the thin film samples (Fig. 3). Because our TDTR measurements require knowledge of the thermal conductivity of the substrate, bare silicon substrates were irradiated with the same range of ion fluences and measured by TDTR (*6*). At the highest ion dose, 3×10^{15} ions cm^{-2}, we observed a factor of 5 increase in the thermal conductivity of the WSe_2 film. This increase in thermal conductivity with ion beam damage is also unprecedented. We inferred from these experiments that ion-induced damage introduces disorder that reduces localization of vibrational energy and enhances the transfer of vibrational energy in the material.

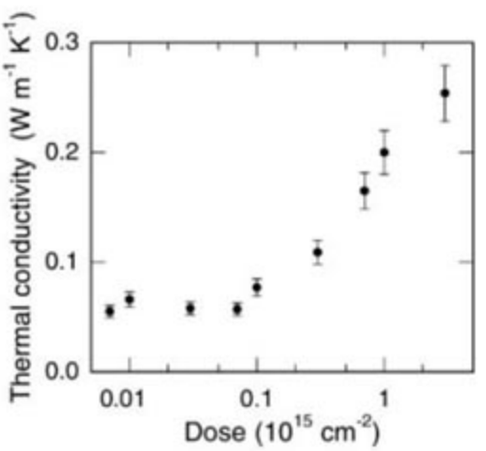

Fig. 3. Thermal conductivity versus irradiation dose for WSe_2 films 26 nm thick. Samples were irradiated with 1-MeV Kr^+ ions to the dose indicated on the *x* axis of the plot. Error bars are the uncertainties propagated from the various experimental parameters used to analyze the data (*6*).

To gain further insight and confidence in our experimental results, we performed molecular dynamics (MD) simulations on model structures. For simplicity and computational efficiency, the atomic interactions in our model compound are described by 6-12 Lennard-Jones potentials:

$$U(r) = 4\varepsilon\left[\left(\frac{\sigma}{r}\right)^{12} - \left(\frac{\sigma}{r}\right)^{6}\right] \quad (1)$$

where ε is the energy scale and σ is the length scale. Two sets of ε and σ parameters were used: For interactions within a single WSe_2 sheet, $\varepsilon = 0.91$ eV and $\sigma = 2.31$ Å, and for the interaction between layers, $\varepsilon = 0.08$ eV and $\sigma = 3.4$ Å. These parameters achieved a good fit to WSe_2 crystal structure and the C_{11} (200 GPa) and C_{33} (50 GPa) elastic constants. For computation efficiency, a cutoff of 5.4 Å was used, with both energy and forces shifted such that they were zero at the

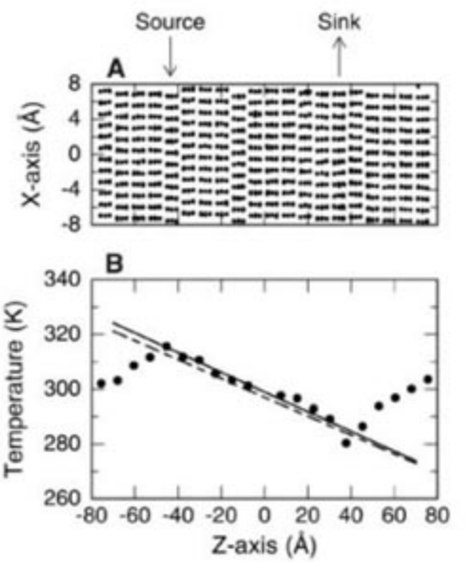

Fig. 4. (**A**) Atomic positions in a model WSe_2 structure showing stacking disorder. The positions of the heat sink and source separated by 8 nm are indicated. (**B**) The steady-state temperature profile obtained from the nonequilibrium, heat source–sink method. The solid line depicts a linear fit to the central region between the heat source and sink. The dashed line is an analogous fit but for the structure with doubled size along the *z* direction with the corresponding separation between the heat source and sink of 16 nm.

cutoff (*18*). The cross-sectional area of the simulation cell is 15.3 × 13.3 Å. Along the (001) direction, two sizes were selected: 160 and 320 Å. Periodic boundary conditions were used for all directions. Newton's equations of motions were solved by the fifth-order predictor corrector algorithm (*18*) with an MD time step, $\Delta t = 1.8 \times 10^{-15}$ s.

The simulation cell for the thermal transport measurement is depicted in Fig. 4. To calculate the thermal conductivity, the we first equilibrated the structure at $T = 300$ K for 100,000 MD time steps. Next, the global thermostat was turned off and thermal energy was added to one WSe_2 sheet and removed from a second sheet, which was located at a distance from the first sheet equal to one-half of the size of the simulation cell along the (001) direction (*19*, *20*). Atomic velocities were scaled such that heat was added or subtracted at a constant rate, 10^{-6} eV per MD time step (*21*). We monitored the temperature profile by averaging the kinetic energy of atoms in each WSe_2 sheet. Because of the small energy barrier for shearing of the WSe_2 structure and the small cross-sectional area of the simulation cell, our model structures exhibited thermally excited local shearing events leading to disorder in the stacking of the WSe_2 sheets (Fig. 4).

After 5 to 20 million MD steps (depending on the system size), a steady-state temperature distribution was established (Fig. 4). The temperature gradient, and thus the thermal conductivity, of 16- and 32-nm-long simulation cells were essentially the same within the statistical standard deviation of 10%, $\Lambda = 0.06$ W m^{-1} K^{-1}. Given the approximate form of the potentials used in our computational work, the agreement between the measured and calculated thermal conductivities was better than we expected. Nevertheless, the low thermal conductivity of the model structure suggests that the ultralow thermal conductivity in disordered, layered crystals is a general phenomenon and not restricted to WSe_2.

Our WSe_2 films are poor electrical conductors in the cross-plane direction; however, if semiconductors with similar structural features and good electrical mobility can be identified, disordered layered crystals may offer a promising route to improved materials for thermoelectric energy conversion.

References and Notes

1. D. G. Cahill, S. K. Watson, R. O. Pohl, *Phys. Rev. B* **46**, 6131 (1992).
2. P. B. Allen, J. L. Feldman, *Phys. Rev. B* **48**, 12581 (1993).
3. R. M. Costescu, D. G. Cahill, F. H. Fabreguette, Z. A. Sechrist, S. M. George, *Science* **303**, 989 (2004).
4. Y. S. Ju, M.-T. Hung, M. J. Carey, M.-C. Cyrille, J. R. Childress, *Appl. Phys. Lett.* **86**, 203113 (2005).
5. S. Moss, M. Noh, K. H. Jeong, D. H. Kim, D. C. Johnson, *Chem. Mater.* **8**, 1853 (1996).
6. Materials and methods are available as supporting material on *Science* Online.
7. W. J. Schutte, J. L. De Boer, F. Jellinek, *J. Solid State Chem.* **70**, 207 (1987).
8. J. A. Wilson, A. D. Yoffe, *Adv. Phys.* **18**, 193 (1969).
9. C. A. Paddock, G. L. Eesley, *J. Appl. Phys.* **60**, 285 (1986).
10. R. J. Stoner, H. J. Maris, *Phys. Rev. B* **48**, 16373 (1993).
11. D. G. Cahill, *Rev. Sci. Instrum.* **75**, 5119 (2004).
12. D. G. Cahill, F. Watanabe, *Phys. Rev. B* **70**, 235322 (2004).
13. K. E. O'Hara, X. Hu, D. G. Cahill, *J. Appl. Phys.* **90**, 4852 (2001).
14. H. T. Grahn, H. J. Maris, J. Tauc, *IEEE J. Quantum Electron.* **25**, 2562 (1989).
15. H.-N. Lin, R. J. Stoner, H. J. Maris, J. Tauc, *J. Appl. Phys.* **69**, 3816 (1991).
16. D. E. Moncton, J. D. Axe, F. J. DiSalvo, *Phys. Rev. B* **16**, 801 (1977).
17. P. A. Medwick, R. O. Pohl, *J. Solid State Chem.* **133**, 44 (1997).
18. M. P. Allen, D. J. Tildesley, *Computer Simulation of Liquids* (Oxford Univ. Press, New York, 1987).
19. A. Maiti, G. D. Mahan, S. T. Pantelides, *Solid State Commun.* **102**, 517 (1997).
20. P. K. Schelling, S. R. Phillpot, P. Keblinski, *Phys. Rev. B* **65**, 144306 (2002).
21. P. Jund, R. Jullien, *Phys. Rev. B* **59**, 13707 (1999).

22. Supported by Office of Naval Research grant nos. N00014-05-1-0250 and N00014-96-0407. Research for this work was performed in the Laser and Spectroscopy Facility and the Center for Microanalysis of Materials of the Frederick Seitz Materials Research Laboratory, University of Illinois, which is partially supported by the U.S. Department of Energy under grant DEFG02-91-ER45439. Use of the Advanced Photon Source was supported by the U.S. Department of Energy, Office of Science, Office of Basic Energy Sciences, under contract no. W-31-109-ENG-38.

Supporting Online Material

www.sciencemag.org/cgi/content/full/1136494/DC1
Materials and Methods
Figs. S1 to S5
References

19 October 2006; accepted 4 December 2006
Published online 14 December 2006;
10.1126/science.1136494
Include this information when citing this paper.

Organic Glasses with Exceptional Thermodynamic and Kinetic Stability

Stephen F. Swallen,[1] Kenneth L. Kearns,[1] Marie K. Mapes,[1] Yong Seol Kim,[1] Robert J. McMahon,[1] M. D. Ediger,[1]* Tian Wu,[2] Lian Yu,[2] Sushil Satija[3]

Vapor deposition has been used to create glassy materials with extraordinary thermodynamic and kinetic stability and high density. For glasses prepared from indomethacin or 1,3-bis-(1-naphthyl)-5-(2-naphthyl)benzene, stability is optimized when deposition occurs on substrates at a temperature of 50 K below the conventional glass transition temperature. We attribute the substantial improvement in thermodynamic and kinetic properties to enhanced mobility within a few nanometers of the glass surface during deposition. This technique provides an efficient means of producing glassy materials that are low on the energy landscape and could affect technologies such as amorphous pharmaceuticals.

Glassy materials combine the disordered structure of a liquid with the mechanical properties of a solid. Amorphous systems can be described in terms of a potential energy landscape, with thermodynamics and kinetics controlled by the minima and barriers on the landscape, respectively (*1*–*3*). Many important issues could be addressed if liquids or glasses with very low energies could be created (*2*, *4*–*6*). For example, it might be possible to definitively understand the Kauzmann entropy crisis, an area of intense recent interest (*1*, *7*–*11*). Kauzmann observed that if the entropy of many supercooled liquids is extrapolated to low temperature, the amorphous state is predicted to have a lower entropy than that of the highly ordered crystal well above absolute zero (*5*, *6*).

Glasses are usually prepared by cooling a liquid, but accessing low energy states by this route is impractically slow (*4*, *12*). If a liquid avoids crystallization as it is cooled, molecular motion eventually becomes too slow to allow the molecules to find equilibrium configurations. This transition to a nonequilibrium state defines the glass transition temperature T_g. Glasses are "stuck" in local minima on the potential energy landscape (*2*, *3*). Because glasses are thermodynamically unstable, lower energies in the landscape are eventually achieved through molecular rearrangements. However, this process is so slow that it is generally impossible to reach states deep in the landscape by this route.

We have discovered that vapor deposition can bypass these kinetic restrictions and produce glassy materials that have extraordinary energetic and kinetic stability and unusually high densities. We demonstrate this for two molecular glass formers: 1,3-bis-(1-naphthyl)-5-(2-naphthyl)benzene (TNB) (T_g = 347 K) and indomethacin (IMC) (T_g = 315 K). For these systems, the most stable glasses are obtained when vapor is deposited onto a substrate controlled near T_g – 50 K. We argue that surface mobility during the deposition process is the mechanism of stable glass formation.

Differential scanning calorimetry (DSC) was used to examine the kinetics and thermodynamics of vapor-deposited samples created by heating crystalline TNB or IMC in a vacuum. Figure 1A shows DSC data for TNB vapor-deposited (blue) onto a substrate held at 296 K.

[1]Department of Chemistry, University of Wisconsin–Madison, Madison, WI 53706, USA. [2]School of Pharmacy, University of Wisconsin–Madison, Madison, WI 53705, USA. [3]Center for Neutron Research, National Institute of Standards and Technology, Gaithersburg, MD 20899, USA.

*To whom correspondence should be addressed. E-mail: ediger@chem.wisc.edu

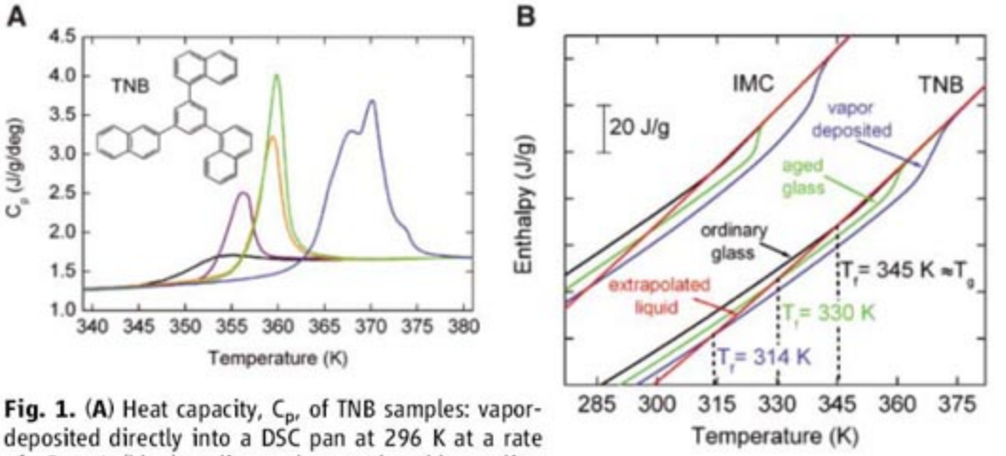

Fig. 1. (**A**) Heat capacity, C_p, of TNB samples: vapor-deposited directly into a DSC pan at 296 K at a rate of ~5 nm/s (blue); ordinary glass produced by cooling the liquid at 40 K/min (black); ordinary glass annealed at 296 K for 174 days (violet), 328 K for 9 days (gold), and 328 K for 15 days (green). (Inset) Structure of TNB. (**B**) Enthalpy of TNB and IMC samples. Heat capacities of the samples shown in (A) are integrated to obtain the curves shown for TNB. Similar experimental conditions were used for IMC (*15*).

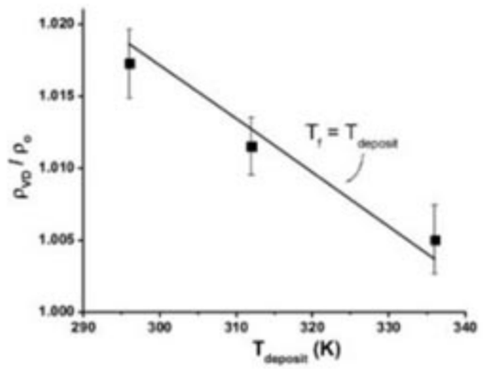

Fig. 2. Density of vapor-deposited TNB films (ρ_{VD}) normalized to the density of the ordinary glass (ρ_o), with both measured at room temperature. Experimental density ratios (filled squares) were calculated from x-ray reflectivity measurements on 100- to 300-nm films by measuring film thickness before and after annealing above T_g (*15*). The solid line indicates the expected density if the samples were prepared in thermal equilibrium with $T_f = T_{deposit}$.

This scan was continued beyond the melting point, after which the sample was cooled into the glass and then scanned again to yield the black curve. This latter curve represents the behavior of an ordinary glass of TNB, with T_g = 347 K, as defined by the onset temperature; it is consistent with previously reported results for TNB (*13*–*15*).

Remarkably, the vapor-deposited sample has a substantially higher onset temperature of 363 K. This result indicates that the vapor-deposited material is kinetically much more stable, because higher temperatures are required to dislodge the molecules from their glassy configurations. For comparison, we isothermally annealed the ordinary glass for 6 months at 296 K and up to 15 days at 328 K (equilibrium was reached at 328 K). Vapor-deposited samples created in only a few hours have much greater kinetic stability than ordinary glasses aged for many days or months below T_g.

To quantify the thermodynamic stability of the vapor-deposited materials, we calculate the fictive temperature (T_f), as defined below. Lower T_f values indicate a lower position in the energy landscape. The enthalpy for TNB and IMC samples, obtained by integrating the heat capacity C_p, is plotted in Fig. 1B. The intersection between these data and the extrapolated supercooled liquid enthalpy (red curve) defines T_f for each sample. For both TNB and IMC, samples prepared by vapor deposition have considerably lower enthalpies and T_f values. On the basis of aging experiments on TNB, we estimate that it would require at least 40 years of annealing an ordinary glass to match T_f for the vapor-deposited sample shown in Fig. 1 (*12*). The similarity of the results for TNB and IMC suggests that vapor deposition can generally produce highly stable glasses.

The thermodynamic stability of these films can also be quantified in comparison with the Kauzmann temperature (T_K), the temperature at which the extrapolated entropy of the supercooled liquid equals that of the crystal (*4*, *5*). We define a figure of merit:

$$\theta_K = \frac{T_g - T_f}{T_g - T_K} \qquad (1)$$

For fragile glassformers such as TNB and IMC, θ_K is a measure of position on the energy landscape, with a value of 1 ($T_f = T_K$) indicating the lowest possible position on the landscape. For TNB, Magill estimated T_K = 270 K (*14*). Vapor deposition of TNB at T_g – 50 K created films with θ_K = 0.43; by this measure, we have proceeded 43% toward the bottom of the energy landscape for amorphous configurations. In comparison, annealing the ordinary glass at 296 K (θ_K = 0.09) or 328 K (θ_K = 0.22) is relatively ineffective. Similar results were observed for IMC deposited at T_g – 50 K, with θ_K = 0.23 to 0.44, depending on deposition rate. These results can be put into context by comparison with Kovac's seminal aging experiments on poly(vinylacetate), where 2 months of annealing achieved $\theta_K \leq 0.17$ (*16*).

Vapor deposition can also create unusually dense glasses. The ratio of the density of vapor-deposited TNB (ρ_{VD}) to that of the ordinary glass (ρ_o, prepared by cooling from the liquid) increases as the deposition temperature is lowered toward T_g – 50 K (Fig. 2). Also shown as the solid line is a prediction of the density if vapor deposition produced an equilibrium supercooled liquid at the deposition temperature (*12*). For this range of deposition temperatures, our samples nearly achieve this upper bound for the density. If we define a fictive temperature based on density, deposition at 296 K produces $T_f \approx$ 300 K, slightly lower than the fictive temperature based on the enthalpy (*15*).

We have used neutron reflectivity to characterize diffusion in glasses of TNB. The high spatial resolution and large contrast in the scattering length of neutrons for hydrogen and deuterium nuclei make this an excellent technique for quantifying molecular motion. As schematically shown in the inset of Fig. 3, 300-nm films were prepared by alternately vapor-depositing 30-nm-thick layers of protio TNB (h-TNB) and deuterio TNB (d-TNB) (*17*). The specular reflectivity R was measured as a function of beam angle relative to the sample surface. This value, multiplied by q^4 for clarity, is plotted as a function of the wave vector q. Reflectivity curves for samples vapor-deposited at different temperatures display diffraction peaks; as expected for our symmetric multilayer samples, only odd diffraction orders are present. For samples deposited at low temperature, diffraction can be observed up to the 13th order, indicating very sharp h-TNB/d-TNB interfaces (*15*).

Time series of neutron reflectivity curves were obtained for two vapor-deposited samples during annealing at 342 K for samples deposited at 330 K (Fig. 4A) or 296 K (Fig. 4B). During 8 hours of annealing, all diffraction peaks (except the first-order peak) for sample A decayed to zero, indicating that substantial interfacial broadening had occurred because of interdiffusion of h-TNB/d-TNB. During the 16 hours of annealing at 342 K for sample B, no detectable interdiffusion occurred, even on the single-nanometer length scale. We emphasize that the only difference between these two samples was the temperature at which the substrate was held during deposition.

Figure 4A illustrates the behavior of an ordinary glass annealed near T_g; as shown elsewhere (*17*), interdiffusion in this sample is characteristic of the equilibrium liquid. In contrast, the sample deposited near T_g – 50 K (Fig. 4B) is kinetically much more stable, in qualitative agreement with the high onset temperature shown for the vapor-deposited sample in Fig. 1A. We can quantify the magnitude of this stability in terms of the equilibrium structural relaxation time

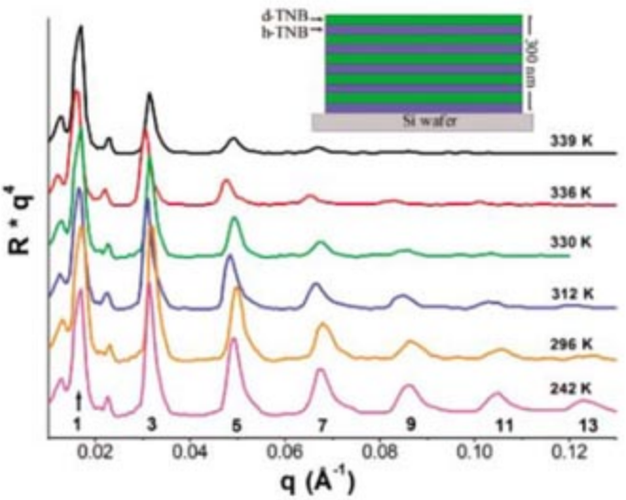

Fig. 3. Neutron reflectivity versus wave vector q for multilayer TNB films vapor-deposited at the specified temperatures. The peak intensities are determined by the sharpness of the h-TNB/d-TNB interfaces, which vary from 1.5 to 9 nm (full width at half maximum of the concentration profile derivative). The diffraction order of each peak is given by the numbers at the bottom. The inset illustrates the structure of the vapor-deposited sample (*15*).

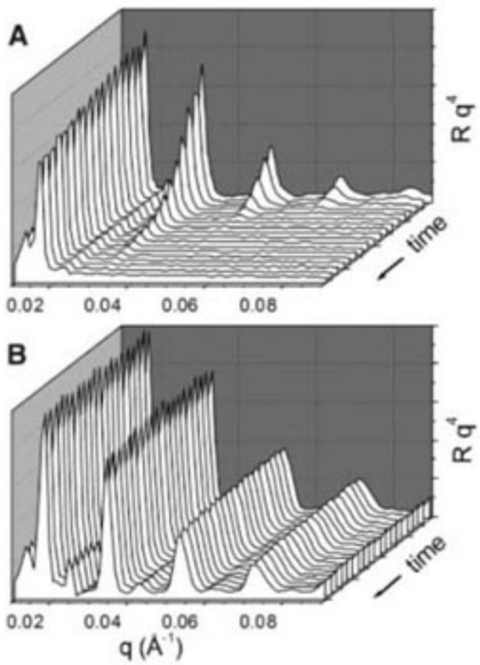

Fig. 4. Neutron reflectivity data for TNB multilayer films continuously annealed at 342 K. The substrate temperature during vapor deposition was (**A**) 330 K and (**B**) 296 K. The decay of the harmonic peaks in (A) occurred over 8 hours and is caused by bulk molecular diffusion (*17*). No detectible diffusion occurred in (B) over 16 hours (*15*).

τ_α, known to be 250 s at 342 K (*18*). The induction time for the sample deposited at $T_g - 50$ K exceeds 200 τ_α. Consistent with this result, we have observed in preliminary experiments that crystal growth rates in stable, vapor-deposited TNB glasses are slower than in ordinary glasses, although the former may contain crystal nuclei.

The reflectivity curves in Fig. 3 provide insight into the mechanism that allows vapor deposition to create unusually stable glasses. The average h-TNB/d-TNB interface widths of the as-deposited samples were extracted from fits to the raw data (*17*) and ranged from 9 nm for the sample deposited at 339 K to 1.5 nm for deposition at 242 K. For all samples deposited at 296 K or above, the interfacial width exceeds the surface roughness (~1.5 nm) as determined by x-ray and neutron reflectivity and the broadening estimated for bulk diffusion during the deposition process (*17*). Deposition at 242 K (T_g – 100 K) produced interfacial widths that are consistent with the surface roughness.

Because the h-TNB/d-TNB interface widths for deposition temperatures above 242 K cannot be explained by surface roughness or bulk diffusion, we tentatively attribute them to enhanced mobility within a few nanometers of the surface of a TNB glass. Such mobility would explain both the broad interfaces observed in the as-deposited samples and the unusually stable glasses formed by vapor deposition. At the deposition rates used in our experiments (0.1 to 5 nm/s), TNB molecules would be a part of the mobile surface layer for ~1 s before they are buried and become part of the bulk glass. If molecules at the surface can substantially rearrange in 1 s, they can find configurations that are near equilibrium configurations at the temperature of the substrate, even if the substrate is well below T_g.

This rapid configuration sampling at the surface would, in a layer-by-layer fashion, produce a bulk glass that is low in the energy landscape with unusually high density and kinetic stability. It would also produce the broad interfaces observed for deposition at temperatures of 296 K and above. Enhanced surface dynamics similar to those in our proposed mechanism have been recently reported. By measuring voltage changes induced by the motions of implanted ions, Cowin and co-workers deduced a marked decrease of the viscosity for the top 3 nm of thin films of supercooled 3-methylpentane (*19*). Numerous studies have found evidence for enhanced mobility at the surface of glassy polymer films (*20*–*23*).

The surface-mobility mechanism for the creation of unusually stable glasses is supported by an order-of-magnitude calculation. TNB samples vapor-deposited at 296 K have interface widths of 2.5 nm, clearly in excess of the width associated with surface roughness. We attribute the additional 1 nm of interface width to surface mobility and, given a deposition rate of 0.1 nm/s, the molecules are within the mobile surface layer for 10 s. Combining this length and time yields an estimate for the surface diffusion coefficient of 5×10^{-16} cm^2/sec. For bulk TNB, this diffusion coefficient is found near T_g, where the structural relaxation time τ_α is a few seconds (*17*, *18*). Thus, surface molecules plausibly remain mobile for several structural relaxation times before becoming buried, arguably long enough to find near-equilibrium configurations at 296 K.

Given the widespread use of vapor-deposition techniques, it is surprising that unusually stable glasses have not been reported previously. In fact, it is commonly reported that vapor-deposition creates low-density glasses with low kinetic and thermodynamic stability (*24*–*26*). As compared with many reported depositions of metallic and organic materials, we have used lower deposition rates and/or substrate temperatures that are nearer to T_g. We observe the creation of highly stable glasses only for substrate temperatures T_{dep}/T_g in the vicinity of 0.85. Additionally, we observe that increasing the deposition rate can considerably decrease the stability of the glasses formed. These observations are all consistent with our proposed mechanism: Faster deposition does not allow as much time for equilibration at the surface and, at low enough temperature, surface molecules will rearrange too slowly to equilibrate. Indeed, the metallic glass community has known for decades that fast, low-temperature deposition is required to prepare high-energy glasses that quench thermodynamically unstable mixtures (*27*).

We speculate that unusually stable glasses can be prepared for many systems that can be vapor-deposited, if surface mobility is enhanced and the substrate temperature is appropriately controlled. We anticipate that the availability of low-energy glasses prepared by vapor deposition and less general routes (*28*) will allow new insights into glass formation and the nature of the lower regions of the energy landscape. Stable glasses could also affect technologies such as amorphous pharmaceuticals, where stability against crystallization is required to retain the enhanced bioavailability of amorphous preparation.

References and Notes

1. C. A. Angell, *J. Res. Natl. Inst. Stand. Technol.* **102**, 171 (1997).
2. P. G. Debenedetti, F. H. Stillinger, *Nature* **410**, 259 (2001).
3. F. H. Stillinger, *Science* **267**, 1935 (1995).
4. M. D. Ediger, C. A. Angell, S. R. Nagel, *J. Phys. Chem.* **100**, 13200 (1996).
5. W. Kauzmann, *Chem. Rev.* **43**, 219 (1948).
6. F. H. Stillinger, *J. Chem. Phys.* **88**, 7818 (1988).
7. R. J. Speedy, *Biophys. Chem.* **105**, 411 (2003).
8. A. Saksaengwijit, J. Reinisch, A. Heuer, *Phys. Rev. Lett.* **93**, 235701 (2004).

9. H. Tanaka, *Phys. Rev. E* **68**, 011505 (2003).
10. D. H. Huang, S. L. Simon, G. B. McKenna, *J. Chem. Phys.* **119**, 3590 (2003).
11. D. V. Matyushov, C. A. Angell, *J. Chem. Phys.* **123**, 034506 (2005).
12. D. J. Plazek, J. H. Magill, *J. Chem. Phys.* **45**, 3038 (1966).
13. C. M. Whitaker, R. J. McMahon, *J. Phys. Chem.* **100**, 1081 (1996).
14. J. H. Magill, *J. Chem. Phys.* **47**, 2802 (1967).
15. Materials and methods are available as supporting material on *Science* Online.
16. A. J. Kovacs, *Fortschr. Hochpolym-Forsch.* **3**, 394 (1963).
17. S. F. Swallen *et al.*, *J. Chem. Phys.* **124**, 184501 (2006).
18. R. Richert, K. Duvvuri, L.-T. Duong, *J. Chem. Phys.* **118**, 1828 (2003).
19. R. C. Bell, H. F. Wang, M. J. Iedema, J. P. Cowin, *J. Am. Chem. Soc.* **125**, 5176 (2003).
20. C. J. Ellison, J. M. Torkelson, *Nat. Mater.* **2**, 695 (2003).
21. S. Kawana, R. A. L. Jones, *Phys. Rev. E* **63**, 021501 (2001).
22. J. L. Keddie, R. A. L. Jones, R. A. Cory, *Faraday Discuss.* **98**, 219 (1994).
23. J. A. Forrest, K. Dalnoki-Veress, J. R. Stevens, J. R. Dutcher, *Phys. Rev. Lett.* **77**, 2002 (1996).
24. F. Faupel *et al.*, *Rev. Mod. Phys.* **75**, 237 (2003).
25. K. Ishii, H. Nakayama, T. Okamura, M. Yamamoto, T. Hosokawa, *J. Phys. Chem. B* **107**, 876 (2003).
26. K. Takeda, O. Yamamuro, H. Suga, *J. Phys. Chem.* **99**, 1602 (1995).
27. D. Turnbull, *Metall. Mater. Trans. A* **12**, 695 (1981).
28. H. Tanaka, R. Kurita, H. Mataki, *Phys. Rev. Lett.* **92**, 025701 (2004).

29. We acknowledge support for this work from NSF CHE-0605136, NSF-0412707, and USDA 2005-01303.

Supporting Online Material

www.sciencemag.org/cgi/content/full/1135795/DC1
Materials and Methods
Fig. S1
References

2 October 2006; accepted 27 November 2006
Published online 7 December 2006;
10.1126/science.1135795
Include this information when citing this paper.

Unexpected Stability of Al_4H_6: A Borane Analog?

X. Li,[1] A. Grubisic,[1] S. T. Stokes,[1] J. Cordes,[1,2] G. F. Ganteför,[1,2] K. H. Bowen,[1]* B. Kiran,[3] M. Willis,[3] P. Jena,[3] R. Burgert,[4] H. Schnöckel[4]

Whereas boron has many hydrides, aluminum has been thought to exhibit relatively few. A combined anion photoelectron and density functional theory computational study of the $Al_4H_6^-$ anion and its corresponding neutral, Al_4H_6, showed that Al_4H_6 can be understood in terms of the Wade-Mingos rules for electron counting, suggesting that it may be a borane analog. The data support an Al_4H_6 structure with a distorted tetrahedral aluminum atom framework, four terminal Al-H bonds, and two sets of counter-positioned Al-H-Al bridging bonds. The large gap between the highest occupied and the lowest unoccupied molecular orbitals found for Al_4H_6, together with its exceptionally high heat of combustion, further suggests that Al_4H_6 may be an important energetic material if it can be prepared in bulk.

Even though aluminum and boron are sister elements in the periodic table, aluminum forms only a few hydrides, whereas boron has many, known as the boranes. The known hydride chemistry of aluminum is limited to AlH_3 and Al_2H_6, seen in cryogenic matrices (*1*, *2*) and perhaps the gas phase (*3*); alane, $(AlH_3)_n$, a polymeric solid; AlH_4^- and its alkali metal salts, the alanates, such as $LiAlH_4$ (*4*); $Al_{13}H^-$ formed in beams (*5*, *6*); and dissociative chemisorption products of $D_2 + Al_n^-$ interactions in beams (*7*). Boron hydrides, in contrast, exhibit a broad diversity of stoichiometries, such as B_2H_6, B_4H_{10}, B_5H_9, B_6H_{10}, and $B_{10}H_{14}$ (*8*–*11*). Given the electronic similarity between aluminum and boron, the lack of a comparable aluminum hydride chemistry is puzzling. Are analogous aluminum hydrides simply unstable under all circumstances, or might there be pathways by which they can be formed and environments in which they are stable?

We explored these questions by rapidly vaporizing aluminum metal in the presence of an abundant, albeit momentary, concentration of hydrogen atoms and the cooling environment of a fast helium gas expansion. These conditions were provided by a pulsed arc discharge source (PACIS) (*5*, *12*). The value of the PACIS source for studying aluminum cluster anion and hydrogen interactions was first realized by Ganteför and co-workers, who used it in photoelectron studies of HAl_{13}^- and similarly sized aluminum cluster anions, each with up to two hydrogen atoms attached (*5*). In our study, such a source provided a doorway into a much wider world of aluminum hydride cluster anions. In a PACIS source, a discharge is struck between an anode and a grounded, metallic sample cathode as helium gas from a pulsed valve flows through the discharge region (Fig. 1). When an extender tube is added to this arrangement, additional gases can be added downstream. In our study, the sample electrode was aluminum, and hydrogen gas was back-filled before each discharge event. Upon initiation of the pulsed discharge, a plasma containing hydrogen atoms (the latter formed by the dissociation of H_2) expanded down the extender tube, cooling, clustering, and reacting along the way. The resulting anions were then subjected to extraction and mass analysis by a time-of-flight mass spectrometer. Their mass spectra revealed that between 1 and 10 hydrogen atoms had been attached to each aluminum cluster anion size. A typical experiment in which aluminum cluster anions, Al_n^- (n = 3 to 20), were generated thus revealed roughly 200 previously unobserved aluminum hydride anions. A por-

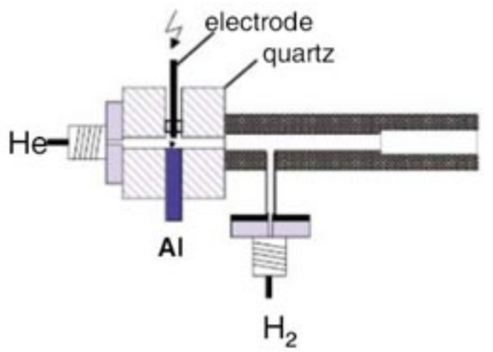

Fig. 1. Schematic diagram of a PACIS source.

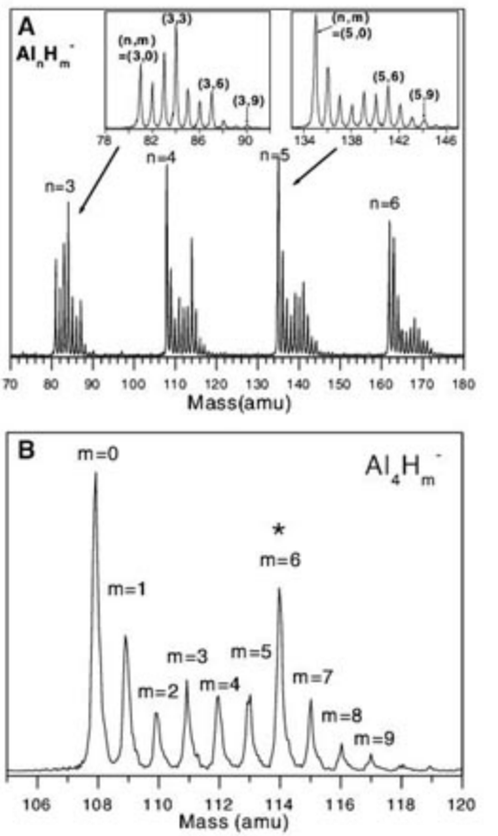

Fig. 2. (**A**) Mass spectrum showing the wide variety of $Al_nH_m^-$ anions that are formed with the PACIS source. Insets show magnified views of selected portions of the mass spectrum, revealing individual $Al_nH_m^-$ species. (**B**) A portion of the mass spectrum showing only the $Al_4H_m^-$ series.

[1]Departments of Chemistry and Materials Science, Johns Hopkins University, Baltimore, MD 21218, USA. [2]Department of Physics, University of Konstanz, 78457 Konstanz, Germany. [3]Department of Physics, Virginia Commonwealth University, Richmond, VA 23284, USA. [4]Institute of Inorganic Chemistry, University of Karlsruhe (TH), 76128 Karlsruhe, Germany.

*To whom correspondence should be addressed. E-mail: kbowen@jhu.edu

tion of such a mass spectrum is presented in Fig. 2A.

Although we have results on many of these species, we chose to introduce this new family of aluminum hydrides by focusing on $Al_4H_6^-$ and two similarly sized hydrides. Figure 2B, which highlights the $Al_4H_m^-$ portion of the aluminum hydride anion mass spectrum, shows that $Al_4H_6^-$ is a magic number species—i.e., a reproducibly intense mass peak relative to its neighbors. Most often, when a peak in a mass spectrum shows this behavior, the species represented by that peak is unusually stable. However, in the case of the anion, $Al_4H_6^-$, we saw no plausible reason for such special stability.

The explanation for its enhanced intensity lies in the photoelectron spectrum of $Al_4H_6^-$. Anion photoelectron spectroscopy was conducted by crossing a mass-selected anion beam with a fixed-frequency photon beam and analyzing the energy of the resultant photodetached electrons. The energetics are governed by the energy-conserving relationship, $h\nu = EBE + EKE$, where $h\nu$ is the photon energy, *EBE* is the electron binding energy, and *EKE* is the electron kinetic energy. $Al_4H_6^-$ anions were generated in a PACIS source as described above and mass-selected by a time-of-flight mass spectrometer. Their excess electrons were photodetached by 4.66-eV photons from the fourth harmonic of a neodymium-doped yttrium aluminum garnet (Nd:YAG) laser and then detected by a magnetic bottle electron energy analyzer (*13*).

The photoelectron spectrum of $Al_4H_6^-$ (Fig. 3A) displays two main features, a largely singular peak at $EBE \approx 1.4$ and two or more closely spaced peaks at higher *EBE* values. All of these peaks arise as a result of photodetachment transitions from the ground electronic state of the $Al_4H_6^-$ anion to the ground and excited electronic states of its corresponding neutral, Al_4H_6. Because the peak at lower *EBE* is due to the ground (anion)–to–ground (neutral) electronic transition, it provides a measurement of the adiabatic electron affinity (EA_a) of neutral Al_4H_6. The EA_a of Al_4H_6 was determined to be 1.25 ± 0.15 eV (where the error is the standard deviation). Also, the vertical detachment energy (*VDE*), which is the *EBE* value of the maxima in the lower-*EBE* peak, was found to be 1.35 ± 0.05 eV. It represents the maximum Franck-Condon overlap between the anion and its corresponding neutral at the structure of the anion. Of more interest, however, is the energy splitting between the lower peak and the first feature among the higher-*EBE* set of peaks. Within Koopmans' approximation, this value is the highest occupied molecular orbital–lowest unoccupied molecular orbital (HOMO-LUMO) gap of the anion's corresponding neutral—i.e., the HOMO-LUMO gap for Al_4H_6. Thus, the HOMO-LUMO gap of neutral Al_4H_6 is 1.9 eV. This very large HOMO-LUMO gap implies unusual stability. The HOMO-LUMO gap of C_{60}, for instance, is ~1.7 eV (*14*). The high stability of neutral Al_4H_6 suggests that it is particularly abundant, leading to enhanced $Al_4H_6^-$ anion formation. Thus, the high stability of neutral Al_4H_6 appears to be the reason for the magic number prominence of anionic $Al_4H_6^-$ in the mass spectrum. The high HOMO-LUMO gap of Al_4H_6 is put into further context by examining the photoelectron spectra of the species immediately adjacent in size, $Al_4H_5^-$ and $Al_4H_7^-$. Their photoelectron spectra are presented in Fig. 3, B and C, respectively. They each display much smaller HOMO-LUMO gaps than does Al_4H_6 (~0.4 and ~0 eV, respectively), showing that Al_4H_6 is indeed unusually stable in comparison with aluminum hydrides of similar stoichiometries.

Having found neutral Al_4H_6 to be a particularly stable species, we conducted electronic structure calculations to determine its structure and the nature of its bonding. These were done at the Density Functional Theory–Generalized Gradient Approximation level of theory using a PerdewWang91 exchange-correlation functional with triple zeta valence polarization basis sets (*15*, *16*). Geometries were optimized without symmetry constraints. Figure 4 presents the lowest energy structure of Al_4H_6 found by means of those calculations. The next higher-energy structures of $Al_4H_6^-$ and Al_4H_6 were 0.33 and 1.07 eV, respectively, above their respective lowest-energy structures. In the lowest-energy structure of Al_4H_6, the aluminum atom framework is a distorted tetrahedron with a terminal hydrogen atom bonded to each aluminum atom and with each of two hydrogen atoms forming counterpositioned bridging bonds across two aluminum atoms. Thus, there are four terminal hydrogen atoms (four Al-H bonds) and two bridging hydrogen atoms. The slight distortion of the aluminum framework's tetrahedral symmetry is due to the presence of the two sets of bridging bonds. These same calculations also gave energetic results that are in excellent agreement with those determined from the photoelectron spectrum of $Al_4H_6^-$. In particular, the calculations

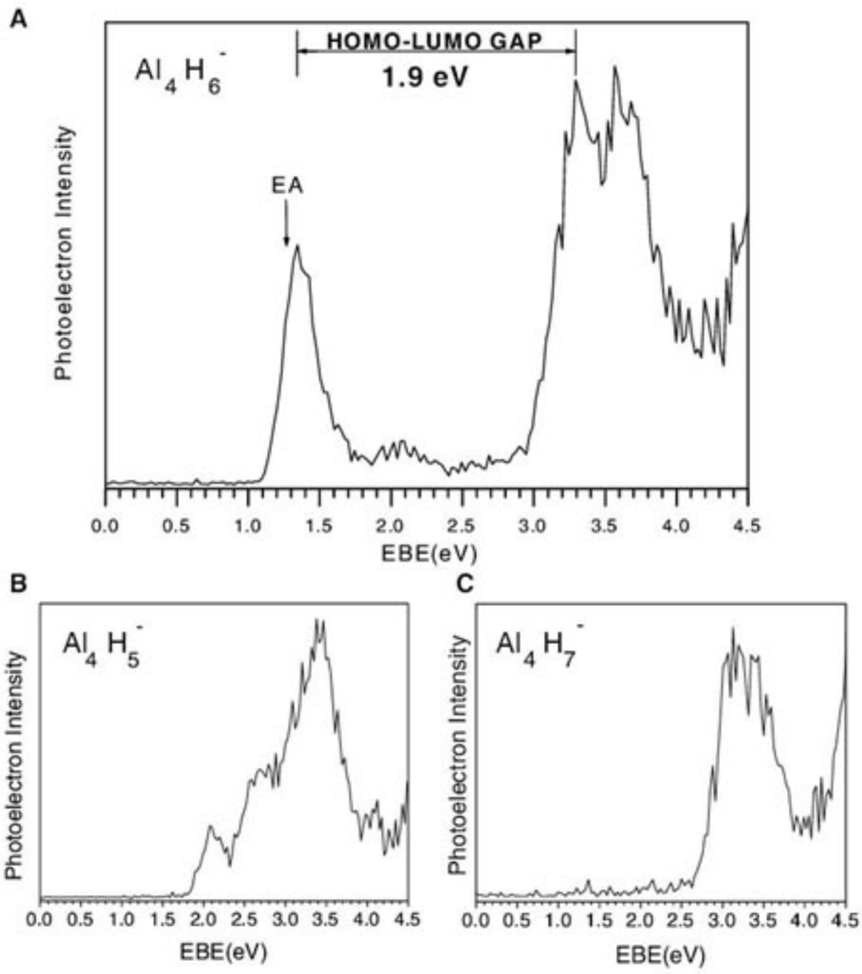

Fig. 3. The photoelectron spectra of (**A**) $Al_4H_6^-$, (**B**) $Al_4H_5^-$, and (**C**) $Al_4H_7^-$, all recorded with 4.66-eV photons.

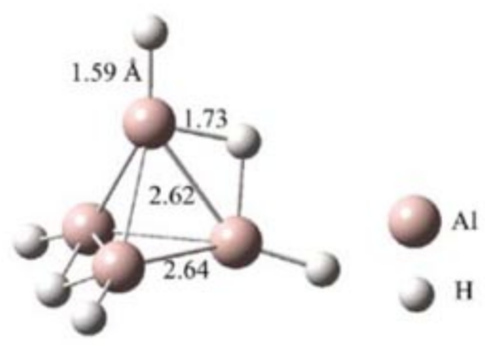

Fig. 4. The calculated structure of neutral Al_4H_6, shown to be a distorted tetrahedron.

predicted a *VDE* value of 1.48 eV and an EA_a value of 1.36 eV. The HOMO-LUMO gap was calculated using time-dependent density functional theory and was found to be 1.85 eV.

Because the structural features seen in Fig. 4 are reminiscent of those in boranes, it is natural to compare the structures of Al_4H_6 and B_4H_6. Although B_4H_6 has not been observed experimentally, calculations have predicted that its structure is the same as that of Al_4H_6 (*17*). Moreover, $B_4H_2R_4$ derivatives of B_4H_6 have been synthesized, and they too display the same structure as that of Al_4H_6 (*18*). Thus, the similarity of the calculated structure of neutral Al_4H_6 to that of boranes led us to investigate whether the Wade-Mingos rules, originally established to relate borane geometries to their electronic structures, might also be applicable to the aluminum hydride species we observed. The best known form of the Wade-Mingos rules (*10*, *19*–*24*) applies to closo-boranes of stoichiometry, $B_nH_n^{2-}$, which contain $(2n + 1)$ valence electron pairs. Of these, n pairs are required by the B-H terminal bonds, leaving $n + 1$ electron pairs for cage bonding. The Wade-Mingos $(n + 1)$ rule states that a borane with $n + 1$ electron pairs for boron cage bonding will have a structure based on an n-vertex polyhedron, such as $B_6H_6^{2-}$, which is an octahedron. In addition to the boranes, Wade-Mingos rules have been successful in relating electronic structure to geometric structure in numerous other classes of cluster compounds.

In exploring the application of Wade-Mingos rules to Al_4H_6, we treated it as $Al_4H_4^{2-}$, analogous to $B_nH_n^{2-}$, although formally Al_4H_6 should be written as $Al_4H_4^{2-} + 2H^+$ to account for all of the nuclei as well as the electrons. Treating Al_4H_6 as $Al_4H_4^{2-}$ is justified because the two bridging hydrogen atoms donate their two electrons to the aluminum skeletal cage. Thus, from an electron-counting perspective, Al_4H_6 can be viewed as $Al_4H_4 + 2e^-$ or $Al_4H_4^{2-}$. In the case of $Al_4H_4^{2-}$, there are 18 valence electrons. Eight of these are involved in forming four Al-H terminal bonds, leaving 10 electrons or five pairs for cage bonding. Because $n + 1 = 5$, n is equal to 4, which implies a tetrahedral structure. A strict application of Wade-Mingos concepts to the $n = 4$ case, however, would instead predict a Jahn-Teller distorted tetrahedral cage, given that the occupied molecular orbitals in tetrahedral symmetry are both degenerate and partially filled. Nevertheless, this symmetry-borne restriction is moot in the case of Al_4H_6, because the presence of two bridging hydrogen atoms decreases its symmetry to D_{2d}. Specifically, the two sets of bridging bonds are each three-center, two-electron bonds in which the Al-Al linkage in each Al-H-Al bridge bond is virtual—i.e., the bridged hydrogen is an integral part of the closo-Al_4H_6 cage. Thus, with only minor caveats, the predicted structure is consistent with our calculated structure in Fig. 4, and although the Wade-Mingos rules were not developed for this particular case, they fit it relatively well. Thus, despite the differences between the hydride chemistries of boron and aluminum, Al_4H_6 displays substantial bonding and structural similarities to the boranes and thus is analogous to them. There are also other interesting touchstones. For example, the bonding in Al_4H_6 would be considered by some to be an example of three-dimensional aromaticity (*25*), several other tetrahedral Al_4 structures have been observed among inorganic clusters in the solid state (*26*, *27*), and before now, $Al_{12}R_{12}^{2-}$ (where R is a *t*-butyl group) was the only example of an aluminum cluster anion reported to adhere to the Wade-Mingos rules (*28*).

Furthermore, it now becomes clear why neither Al_4H_5 nor Al_4H_7 exhibit notable HOMO-LUMO gaps (Fig. 3, B and C). Both Al_4H_5 and Al_4H_7 have odd numbers of valence electrons (17 and 19, respectively), and the Wade-Mingos rules deal only with even numbers of electrons—i.e., with electron pairs. Thus, the large HOMO-LUMO gap of Al_4H_6 and the small HOMO-LUMO gaps of Al_4H_5 and Al_4H_7 are consistent with the Wade-Mingos rules.

Al_4H_6 is an impressive high–energy density molecule or cluster that may have application in propulsion. We calculated the heat of combustion of Al_4H_6 to the products, Al_2O_3 and water, to be 438 kcal/mol, ~2.6 times greater than that of methane. Moreover, given the thermodynamic driving force required to go all the way to alumina and water, it is unlikely that the combustion products of Al_4H_6 will stop at some intermediate species as boranes are known to do. Furthermore, the large HOMO-LUMO gap for Al_4H_6 implies that it may be relatively stable and perhaps can be synthesized in bulk quantities. If so, Al_4H_6 and related species could be important energetic materials.

References and Notes

1. L. Andrews, X. Wang, *Science* **299**, 2049 (2003).
2. F. A. Kurth, R. A. Eberlein, H. Schnöckel, A. J. Downs, C. R. Pulham, *J. Chem. Soc.* **16**, 1302 (1993).
3. P. Breisacher, B. Siegal, *J. Am. Chem. Soc.* **86**, 5053 (1964).
4. F. A. Cotton, G. Wilkinson, *Advanced Inorganic Chemistry* (Interscience, New York, ed. 2, 1966).
5. S. Burkart *et al.*, *Chem. Phys. Lett.* **301**, 546 (1999).
6. B. K. Rao, P. Jena, S. Burkart, G. Ganteför, G. Seifert, *Phys. Rev. Lett.* **86**, 692 (2001).
7. L.-F. Cui, X. Li, L.-S. Wang, *J. Chem. Phys.* **124**, 054308 (2006).
8. N. N. Greenwood, A. Earnshaw, *Chemistry of the Elements* (Elsevier Science, Amsterdam, ed. 2, 1997).
9. W. N. Lipscomb, *Boron Hydrides* (W. A. Benjamin, New York, 1963).
10. K. J. Wade, *Adv. Inorg. Chem. Radiochem.* **18**, 1 (1976).
11. R. E. Williams, *Chem. Rev.* **92**, 177 (1992).
12. H. R. Siekmann, C. Lueder, J. Faehrmann, H. O. Lutz, K. H. Meiwes-Broer, *Zeit. Phys. D* **20**, 417 (1991).
13. M. Gerhards, O. C. Thomas, J. M. Nilles, W.-J. Zheng, K. H. Bowen, *J. Chem. Phys.* **116**, 10247 (2002).
14. S. H. Yang, C. L. Pettiette, J. Conceicao, O. Cheshnovsky, R. E. Smalley, *Chem. Phys. Lett.* **139**, 233 (1987).
15. All calculations were done with the use of Gaussian 03 software, Revision C.02, M. J. Frisch *et al.* (Guassian Inc., Wallingford, CT, 2004).
16. R. Ahlrichs, S. D. Elliott, *Phys. Chem. Chem. Phys.* **1**, 13 (1999).
17. A. Neu *et al.*, *Angew. Chem. Int. Ed. Engl.* **36**, 2117 (1997).
18. A. Neu, T. Mennekes, P. Paetzold, U. Englert, M. Hofmann, P. R. Schleyer, *Inorg. Chim. Acta* **289**, 58 (1999).
19. K. Wade, *Chem. Commun.* **1971**, 792 (1971).
20. D. M. P. Mingos, *Nature Phys. Sci.* **236**, 99 (1972).
21. J. W. Lauher, *J. Am. Chem. Soc.* **100**, 5305 (1978).
22. E. D. Jemmis, M. M. Balakrishnarajan, P. D. Pancharatna, *J. Am. Chem. Soc.* **123**, 4313 (2001).
23. M. M. Balakrishnarajan, R. Hoffman, *J. Am. Chem. Soc.* **126**, 13119 (2004).
24. M. A. Cavanaugh, T. P. Fehlner, R. Stramel, M. E. O'Neill, K. Wade, *Polyhedron* **4**, 687 (1985).
25. P. R. Schleyer, K. Najafian, *Inorg. Chem.* **37**, 3454 (1998).
26. C. Dohmeier, D. Loos, H. Schnöckel, *Angew. Chem.* **108**, 141 (1996).
27. G. Linti, H. Schnöckel, W. Uhl, N. Wiberg, *Molecular Clusters of the Main Group Elements*, M. Drieß, H. Nöth, Eds. (Wiley-VCH, Weinheim, Germany, 2002).
28. W. Hiller, K.-W. Klinkhammer, W. Uhl, J. Wagner, *Angew. Chem. Ed. Int. Engl.* **30**, 179 (1991).

29. Supported by the Air Force Office of Scientific Research (K.B.), the Office of Basic Energy Sciences, Department of Energy (P.J.), and the Deutsche Forschungsgemeinschaft (G.G. and H.S.). K.B. also acknowledges valuable conversations with J. Muckerman and B. Eichhorn.

11 August 2006; accepted 13 November 2006
10.1126/science.1133767

Divalent Metal Nanoparticles

Gretchen A. DeVries, Markus Brunnbauer, Ying Hu, Alicia M. Jackson, Brenda Long, Brian T. Neltner, Oktay Uzun, Benjamin H. Wunsch, Francesco Stellacci*

Nanoparticles can be used as the building blocks for materials such as supracrystals or ionic liquids. However, they lack the ability to bond along specific directions as atoms and molecules do. We report a simple method to place target molecules specifically at two diametrically opposed positions in the molecular coating of metal nanoparticles. The approach is based on the functionalization of the polar singularities that must form when a curved surface is coated with ordered monolayers, such as a phase-separated mixture of ligands. The molecules placed at these polar defects have been used as chemical handles to form nanoparticle chains that in turn can generate self-standing films.

Nanoparticles that consist of crystals of tens to thousands of atoms have been used as "artificial atoms" to form supracrystals that mimic ionic solids (*1*) or to form the nanoscale equivalent of ionic liquids (*2*). Breaking the interaction symmetry in these isotropic and almost spherical materials is a major challenge. It is increasingly evident that nanoparticles would

become a much more powerful research tool if it were possible to place a known small number of molecules in their ligand shell to enable directional assembly, for example. This would enlarge the scope of potential applications, because anisotropic assemblies have distinctive properties that cannot be found or produced in isotropic assemblies (*3*, *4*). Indeed, a large research effort to direct the assembly of nanoparticles (NPs), based primarily on biomolecules (*5*–*9*) or other templating agents (*10*), has been hindered by a lack of control over the number of receptors that interact with the templating agent. Approaches based solely on stoichiometry tend to require dilute aqueous solutions, resulting in limited throughput (*11*, *12*). Recently, creative methods to introduce single valency in NPs have been developed, mostly through solid-state reactions (*13*–*16*). We present an approach to functionalize monolayer protected metal NPs at two diametrically opposed points that exist as a consequence of the topological nature (*17*, *18*) of the particles. Specifically, we have made NPs that act as divalent building blocks ("artificial monomers"), and can be reacted with complementary divalent molecules to form chains that can then produce self-standing films.

Monolayer protected metal NPs are supramolecular assemblies consisting of a metallic core coated with a self-assembled monolayer (SAM) composed of one or more types of thiol-terminated molecules (ligands). It is known that molecules in SAMs on flat gold surfaces form a two-dimensional (2D) crystal in which every molecule conforms to the same tilt angle and direction relative to the surface normal (*19*, *20*) in order to maximize the van der Waals interactions with its nearest neighbors. Landman and coworkers (*21*) addressed the question of the morphology of the ligand shell SAM on the faceted surface of a gold NP. They found that ligand molecules conform to one single tilt angle relative to a common particle diameter rather than assuming their equilibrium tilt angle on each crystallographic facet, which would generate a large number of line defects along facet edges. That is, the vectorial projection of the tilted ligand molecules propagates around the particle. This needs to be reconciled with the fact that on a topological sphere a 2D crystal cannot exist unless two separate point defects are present (*22*, *23*). This is commonly known as the "hairy ball theorem" that states that it is not possible to "align hairs" onto a sphere without generating two singularities (such as the whirl on the back of our heads). Recently, we have shown (*18*, *24*) that mixtures of thiolated molecules, which on flat gold surfaces separate into randomly distributed domains (*25*), form ordered alternating phases (ripples) when assembled on surfaces with a positive Gaussian curvature, such as the core of an NP (Fig. 1A). These types of domains will profoundly demarcate the two diametrically opposed singularities at the particle poles, where the rings collapse into points (Fig. 1B). We conjecture that, in the case of a self-assembled ligand shell, the polar singularities manifest themselves as defect points, that is, sites at which the ligands must assume a nonequilibrium tilt angle. Ligands at the poles, being not optimally stabilized by intermolecular interactions with their neighbors, should be the first molecules to be replaced in place-exchange reactions (SOM Text S1).

Gold NPs coated with a binary mixture of 1-nonanethiol (NT) and 4-methylbenzenethiol (MBT) were synthesized and characterized by scanning tunneling microscopy (STM). Ordered rings similar in nature and spacing to the ones observed previously (*18*) were found. These molecules were chosen for multiple reasons: They have a strong driving force for phase separation and a large STM contrast, and are terminated with unreactive methyl groups. Transmission electron microscopy (TEM) was used to determine the size distribution and the molecular weight of the NPs. To place-exchange at the polar defects, the particles were dissolved in a solution containing 40 molar equivalents (relative to the moles of particles) of 11-mercaptoundecanoic acid (MUA) activated by N-hydroxysuccinimide. After stirring for 30 min, the reaction was rapidly quenched by filtration over a Sephadex column or by inducing precipitation with deionized water. A two-phase "polymerization" reaction inspired by the well-known procedure to synthesize nylon was then performed by combining an organic (toluene) phase containing the MUA functionalized particles with a water phase containing divalent 1,6-diaminohexane (DAH) (Fig. 1C).

Within a few minutes, a precipitate begins to form at the water-toluene interface (fig. S1); after a few hours, the reaction reaches equilibrium. The precipitate can be re-dissolved in tetrahydrofuran (THF) and dropped onto a TEM grid or, conversely, collected directly on a TEM grid and rinsed with THF. TEM images in both cases show a large population of linear chains of NPs, ranging from 3 to 20 NPs in length (Fig. 2). The low fraction of branched chains and the absence of 3D aggregates in the images strongly supports the idea of selective functionalization at the two opposed polar defects and suggests that polar singularities react even faster than other defects in the ligand shell.

Many control experiments were performed to observe the formation (or lack thereof) of a precipitate and the presence or absence of chains in TEM images of both the precipitate and the toluene phase (fig. S2). Mixed-ligand rippled NPs showed precipitate only when pole-functionalized with MUA, either activated or not activated. NPs containing carboxylic acid groups everywhere in the ligand shell formed, as expected, only large 3D aggregates resulting from nondirectional interparticle bonding. In general, precipitate was not observed when DAH was not present in the water phase or when the particles lacked carboxylic acid terminated ligands, proving that the precipitate is a product of an amide-coupling reaction leading to an amide bond (in the case of activation) or to a salt. A statistical analysis was

Department of Materials Science and Engineering, Massachusetts Institute of Technology, Cambridge, MA 02139, USA.

*To whom correspondence should be addressed. E-mail: frstella@mit.edu

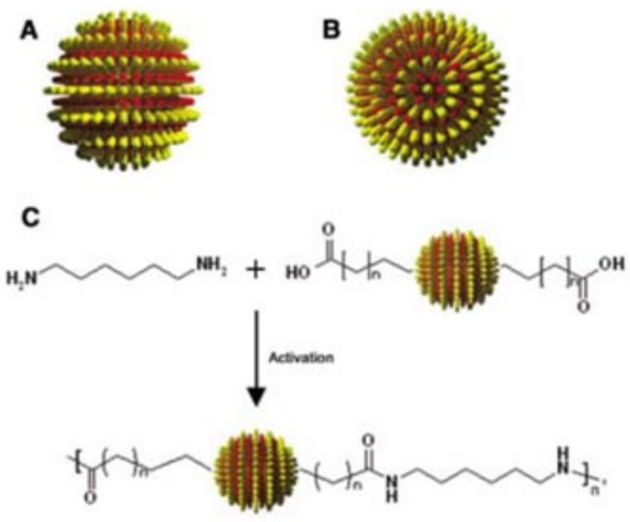

Fig. 1. From rippled particles to NP chains. Idealized drawing of (**A**) a side view and (**B**) a top view of a rippled particle showing the two polar defects that must exist to allow the alternation of concentric rings. (**C**) Schematic depiction of the chain formation reaction.

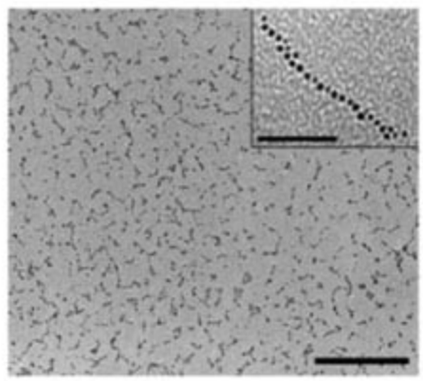

Fig. 2. TEM images of chains that compose the precipitate obtained when MUA pole-functionalized rippled NPs are reacted with DAH in a two-phase reaction. Scale bars 200 nm, inset 50 nm.

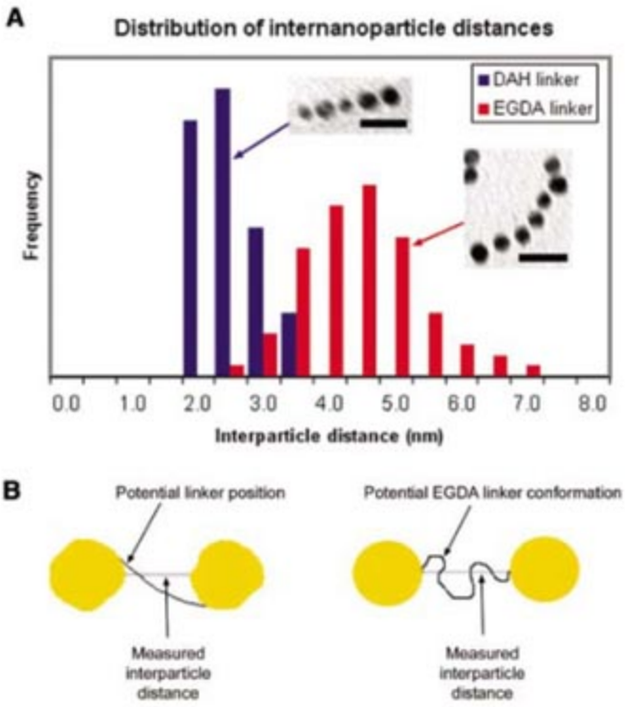

Fig. 3. Variation in interparticle distance with linker molecule. (**A**) Distribution of interparticle distances in chains with DAH linkers (blue) and EGDA linkers (red). The average interparticle distance for DAH was 2.2 nm ± 0.4 nm; for EGDA, it was 4.2 nm ± 0.9 nm. Note that the measured distributions barely overlap. Insets show TEM images of representative chains of each type. Scale bars, 20 nm. (**B**) Schematics illustrating (left) the potential geometry of NPs that could result in the measured interparticle distances being smaller than the length of the linker and (right) the conformational freedom of EGDA that could result in the observed wide distribution of interparticle distances for this type of chain.

performed on chains and controls resulting from one-phase syntheses (*26*). After analyzing more than 40 samples with a total population exceeding 50,000 particles, it was found that the average fraction of particles in chains was 20% (SD = 8%), whereas in all control experiments only 3 to 5% of the NPs were found in chainlike structures. The one-phase synthesis had a lower yield than the interfacial two-phase reaction.

To further prove that the chains observed in our TEM images were due to molecular linking of our particles, the synthesis was performed with one of two divalent linking molecules of different lengths: DAH and *O,O'*-Bis(2 aminoethyl)octadecaethylene glycol (EGDA). We then measured the average interparticle separation along the chain (defined as the distance between the two nearest points or facets). Assuming an all-trans conformation for the molecular linkers (i.e., two MUA molecules covalently bonded to either DAH or EGDA), the expected interparticle distance would be 3.6 and 9.6 nm, respectively. Analysis of TEM images showed an average interparticle separation of 2.2 nm (SD = 0.4 nm) for DAH and of 4.2 nm (SD = 0.9 nm) for EGDA (Fig. 3A), proving that the observed chains are kept together by the molecular linkers. The larger spread in the EGDA distribution was expected because of its greater conformational freedom (Fig. 3B). Evidence that chains are present in solution (as opposed to being caused by solvent drying) was also obtained through light-scattering experiments. We found an increase in scattering intensity for THF solutions of chains as compared with solutions of identical optical density containing only the starting particles (fig. S3), proving the presence of aggregates in solution. Moreover, NPs of two different sizes (average diameter 10 and 20 nm, respectively) were pole-functionalized with 16-mercapto-1-hexadecylamine and reacted with sebacoyl chloride (a divalent molecule) to form chains of random composition (fig. S4). When the same particles were cast on a TEM grid without previous pole functionalization or without reacting with sebacoyl chloride, primarily isolated particles were obtained. To prove the dynamic nature of the chains, we exposed them to a large excess of NT for 3 days and observed only isolated particles in TEM images (fig. S5). Poles provide a distinctive way to place NPs on a surface with their ripples parallel to the substrate plane. STM images of samples prepared in this way lack the striations present when the sample is prepared such that the ripples are perpendicular to the substrate plane (fig. S6).

Place-exchange reactions have been thoroughly studied by Murray and co-workers (*27*–*29*). They found that molecules exchange first at defects in the ligand shell or at corners and edges of the core crystal. Using nuclear magnetic resonance, they calculated the initial rate of the ligand-exchange reaction: For 1-octanethiol–coated NPs they found a second-order reaction rate constant of 3 10^{-2} M^{-1} s^{-1} (*27*). In our system, the place-exchange reaction reaches equilibrium (at least for pole functionalization) after 10 min (*30*). Given that the number of NPs that contain at least one MUA molecule in their ligand shells can be experimentally evaluated (by making the conservative assumption that every MUA-functionalized particle will react to form an insoluble chain), the second-order rate constant was found to be 1.67 M^{-1} s^{-1}, about two orders of magnitude larger than that observed for homoligand NPs (*27*). Applying the fastest second-order rate constant published (*27*), the number of MUA molecules that would have reacted at defects other than the poles under our reaction conditions is only 1 MUA molecule per 100 NPs. It should be pointed out that (i) we assume that every chain precipitates but observe few dimers in TEM images of the precipitate, hence they must still be soluble; and (ii) we assume that only one MUA molecule is located at each pole. Faster rates of reaction would be obtained if any of these assumptions were removed. These kinetic experiments show that defects at the molecularly defined polar singularities of mixed ligand NPs are thermodynamically distinct from those at crystallographically defined vertices of the core crystal. Most experiments were performed with particles with an average diameter of ~4 nm; as the size of the particles changes, it is reasonable to expect that the rate of polar reactions will vary. The polar singularities will exist only in a certain size range: On surface hemispheres with a radius larger than 20 nm, ripples do not form (*18*), and a similar behavior is expected on NPs. Investigations are under way to determine the lower size limit; we have observed ripples and chains in NPs as small as 3 nm in diameter.

Enough NP chains at the water-toluene interface have been produced to form a continuous film as large as 1 cm^2 (fig. S7). Our preliminary conclusion is that these films (whose thickness can reach 60 μm) must be composed of multiple interwoven chains. Whereas the chains described here are soluble in dichloromethane (DCM), the films when placed in DCM quickly lose any unreacted particles but maintain their structural integrity and then take weeks to dissolve. The van der Waals interactions between the ligand shells of the particles together with the interchain morphology provide enough mechanical strength to make these purely NP films self-standing. Control experiments show that, in situations where chains are not formed, one of two extreme cases happen. When the entire ligand shell can react with diamine (e.g., there is carboxylic acid in the ligand shell), coarse powders that are insoluble in any solvent are formed. When the ligand shell cannot react with diamines, semicontinuous films form, but only after the toluene has completely evaporated; these materials can at times be self-standing but always readily dissolve in organic solvents.

References and Notes

1. E. V. Shevchenko, D. V. Talapin, N. A. Kotov, S. O'Brien, C. B. Murray, *Nature* **439**, 55 (2006).
2. A. B. Bourlinos *et al.*, *Eur. Phys. J. E* **20**, 109 (2006).
3. S. A. Maier *et al.*, *Adv. Mater.* **13**, 1501 (2001).
4. K. G. Thomas, S. Barazzouk, B. I. Ipe, S. T. S. Joseph, P. V. Kamat, *J. Phys. Chem. B* **108**, 13066 (2004).
5. N. L. Rosi, C. S. Thaxton, C. A. Mirkin, *Angew. Chem. Int. Ed.* **43**, 5500 (2004).
6. G. D. Bachand *et al.*, *Nano Lett.* **4**, 817 (2004).
7. G. L. Wang, R. W. Murray, *Nano Lett.* **4**, 95 (2004).
8. M. G. Warner, J. E. Hutchison, *Nat. Mater.* **2**, 272 (2003).
9. E. Katz, I. Willner, *Angew. Chem. Int. Ed.* **43**, 6042 (2004).
10. Z. Y. Tang, N. A. Kotov, *Adv. Mater.* **17**, 951 (2005).
11. A. H. Fu *et al.*, *J. Am. Chem. Soc.* **126**, 10832 (2004).
12. J. P. Novak *et al.*, *J. Am. Chem. Soc.* **122**, 12029 (2000).
13. S. Praharaj, S. Nath, S. K. Ghosh, S. Kundu, T. Pal, *Langmuir* **20**, 9889 (2004).

14. K. M. Sung, D. W. Mosley, B. R. Peelle, S. G. Zhang, J. M. Jacobson, *J. Am. Chem. Soc.* **126**, 5064 (2004).
15. J. G. Worden, A. W. Shaffer, Q. Huo, *Chem. Commun.* **2004**, 518 (2004).
16. F. W. Huo, A. K. R. Lytton-Jean, C. A. Mirkin, *Adv. Mater.* **18**, 2304 (2006).
17. D. R. Nelson, *Nano Lett.* **2**, 1125 (2002).
18. A. M. Jackson, J. W. Myerson, F. Stellacci, *Nat. Mater.* **3**, 330 (2004).
19. J. C. Love, L. A. Estroff, J. K. Kriebel, R. G. Nuzzo, G. M. Whitesides, *Chem. Rev.* **105**, 1103 (2005).
20. F. Schreiber, *Prog. Surf. Sci.* **65**, 151 (2000).
21. W. D. Luedtke, U. Landman, *J. Phys. Chem. B* **102**, 6566 (1998).
22. H. Poincare, *J. Math Pure Appl.* **1**, 167 (1885).
23. M. Eisenberg, R. Guy, *Am. Math. Mon.* **86**, 571 (1979).
24. A. M. Jackson, Y. Hu, P. J. Silva, F. Stellacci, *J. Am. Chem. Soc.* **128**, 11135 (2006).
25. R. K. Smith *et al.*, *J. Phys. Chem. B* **105**, 1119 (2001).
26. The one-phase chaining reaction is less efficient than the two-phase reaction for many reasons: Mainly, it is challenging to get the exact stoichiometric ratio of nanoparticles to divalent molecules. The kinetics of the polymerization reaction are also slower. However, the one-phase reaction product can be directly cast onto TEM grids from solution with no intermediate processing, and consequently it can be quantitatively analyzed.
27. M. J. Hostetler, A. C. Templeton, R. W. Murray, *Langmuir* **15**, 3782 (1999).
28. Y. Song, R. W. Murray, *J. Am. Chem. Soc.* **124**, 7096 (2002).
29. R. L. Donkers, Y. Song, R. W. Murray, *Langmuir* **20**, 4703 (2004).
30. As determined by timed experiments. The amount of pole-functionalized nanoparticles that precipitate can be measured through optical spectroscopy of the organic phase in the two-phase polymerization system. See SOM Materials and Methods for details.
31. The authors are grateful to V. Vitelli and D. Nelson for helpful discussions. The financial support of the National Science Foundation (Nanotechnology Interdisciplinary Research Team Division of Materials Research-0303973) and of the Petroleum Research Foundation are acknowledged. F.S. is grateful to 3M, DuPont, and the Packard Foundation for the young faculty awards. G.A.D. acknowledges support from the Department of Defense National Defense Science and Engineering Graduate Fellowship, and A.M.J. from the Collamore Fellowship for graduate students. This work made use of the shared facilities of the Material Research Science and Education Center Program of the National Science Foundation under award DMR 02-13282.

Supporting Online Material

www.sciencemag.org/cgi/content/full/315/5810/358/DC1
Materials and Methods
SOM Text
Figs. S1 to S7
References

28 July 2006; accepted 6 December 2006
10.1126/science.1133162

Global-Scale Similarities in Nitrogen Release Patterns During Long-Term Decomposition

William Parton,[1] Whendee L. Silver,[2] Ingrid C. Burke,[1,3] Leo Grassens,[4] Mark E. Harmon,[5] William S. Currie,[6] Jennifer Y. King,[7] E. Carol Adair,[8] Leslie A. Brandt,[8] Stephen C. Hart,[9] Becky Fasth[5]

Litter decomposition provides the primary source of mineral nitrogen (N) for biological activity in most terrestrial ecosystems. A 10-year decomposition experiment in 21 sites from seven biomes found that net N release from leaf litter is dominantly driven by the initial tissue N concentration and mass remaining regardless of climate, edaphic conditions, or biota. Arid grasslands exposed to high ultraviolet radiation were an exception, where net N release was insensitive to initial N. Roots released N linearly with decomposition and exhibited little net N immobilization. We suggest that fundamental constraints on decomposer physiologies lead to predictable global-scale patterns in net N release during decomposition.

Litter decomposition converts the products of photosynthesis to inorganic components and stable soil organic matter. Decomposition releases more carbon (C) annually than fossil fuel combustion (*1*, *2*), and it represents the primary source of nutrients for plants, and both nutrients and energy for microbes, over biological time scales (*3*, *4*). This is particularly true for the supply of nitrogen (N), which lacks a notable geologic input and is commonly a limiting element to plant growth (*5*). Internal recycling of N from litter decomposition thus provides a key resource for ecosystem productivity.

Litter decomposition is a lengthy process generally requiring years to decades for completion, and considerable N remains in litter after the initial decomposition phase (*6*–*8*). The vast majority of decomposition studies have been conducted over short time periods (<5 years), and at local scales using site-specific litters (*9*–*11*), making cross-site comparisons difficult. The lack of long-term broad-scale studies on litter decomposition and nutrient release inhibits our ability to accurately predict ecosystem C balance and response to environmental change at regional and global scales. The Long-Term Intersite Decomposition Experiment (LIDET) was a 10-year effort encompassing most of the world's biomes designed to determine long-term controls on decomposition and nutrient immobilization or mineralization. The study used several leaf and root litters that differed in chemical quality, with a core set of five to six leaf litters and three root litters that were decomposed at all sites (*12*). This data set is unique in that it encompasses the global array of climatic conditions (Table 1), includes a wide range of soil types and associated soil microbial community compositions, and was carried out over an unprecedented time span. Our goal was to use the LIDET core litter data set (*1*) from upland terrestrial sites to determine which combination of climate, initial litter chemistry, and site-specific characteristics (e.g., those derived from edaphic conditions and decomposer biota) best predict long-term patterns in litter N dynamics during decomposition (*1*, *10*, *12*–*14*). The data set included seven biomes, each with at least two replicate sites (n = 21 sites). We used mean annual temperature and precipitation, actual evapotranspiration, and the climatic decomposition index (CDI) as potential predictors of decomposition rates and N dynamics (Table 1). The CDI incorporates seasonality in temperature and moisture and has been shown to be well correlated with decomposition rates over 1 to 5 years (*1*). The core litters were chosen to encompass a wide range of C:N ratios, and concentrations of N, lignin, and other secondary compounds (Table 1, table S2).

CDI was the best predictor of decomposition rates globally (correlation coefficient r^2 = 0.68). Leaf and root litter decomposition were slowest in the cold, dry regions, such as boreal forest and tundra, and fastest in the warm, moist tropical forests (Fig. 1). A notable exception was the rapid leaf litter decomposition rate in arid-zone perennial grasslands despite a CDI of 0.11 (Fig. 1C); these ecosystems may have been affected by ultraviolet (UV) radiation (*15*–*17*) in addition to climate.

Unlike patterns in mass loss, net N immobilization and release in leaf litter were strongly

[1]Natural Resource Ecology Laboratory, Colorado State University, 200 West Lake, Campus Mail 1499, Fort Collins, CO 80523–1499, USA. [2]Ecosystem Science Division, Department of Environmental Science, Policy, and Management, 137 Mulford Hall #3114, University of California, Berkeley, CA 94720, USA. [3]Department of Forest, Rangeland, and Watershed Stewardship, and Graduate Degree Program in Ecology, Colorado State University, Fort Collins, CO 80523–1472, USA. [4]LSI Logic Inc., 1636 Southwest 26th Street, Loveland, CO 80227, USA. [5]Department of Forest Science, Oregon State University, Corvallis, OR 97331, USA. [6]School of Natural Resources and Environment, University of Michigan, Ann Arbor, MI 48103, USA. [7]Department of Soil, Water, and Climate and Department of Ecology, Evolution, and Behavior, University of Minnesota, 439 Borlaug Hall, 1991 Upper Buford Circle, St. Paul, MN 55108, USA. [8]Department of Ecology, Evolution, and Behavior, University of Minnesota, 100 Ecology Building, 1987 Upper Buford Circle, St. Paul, MN 55108, USA. [9]School of Forestry and Merriam-Powell Center for Environmental Research, Northern Arizona University, Flagstaff, AZ 86011, USA.

Table 1. Climate data for the seven biomes used in this study. The mean time to the initiation of net N release (TNET) is given in years for each leaf litter species and biome and was calculated using the best-fit equation to determine the point of maximum net N immobilization (*18*). Mean precipitation (PPT), temperature (TMP), actual evapotranspiration (AET), and the climatic decomposition index (*37*) are shown. TRAE, *Triticum aestivum*; PIRE, *Pinus resinosa*; THPL, *Thuja plicata*; ACSA, *Acer saccharum*; QUPR, *Quercus prinus*; DRGL, *Drypetes glauca*.

Biome	Mean annual PPT (mm)	Mean annual TMP (°C)	Climatic decomposition index (CDI)	Mean AT (mm)	TRAE 0.38% N TNET	PIRE 0.58% N TNET	THPL 0.62% N TNET	ACSA 0.80% N TNET	QUPR 1.02% N TNET	DRGL 1.98% N TNET
Arid grassland	331	13.0	0.11	1490	–	–	–	–	–	–
Humid grassland	807	9.8	0.30	1138	3.5	3	3.9	1.75	1.6	0.25
Tundra	788	−6.0	0.09	589	9.5	7.6	6.4	2.6	1.6	0.5
Boreal forest	750	0.0	0.12	830	6.4	4	4	2.6	1.3	0.5
Coniferous forest	1840	11.2	0.27	1058	3.8	2.6	2.2	1.4	0.7	0.25
Deciduous forest	1485	8.8	0.32	1070	1.85	1.1	0.9	0.8	0.33	0.2
Tropical forest	3210	23.6	0.78	1429	0.4	0.6	0.35	0.5	0.2	0.1

controlled by initial tissue N concentrations regardless of climate, other litter quality parameters, or site characteristics. A single, continuous nonlinear regression derived from the data explained 77% of the variability in net N immobilization and release as a function of initial leaf litter N concentrations and mass remaining for all forested biomes, humid grasslands, and tundra ecosystems (Fig. 2) (*18*). Patterns in net N immobilization and release were clearly delineated into four categories based on the initial leaf litter N concentrations (Table 1): high N (1.98% N, *Drypetes glauca*), intermediate N (1.02% N, *Quercus prinus*), low N [0.58 to 0.80% N, *Pinus resinosa* (decomposed at all but four sites), *Thuja plicata*, *Acer saccharum*], and very low N (0.39% N, *Triticum aestivum*). Litter high in initial N content had the best fit to the equation (r^2 = 0.91), although we could still explain 47% of the variation with the low-N litter that had the poorest fit. Leaf litters with intermediate to high initial N concentrations showed little or no net N immobilization, defined as the fraction of original $N > 1$ (Fig. 2, A and B). Substantial net N release started when ~40% of the mass was lost. The maximum fraction of original N immobilized increased as the initial N concentration decreased to low and very low levels (Fig. 2, A to D). There was also a general pattern of increased variance of the fraction of N remaining as the initial N content of the leaf litter decreased. On average, 170% of the initial N was immobilized (net) in the litter with very low initial N, and net N release occurred only after 60% of the mass had been lost.

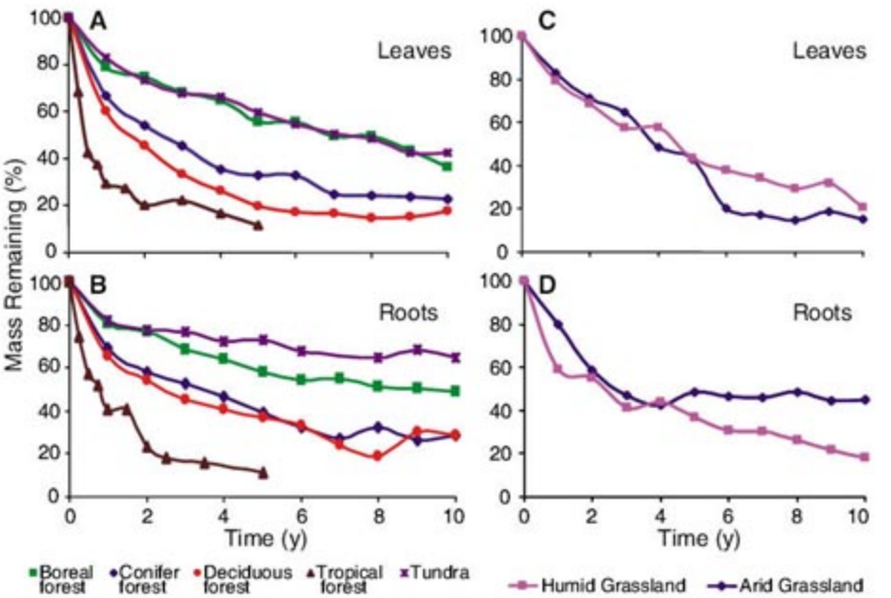

Fig. 1. Average mass remaining as a function of time for LIDET core leaf (n = 5 to 6 species) and root (n = 3 species) litters decomposed in 21 sites. (**A**) Leaf litter decomposed in forest and tundra biomes; (**B**) root litter decomposed in forest and tundra biomes; (**C**) leaf litter decomposed in humid and arid grasslands; (**D**) root litter decomposed in humid and arid grasslands. Each species and litter type was decomposed in replicate bags and collected at multiple time points. Results show that leaf and root litter decomposition rates generally increase as the CDI increases (Table 1). In arid grasslands, leaf litter decomposed more rapidly than expected (based on the CDI), possibly due to photodegradation.

These data demonstrate that fundamental constraints on microbial physiology lead to predictable patterns in net N immobilization and release during long-term decomposition. Patterns in net N immobilization and release have been shown to be related to the initial N concentration of specific leaf litters (*19*, *20*), but these relations were thought to be dependent upon climate, other litter chemical characteristics (*7*), edaphic conditions (*21*, *22*), or microbial community composition (*23*, *24*). Theoretically the C:N ratio should dominantly control net N release during litter decomposition because microbial decomposers should only release N when their N requirements have been met. At low C:N ratios (e.g., high N concentrations), decomposers meet their N requirements directly from the litter. At higher initial C:N ratios, net immobilization typically occurs as microbes access N exogenous to the litter and convert it to microbial biomass or exoenzymes [e.g., (*25*)]. Immobilization of exogenous N is presumably controlled by N availability in the environment. Patterns in net N release and immobilization should thus be dependent upon the relative C:N ratios of the decomposer organisms and the substrate, as well as N availability in the environment. Here we show that leaf litter N dynamics can be predicted at broad spatial and long temporal scales based only on the initial litter N concentration and the mass remaining during decomposition.

Net N release started when the average C:N ratio of the leaf litter was less than 40 (a range of 31 to 48). This is somewhat lower than in a 6-year decomposition study across Canada (C:N = 55) (*22*). The Canadian study used a narrower range of initial litter N and reported no relation between initial N concentration and rates of net N release. However, when net N release and immobilization are examined per unit of mass remaining, results were similar to the LIDET study.

As with mass loss, there was one exception to the pattern of net N release from the LIDET study. In arid-zone perennial grasslands, leaf litters with low and very low initial N concentrations showed a linear trend of net N release

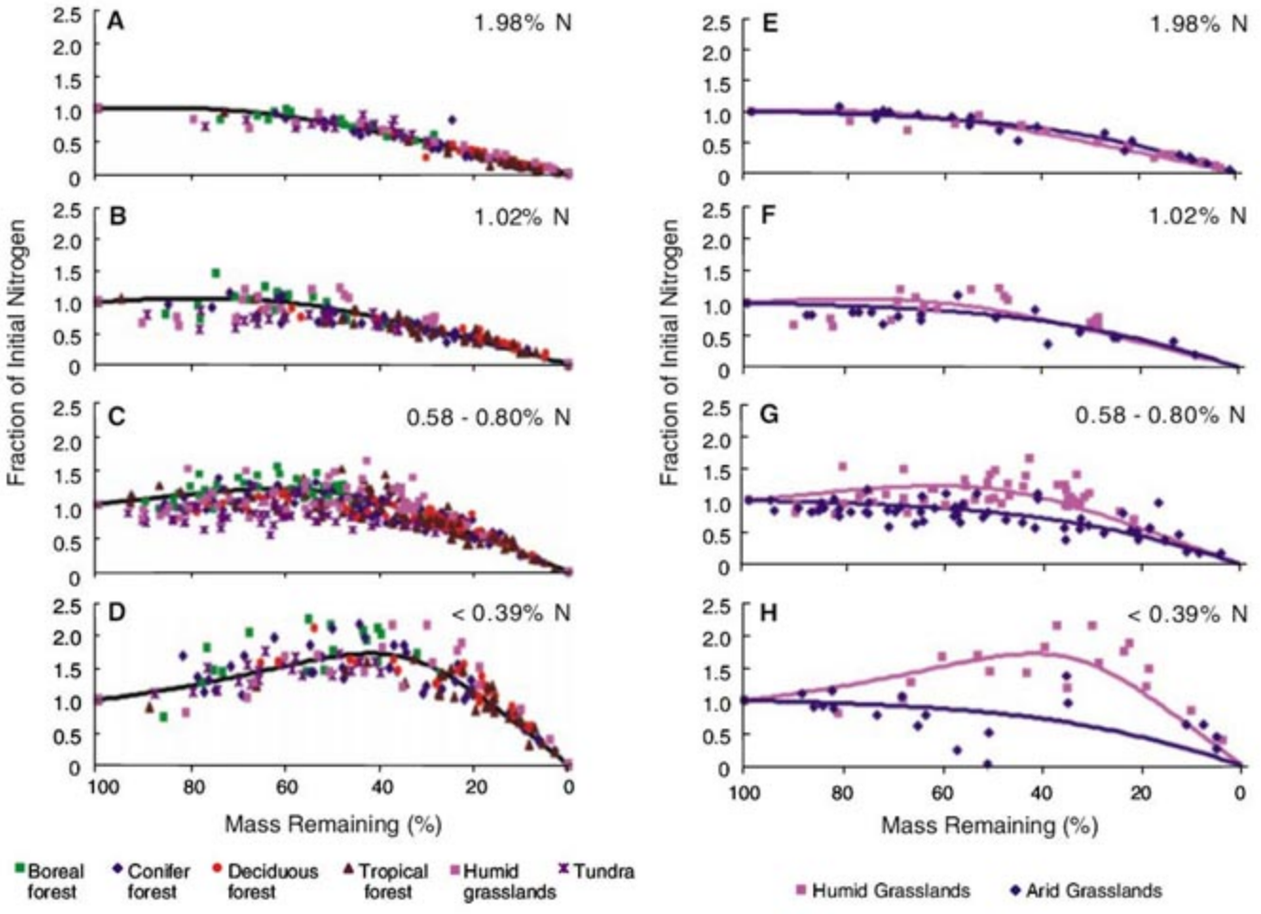

Fig. 2. Fraction of original litter N remaining as a function of the leaf litter mass remaining for tundra, grassland, and forest biomes. (**A**) to (**D**) include all biomes except arid grasslands; (**E**) to (**H**) compare arid and humid grasslands. Data are divided into litter high in initial N (A and E), intermediate initial N (B and F), low initial N (C and G), and extremely low initial N (D and H). The lines on the graphs show the best-fit model for describing the pattern of fraction of original N as a function of the initial N concentration of the litter (*18*). Model results match the observed data and show that net N immobilization, defined as an absolute increase in N concentration of the litter, is highest for the leaf litter with very low initial N concentration and decreases to minimal values for high initial N concentration of leaf litter. Leaf litter in arid grasslands was an exception showing no N immobilization in the low and very low N litters.

with little or no net N immobilization (Fig. 2, E and F). The pattern of net N release versus mass remaining for arid grasslands could be described by an equation with no effect of initial litter N concentration (*18*) (Fig. 2, E to H). This contrasts with the results from humid grasslands that exhibited increasing net N immobilization as the initial N concentration of the leaf litter decreased (Fig. 2, E to H). Leaf litters decomposed faster in humid grasslands than in arid grasslands during the early stages of decomposition, but decomposition increased more rapidly in arid grasslands after the first 3 to 5 years to a level equivalent to that of deciduous forests (Fig. 1). This was surprising given that the CDI for arid grasslands is <50% that of the humid grassland and deciduous forest biomes. The effect was not seen for root tissues, which were decomposed below ground and decayed faster in humid grasslands than in arid grasslands (Fig. 1D). The rapid increase in leaf litter decomposition during the later stages of decomposition and the linear net N release regardless of initial N concentration in arid grasslands may be caused by photodegradation. Arid grasslands typically have less than 100 g m^{-2} of standing live and dead plant tissues, whereas humid grasslands have more than 400 g m^{-2} aboveground plant biomass that intercepts most of the solar radiation before it gets to the surface leaf litter (*26*). Studies conducted during the early stages of decomposition (1 to 3 years) in arid grasslands have produced conflicting results regarding the effects of UV radiation on decomposition processes (*15*, *27*, *28*). However, recent studies suggest that where biotic decomposition is not favored (such as high litter lignin:N ratio and low moisture availability typical of arid grasslands), the abiotic process of photodegradation may predominate (*16*). This mechanism could explain the lack of a strong correlation between N concentration and decomposition, as well as the absence of net N immobilization at these sites.

Contrary to patterns of net N immobilization and release with mass loss, the time required to initiate net N release (TNET) was sensitive to initial tissue chemistry and climate. The TNET was inversely correlated with initial litter N and CDI ($r^2 = 0.77$, $P < 0.01$) (Table 1). The relation with CDI reflects the climatic controls on decomposition rate. The humid tropical biome had the lowest TNET values, ranging from 0.5 year for very low initial N litter to less than 0.1 year for high initial N litter. In the tundra and boreal forest biomes, it took more than 7 years for net N release to occur in litter with very low initial N, but only 0.5 year for net N

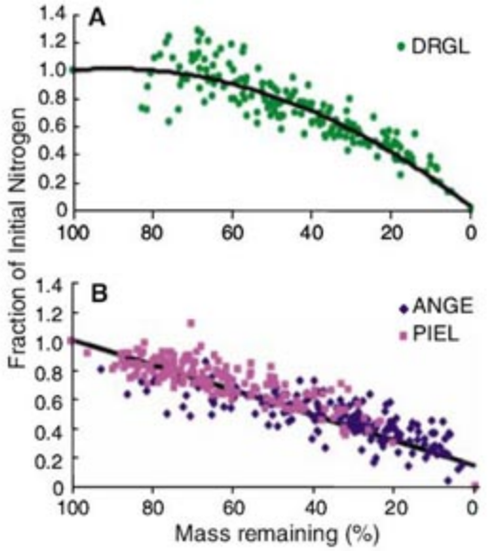

Fig. 3. Fraction of original root litter N remaining as a function of the litter mass remaining for *Drypetes glauca* root litter (**A**), and *Andropogon gerardi* and *Pinus elliottii* root litter (**B**), decomposing at the LIDET sites. Net N immobilization was minimal for decomposing root litter, with N being released as soon as decomposition of root litter starts. The equation for the DRGL roots is $y = -0.0001x^2 + 0.0221x + 0.0192$, $r^2 = 0.90$; the relation for the PIEL and ANGE roots is $y = 0.0087x + 0.1409$, $r^2 = 0.87$.

release from litter high in initial N. The TNET was at least 50% faster for most leaf litters decomposed in temperate deciduous forests when compared to coniferous forests and humid grasslands, all with similar CDIs (Table 1). Within a given CDI level, other factors such as edaphic conditions or decomposer communities may contribute to the differences observed (*29*, *30*). At the highest leaf litter N concentrations, all biomes experienced net N release during the first year of decomposition.

Root litter N followed a linear pattern with mass remaining (Fig. 3) and could best be described by two equations. The first was for *D. glauca* roots, which demonstrated a small amount of net N immobilization early in decomposition for a range of sites, possibly due to slightly higher concentrations of nonpolar extractives and slightly lower acid extractable carbohydrates concentrations than the other species (table S2). The second equation described net N release for the pine and grass roots that did not immobilize N during decomposition. A comparison of litter N dynamics during decomposition of pine and grass roots with leaf litter of similar initial N concentration (Figs. 2 and 3) showed that N was released from roots much more rapidly than from leaf litter. Roots released N as soon as litter decomposition was initiated (C:N ratio > 50). Microbial decomposers in the soil may have greater access to moisture, organic matter, and mineral N than microbes involved in leaf litter decomposition at the soil surface, which would facilitate net N release during decomposition (*31*). Similar patterns in net N release in roots have been described for native root litter decomposed in situ in grasslands (*32*), temperate broadleaf forests (*33*), temperate conifer forests (*34*), and moist and humid tropical forests (*35*, *36*).

Our data show that the initial N concentration of leaf litter is a dominant driver of net N immobilization and release during long-term litter decomposition at a global scale. This occurs regardless of climate, other litter chemical properties, edaphic conditions, or soil microbial communities. Our data also show that N can be released early in decomposition from high-quality litters in environments that support low decomposition rates. The time required to initiate net N release was predicted from the initial N of the litter and the CDI across biomes, but required more site information within a given CDI. Roots generally lost N linearly with mass loss during decomposition. Because N release during decay plays a fundamental role in net ecosystem production, improved understanding of the controls on net N release during decomposition is likely to greatly improve our ability to predict terrestrial C dynamics at global and regional scales.

References and Notes

1. H. L. Gholz, D. Wedin, S. Smitherman, M. E. Harmon, W. J. Parton, *Global Change Biol.* **6**, 751 (2000).
2. I. C. Prentice *et al.*, in *Climate Change 2001: The Scientific Basis: Contribution of Working Group I to the Third Assessment Report of the Intergovernmental Panel on Climate Change*, J. T. Houghton *et al.*, Eds. (Cambridge Univ. Press, Cambridge, 2001), pp. 183–231.
3. B. Moore, B. H. Braswell, *Ambio* **23**, 4 (1994).
4. W. S. Currie, *Global Change Biol.* **9**, 919 (2003).
5. P. M. Vitousek, R. W. Howarth, *Biogeochemistry* **13**, 87 (1991).
6. J. D. Lousier, D. Parkinson, *Can. J. For. Res.* **9**, 449 (1979).
7. B. Berg, C. McClaugherty, *Can. J. Bot.* **67**, 1148 (1989).
8. B. Berg, *For. Ecol. Manage.* **133**, 13 (2000).
9. J. D. Aber, J. M. Melillo, C. A. McClaugherty, *Can. J. Bot.* **68**, 2201 (1990).
10. R. Aerts, *Oikos* **79**, 439 (1997).
11. G. Cadisch, K. E. Giller, Eds., *Driven by Nature: Plant Litter Quality and Decomposition* (CAB International, Oxon, UK, 1997).
12. Long-Term Intersite Decomposition Experiment Team (LIDET), *Meeting the Challenges of Long-Term, Broad-Scale Ecological Experiments* (Publication No. 19, U.S. Long Term Ecological Research Network Office, Seattle, WA, 1995).
13. W. M. Post, J. Pastor, *Clim. Change* **34**, 253 (1996).
14. D. L. Moorhead, W. S. Currie, E. B. Rastetter, W. J. Parton, M. E. Harmon, *Global Biogeochem. Cycles* **13**, 575 (1999).
15. J. Rozema *et al.*, *Plant Ecol.* **128**, 284 (1997).
16. V. A. Pancotto, O. E. Sala, T. M. Robson, M. M. Caldwell, A. L. Scopel, *Global Change Biol.* **11**, 1982 (2005).
17. A. T. Austin, L. Vivanco, *Nature* **442**, 555 (2006).
18. Materials and methods are available as supporting material on *Science* Online.
19. E. H. Richards, A. G. Norman, *Biochem. J.* **25**, 1769 (1931).
20. J. D. Aber, J. M. Melillo, *Can. J. Bot.* **60**, 2263 (1982).
21. S. E. Hobbie, P. M. Vitousek, *Ecology* **81**, 1867 (2000).
22. T. R. Moore, J. A. Trofymow, C. E. Prescott, J. Fyles, B. D. Titus, *Ecosystems* **9**, 46 (2006).
23. M. H. Beare *et al.*, *Ecol. Monogr.* **62**, 569 (1992).
24. S. D. Frey, M. Knorr, J. L. Parrent, R. T. Simpson, *For. Ecol. Manage.* **196**, 159 (2004).
25. S. D. Frey, E. T. Elliott, K. Paustian, G. A. Peterson, *Soil Biol. Biochem.* **32**, 689 (2000).
26. D. S. Schimel *et al.*, *Ecology* **72**, 672 (1991).
27. H. A. Verhoef, J. M. H. Verspagen, H. R. Zoomer, *Biol. Fertil. Soils* **31**, 366 (2000).
28. S. A. Moody *et al.*, *Plant Ecol.* **154**, 27 (2001).
29. J. D. Aber, J. M. Melillo, K. J. Nadelhoffer, C. A. McClaugherty, J. Pastor, *Oecologia* **66**, 317 (1985).
30. J. E. Barrett, R. L. McCulley, D. R. Lane, I. C. Burke, W. K. Lauenroth, *J. Veg. Sci.* **13**, 383 (2002).
31. W. L. Silver, R. K. Miya, *Oecologia* **129**, 407 (2001).
32. T. R. Seastedt, W. J. Parton, D. S. Ojima, *Can. J. Bot.* **70**, 384 (1992).
33. M. E. Dornbush, T. M. Isenhart, J. W. Raich, *Ecology* **83**, 2985 (2002).
34. H. Chen, M. E. Harmon, J. Sexton, B. Fasth, *Can. J. For. Res.* **32**, 320 (2002).
35. W. L. Silver, K. A. Vogt, *J. Ecol.* **8**, 729 (1993).
36. W. L. Silver *et al.*, *Global Change Biol.* **11**, 290 (2005).
37. W. J. Parton, D. S. Schimel, D. S. Ojima, C. V. Cole, in *Quantitative Modeling of Soil Formation Processes*, R. B. Bryant, R. W. Arnold, Eds. (SSSA Special Publication 39 ASA, CSSA, and SSA, Madison, WI, 1994), pp. 147–167.

38. The LIDET study was supported by NSF Ecosystems Studies grants BSR-8805390 and BSR-9180329 to Oregon State University, NSF Shortgrass Steppe LTER grant DEB-350273, NSF IRC grant DEB-9977066, and University of Tennessee–Battelle, LLC (U.S. Department of Energy) subcontract grant 4000050162. This work was conducted as part of the Long-Term Intersite Decomposition Working Group supported by the National Center for Ecological Analysis and Synthesis, a Center funded by NSF (grant DEB-0072909), University of California, Santa Barbara. W.S. was also supported by NSF grants DEB-0218039, DEB-0219104, and the California Agricultural Experiment Station (7069-MS). W.P. was supported by DOE ORNL grant 533906, NSF grant DEB-0217631, and the NSF UV radiation project at the University of Minnesota. We thank H. Gholz for invaluable input on previous versions of this manuscript, and S. Lutz, C. Keough, and L. Richards for assistance in analyzing the extensive LIDET litter decay data set.

Supporting Online Material

www.sciencemag.org/cgi/content/full/315/5810/361/DC1
Materials and Methods
Tables S1 to S3
References

7 September 2006; accepted 5 December 2006
10.1126/science.1134853

Water Solubility in Aluminous Orthopyroxene and the Origin of Earth's Asthenosphere

Katrin Mierdel,[1] Hans Keppler,[1,2]* Joseph R. Smyth,[2,3] Falko Langenhorst[2,4]

Plate tectonics is based on the concept of rigid lithosphere plates sliding on a mechanically weak asthenosphere. Many models assume that the weakness of the asthenosphere is related to the presence of small amounts of hydrous melts. However, the mechanism that may cause melting in the asthenosphere is not well understood. We show that the asthenosphere coincides with a zone where the water solubility in mantle minerals has a pronounced minimum. The minimum is due to a sharp decrease of water solubility in aluminous orthopyroxene with depth, whereas the water solubility in olivine continuously increases with pressure. Melting in the asthenosphere may therefore be related not to volatile enrichment but to a minimum in water solubility, which causes excess water to form a hydrous silicate melt.

Earth's asthenosphere is often assumed to roughly coincide with the low-velocity zone, a layer of reduced seismic velocities and increased attenuation of seismic waves. The low-velocity zone usually begins at a depth of 60 to 80 km below the oceans and ends around 220 km (*1*). Below continental shields, the upper boundary is depressed to 150 km. The seismic characteristics of the low-velocity zone could be easily explained by the presence of a small frac-

Table 1. Experimental results on water solubility in aluminum-saturated enstatite. All experiments were carried out using an oxide-hydroxide mixture as starting material, except as noted. Number of infrared measurements refers to the numbers of different spots measured, usually on different crystals. Water contents (in ppm by weight) were calculated from the infrared data according to two different extinction coefficients, from Bell *et al.* (*13*) and from Paterson (*28*). Errors are one standard deviation. Water contents in atoms H per 10^6 Si can be obtained by multiplying by a factor of 22.3. All data reported here for a given pressure and temperature were included in the calibration of the thermodynamic model of water solubility. Solid phases detected refer to those phases that could be directly observed by x-ray diffraction or Raman spectroscopy. However, all the samples must have contained some aluminous phase, probably spinel or pyrope, as the aluminum content of the orthopyroxene was always several weight % lower than the aluminum content of the starting material. A fluid phase was always present during the experiments, as all samples released considerable amounts of water upon opening of the capsules. No evidence for melting was seen, as the run products were usually loose powders without interstitial glass. Some fluffy material and isolated glass beads probably represent material precipitated from the fluid upon quenching. En, enstatite; Sp, spinel; Ol, olivine; Prp, pyrope; Crn, corundum; Ky, kyanite; Sr, sapphirine; Prl, pyrophyllite. Al contents in enstatite were sometimes slightly inhomogeneous. The numbers and standard deviations given were usually derived from more than 100 individual analyses of different crystals in the charge. The molar Mg/Si ratio in all samples is equal to 1 within the error of the measurement.

Sample	*T* (°C)	*P* (kbar)	Duration (hours)	Number of infrared measurements	Water content (ppm)		Solid phases detected	Al_2O_3 content in enstatite (weight %)
					Bell *et al.* (*13*)	Paterson (*28*)		
En63	800	15	168	2	8420 ± 750	6280 ± 235	En, Crn	9.2 ± 0.99
En59/4	900	15	70	6	3710 ± 795	2810 ± 575	En, Ol, Sp, Sr	10.05 ± 0.85
En59/1	900	15	168	5	8380 ± 3030	6730 ± 2280	En, Crn	8.99 ± 1.5
En59	900	15	168	14	8290 ± 2650	6720 ± 2210	En, Crn	11.9 ± 2.22
En60	1000	15	120	6	3110 ± 600	2440 ± 465	En	8.28 ± 2.2
En47*	1100	15	120	5	2460 ± 960	1860 ± 780	En, Ol, Sp	6.7 ± 1.33
En47/1	1100	15	120	4	1730 ± 450	1340 ± 325	En	8.77 ± 2.16
En47/2	1100	15	168	2	1590 ± 185	1290 ± 255	En, Sp, (Ol)	8.96 ± 1.46
En86	800	25	168	2	4670 ± 655	3590 ± 600	En, Ky	6.67 ± 2.44
En85	900	25	168	4	6400 ± 1330	5040 ± 885	En	5.57 ± 1.56
En84	1100	25	120	2	1420 ± 115	1080 ± 190	En, Ol	5.4 ± 0.84
En87*	1000	35	120	2	1680 ± 490	1140 ± 340	En, Prp	1.73 ± 0.21
En87/2	1000	35	120	6	2370 ± 450	1640 ± 435	En, Ol, Prp	1.21 ± 0.61
En70*	1100	35	168	1	1230	960	En, Ol, Prp	1.75 ± 0.65
En90/1	1100	35	120	3	1500 ± 305	1150 ± 280	En, Ol, Prp, Prl	1.57 ± 0.25

*Synthesized from gels.

tion of partial melt as intergranular film (*1*, *2*). Some water is required to generate such a partial melt in the mantle, as mantle temperatures at the relevant depths are below the dry melting point of peridotite but above the water-saturated solidus (*3*, *4*). Originally, it was believed that the top of the low-velocity zone corresponds to the stability limit of hydrous phases such as phlogopite or hornblende (*5*, *6*). However, this is unlikely because the solubility of water (and of alkalis) in nominally anhydrous mantle minerals (*7*–*9*) is so high that separate hydrous phases such as amphiboles and phlogopite are not stable in an upper mantle of pyrolite composition.

If the low-velocity zone were due to partial melting, the existence of a lower boundary would be even more difficult to understand, as the geotherm remains above the water-saturated solidus with increasing depth. Moreover, it is unclear whether low degrees of partial melt in the mantle would form an intergranular film (*10*), as dry basaltic melts do not wet mantle minerals and therefore tend to form isolated pockets. Accordingly, alternative models have been proposed. These models (*10*, *11*) are based on the observation that water dissolved in mantle minerals such as olivine reduces both the strength of the mineral and the seismic velocities. The boundary between lithosphere and asthenosphere may then correspond to a boundary in intracrystalline water content, with the asthenosphere being water-rich, whereas the oceanic lithosphere is depleted in water as a result of the melt extraction at mid-ocean ridges. The presence of partial melt in the asthenosphere is not required in these models. However, they cannot explain the existence of a low-velocity zone below continental shields, as the mechanism of magma production below continents is very different from that prevailing at mid-ocean ridges.

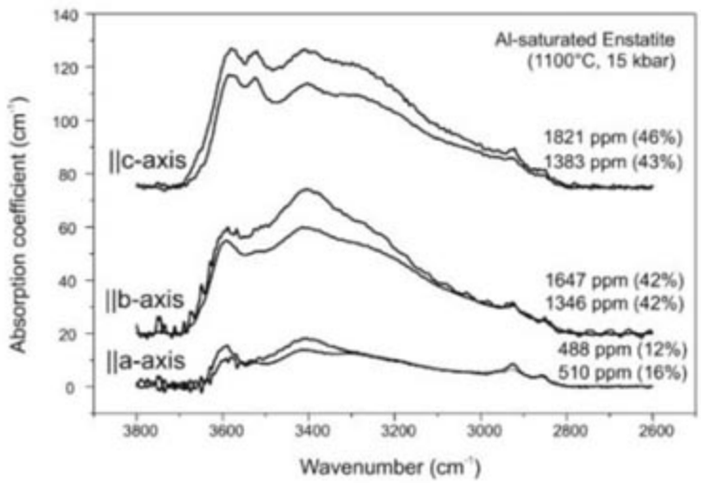

Fig. 1. Polarized infrared spectra of two aluminum-saturated enstatite crystals synthesized at 1100°C and 15 kbar. Water contents (in ppm) correspond to the absorbances measured parallel to the three crystallographic axes. Bulk water contents are obtained by adding these values. Numbers in parentheses denote percentage of total water observed in each of the three directions of polarization. The spectra shown here and in Fig. 2 were obtained from the raw data by subtracting a linear baseline defined by the points at 3800 cm^{-1} and 2800 cm^{-1}. The two weak features between 2800 cm^{-1} and 3000 cm^{-1} could be due to organic surface contamination. However, they persisted after repolishing and they may therefore be intrinsic to the sample.

[1]Institut für Geowissenschaften, Universität Tübingen, Wilhelmstr. 56, 72074 Tübingen, Germany. [2]Bayerisches Geoinstitut, Universität Bayreuth, 95440 Bayreuth, Germany. [3]Department of Geological Sciences, University of Colorado, Boulder, CO 80309, USA. [4]Institut für Geowissenschaften, Friedrich-Schiller-Universität Jena, Burgweg 11, 07749 Jena, Germany.

*To whom correspondence should be addressed. E-mail: hans.keppler@uni-bayreuth.de

All models of the low-velocity zone depend on the presence of water and its solubility in mantle minerals. The main constituents of the upper mantle are olivine and orthopyroxene (enstatite). The water solubility in both olivine and Al-free orthopyroxene is quite comparable and increases with pressure and temperature (*7–9*, *12*). However, aluminum is known to greatly enhance water solubility in orthopyroxene, and at high Al contents, water in orthopyroxene may dominate the water budget in the mantle. Throughout Earth's upper mantle, olivine and orthopyroxene usually coexist with small amounts of an aluminous phase such as spinel or garnet. Therefore, we experimentally studied the solubility of water in aluminous $MgSiO_3$ enstatite in equilibrium with spinel or garnet (i.e., under conditions of aluminum saturation).

Experiments were carried out in an end-loaded piston-cylinder apparatus. Mixtures of $Mg(OH)_2$, $Al(OH)_3$, and SiO_2 were sealed in platinum-rhodium ($Pt_{0.95}Rh_{0.05}$) capsules together with about 20 weight % of liquid water. The stoichiometry of the starting mixture was chosen to correspond to aluminous orthopyroxene plus small amounts of olivine and spinel or garnet. In some experiments, homogeneous mixtures of the starting chemicals were used. In most experiments, however, alternating layers with low and high silica content were introduced into the capsule to reduce nucleation rates so as to grow larger crystals. In addition, some experiments were carried out with amorphous gels and liquid water as starting material. Experiments were run at 15 to 35 kbar and 800° to 1100°C for a few days. After the experiments, the capsules were opened. Capsules that did not release excess water after the experiment were discarded. Perfectly clear and inclusion-free single crystals of orthopyroxene were picked from the charges, optically oriented, and doubly polished. Polarized infrared spectra (Fig. 1) were measured with a Bruker IFS 125 Fourier-transform infrared spectrometer coupled with an IRscope I microscope (tungsten source, CaF_2 beam splitter, narrow-band mercury cadmium telluride detector, Al strip polarizer on KRS 5 substrate). Water contents were calculated from the infrared data with the use of the extinction coefficients of Bell *et al*. (*13*). Chemical analyses were carried out with a JEOL 8900 RL electron microprobe (15 kV, 15 nA, 120 s counting time per spot, focused beam).

The water contents in the aluminous pyroxenes are strikingly high, reaching values close to 1 weight % at low pressures and temperatures (Table 1 and Fig. 2). Water solubilities clearly decrease with both pressure and temperature, opposite to the behavior observed for olivine and Al-free enstatite. The high water solubilities are correlated with anomalously high Al contents in the pyroxenes, which are much higher than those predicted from existing thermodynamic models and experimental calibrations (*14–16*). However, in previous studies, only a few experiments were carried out at the low pressures and temperatures where we observe high Al and water contents, and the water fugacity was probably not carefully controlled in all experiments. The high water contents appear to be intrinsic to the pyroxenes. The presence of foreign phases in the crystals is unlikely, because the infrared bands are strongly polarized (Fig. 1) and measurements were taken only on perfectly clear and optically inclusion-free crystals. To rule out any impurities at the submicroscopic level, we investigated several orthopyroxene crystals by transmission electron microscopy. The structure of the pyroxene crystals (Fig. 3) is undisturbed without any foreign phases or linear and planar defects. The high water contents are therefore definitively due to OH point defects in the structure.

Electron microprobe analyses suggest that most of the water is dissolved by the coupled substitution of $Al^{3+} + H^+$ for Si^{4+} and by the substitution of $Al^{3+} + H^+$ for 2 Mg^{2+}. Both substitutions appear to occur with roughly equal abundance; that is, Al is distributed about equally among tetrahedral and octahedral sites, irrespective of water content. Both substitution

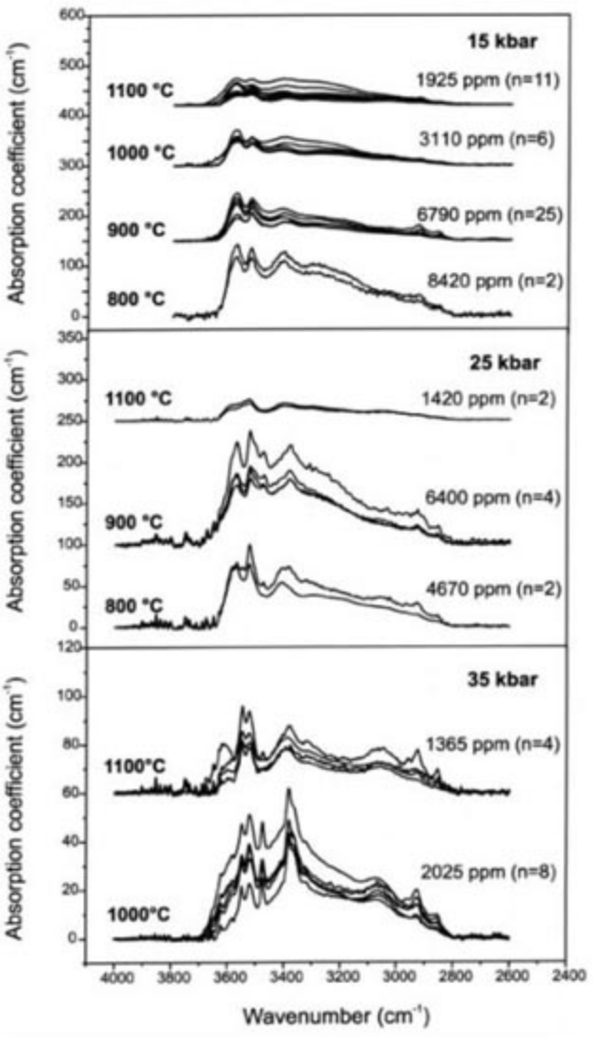

Fig. 2. Polarized infrared spectra (electrical field vector E parallel to the crystallographic *c* axis) and total water contents of aluminum-saturated enstatite at 800° to 1100°C and 15 to 35 kbar. Numbers are average water contents derived from the bulk water contents of all samples synthesized at a given pressure and temperature; *n* is the number of measurements. Bulk water contents were calculated as explained in Fig. 1. The water content of the sample synthesized at 25 kbar and 800°C, where only two crystals could be measured, is probably somewhat below the real water solubility under these conditions.

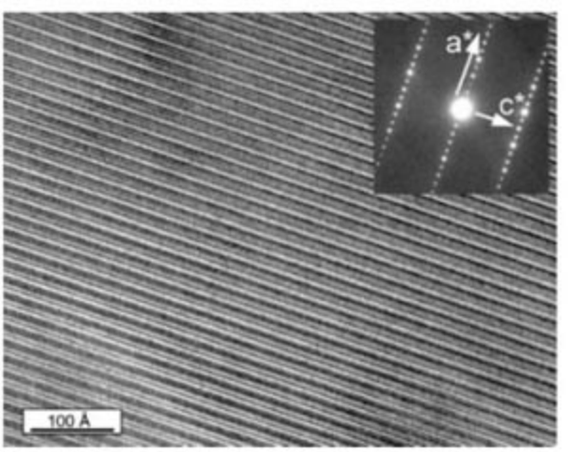

Fig. 3. Representative high-resolution transmission electron microscopy image taken along the [010] direction and corresponding selected area electron diffraction pattern (inset; *a** and *c** axes are shown) of an aluminum-saturated enstatite with 0.75 weight % water. The sample was synthesized at 15 kbar and 900°C. No evidence for foreign phases or planar defects can be detected in this image.

mechanisms imply a molar 1:1 ratio between Al and H. This is consistent with the observation that the "excess" of aluminum in the orthopyroxenes relative to existing calibrations (*14*–*16*) roughly equals the water content, if both Al_2O_3 and H_2O are expressed in molar fractions. The substitution mechanism was confirmed by a single-crystal x-ray diffraction structure refinement of one aluminous pyroxene containing 7500 ppm (by weight) of water. The structure refinement yielded 5% vacancies on one of the Mg sites [M2 (*17*)], consistent with H^+ substituting for Mg^{2+} and a significantly enlarged polyhedral volume of one of the Si sites [Si2 (*17*)] of 1.6575 $Å^3$, consistent with a substitution of $Al^{3+} + H^+$ for Si^{4+}. Structurally, the decrease in H and Al contents with increasing pressure results from the pressure destabilization of tetrahedral Al.

The systematic variations in water content with pressure and temperature observed in this study (Fig. 2) suggest that the water contents represent true equilibrium solubility. This is also supported by the observation that runs with different starting materials (oxide mixture and gels) yield similar results. To describe the water solubility in orthopyroxene coexisting with olivine and an aluminous phase as a function of pressure, temperature, and water fugacity, we calibrated a model that describes the water solubility in aluminous enstatite as the sum of the water solubility in Al-free enstatite and the water solubility coupled to aluminum. The water solubility in Al-free enstatite was previously calibrated (*8*, *9*) and can be expressed as

$$c_{water} = A\, f_{H_2O} \exp\left(\frac{-\Delta H^{1bar}}{RT}\right) \exp\left(\frac{-\Delta V^{solid} P}{RT}\right) \quad (1)$$

where A = 0.01354 ppm/bar, f_{H_2O} is water fugacity [calculated using the equation of state of (*18*)], ΔH^{1bar} = –4563 J/mol, ΔV^{solid} = 12.1 cm^3/mol, R is the gas constant, P is pressure, and T is absolute temperature. The additional water solubility due to Al can then be described by

$$c^{Al}_{water} = A^{Al} (f_{H_2O})^{1/2} \exp\left(\frac{-\Delta H^{1bar}_{Al}}{RT}\right) \exp\left(\frac{-\Delta V^{solid}_{Al} P}{RT}\right) \quad (2)$$

Note, however, that in Eq. 2 water fugacity enters as a square-root term (*19*) because the coupled substitution with Al yields isolated OH groups, unlike the OH pairs that result from the substitution of 2 H^+ for Mg^{2+} in pure enstatite (*8*, *9*). A least-squares fit of all experimental data to Eq. 2 yielded A^{Al} = 0.042 ppm/$bar^{0.5}$, ΔH^{1bar}_{Al} = –79,685 J/mol, and ΔV^{solid}_{Al}= 11.3 cm^3/mol. The total water solubility in orthopyroxene coexisting with olivine and either spinel or pyrope can now be calculated at any pressure and temperature by adding the results from Eqs. 1 and 2. This is consistent with observations from previous studies that the water solubility coupled to Al and the water solubility in Al-free enstatite are due to different and independent defects, with the bulk water solubility being the sum of the individual defect solubilities (*8*, *20*). Only pressure and temperature are required to calculate the equilibrium water content in the Al-saturated orthopyroxene. This is because according to the phase rule, in a four-component system (MgO-Al_2O_3-SiO_2-H_2O) the coexistence of four phases (orthopyroxene, olivine, aluminous phase, and fluid) only leaves two degrees of freedom. Therefore, if pressure and temperature are given, all compositional variables in the system are determined.

Bulk mantle water solubility has a pronounced minimum (Fig. 4) between 150 and 200 km depth, coinciding with the location of the seismic low-velocity zone (shaded) below continental shields. The minimum is due to the sharp decrease of water solubility in aluminous orthopyroxene with temperature and also with pressure, whereas water solubility in olivine continuously increases with pressure and temperature (*7*, *12*). As shown in Fig. 4, at a bulk water content of about 800 ppm, the mantle in the low-velocity zone would be oversaturated with water (i.e., the water activity would equal 1). However, as the geotherm at this depth is located above the water-saturated peridotite solidus (*3*, *4*) of about 1000°C, a hydrous melt will form in the presence of sufficient amounts of water. Because the temperature of the geotherm is far above the water-saturated solidus under these conditions, a water activity around 0.1 is probably sufficient to induce melting (*21*). This water activity would imply that a few hundred ppm of water are sufficient to generate a small fraction of hydrous melt in the asthenosphere. Such water contents are to be expected in the upper mantle (*22*–*24*). If the same calculation is carried out for a hotter oceanic geotherm (Fig. 4, right panel), the upper boundary of the zone of minimum water solubility is lifted to a depth of only 60 to 80 km, consistent with the position of the low-velocity zone below oceans. Moreover, this behavior also provides a straightforward explanation for the seismic observation that the top of the low-velocity zone is very sharp and well defined, whereas the lower boundary is more diffuse and difficult to locate (*2*, *25*). As the water solubility in mantle minerals sharply increases with decreasing depth, the fraction of partial melt in equilibrium with these minerals will also sharply decrease at the asthenosphere-lithosphere boundary. On the other hand, toward the lower boundary of the asthenosphere, the decrease in

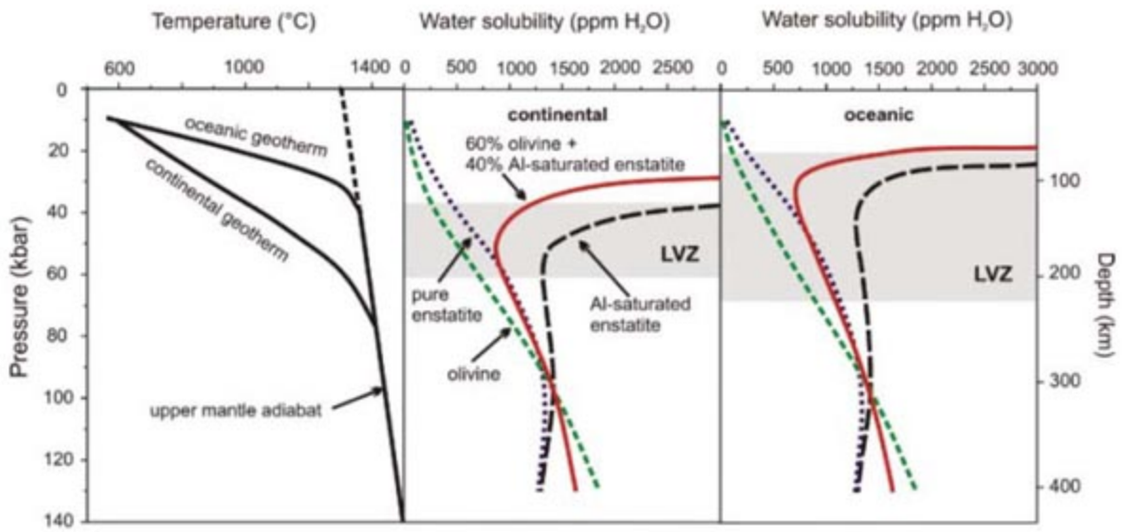

Fig. 4. Water solubility (in ppm by weight) in upper-mantle minerals as a function of depth for a typical continental shield and oceanic geotherm (*26*). The typical position of the low-velocity zone (LVZ) below continental shields and below oceans is shaded in gray. Water solubility in olivine is according to Kohlstedt *et al.* (*7*). Water solubility in aluminum-saturated enstatite was calculated from Eqs. 1 and 2. Recently (*27*), it was suggested that the infrared extinction coefficient of water in olivine may be considerably smaller than previously thought. If this new calibration were applied, the water solubility in olivine would increase by a factor of about 2.5. This would somewhat sharpen the minimum in the bulk water solubility curves shown above and move them to higher water contents. It would not, however, change the general shape of the curves or the position of the inferred boundaries of the asthenosphere. The effect of using different experimental data for water solubility in olivine as well as the effect of changing the ratio of orthopyroxene to olivine is further discussed in (*21*).

melt fraction will be more gradual, reflecting the gradual increase of water solubility in olivine and orthopyroxene.

Our results therefore support the concept that the low-velocity zone may be related to partial melting (*1*, *2*, *6*). However, even in the absence of melting, the partitioning of water between olivine and orthopyroxene would strongly depend on depth. The high water solubilities in aluminous orthopyroxene at low pressure and temperature will effectively "dry out" olivine, and this may also contribute to a stiffening of the lithosphere. In any case, however, our results imply that the existence of an asthenosphere—and therefore of plate tectonics as we know it—is possible only in a planet with a water-bearing mantle.

References and Notes

1. D. L. Anderson, *Theory of the Earth* (Blackwell Scientific, Boston, 1989).
2. D. L. Anderson, C. Sammis, *Phys. Earth Planet. Inter.* **3**, 41 (1970).
3. I. Kushiro, Y. Syono, S. Akimoto, *J. Geophys. Res.* **73**, 6023 (1968).
4. T. Kawamoto, J. R. Holloway, *Science* **276**, 240 (1997).
5. I. B. Lambert, P. J. Wyllie, *Nature* **219**, 1240 (1968).
6. I. B. Lambert, P. J. Wyllie, *Science* **169**, 764 (1970).
7. D. L. Kohlstedt, H. Keppler, D. C. Rubie, *Contrib. Mineral. Petrol.* **123**, 345 (1996).
8. M. Rauch, H. Keppler, *Contrib. Mineral. Petrol.* **143**, 525 (2002).
9. K. Mierdel, H. Keppler, *Contrib. Mineral. Petrol.* **148**, 305 (2004).
10. S.-I. Karato, H. Jung, *Earth Planet. Sci. Lett.* **157**, 193 (1998).
11. G. Hirth, D. L. Kohlstedt, *Earth Planet. Sci. Lett.* **144**, 93 (1996).
12. Y.-H. Zhao, S. B. Ginsberg, D. L. Kohlstedt, *Contrib. Mineral. Petrol.* **147**, 155 (2004).
13. D. R. Bell, P. D. Ihinger, G. R. Rossman, *Am. Mineral.* **80**, 465 (1995).
14. P. A. Danckwerth, R. C. Newton, *Contrib. Mineral. Petrol.* **66**, 189 (1978).
15. D. Perkins, T. J. B. Holland, R. C. Newton, *Contrib. Mineral. Petrol.* **78**, 99 (1981).
16. T. Gasparik, *Phase Diagrams for Geoscientists: An Atlas of the Earth's Interior* (Springer-Verlag, Berlin, 2003).
17. M. Cameron, J. J. Papike, *Rev. Mineral.* **7**, 5 (1980).
18. K. S. Pitzer, S. M. Sterner, *J. Chem. Phys.* **101**, 3111 (1994).
19. R. Lu, H. Keppler, *Contrib. Mineral. Petrol.* **129**, 35 (1997).
20. R. Stalder, H. Skogby, *Eur. J. Mineral.* **14**, 1139 (2002).
21. See supporting material on *Science* Online.
22. D. R. Bell, G. R. Rossman, *Science* **255**, 1391 (1992).
23. J. Ingrin, H. Skogby, *Eur. J. Mineral.* **12**, 543 (2000).
24. N. Bolfan-Casanova, *Mineral. Mag.* **69**, 229 (2005).
25. C. A. Rychert, K. M. Fischer, S. Rondenay, *Nature* **436**, 542 (2005).
26. D. L. Turcotte, G. Schubert, *Geodynamics* (Cambridge Univ. Press, Cambridge, ed. 2, 2002).
27. D. R. Bell, G. R. Rossman, J. Maldener, D. Endisch, F. Rauch, *J. Geophys. Res.* **108**, 10.1029/2001JB000679 (2003).
28. M. S. Paterson, *Bull. Mineral.* **105**, 20 (1982).

29. Supported by a Deutsche Forschungsgemeinschaft Leibniz award (H.K.) and by the Alexander von Humboldt Foundation and NSF grant EAR 0337611 (J.R.S.).

Supporting Online Material

www.sciencemag.org/cgi/content/full/315/5810/364/DC1
SOM Text
Figs. S1 and S2
References

21 September 2006; accepted 23 November 2006
10.1126/science.1135422

A Semi-Empirical Approach to Projecting Future Sea-Level Rise

Stefan Rahmstorf

A semi-empirical relation is presented that connects global sea-level rise to global mean surface temperature. It is proposed that, for time scales relevant to anthropogenic warming, the rate of sea-level rise is roughly proportional to the magnitude of warming above the temperatures of the pre–Industrial Age. This holds to good approximation for temperature and sea-level changes during the 20th century, with a proportionality constant of 3.4 millimeters/year per °C. When applied to future warming scenarios of the Intergovernmental Panel on Climate Change, this relationship results in a projected sea-level rise in 2100 of 0.5 to 1.4 meters above the 1990 level.

Understanding global sea-level changes is a difficult physical problem, because complex mechanisms with different time scales play a role (*1*), including thermal expansion of water due to the uptake and penetration of heat into the oceans, input of water into the ocean from glaciers and ice sheets, and changed water storage on land. Ice sheets have the largest potential effect, because their complete melting would result in a global sea-level rise of about 70 m. Yet their dynamics are poorly understood, and the key processes that control the response of ice flow to a warming climate are not included in current ice sheet models [for example, meltwater lubrication of the ice sheet bed (*2*) or increased ice stream flow after the removal of buttressing ice shelves (*3*)]. Large uncertainties exist even in the projection of thermal expansion, and estimates of the total volume of ice in mountain glaciers and ice caps that are remote from the continental ice sheets are uncertain by a factor of two (*4*). Finally, there are as yet no published physically based projections of ice loss from glaciers and ice caps fringing Greenland and Antarctica.

For this reason, our capability for calculating future sea-level changes in response to a given surface warming scenario with present physics-based models is very limited, and models are not able to fully reproduce the sea-level rise of recent decades. Rates of sea-level rise calculated with climate and ice sheet models are generally lower than observed rates. Since 1990, observed sea level has followed the uppermost uncertainty limit of the Intergovernmental Panel on Climate Change (IPCC) Third Assessment Report (TAR), which was constructed by assuming the highest emission scenario combined with the highest climate sensitivity and adding an ad hoc amount of sea-level rise for "ice sheet uncertainty" (*1*).

While process-based physical models of sea-level rise are not yet mature, semi-empirical models can provide a pragmatic alternative to estimate the sea-level response. This is also the approach taken for predicting tides along coasts (for example, the well-known tide tables), where the driver (tidal forces) is known, but the calculation of the sea-level response from first principles is so complex that semi-empirical relationships perform better. Likewise, with current and future sea-level rise, the driver is known [global warming (*1*)], but the computation of the link between the driver and the response from first principles remains elusive. Here, we will explore a semi-empirical method for estimating sea-level rise.

As a driver, we will use the global average near-surface air temperature, which is the standard diagnostic used to describe global warming. Figure 1 shows a schematic response to a step-function increase in temperature, after climate and sea level parameters were at equilibrium. We expect sea level to rise as the ocean takes up heat and ice starts to melt, until (asymptotically) a new equilibrium sea level is reached. Paleoclimatic data suggest that changes in the final equilibrium level may be very large: Sea level at the Last Glacial Maximum, about 20,000 years ago, was 120 m lower than the current level, whereas global mean temperature was 4° to 7°C lower (*5*, *6*). Three million years ago, during the Pliocene, the average climate was about 2° to 3°C warmer and sea level was

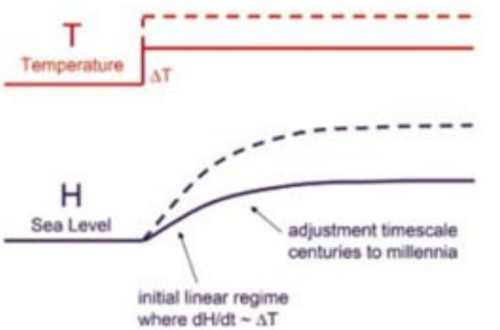

Fig. 1. Schematic of the response of sea level to a temperature change. The solid line and the dashed line indicate two examples with different amplitude of temperature change.

Potsdam Institute for Climate Impact Research, 14473 Potsdam, Germany. E-mail: rahmstorf@ozean-klima.de

25 to 35 m higher (*7*) than today's values. These data suggest changes in sea level on the order of 10 to 30 m per °C.

The initial rate of rise is expected to be proportional to the temperature increase

$$dH/dt = a\,(T - T_0) \qquad (1)$$

where H is the global mean sea level, t is time, a is the proportionality constant, T is the global mean temperature, and T_0 is the previous equilibrium temperature value. The equilibration time scale is expected to be on the order of millennia. Even if the exact shape of the time evolution $H(t)$ is not known, we can approximate it by assuming a linear increase in the early phase; the long time scales of the relevant processes give us hope that this linear approximation may be valid for a few centuries. As long as this approximation holds, the sea-level rise above the previous equilibrium state can be computed as

$$H(t) = a\int_{t0}^{t}(T(t') - T_0)\,dt' \qquad (2)$$

where t' is the time variable.

We test this relationship with observed data sets of global sea level (*8*) and temperature [combined land and ocean temperatures obtained from NASA (*9*)] for the period 1880–2001, which is the time of overlap for both series. A highly significant correlation of global temperature and the rate of sea-level rise is found ($r = 0.88$, $P = 1.6 \times 10^{-8}$) (Fig. 2) with a slope of $a = 3.4$ mm/year per °C. If we divide the magnitude of equilibrium sea-level changes that are suggested by paleoclimatic data (*5*–*7*) by this rate of rise, we obtain a time scale of 3000 to 9000 years, which supports the long equilibration time scale of sea-level changes.

The baseline temperature T_0, at which sea-level rise is zero, is 0.5°C below the mean temperature of the period 1951–1980. This result is consistent with proxy estimates of temperatures in the centuries preceding the modern warming (*10*), confirming that temperature and sea level were not far from equilibrium before this modern warming began. This is consistent with the time scale estimated above and the relatively stable climate of the Holocene (the past 10,000 years).

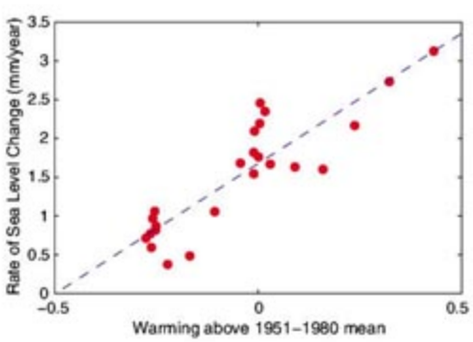

Fig. 2. Correlation of temperature and the rate of sea-level rise for the period 1881–2001. The dashed line indicates the linear fit. Both temperature and sea-level curves were smoothed by computing nonlinear trend lines, with an embedding period of 15 years (*14*). The rate of sea-level change is the time derivative of this smoothed sea-level curve, which is shown in Fig. 3. Data were binned in 5-year averages to illustrate this correlation.

In Fig. 3, we compare the time evolution of global mean temperature, converted to a "hindcast" rate of sea-level rise according to Eq. 1, with the observed rate of sea-level rise. This comparison shows a close correspondence of the two rates over the 20th century. Like global temperature evolution, the rate of sea-level rise increases in two major phases: before 1940 and again after about 1980. It is this figure that most clearly demonstrates the validity of Eq. 1. Accordingly, the sea level that was computed by integrating global temperature with the use of Eq. 2 is in excellent agreement with the observed sea level (Fig. 3), with differences always well below 1 cm.

We can explore the consequences of this semi-empirical relationship for future sea levels (Fig. 4), using the range of 21st century temperature scenarios of the IPCC (*1*) as input into Eq. 2. These scenarios, which span a range of temperature increase from 1.4° to 5.8°C between 1990 and 2100, lead to a best estimate of sea-level rise of 55 to 125 cm over this period. By including the statistical error of the fit shown in Fig. 2 (one SD), the range is extended from 50 to 140 cm. These numbers are significantly higher than the model-based estimates of the IPCC for the same set of temperature scenarios, which gave a range from 21 to 70 cm (or from 9 to 88 cm, if the ad hoc term for ice sheet uncertainty is included). These semi-empirical scenarios smoothly join with the observed trend in 1990 and are in good agreement with it during the period of overlap.

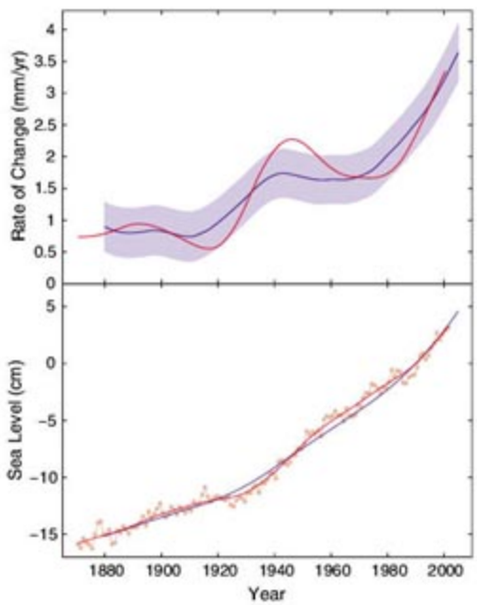

Fig. 3. (**Top**) Rate of sea-level rise obtained from tide gauge observations (red line, smoothed as described in the Fig. 2 legend) and computed from global mean temperature from Eq. 1 (dark blue line). The light blue band indicates the statistical error (one SD) of the simple linear prediction (*15*). (**Bottom**) Sea level relative to 1990 obtained from observations (red line, smoothed as described in the Fig. 2 legend) and computed from global mean temperature from Eq. 2 (blue line). The red squares mark the unsmoothed, annual sea-level data.

We checked that this analysis is robust within a wide range of embedding periods (i.e., smoothing) of the observational time series. The slope found in Fig. 2 varies between 3.2 and 3.5 mm/year per °C for any embedding period between 2 and 17 years, causing only minor variations in the projected sea level. For short embedding periods (around 5 years), the rate of sea-level rise (Fig. 3, top) closely resembles that shown in (*8*) with large short-term fluctuations. For embedding dimensions longer than 17 years, the slope starts to decline, because the acceleration of sea-level rise since 1980 (Fig. 3) is then progressively lost by excessive smoothing. For very long embedding periods (30 years), the rate of sea-level rise becomes rather flat such as that shown in (*11*).

The linear approximation (Eq. 1) is only a simplistic first-order approximation to a number of complex processes with different time scales. The statistical error included in Fig. 4 does not include any systematic error that arises if the linear relationship breaks down during the forecast period. We can test for this systematic error using climate models, if only for the thermal expansion component of sea-level rise that these models capture. For this test, we used the CLIMBER-3α climate model (*12*), which uses a simplified atmosphere model coupled to a three-dimensional general circulation ocean model with free surface (i.e., that vertically adjusts). We used a model experiment initialized from an equilibrium state of the coupled system in the year 1750 and, with historic radiative forcing, forced changes until the year 2000. After 2000, the model was forced with the IPCC A1FI scenario. The global mean temperature increases by 0.8°C in the 20th century and by 5.0°C from 1990 to 2100 in this experiment.

Temperature and sea-level rise data from this model for the time period 1880–2000 were treated like the observational data in the analysis presented above, and graphs corresponding to Figs. 2 and 3 look similar to those derived from the observational data (figs. S1 and S2). The slope found is only 1.6 mm/year per °C (i.e., half of the observed slope) because only the thermal expansion component is modeled. Using the semi-empirical relation as fitted to the period 1880–2000, we predicted the sea level for the 21st century (fig. S3). Up to the year 2075, this predicted sea level remains within 5 cm of the actual (modeled) sea level. By the year 2100, the predicted level is 51 cm whereas the actual (modeled) level is 39 cm above that of 1990 (i.e., the semi-empirical formula overpredicts sea level by 12 cm).

For the continental ice component of sea-level rise, we do not have good models to test how the

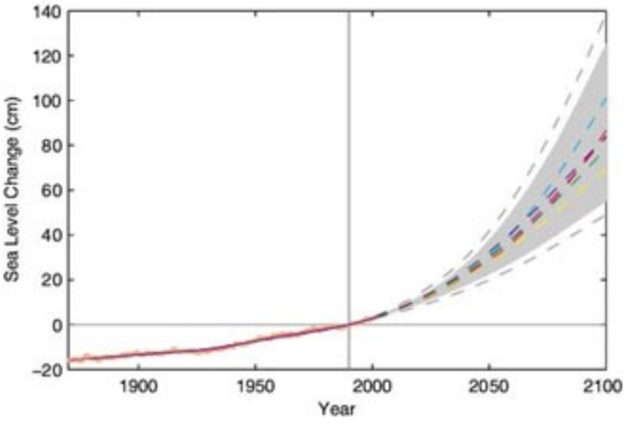

Fig. 4. Past sea level and sea-level projections from 1990 to 2100 based on global mean temperature projections of the IPCC TAR. The gray uncertainty range spans the range of temperature rise of 1.4° to 5.8° C, having been combined with the best statistical fit shown in Fig. 2. The dashed gray lines show the added uncertainty due to the statistical error of the fit of Fig. 2. Colored dashed lines are the individual scenarios as shown in (*1*); the light blue line is the A1FI scenario, and the yellow line is the B1 scenario.

linear approximation performs, although the approximation is frequently used by glaciologists ("degree-days scheme"). Given the dynamical response of ice sheets observed in recent decades and their growing contribution to overall sea-level rise, this approximation may not be robust. The ice sheets may respond more strongly to temperature in the 21st century than would be suggested by a linear fit to the 20th century data, if time-lagged positive feedbacks come into play (for example, bed lubrication, loss of buttressing ice shelves, and ocean warming at the grounding line of ice streams). On the other hand, many small mountain glaciers may disappear within this century and cease to contribute to sea-level rise. It is therefore difficult to say whether the linear assumption overall leads to an over- or underestimation of future sea level. Occam's razor suggests that it is prudent to accept the linear assumption as reasonable, although it should be kept in mind that a large uncertainty exists, which is not fully captured in the range shown in Fig. 4.

Regarding the lowest plausible limit to sea-level rise, a possible assumption may be that the rate shown in Fig. 3 stops increasing within a few years (although it is difficult to see a physical reason for this) and settles at a constant value of 3.5 mm/year. This implies a sea-level rise of 38 cm from 1990 to 2100. Any lower value would require that the rate of sea-level rise drops despite rising temperature, reversing the relationship found in Fig. 2.

Although a full physical understanding of sea-level rise is lacking, the uncertainty in future sea-level rise is probably larger than previously estimated. A rise of over 1 m by 2100 for strong warming scenarios cannot be ruled out, because all that such a rise would require is that the linear relation of the rate of sea-level rise and temperature, which was found to be valid in the 20th century, remains valid in the 21st century. On the other hand, very low sea-level rise values as reported in the IPCC TAR now appear rather implausible in the light of the observational data.

The possibility of a faster sea-level rise needs to be considered when planning adaptation measures, such as coastal defenses, or mitigation measures designed to keep future sea-level rise within certain limits [for example, the 1-m long-term limit proposed by the German Advisory Council on Global Change (*13*)].

References and Notes

1. J. T. Houghton *et al.*, Eds., *Climate Change 2001: The Scientific Basis* (Cambridge Univ. Press, Cambridge, 2001).
2. H. J. Zwally *et al.*, *Science* **297**, 218 (2002).
3. E. Rignot *et al.*, *Geophys. Res. Lett.* **31**, 18 (2004).
4. S. C. B. Raper, R. J. Braithwaite, *Nature* **439**, 311 (2006).
5. C. Waelbroeck *et al.*, *Quat. Sci. Rev.* **21**, 295 (2002).
6. T. Schneider von Deimling, A. Ganopolski, H. Held, S. Rahmstorf, *Geophys. Res. Lett.* **33**, L14709 (2006).
7. H. J. Dowsett *et al.*, *Global Planet. Change* **9**, 169 (1994).
8. J. A. Church, N. J. White, *Geophys. Res. Lett.* **33**, L01602 (2006).
9. J. Hansen *et al.*, *J. Geophys. Res. Atmos.* **106**, 23947 (2001).
10. P. D. Jones, M. E. Mann, *Rev. Geophys.* **42**, RG2002 (2004).
11. S. Jevrejeva, A. Grinsted, J. C. Moore, S. Holgate, *J. Geophys. Res.* **111**, 09012 (2006).
12. M. Montoya *et al.*, *Clim. Dyn.* **25**, 237 (2005).
13. German Advisory Council on Global Change, "The future oceans: warming up, rising high, turning sour," (Wissenschaftlicher Beirat der Bundesregierung Globale Umweltveränderungen Special Report, Berlin, 2006); (www.wbgu.de/wbgu_sn2006_en.pdf).
14. J. C. Moore, A. Grinsted, S. Jevrejeva, *Eos* **86**, 226 (2005).
15. The statistical error was calculated by means of the Matlab function "polyval" for the linear fit shown in Fig. 2.

16. The author thanks J. Church for providing the observational data and M. Stöckmann for the model data. They as well as J. Gregory and B. Hare are thanked for valuable discussions.

Supporting Online Material

www.sciencemag.org/cgi/content/full/1135456/DC1
Figs. S1 to S3

22 September 2006; accepted 4 December 2006
Published online 14 December 2006;
10.1126/science.1135456
Include this information when citing this paper.

Nonequilibrium Mechanics of Active Cytoskeletal Networks

Daisuke Mizuno,[1] Catherine Tardin,[1] C. F. Schmidt,[1,2]* F. C. MacKintosh[1]*

Cells both actively generate and sensitively react to forces through their mechanical framework, the cytoskeleton, which is a nonequilibrium composite material including polymers and motor proteins. We measured the dynamics and mechanical properties of a simple three-component model system consisting of myosin II, actin filaments, and cross-linkers. In this system, stresses arising from motor activity controlled the cytoskeletal network mechanics, increasing stiffness by a factor of nearly 100 and qualitatively changing the viscoelastic response of the network in an adenosine triphosphate–dependent manner. We present a quantitative theoretical model connecting the large-scale properties of this active gel to molecular force generation.

Mechanics directly control many functions of cells, including the generation of forces, motion, and the sensing of external forces (*1*). The cytoskeleton is a network of semiflexible linear protein polymers (actin filaments, microtubules, and intermediate filaments) that is responsible for most of the mechanical functions of cells. It differs from common polymer materials in both the complexity of composition and the fact that the system is not at thermodynamic equilibrium. Chemical nonequilibrium drives mechanoenzymes (motor proteins) that are the force generators in cells. The cytoskeleton is thus an active material that can adapt its mechanics and perform mechanical tasks such as cell locomotion or cell division.

Here, we show how nonequilibrium motor activity controls the mechanical properties of a simple three-component in vitro model cytoskeletal network. The nonequilibrium origin of this active control mechanism can be seen directly in the violation of a fundamental theorem of statistical physics, the fluctuation-dissipation (FD) theorem, which links thermal fluctuations of systems to their response to external forces. The FD theorem is a generalization of Einstein's description of Brownian motion (*2*). Although it is valid only in equilibrium, its possible extension to out-of-equilibrium systems such as granular materials and living cells has been debated (*3*–*5*). Prior studies in cells have suggested violations of the FD theorem (*3*), but this has not been directly observed. We show that an in vitro model system consisting of a cross-linked

[1]Department of Physics and Astronomy, Vrije Universiteit, 1081HV Amsterdam, Netherlands. [2]III. Physikalisches Institut, Fakultät für Physik, Georg-August-Universität, 37077 Göttingen, Germany.

*To whom correspondence should be addressed. E-mail: cfs@nat.vu.nl (C.F.S.); fcm@nat.vu.nl (F.C.M.)

actin network with embedded force-generating myosin II motors strongly violates the FD theorem and that it does so because of the contractility of the acto-myosin system.

Actin and myosin are key components in muscle contraction and cell motility (*6*, *7*). Myosin motor domains, or heads, bind to actin filaments (F-actin) and generate force via the hydrolysis of adenosine triphosphate (ATP), resulting in motion along the polar actin filaments. At low salt concentrations, myosin II can form multimeric bipolar structures in vitro (Fig. 1A) (*8*). These "minifilaments" can link different actin filaments and move these filaments relative to each other (*9*). In the absence of ATP, these motor complexes statically cross-link F-actin and generate bundles that can be seen in a light microscope (Fig. 1B). In the presence of ATP, minifilaments generate contractile forces that can result in actin aggregation and phase separation (Fig. 1C), a phenomenon known as superprecipitation (*10*). To stabilize the networks and delay the onset of superprecipitation, we used F-actin cross-linked by biotin and neutravidin.

We measured the mechanical properties of these networks by active microrheology (AMR) (*11*–*13*), in which micrometer-sized embedded probe particles are manipulated by a sinusoidally oscillated optical trap, generating a force F at frequency ω. The response function $\alpha(\omega)$ is obtained from the measured probe particle displacement $u(\omega)$:

$$\alpha(\omega) = u(\omega)/F \qquad (1)$$

For a simple incompressible and homogeneous elastic medium, this response function is related to the shear modulus G or stiffness of the medium via a generalization of the Stokes relation (*13*–*17*) $\alpha = 1/(6\pi Ga)$, where a is the probe particle radius. For materials with dissipation, the displacement u and force F are not in phase, which results in a complex response function. In this case, the shear modulus is $G = G' + iG''$, where G' is the elastic modulus and G'' is the viscous modulus. For cross-linked actin (1 mg/ml) gels, we found a predominantly elastic response in which G' is much larger than G'' in the range of frequencies below 100 Hz. The measured moduli are consistent both with experiments on similar actin gels (*18*) and with theoretical predictions for actin networks with an average distance of about 2 to 3 μm between cross-links (*13*, *19*).

To characterize motor-generated activity, we used passive microrheology (PMR), which consists of recording the spontaneous displacement fluctuations of a probe particle without applied forces (*13*–*16*). In an equilibrium system, only thermal forces act on the probe, and the power spectral density

$$C(\omega) = \int \langle u(t)u(0) \rangle \exp(i\omega t)\, dt \qquad (2)$$

of the displacement fluctuations $u(t)$ is directly related to the mechanical response of the material by the FD theorem,

$$\alpha''(\omega) = \frac{\omega}{2k_B T} C_{eq}(\omega) \text{ (equilibrium only)} \quad (3)$$

where $\alpha''(\omega)$ is the imaginary part of the response function, k_B is the Boltzmann constant, and T is absolute temperature. Because we can independently measure the left side of Eq. 3 with AMR and the right side with PMR, we can search for signatures of motor activity in the form of violations of the FD theorem.

As a control, we first verified the FD theorem as expressed in Eq. 3 for an equilibrium sample by directly comparing $\alpha''(\omega)$ measured with AMR and $\omega C(\omega)/2k_B T$ measured with PMR. For cross-linked actin without myosin, the agreement with Eq. 3 is shown in Fig. 2A.

Active processes create additional fluctuations and are expected to make the right side of Eq. 3 larger than the left side, thus violating the FD theorem. Indirect evidence for this has been reported in cells (*3*). We started with experiments at 3.5 mM ATP, where motors are expected to be active. Interestingly, we saw no difference between AMR and PMR results for up to 5 hours (Fig. 2A). At longer times, however, a clear difference developed in the form of strongly enhanced fluctuations at frequencies below 10 Hz (Fig. 2B). The appearance of these nonequilibrium fluctuations after a time lag can be explained by a switching of the myosin minifilaments from a nonprocessive mode, which cannot generate forces between actin filaments, to a processive tension-generating mode. Such a transition is expected because the ratio of attached to unattached time (duty ratio) of myosin increases with decreasing ATP concentration, when motor release induced by ATP binding becomes the rate-limiting step in the chemical cycle (*20*). Consistent with this, the lag time increased with increasing initial ATP concentra-

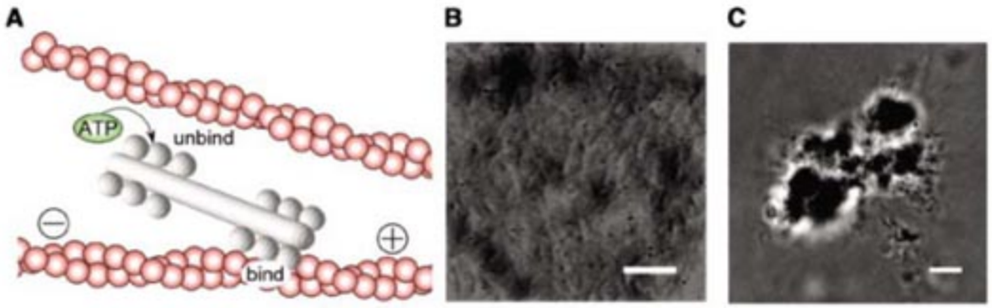

Fig. 1. (**A**) Schematic of a bipolar myosin filament interacting with two actin filaments. Polarity of actin is indicated by the +/− signs (myosin moves toward the plus end). (**B**) Differential interference contrast microscopy image of bundled actin filaments at high salt concentration ([KCl] = 150 mM, actin concentration 1 mg/ml, myosin concentration 170 nM, no cross-links). As ATP depletes, thick acto-myosin bundles form without phase separation. (**C**) At low salt concentration ([KCl] = 50 mM), active myosin filaments result in contraction of the actin network to form dense acto-myosin aggregates (superprecipitation). Scale bars, 5 μm.

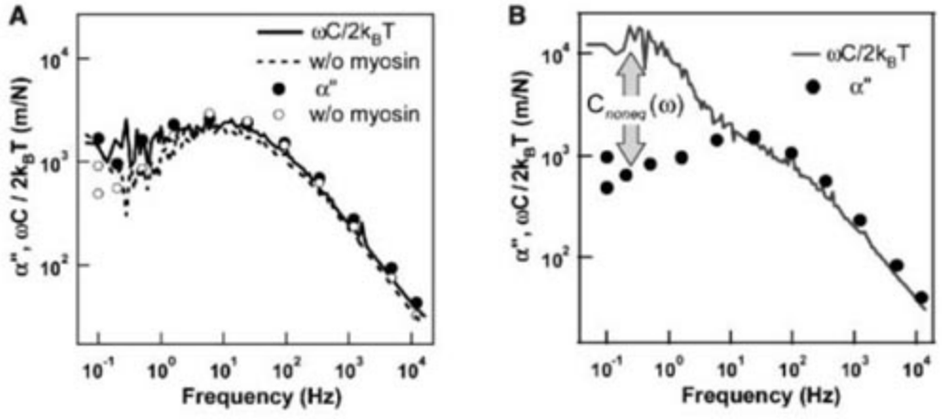

Fig. 2. Mechanical response of cross-linked nonactive and active gels (actin and myosin concentrations as in Fig. 1). (**A**) The imaginary part of the response function α'' measured by AMR (circles) and the normalized power spectrum $\omega C(\omega)/2k_B T$ measured by PMR (lines). Open circles and the dashed line denote cross-linked actin without myosin; solid circles and the solid line denote networks with myosin 2.5 hours after sample preparation. For up to 5 hours, α'' and $\omega C(\omega)/2k_B T$ with and without myosin show good agreement, indicating that myosin activity did not yet produce observable nonequilibrium fluctuations. (**B**) The same as (A) but 6.8 hours after sample preparation (with myosin). Below 10 Hz, nonequilibrium fluctuations are observable as an enhancement of $\omega C(\omega)/2k_B T$ relative to α''.

tion. We also performed experiments at low ATP concentrations stabilized with an ATP regenerating system (*13*). At ATP concentrations below ~60 μM, we observed stable active fluctuations in the gels lasting for several hours.

Along with the nonequilibrium fluctuations, we saw a strong stiffening of the networks due to motor activity. This is apparent in the reduced response or compliance of the network (Fig. 3A). The shear modulus can be calculated using the generalized Stokes formula (*14*–*17*) (Fig. 3B). Here, the network stiffness increases by a factor of almost 100 depending on the ATP concentration. The stiffening of the network is related to the well-known strain stiffening response of actin gels under external stress (*18*, *19*, *21*): The contractile activity of motors results in internal tensile stresses in the actin filaments, which make the network more rigid. Unlike stiffening due to anisotropic shear stress, however, we expect that stresses induced by the motors are isotropic, which should lead to more pronounced stiffening because filaments of all orientations can participate.

The hypothesis that the observed stiffening is due to isotropically tensed filaments can be tested quantitatively by an examination of the frequency dependence of the stiffening. For relaxed actin gels, the stiffness of the networks increases with frequency in the form of a power law as $G \approx (-i\omega)^{3/4}$ (*15*, *22*, *23*). Given the inverse relationship between response and stiffness, this is consistent with the behavior of our model system either in the absence of motors or at high ATP concentrations (Figs. 2A and 3A). With the onset of nonequilibrium activity, however, the power law changed toward a slope of ½, which is consistent with the prediction for filaments under tension (*24*). The full frequency dependence (green curve in Fig. 3A) is derived in (*13*). This frequency dependence also rules out another possible explanation for the observed stiffening of the network, namely an increased cross-linking of actin by inactive myosin. Cross-links alone will not change the $\omega^{-3/4}$ frequency dependence (*22*, *25*). Thus, the increased stiffness seen in Fig. 3B is most likely the result of motor-induced tension in the network strands.

Given the presence of both cross-links and myosin minifilaments in our system, we expect that the myosins generate contractile tension in actin filaments between cross-link points (Fig. 4A). We find rates on the order of a fraction of a micrometer per second in the movement of probe particles (Fig. 4B), consistent with typical rates of myosin motility. This slow buildup of strain implies quasi-static elastic deformations that include network compression. Increased filament density would imply a local reduction of the solvent/buffer, just as squeezing a sponge expels liquid. Given the stochastic binding kinetics of the myosins, the minifilaments eventually let go, which results in a fast relaxation of the network strain (Fig. 4B). The rate at which the network can relax is determined by the dissipation due to the inflow of solvent

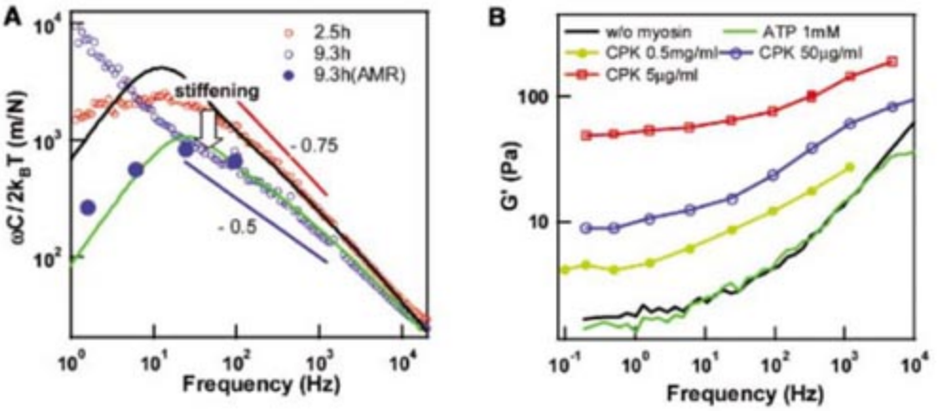

Fig. 3. Effect of filament tension on the response of the active networks (actin and myosin concentrations as in Fig. 1). (**A**) Spectra $\omega C(\omega)/2k_BT$ measured with PMR at 2.5 hours (open red circles) and 9.3 hours (open blue circles) and α'' measured with AMR at 9.3 hours (solid blue circles) after sample preparation (initial [ATP] = 3.5 mM). In the presence of nonequilibrium activity, the response function is reduced, indicating a stiffer sample, which can be fully accounted for by prestress/tension of filaments. Theoretical predictions (*13*) are shown for a network with filament tension of 0.1 pN, cross-link distance $l_c = 2.6$ μm (green curve), and no tension with the same l_c (black curve). Independently known parameters: friction coefficient $\zeta = 0.00377$ Pa·s, persistence length $l_p = 17 \times 10^{-6}$ m, probe radius $a = 2.5$ μm. (**B**) Shear modulus $G'(\omega)$ at controlled [ATP]: green line, 1 mM ATP, same as control (black line, no myosin). Lower [ATP] stabilized below ~60 μM by creatine phosphokinase (CPK): ochre line, [CPK] = 0.5 mg/ml; blue line, 50 μg/ml; red line, 5 μg/ml.

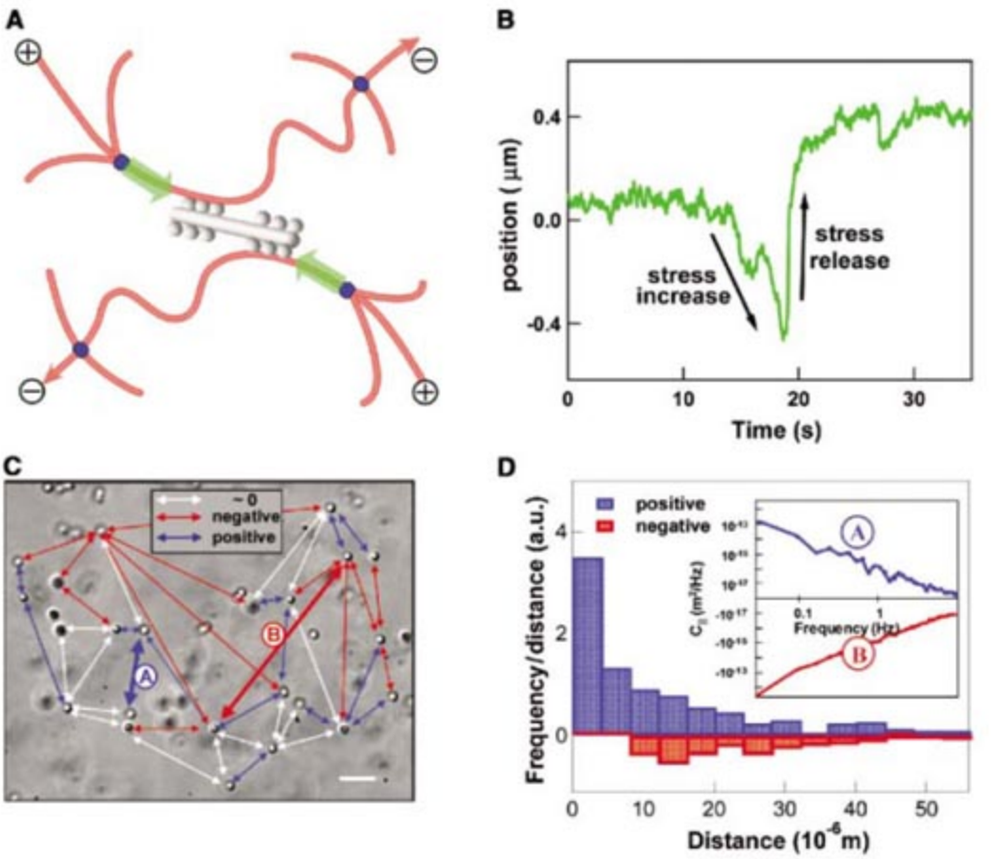

Fig. 4. (**A**) Schematic illustration of tension development in actin filaments (red). Myosin minifilaments (gray) cause network contraction between cross-links (blue). (**B**) Typical contractile event reflected in the motion of a probe particle. (**C**) Correlated motion of particle pairs (diameter 1.1 μm; scale bar, 5 μm) can be measured by video microscopy (*13*, *16*). In equilibrium, cross-correlations must be positive (*16*, *17*, *27*); nonequilibrium forces can lead to positive (blue arrows), negative (red arrows), or no correlations (white arrows). (**D**) Histogram of particle pairs showing positive (blue) and negative (red) correlations dependent on distance. The frequency (vertical axis) was normalized by distance to compensate for the increasing probability of finding a second bead at a given distance. Inset: representative cross-correlation spectra [particle pairs A and B in (C)] with positive (blue) and negative (red) correlations. Negative correlations are observed only at low frequencies, where nonequilibrium behavior is apparent in Fig. 2B.

(like the swelling of a sponge). Time scales for this process are expected to be on the order of $\eta(r/\xi)^2/G$ (*15*, *17*), where ξ (~0.3 μm) is the mesh size of the network and r is a typical length scale of deformation. If we take the cross-linking distance as r (~3 μm), this gives a relaxation time of ~0.1 s, which is consistent with the observed relaxation in Fig. 4B and the appearance of motor activity in Fig. 2B.

To further test the hypothesis that the nonequilibrium effects we observe are due to contractile/compressive gel deformations, we also examined the correlated motions of pairs of particles within the network (Fig. 4, C and D). The observed anticorrelations in particular are not expected in equilibrium, but they are consistent with the contractile forces sketched in Fig. 4A.

Thus, actin, myosin, and cross-links are sufficient to capture essential and general features of contractility and mechanical adaptation in cytoskeletal networks. These observations suggest mechanisms by which cells could rapidly modulate their stiffness by flexing their internal "muscles" without changing the density, polymerization, or bundling state of F-actin. Cells can actively adapt their elasticity to the mechanics of the extracellular matrix (*26*) or to an externally applied force (*1*), and motors could be the cause for that. From a materials perspective, this in vitro model system exhibits an active state of matter that adjusts its own mechanical stiffness via internal forces. This work can be a starting point for exploring both model systems and cells in quantitative detail, with the aim of uncovering the physical principles underlying the active regulation of the complex mechanical functions of cells.

References and Notes

1. P. A. Janmey, D. A. Weitz, *Trends Biochem. Sci.* **29**, 364 (2004).
2. A. Einstein, *Ann. Phys.* **17**, 549 (1905).
3. A. W. C. Lau, B. D. Hoffman, A. Davies, J. C. Crocker, T. C. Lubensky, *Phys. Rev. Lett.* **91**, 198101 (2003).
4. L. Le Goff, F. Amblard, E. M. Furst, *Phys. Rev. Lett.* **88**, 018101 (2002).
5. G. D'Anna, P. Mayor, A. Barrat, V. Loreto, F. Nori, *Nature* **424**, 909 (2003).
6. D. Bray, *Cell Movements: From Molecules to Motility* (Garland, New York, ed. 2, 2001).
7. G. Laevsky, D. A. Knecht, *J. Cell Sci.* **116**, 3761 (2003).
8. E. Reisler, C. Smith, G. Seegan, *J. Mol. Biol.* **143**, 129 (1980).
9. D. Humphrey, C. Duggan, D. Saha, D. Smith, J. Kas, *Nature* **416**, 413 (2002).
10. T. Hayashi, K. Maruyama, *J. Biochem. (Tokyo)* **78**, 1031 (1975).
11. L. A. Hough, H. D. Ou-Yang, *Phys. Rev. E* **65**, 021906 (2002).
12. D. Mizuno, Y. Kimura, R. Hayakawa, *Phys. Rev. Lett.* **87**, 088104 (2001).
13. See supporting material on *Science* Online.
14. T. G. Mason, D. A. Weitz, *Phys. Rev. Lett.* **74**, 1250 (1995).
15. F. Gittes, B. Schnurr, P. D. Olmsted, F. C. MacKintosh, C. F. Schmidt, *Phys. Rev. Lett.* **79**, 3286 (1997).
16. J. C. Crocker *et al.*, *Phys. Rev. Lett.* **85**, 888 (2000).
17. A. J. Levine, T. C. Lubensky, *Phys. Rev. Lett.* **85**, 1774 (2000).
18. M. L. Gardel *et al.*, *Science* **304**, 1301 (2004).
19. F. C. Mackintosh, J. Kas, P. A. Janmey, *Phys. Rev. Lett.* **75**, 4425 (1995).
20. C. Veigel *et al.*, *Nature* **398**, 530 (1999).
21. C. Storm, J. J. Pastore, F. C. MacKintosh, T. C. Lubensky, P. A. Janmey, *Nature* **435**, 191 (2005).
22. F. Gittes, F. C. MacKintosh, *Phys. Rev. E* **58**, R1241 (1998).
23. D. C. Morse, *Macromolecules* **31**, 7044 (1998).
24. A. Caspi, M. Elbaum, R. Granek, A. Lachish, D. Zbaida, *Phys. Rev. Lett.* **80**, 1106 (1998).
25. G. H. Koenderink, M. Atakhorrami, F. C. MacKintosh, C. F. Schmidt, *Phys. Rev. Lett.* **96**, 138307 (2006).
26. D. E. Discher, P. Janmey, Y. L. Wang, *Science* **310**, 1139 (2005).
27. M. Buchanan, M. Atakhorrami, J. F. Palierne, C. F. Schmidt, *Macromolecules* **38**, 8840 (2005).

28. We thank M. Atakhorrami, G. H. Koenderink, D. Pine, and D. A. Weitz for helpful discussions, and K. Vermeulen for sample preparation. Supported by the Deutsche Forschungsgemeinschaft Research Center for Molecular Physiology of the Brain (C.F.S.). This work is part of the research program of the Stichting voor Fundamenteel Onderzoek der Materie (FOM), which is funded by the Nederlandse Organisatie voor Wetenschappelijk Onderzoek (NWO).

Supporting Online Material

www.sciencemag.org/cgi/content/full/315/5810/370/DC1
Materials and Methods
SOM Text
Movies S1 to S4
References

28 August 2006; accepted 5 December 2006
10.1126/science.1134404

An Inward-Facing Conformation of a Putative Metal-Chelate–Type ABC Transporter

H. W. Pinkett,[1] A. T. Lee,[1] P. Lum,[1]* K. P. Locher,[2] D. C. Rees[1]†

The crystal structure of a putative metal-chelate–type adenosine triphosphate (ATP)–binding cassette (ABC) transporter encoded by genes *HI1470* and *HI1471* of *Haemophilus influenzae* has been solved at 2.4 angstrom resolution. The permeation pathway exhibits an inward-facing conformation, in contrast to the outward-facing state previously observed for the homologous vitamin B_{12} importer BtuCD. Although the structures of both HI1470/1 and BtuCD have been solved in nucleotide-free states, the pairs of ABC subunits in these two structures differ by a translational shift in the plane of the membrane that coincides with a repositioning of the membrane-spanning subunits. The differences observed between these ABC transporters involve relatively modest rearrangements and may serve as structural models for inward- and outward-facing conformations relevant to the alternating access mechanism of substrate translocation.

Transporters catalyze the thermodynamically unfavorable translocation of substrates against a transmembrane concentration gradient through the coupling to a second, energetically favorable process. One of the most widespread families of transporters, the adenosine triphosphate (ATP)–binding cassette (ABC) family (*1*–*4*), uses the binding and hydrolysis of ATP to power substrate translocation. ABC transporters are minimally composed of four domains, with two transmembrane domains (TMDs) and two ABCs or nucleotide-binding domains (NBDs) located in the cytoplasm. Although diverse with respect to physiological function and TMD architecture, ABC transporters are characterized by two highly conserved NBDs that contain critical sequence motifs for ATP binding and hydrolysis, including the P loop present in many nucleotide-binding proteins and the ABC signature or C-loop motif [Leu-Ser-Gly-Gly-Gln (LSGGQ)] that is specific to ABC transporters. These similarities suggest a common mechanism by which ABC transporters orchestrate a sequence of nucleotide- and substrate-dependent conformational changes that translocate the substrate across the membrane through interconversion of outward- and inward-facing conformations; this type of "alternating access" model has been generally found to provide a productive framework for the mechanistic characterization of transporters (*5*). For prokaryotic ABC transporters functioning as importers, substrate translocation is also dependent on high-affinity periplasmic-binding proteins (*6*) that deliver the ligand to the outward-facing state of the cognate transporter.

The HI1470/1 transporter from *Haemophilus influenzae* belongs to the family of binding protein–dependent bacterial ABC transporters that mediate the uptake of metal-chelate species, including heme and vitamin B_{12} (*7*). Because iron is often an essential nutrient, members of this family are widely distributed throughout bacteria, including pathogenic organisms such as *H. influenzae* (*8*). The molecular architecture for

[1]Division of Chemistry and Chemical Engineering, Howard Hughes Medical Institute, MC 114-96, California Institute of Technology (Caltech), Pasadena, CA 91125, USA. [2]Institute of Molecular Biology and Biophysics, ETH Zurich, 8093 Zurich, Switzerland.

*Present address: Department of Biological Sciences, University of Southern California, Los Angeles, CA 90089, USA. †To whom correspondence should be addressed. E-mail: dcrees@caltech.edu

this family of ABC transporters was established by the structure of BtuCD, the B_{12} importer from *Escherichia coli* (*9*). The transporter encoded by genes *HI1470* and *HI1471* of *H. influenzae* (*10*) exhibits 24 and 33% sequence identity to the ABC subunit BtuD and the membrane-spanning subunit BtuC, respectively, and was identified as a promising candidate for structural study during the original screen of homologs explored in the BtuCD analysis (*9*). After overexpression and purification in decylmaltoside of a histidine-tagged construct, the crystal structure of the intact, nucleotide-free HI1470/1 transporter was phased by isomorphous and multiwavelength anomalous diffraction methods and refined at 2.4 Å resolution (*11*).

The overall molecular organization of HI1470/1 (Fig. 1A) resembles that observed previously for BtuCD (*9*), with the functional unit consisting of two copies each of the HI1471 membrane-spanning subunits and of the HI1470 ABC subunits (Fig. 1, B and C). The root mean square deviations (RMSDs) in Cα positions between structurally equivalent residues in the individual subunits of HI1470/1 and BtuCD are ~1.5 Å; the corresponding RMSD after superposition of equivalent residues in all four subunits of these transporters is 2.4 Å. Each pair of HI1470 or HI1471 subunits in HI1470/1 is closely related (RMSDs ~1 Å) by a rotational operation that is close to an exact two-fold axis (rotation angle ~180.5°) passing through the center of the transporter. By means of the program HOLE (*12*), an evaluation of the permeation pathway that surrounds this axis reveals an important difference related to the detailed arrangement of subunits between HI1470/1 and BtuCD (Fig. 2): Although both transporters maintain a tapered pathway through the membrane-spanning subunits, the pathways open to opposite sides of the membrane, such that HI1470/1 and BtuCD adopt inward- and outward-facing conformations, respectively.

Each subunit of the membrane-spanning HI1471 contains 10 transmembrane helices (Fig. 1B), packed in a similar fashion to that observed for BtuC with the N and C termini located in the cytoplasm (*9*). Two noteworthy aspects of the rather intricate topology of the helical arrangement are the positioning of the helix TM2 through the center of the subunit (which places TM2 in proximity to most of the other membrane-spanning helices) and the similarities in helix packing between the N- and C-terminal halves of HI1471, although with opposite polarities through the membrane. This similarity in packing is particularly evident for the sets of helices (TM2 to TM5 and TM7 to TM10) that are approximately related by a two-fold axis in the plane of the membrane (Fig. 3A). Internal symmetry of this type is rather frequently observed in channels and transporters (*13*). For HI1471 and BtuC, this internal symmetry extends to the construction of the permeation pathway surrounding the molecular two-fold axis (Fig. 3B). Interactions between transmembrane subunits are dominated by contacts between helices TM5 and TM10 and the extramembrane helix 5a, with residues from TM3 and TM8 lining the permeation pathway. Notably, the regular helical structures of TM3 and TM8 are maintained only to about the center of the TMD and extend in a nonhelical, irregular

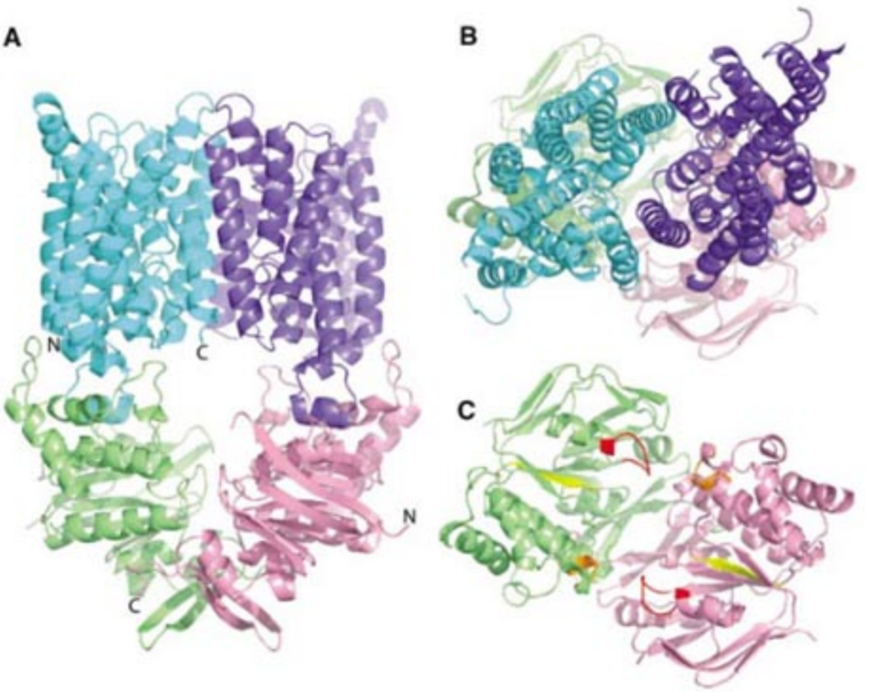

Fig. 1. (**A**) The ABC transporter HI1470/1 consists of four subunits: two membrane-spanning HI1471 subunits (cyan and blue) and two nucleotide-binding HI1470 subunits (green and pink). The molecular rotation axis is vertical, with the cytoplasmic-facing surface of the transporter toward the bottom. The locations of the N and C termini for one subunit each of HI1470 and HI1471 are indicated. (**B**) A view of HI1470/1 rotated 90° from that of (A), looking down the molecular two-fold axis toward the membrane-spanning subunits from the periplasmic surface. (**C**) A view of the HI1470 ABC subunits from the same direction as in (B), looking down the molecular two-fold axis toward the face of the NBDs interacting with the membrane-spanning subunits. The Walker A or P-loop motif (residues 40 to 46) is colored red, the Walker B motif (residues 148 to 154) is colored yellow, and the ABC signature motif (residues 129 to 133) is colored orange. The Walker A or P-loop motif is found at the N-terminal end of helix h1 that is surrounded by the two β sheets of the catalytic core domain. Ribbon diagrams in this report were prepared and rendered with the program PyMOL (*32*).

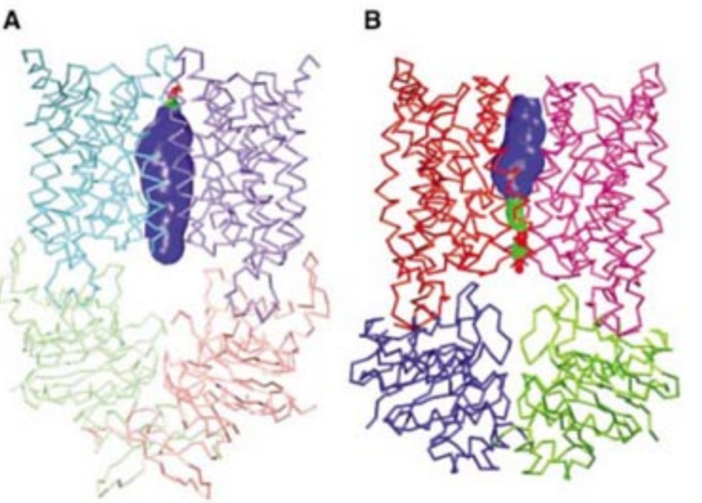

Fig. 2. Visualization of the permeation pathways of HI1470/1 and BtuCD with the program HOLE (*12*). (**A**) The permeation pathway generated by the two HI1471 subunits is narrow at the periplasmic surface and open to the cytoplasm, which are located toward the top and bottom of the figure, respectively. (**B**) In contrast, the pathway for BtuC is closed at the cytoplasm and open to the periplasm. The HOLE representation of the pore surface is shown in a multicolored form that was displayed and rendered with the program VMD (*33*). Red, green, and blue surfaces designate regions of the permeation pathway with effective radii <0.6, 0.6 to 1.15, and >1.15 Å, respectively. The calculated diameters at the widest part of the pathways illustrated for HI1470/1 and BtuCD are ~11 and 9 Å, respectively. The permeation pathway in BtuCD is of sufficient size to accommodate a corrin ring but not the entire B_{12} molecule (*9*); the ligand for HI1470/1 has not been identified.

fashion through the remainder of the membrane (*9*). Extended polypeptide chain conformations have been previously noted along the permeation pathways of other transporters (*14*–*18*).

HI1470 (Fig. 1C) exhibits the characteristic fold that was first observed for the ABC subunit HisP (*19*) and subsequently observed for other members of this family. ABC subunits are organized into two domains: a highly conserved catalytic core domain containing the P loop and a structurally more diverse α-helical domain with the ABC signature motif, LSGGQ. The catalytic core domain consists of two β sheets (a predominantly parallel β sheet containing the P loop and a smaller, antiparallel β sheet) that together surround an α helix (h1) extending away from the P loop. Although there are conserved elements of the α-helical domain between different ABC transporters, this region in general is more variable among members of the ABC family (*20*), and the relative orientation of the helical and catalytic domains is sensitive to the nucleotide state (*21*). As with BtuCD and the drug exporter Sav1866 (*22*), the region of the NBD that interacts with the TMD primarily involves the Q loop in the α-helical domain. The Q loop contains a conserved glutamine (Gln^{73} in HI1470) that participates in the binding of nucleotide to the NBD; the corresponding residue in BtuD (Gln^{80}) was observed to interact with cyclotetravanadate that occupies the nucleotide-binding site. The Q loop has been observed to be conformationally variable, and changes in this region have been proposed to be involved in the coupling of nucleotide hydrolysis to the conformational state of the TMDs (*23*).

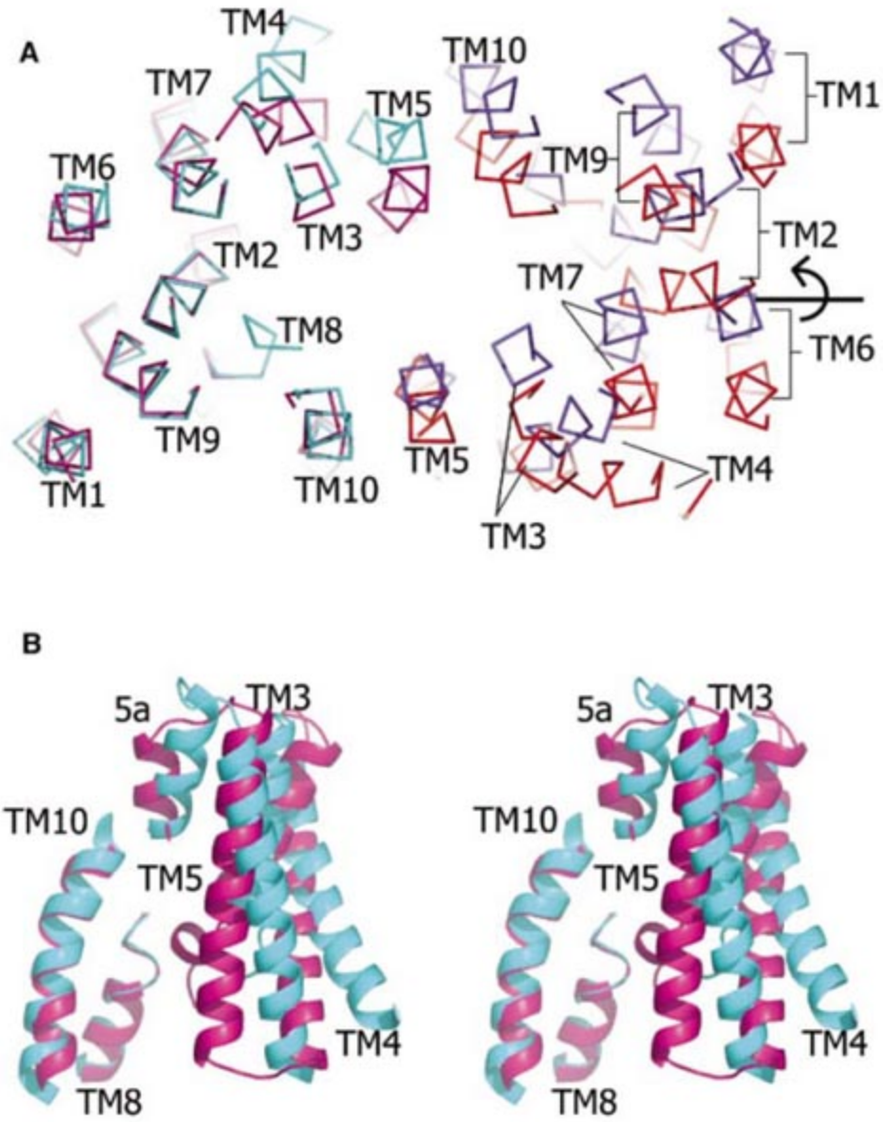

Fig. 3. (**A**) Comparison of the homologous membrane-spanning subunits HI1471 and BtuC, after superposition of TM2 in subunit A (to the left) of each structure, as viewed down the molecular two-fold axis from the periplasm. With the exceptions of TM3 to TM5, the helices in the A subunits of HI1471 (cyan) and BtuC (purple) superimpose closely. In contrast, interconversion of the B subunits (to the right) between these two structures (blue and red, respectively) requires an ~9° twist (indicated by the curved arrow) about an axis oriented in the direction shown to the right, which passes through the helical domain of the ABC subunit. (**B**) Stereoview of a superposition of helices TM3, TM4, TM5, TM8, TM10, and 5a in subunit A of HI1471 (cyan) and BtuC (purple), as viewed from within the permeation pathway with the molecular two-fold axis vertical. The internal symmetry–relating helices TM3 and TM8 and TM5 and TM10, as well as the irregular structures of TM3 and TM8, may be observed. The extramembrane helix 5a helps restrict the permeation pathway on the periplasmic side of HI1470/1.

Although the overall architecture of the intact HI1470/1 transporter resembles that of BtuCD, more detailed comparisons highlight differences in tertiary and quaternary arrangements between structures that may be functionally relevant. Relative to a structurally conserved core of seven helices (TM1, TM2, and TM6 to TM10) that is maintained between the TMDs of HI1471 and BtuC (Fig. 3A), three helices (TM3, TM4, and TM5) differ significantly between the two structures (Fig. 3, A and B). These differences are evident in a comparison of HI1470 and BtuC subunits based on superposition of the central TM2 helix (Fig. 3A). Among the more substantial rearrangements between the two structures is a 20° shift in the helix axis of TM5 (Fig. 3B). Because TM5 participates in the subunit-subunit interface surrounding the molecular two-fold axis, these tertiary structure changes are coupled to quaternary changes in the relative positions of the TMDs, as evidenced by the alteration in the crossing angle between helices TM5 and TM10 from −143° in BtuCD to −163° in HI1470/1. When the conserved seven-helical core is used to superimpose one BtuC subunit and one HI1471 subunit, a twist of ~9° about an axis that is approximately normal to the molecular two-fold axis is required to superimpose the partner TMD subunits (Fig. 3A). The combination of the repositioning of helices TM3 to TM5 with the overall twist motion across the subunit-subunit interface between TMDs has substantial consequences for the permeation pathway. In HI1470/1, the change in orientation of TM5 simultaneously closes access to the periplasm while opening the pathway to the cytoplasm; in contrast, cytoplasmic access to the permeation pathway is closed in BtuCD by residues in the loop between TM4 and TM5. An important additional contribution to the periplasmic restriction in HI1470/1 is provided by the extramembrane helical element 5a immediately following TM5.

The ABC subunits of both HI1470/1 and BtuCD pack together such that the P loop of one subunit opposes the signature motif of the other, in a manner originally proposed from modeling studies (*24*) and subsequently observed for Rad50 (*25*). The closed state with the most extensive interface between ABC subunits is associated with the ATP-bound form and has been structurally characterized in isolated ABC subunits (*26*–*28*) and in the intact ABC transporter Sav1866 (*22*). Relative to this closed state, the dimers of HI1470 and BtuD that are present in the corresponding structures of the nucleotide-free transporters each exhibit more open conformations, because the catalytic domains have opened up by rotations of 20° to 25° relative to the closed dimer of MalK, the ABC subunit of the maltose transporter (*27*). The

HI1470 dimer arrangement most closely resembles the "semi-open" (*27*) or post-ATP hydrolysis, adenosine diphosphate–bound (*29*) forms of the MalK dimer, with RMSDs of 2.7 Å between these structures for the conserved structural elements of the catalytic domains in the dimer, as compared to 4.3 Å with the closed state of MalK. The similarity of the BtuD dimer to the semi-open state of MalK has been previously noted (*27*), although the distinctions between BtuD and the semi-open and closed states of MalK (RMSDs of 2.3 and 2.9 Å) are not as clear for BtuD as for HI1470. Direct comparisons of the BtuD and HI1470 dimers further indicate that the latter has a more open conformation than the former. For example, the distance between the P loop and signature sequence on different subunits is greater in the HI1470 dimer than in BtuD, as is the separation between the signature sequences on different subunits in these two structures (Fig. 4A). Although there are important differences, this comparative analysis suggests that, despite the absence of nucleotides, the arrangement of ABC subunits observed in BtuCD more closely resembles the closed conformation than does HI1470/1.

Although a detailed mechanistic description will clearly require biochemical and structural characterization of multiple states of an ABC transporter system (including bound nucleotides, substrate, and binding protein), the observation that the permeation pathways of HI1470/1 and BtuCD are oriented in opposite directions can help identify structural elements underlying this transition. The conformational transformations relating HI1470/1 and BtuCD, although maintaining the overall two-fold molecular symmetry, do not exclusively involve rigid body movements of individual subunits (Fig. 3A). Still, the rigid body description provides a useful reference framework for this analysis; for example, when the entire HI1470/1 and BtuCD transporters are superimposed so that the two-fold axes coincide, the transformation that is calculated for the catalytic core domain of individual ABC subunits between the two structures corresponds to a rotation of ~10° about an axis tilted 13° from the molecular two-fold axis. The rotation axis corresponding to this transformation passes near the P loop (Fig. 4A), with the consequence that the structural adjustments

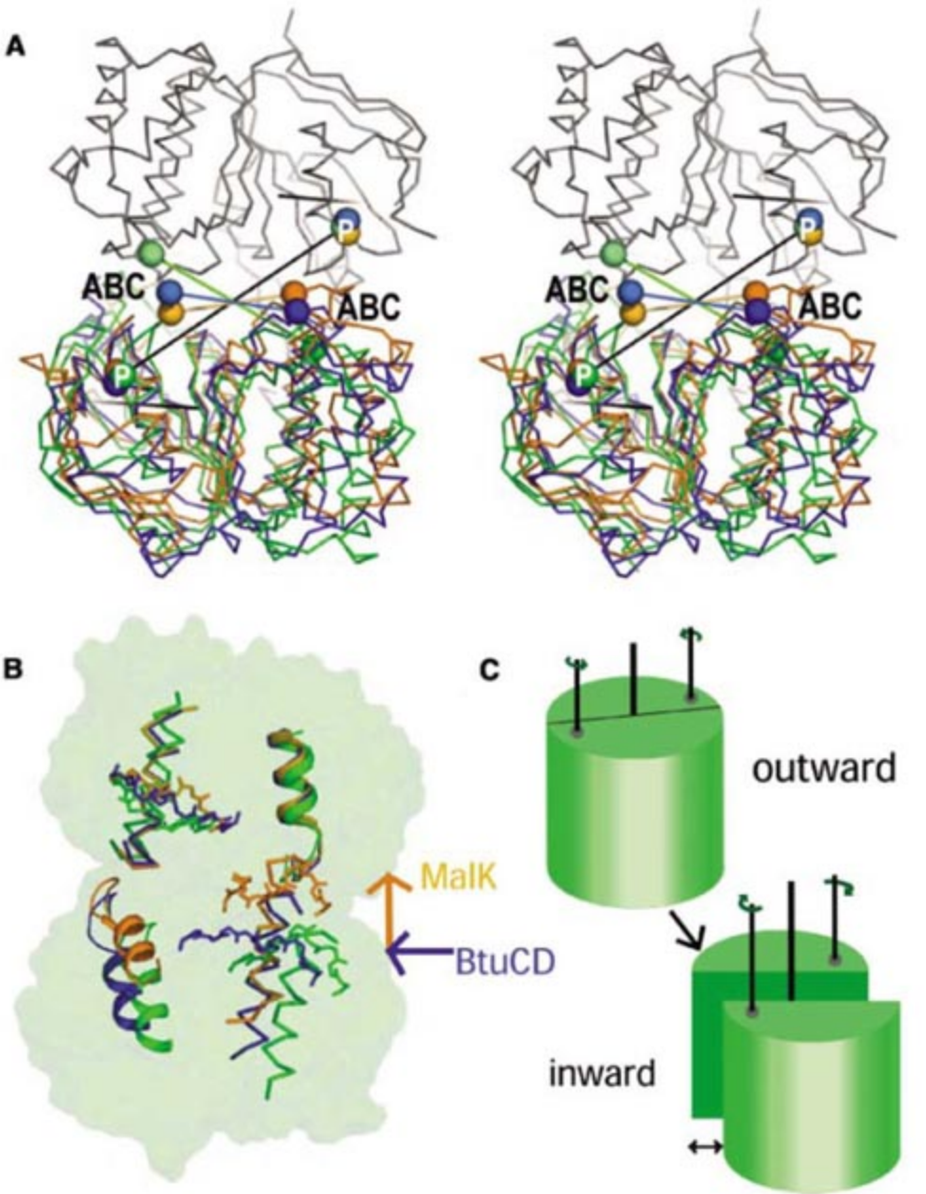

Fig. 4. Relationships between dimeric ABC structures. (**A**) Stereoview of the dimers of HI1470 (green), BtuD (blue; PDB 1L7V), and the ATP-bound state of MalK (orange; PDB 1Q12) based on a superposition of residues in the catalytic core domains of both subunits. At the bottom, one subunit from each structure is indicated by the appropriately colored Cα trace, whereas the trace of the second subunit from HI1470 is indicated in gray at the top. The spheres identify the P-loop and ABC sequence motifs. The closely overlapping spheres labeled with the letter "P" in each image indicate the positions of Gly^{43}, Gly^{38}, and Gly^{41} used to mark the P loops of HI1470, BtuD, and MalK, respectively; the other spheres designate the locations of Gly^{131}, Gly^{129}, and Gly^{136} denoting the ABC signature motif of these same structures. Fig. 1C highlights these same elements in the HI1470 dimer (rotated ~60° about an axis normal to the page). Although the intersubunit spacings between the P loops within all three dimers are similar (~35 Å; black line), the separations between signature motifs within each dimer are 16, 16, and 24 Å in MalK (orange), BtuD (teal), and HI1470 (green), respectively. The spacings between the P loop and signature motif in different subunits are 11, 14, and 16 Å in MalK, BtuD, and HI1470, respectively. The rotation axes relating the catalytic domains of corresponding BtuD and HI1470 subunits pass near the P loops of these structures and are illustrated as black lines tilted ~13° from the normal to the viewing direction. The locations of these axes are reflected in the similar distances between P loops in the three dimeric ABC structures, whereas separations involving the signature motifs vary more widely because these regions are farther from the rotation axes. (**B**) Comparison of the ABC dimers of HI1470/1 (green), BtuD (blue), and ATP-bound MalK (orange) as viewed from the membrane in the same orientation as in (A). The subunits are superimposed onto the conserved regions of the catalytic core domain of one subunit (chain C) of HI1470 (top subunit). The P loops and h1 helices are depicted as ribbons, the signature sequence and associated helix are depicted as a Cα trace, and the main chain atoms in the Q loop are depicted as thick bonds. Although these elements overlap in the top (superimposed) subunits, substantial variation is evident in the lower subunit, particularly the translational shift along the dimer interface between the Q loops and signature motifs of the intact HI1470 and BtuD (blue arrow). In comparison, these elements in MalK are rotated about a hinge axis in a tweezers-type motion (*27*) to close up the interface relative to BtuD (yellow arrow). (**C**) A schematic representation illustrating how rotations about local axes in each subunit, parallel to the molecular two-fold axis of the dimer, create a translational shift along the dimer interface. These rotations can consequently be coupled to a twisting motion of the associated membrane-spanning subunits to interconvert inward- and outward-facing conformations.

are relatively modest in the catalytic core domain between structures but increase with increasing distance from this region, as is particularly evident for the ABC signature sequence. When the catalytic domains of one NBD in the intact HI1470/1 transporter and one NBD in the intact BtuCD transporter are superimposed, the relative positions of the partner NBDs observed in these structures are shifted by a translation or screw component of ~4.5 Å along an axis parallel to the interface between NBDs (Fig. 4B); this translational component repositions the two NBDs in a direction perpendicular to that generated by the tweezers-type motion observed between different nucleotide states of MalK (*27*), which also corresponds to the hinge motion between BtuD and the closed form of MalK. Notably, the direction of this translational shift coincides with the direction of the twist motion observed between the TMDs of HI1470/1 and BtuCD (Fig. 3A). This screw component arises from the coupling of the local rotation axes relating individual NBDs in different structures to the molecular two-fold rotation, which generates a displacement along the subunit-subunit interface as the separation between NBDs varies (Fig. 4C). The linkage between NBD positioning and the twist between TMDs supports a coupling mechanism connecting the permeation pathway and nucleotide state of the transporter, where the ABCs can remain juxtaposed during the transport cycle.

The structures of HI1470/1 and BtuCD demonstrate that inward- and outward-facing conformations of an importer-type ABC transporter may be accommodated with relatively little change in overall architecture. Because neither HI1470/1 nor BtuCD were crystallized in the presence of nucleotide, binding protein, or ligand, the energetic basis of the differential stabilization of alternate conformations is not obvious; one possibility is that the substitution of the native bilayer with detergent has shifted the equilibrium between inward- and outward-facing conformations. A comparable phenomenon has recently been discussed for the conformation of the voltage sensor in potassium channels (*30*). Lattice contacts overlapping the molecular two-fold axis of HI1470 and the periphery of BtuD could also play a role in stabilizing the observed conformations of the ABCs. Consequently, despite the differences in structures of HI1470/1 and BtuCD, it is not possible to establish the correspondence between nucleotide state and transporter conformation with certainty; however, the closer juxtaposition of ABC subunits in BtuCD relative to HI1470/1 suggests that the outward-facing conformation of the transporter corresponds to the closed (ATP) state of the NBDs, as suggested by Chen and Davidson (*27*) and as observed for Sav1866 by Dawson and Locher (*22*). A notable aspect of the switch in translocation pathways between inward- and outward-facing conformation is the packing rearrangement of helices TM3 to TM5 with respect to the remainder of the TMD. In view of the internal duplication evident in the helix packing arrangements of HI1470/1 and BtuCD, as well as other channels and transporters (*13*), this suggests the possibility that the internal symmetry is inherent in the mechanistic transition between inward- and outward-facing conformations. The roles of binding protein, ligand, and particularly nucleotide binding and hydrolysis in driving these conformational transitions remain crucial mechanistic issues.

References and Notes

1. I. B. Holland, S. P. C. Cole, K. Kuchler, C. F. Higgins, Eds. *ABC Proteins: From Bacteria to Man* (Academic Press, London, 2003).
2. K. P. Locher, *Curr. Opin. Struct. Biol.* **14**, 426 (2004).
3. A. L. Davidson, J. Chen, *Annu. Rev. Biochem.* **73**, 241 (2004).
4. E. Biemans-Oldehinkel, M. K. Deoven, B. Poolman, *FEBS Lett.* **580**, 1023 (2006).
5. L. Guan, H. R. Kaback, *Annu. Rev. Biophys. Biomol. Struct.* **35**, 67 (2006).
6. F. A. Quiocho, P. Ledvina, *Mol. Microbiol.* **20**, 17 (1996).
7. W. Köster, *Res. Microbiol.* **152**, 291 (2001).
8. J. H. Crosa, A. R. Mey, S. M. Payne, Eds. *Iron Transport in Bacteria* (ASM Press, Washington, DC, 2004).
9. K. P. Locher, A. T. Lee, D. C. Rees, *Science* **296**, 1091 (2002).
10. R. D. Fleischmann *et al.*, *Science* **269**, 496 (1995).
11. Materials and methods are available as supporting material on *Science* Online.
12. O. S. Smart, J. G. Neduvelil, X. Wang, B. A. Wallace, M. S. Sansom, *J. Mol. Graphics* **14**, 354 (1996).
13. O. Pornillos, G. Chang, *FEBS Lett.* **580**, 358 (2006).
14. K. Murata *et al.*, *Nature* **407**, 599 (2000).
15. C. Toyoshima, M. Nakasako, H. Nomura, H. Ogawa, *Nature* **405**, 647 (2000).
16. R. Dutzler, E. B. Campbell, M. Cadene, B. T. Chait, R. MacKinnon, *Nature* **415**, 287 (2002).
17. C. Hunte *et al.*, *Nature* **435**, 1197 (2005).
18. A. Yamashita, S. Singh, T. Kawate, Y. Jin, E. Gouaux, *Nature* **437**, 215 (2005).
19. L.-W. Hung *et al.*, *Nature* **396**, 703 (1998).
20. L. Schmitt, H. Benabdelhak, M. A. Blight, I. B. Holland, M. T. Stubbs, *J. Mol. Biol.* **330**, 333 (2003).
21. N. Karpowich *et al.*, *Structure* **9**, 571 (2001).
22. R. J. P. Dawson, K. P. Locher, *Nature* **443**, 180 (2006).
23. P. M. Jones, A. M. George, *Proc. Natl. Acad. Sci. U.S.A.* **99**, 12639 (2002).
24. P. M. Jones, A. M. George, *FEMS Microbiol. Lett.* **179**, 187 (1999).
25. K.-P. Hopfner *et al.*, *Cell* **101**, 789 (2000).
26. P. C. Smith *et al.*, *Mol. Cell* **10**, 139 (2002).
27. J. Chen, G. Lu, J. Lin, A. L. Davidson, F. A. Quiocho, *Mol. Cell* **12**, 651 (2003).
28. J. Zaitseva *et al.*, *EMBO J.* **25**, 3432 (2006).
29. G. Lu, J. M. Westbrooks, A. L. Davidson, J. Chen, *Proc. Natl. Acad. Sci. U.S.A.* **102**, 17969 (2005).
30. S. Y. Lee, A. Lee, J. Y. Chen, R. MacKinnon, *Proc. Natl. Acad. Sci. U.S.A.* **102**, 15441 (2005).
31. H. M. Berman *et al.*, *Nucleic Acids Res.* **28**, 235 (2000).
32. W. L. DeLano, *The PyMOL Molecular Graphics System* (DeLano Scientific, San Carlos, CA, 2002).
33. W. Humphrey, A. Dalke, K. Schulten, *J. Mol. Graphics* **14**, 33 (1996).

34. We thank L. Thomas and J. Kaiser for their contributions to the structure determination, N. Kadaba and J. B. Howard for discussions, and the staff of the Stanford Synchrotron Radiation Laboratory (SSRL) for their assistance during crystal screening and data collection. This work was supported in part by NIH grant GM45162. We acknowledge support for fellowships from the James Irvine Foundation (H.W.P.) and NIH (P.L.), the Vallee Foundation (D.C.R.), the Parsons Foundation for computational resources, and the Gordon and Betty Moore Foundation for support of the Molecular Observatory at Caltech. SSRL is supported by DOE and NIH. Coordinates have been deposited in the Protein Data Bank (PDB) [www.rcsb.org/pdb; (*31*)] as entry 2NQ2 for release upon publication.

Supporting Online Material

www.sciencemag.org/cgi/content/full/1133488/DC1
Materials and Methods
Figs. S1 to S3
Table S1
References

4 August 2006; accepted 30 November 2006
Published online 7 December 2006;
10.1126/science.1133488
Include this information when citing this paper.

Antibody Class Switching Mediated by Yeast Endonuclease–Generated DNA Breaks

Ali A. Zarrin,[1] Catherine Del Vecchio,[1] Eva Tseng,[1] Megan Gleason,[1] Payam Zarin,[1] Ming Tian,[2] Frederick W. Alt[1]*

Antibody class switching in activated B cells uses class switch recombination (CSR), which joins activation-induced cytidine deaminase (AID)–dependent double-strand breaks (DSBs) within two large immunoglobulin heavy chain (IgH) locus switch (S) regions that lie up to 200 kilobases apart. To test postulated roles of S regions and AID in CSR, we generated mutant B cells in which donor Sμ and accepter Sγ1 regions were replaced with yeast I-SceI endonuclease sites. We found that site-specific I-SceI DSBs mediate recombinational IgH locus class switching from IgM to IgG_1 without S regions or AID. We propose that CSR evolved to exploit a general DNA repair process that promotes joining of widely separated DSBs within a chromosome.

During an immune response, activated B cells switch from production of immunoglobulin M (IgM) antibodies to antibody classes (IgG, IgE, or IgA) that have different immunological functions (*1*). In mice, immunoglobulin heavy chain (IgH) constant region exons (termed C_H genes) lie within a chromosomal region that spans 200 kb (Fig. 1A). IgH class switching occurs by a process, termed class switch recombination (CSR), in which the IgM C_H (Cμ) gene is replaced with a downstream C_H gene. CSR occurs between

large (1- to 12-kb), repetitive switch (S) region sequences that lie upstream of given C_H genes (Fig. 1A). Gene-targeted deletion of S regions (*2*–*4*) or their replacement with non–S region sequences (*4*, *5*) greatly diminishes CSR, indicating that S regions are specialized targets for CSR events. CSR requires activation-induced cytidine deaminase (AID) (*6*), which deaminates cytosine residues in DNA (*1*), and transcription through S regions as a means of AID access (*1*, *7*). Certain DNA repair pathways have been coopted to process deaminated cytidines in S regions into DNA double-strand breaks (DSBs) (*8*), which are CSR intermediates (*9*–*11*). Joining of a DSB within the donor Cμ S region (Sμ) to a DSB within a downstream S region completes CSR (*1*).

During CSR, AID introduces multiple DSBs into S regions, with some being joined between two S regions to effect CSR and others being rejoined or joined to other DSBs within the same S region to generate internal S region deletions (*12*). DSB response proteins, including ATM, 53BP1, and H2AX, are necessary for normal joining of CSR DSBs, potentially because they facilitate end joining (*13*) and/or contribute to bringing two different S regions together in a process referred to as synapsis (*14*, *15*). S regions might function in synapsis by generating unusual structures or binding synapsis factors (*16*). In the V(D)J recombination process that assembles Ig variable-region V, D, and J segments to generate antibody diversity, synapsis is carried out by the RAG endonuclease that cleaves the segments (*1*). By analogy, AID also might function in S region synapsis, perhaps via interactions of S region–bound AID molecules and unknown cofactors (*17*). Alternatively, S regions may simply serve as targets for AID-generated DSBs and have no requisite downstream functions. The latter possibility leaves unanswered the question of how DSBs in donor Sμ and acceptor downstream S regions are synapsed.

To elucidate CSR synapsis mechanisms, we asked whether recombinational IgH class switching in B cells could be established without S regions or AID. Specifically, we asked whether site-specific DSBs could replace Sγ1, or both Sμ and Sγ1, in mediating class switching to IgG1. To generate the DSBs, we selected the yeast I-SceI endonuclease (*18*), which recognizes an 18–base pair (bp) target that is rare in the mammalian genome (*19*) and which generates DSBs with staggered ends (Fig. 1A) (*18*). We used gene targeting to generate the ΔSγ1/I-SceI^a allele by replacing the 12-kb endogenous Sγ1 on the γ_1^a allele of an γ_1^a/γ_1^b F1 embryonic stem (ES) cell line with a cassette that contained two I-SceI sites in inverted orientation flanking 500 bp of sequence (*Xpf* intron) that has no inherent CSR activity (Fig. 1, A and B, and fig. S1) (*5*). We used this strategy to mimic the internal S region deletion versus long-range CSR events that occur during normal CSR. Thus, the two I-SceI sites flanking the inert spacer allow us to estimate the frequency with which DSBs are joined at short range (500 bp) relative to the frequency at which they are joined over long range (100 kb) to Sμ DSBs. For replacement of both Sμ and Sγ1, we started with ES cells harboring a ΔSγ1/I-SceI^a allele, deleted the 4.6-kb Sμ region (*3*), and then replaced Sμ with two I-SceI sites in inverted orientation (Fig. 1, A and B). The resulting allele, in which both Sμ and Sγ1 were replaced with I-SceI sites, was termed ΔSμΔSγ1/I-SceI^a (Fig. 1B and fig. S1). We also selected ES cells homozygous for the ΔSμΔSγ1/I-SceI^a allele (fig. S1B). We used targeted ES cells to generate normal splenic B cells via RAG-2–deficient blastocyst complementation (*20*).

To assess effects of the Sγ1 replacement, we assayed IgG_1 secretion in activated mutant B cells. In normal B cells, IgG_1 secretion only occurs via CSR events that place Cγ1 in the position of Cμ. Splenocytes from wild-type F1 ES cells or F1 ES cells harboring the ΔSγ1/I-SceI^a allele were cultured with CD40 antibodies (anti-CD40) plus interleukin-4 (IL-4) and separately with bacterial lipopolysachride (LPS) plus IL-4, which induces transcription from a promoter upstream of Sγ1 and, as a result, induces CSR between Sμ and Sγ1 (*1*). After stimulation, targeted and wild-type alleles were similarly transcribed (fig. S2). We used a specific antibody to measure secreted IgG_1^a as an index of switching on targeted IgH^a alleles. With either activation protocol, secretion of IgG_1^a by the ΔSγ1/I-SceI^a or ΔSμΔSγ1/I-SceI^a F1 B cells after 6 days of activation was reduced, on average, more than 100-fold, to nearly background quantities

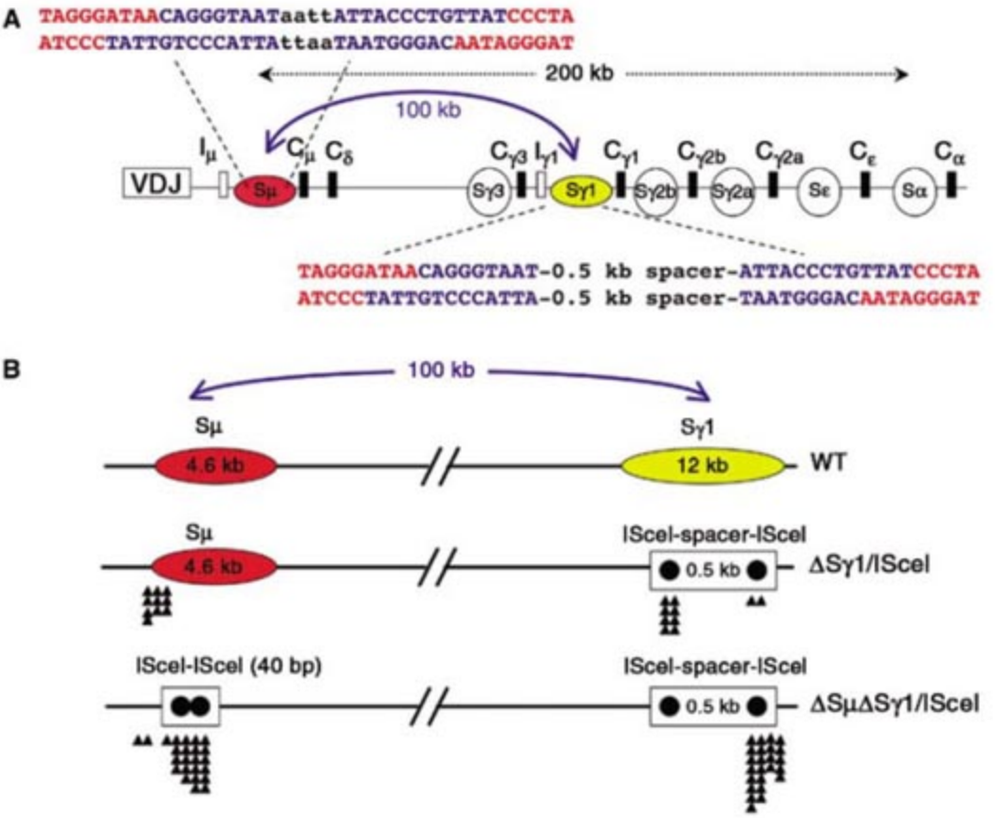

Fig. 1. Gene targeting strategy and recombination breakpoints. (**A**) Genomic organization of the mouse IgH constant region locus. Black rectangles denote C_H exons, and ovals denote S regions. Sμ and Sγ1 are about 100 kb apart. The Sγ1^a (12 kb) was first targeted by homologous recombination and replaced with outlined I-SceI cassette to generate ΔSγ1/I-SceI^a (fig. S1). Subsequently the 4.6-kb Sμ^a was replaced with two I-SceI sites by using a targeting vector described previously (*3*). The two inserted I-SceI sites in the Sγ1 region are in inverted orientation flanking 500 bp of intron from the *Xpf* gene. The I-SceI sites in the Sμ region are in inverted orientation separated by a 4-bp spacer (AATT). The staggered cleavage site of I-SceI is depicted by red and blue colors. The location of the V(D)J exon at the 5′ end of the IgH constant region locus is indicated. The locations of intronic (I) promoters for μ and γ1 from which germline transcription initiates are designated as open rectangular boxes. (**B**) Schematic summary of I-SceI replacements. The Sμ and Sγ1 regions are depicted with red and yellow ovals, respectively. The I-SceI cassettes are drawn as black solid circles in a rectangular box. Small solid triangles represent the location of DNA junctions between Sμ and ΔSγ1/I-SceI^a or between ΔSμ/I-SceI^a and ΔSγ1/I-SceI^a. Sequences of these junctions are shown in figs. S8 and S9.

[1]Howard Hughes Medical Institute, Children's Hospital, CBR Institute for Biomedical Research, and Department of Genetics, Harvard University Medical School, Boston, MA 02115, USA. [2]Department of Molecular Genetics and Microbiology, University of Texas at Austin, Austin, TX 78712, USA.

*To whom correspondence should be addressed. E-mail: alt@enders.tch.harvard.edu

(Fig. 2, A and B). However, infection of activated ΔSγ1/I-SceI^a or ΔSμΔSγ1/I-SceI^a B cells with a retrovirus (pMX–I-SceI) that expresses I-SceI stimulated $IgG_1{}^a$ secretion by 50-fold or more to quantities that, on average, were about 10 to 20% of those of wild type (Fig. 2, A and B). As a control, pMX–I-SceI infection of wild-type B cells had no obvious effect on $IgG_1{}^a$ switching (Fig. 2, A and B). Amounts of retroviral infection in different experiments ranged from 20 to 70% of the cells (fig. S3). Therefore, many cells in assayed populations were not exposed to pMX–I-SceI, which means that the relative efficiency of I-SceI–dependent switching to IgG_1 on the targeted alleles of pMX–I-SceI–infected B cells, as compared with bona fide CSR to IgG_1 on wild-type alleles, was even higher than observed.

We confirmed the surprisingly high amounts of $IgG_1{}^a$ switching in the pMX–I-SceI–infected mutant B cells by several independent methods, including B cell hybridoma analyses (fig. S4), flow cytometry (fig. S3), and enzyme-linked immune spot (ELISpot) assays. ELISpot allows quantitative assessment of the frequency of antibody secreting cells at the single cell level. For these experiments, B cells homozygous for the ΔSμΔSγ1/I-SceI^a allele were stimulated with LPS and IL-4 or anti-CD40 and IL-4 for 4 days with or without pMX–I-SceI infection. Although we observed no IgG_1 switching in uninfected ΔSμΔSγ1/I-SceI^a homozygous B cells, nearly 10% of pMX–I-SceI–infected cells switched to IgG_1 (Fig. 2C and fig. S5). In control experiments, about 40% of similarly stimulated wild-type cells switched to IgG_1 (fig. S5). Thus, switching on S region mutant alleles approached 20% of wild-type quantities, with the highest amounts appearing to correspond with the highest amounts of retroviral infection. Lastly, ΔSμΔSγ1/I-SceI^a homozygous B cells stimulated only with LPS showed a similar amount of IgG_1 switching [about 7% (Fig. 2C and fig. S5)] as when stimulated with LPS and IL-4 or anti-CD40 and IL-4. This result is noteworthy because LPS stimulation of normal B cells does not induce transcription through the Sγ1 region and, correspondingly, does not substantially up-regulate IgG_1 switching (fig. S5) (*1*).

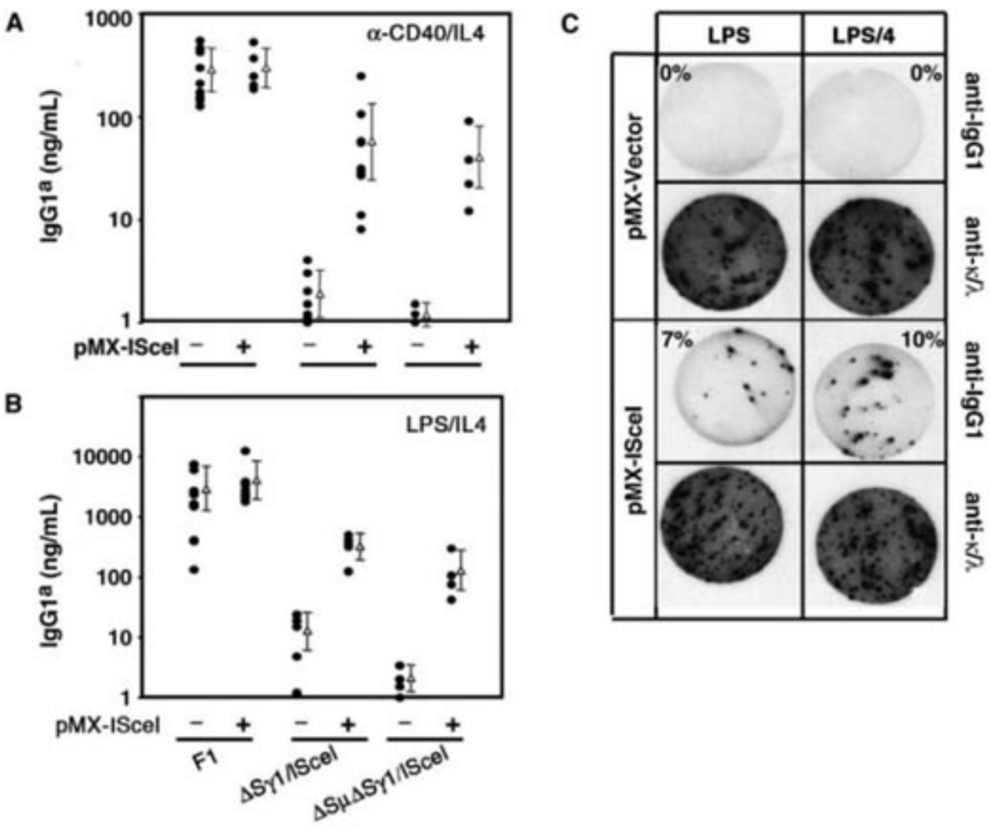

Fig. 2. CSR in wild-type or targeted B cells. (**A** and **B**) Enzyme-linked immunosorbent assay (ELISA). Wild-type (F1), ΔSγ1/I-SceI^a, or ΔSμΔSγ1/I-SceI^a B cells were cultured in the presence of anti-CD40 and IL-4 (A) or LPS and IL-4 (B) and assayed for secretion of $IgG_1{}^a$. The amount of $IgG_1{}^a$ secreted in the presence of pMX–I-SceI or in its absence (uninfected or pMX vector alone) is shown. Each solid circle represents the measurements for one mouse. Error bars represent standard deviation of the mean (open triangles) of two or three independent experiments, each done with cells from a different mouse. (**C**) ELISpot assays ELISpot measured the frequency of IgG_1-producing cells in populations of homozygous ΔSμΔSγ1/I-SceI^a B cells stimulated with LPS, LPS and IL-4. The cells were infected with pMX vector alone or pMX–I-SceI and after 4 days plated at different dilutions. The ratio of IgG_1-producing B cells to the total number of B cells was determined by staining the cells after 12 to 18 hours with antibodies against IgG_1 or κ/λ. Noninfected homozygous mutant cells or homozygous mutant cells infected with pMX vector showed negligible switching to IgG_1. A table summarizing the ELISpot assays on three to four different chimeras using different stimulation conditions is depicted in fig. S5.

To test whether the I-SceI–dependent switching to IgG_1 in mutant cells required AID, we generated IgM^a-producing hybridomas from ΔSμΔSγ1/I-SceI^a B cells. As for hybridomas from wild-type B cells, the mutant B cell hybridomas did not express detectable AID (Fig. 3A). In addition, Northern blots failed to reveal germline Cγ1 transcripts in these hybridomas (fig. S6). We infected ΔSμΔSγ1/I-SceI^a hybridomas with pMX–I-SceI and performed ELISpot after 6 days. In these experiments, on average, 7% of the ΔSμΔSγ1/I-SceI^a hybridomas cells switched to IgG_1 production (Fig. 3, B and C, and fig. S7), indicating that I-SceI–mediated class switching to IgG_1 can be induced in the absence of AID and in the absence of readily detectable Cγ1 locus transcripts.

We used polymerase chain reaction (PCR) to characterize recombination junctions from individual ΔSγ1/I-SceI^a $IgG_1{}^a$-producing hybridomas and found Sμ sequences fused, at various sites within Sμ, to one or the other I-SceI site (Fig. 1B and fig. S8, A and B), which along with the I-SceI dependence of these junctions confirmed that I-SceI was responsible for generating downstream acceptor DSBs. Further analyses of several junctions that used the 5′ I-SceI site revealed that half had alterations of the retained 3′ I-SceI site (fig. S8C), consistent with I-SceI cutting these sites with high efficiency (*19*, *21*). All Sμ–I-SceI junctions analyzed had a high frequency of mutations (5.5×10^{-3} per base pair) within the Sμ sequence just upstream of the junction, as expected for involvement of AID in the generation of donor Sμ DSBs (*22*). In contrast, analyzed junctions had only a background frequency of mutations (1×10^{-4} per bp) in the 500-bp *Xpf* intron directly downstream of the 5′ I-SceI site, consistent with downstream DSBs being generated by I-SceI (fig. S8, A to C). These results show that AID-induced DSBs in Sμ can be joined to DSBs generated by other processes, in this case I-SceI, supporting the notion that such joining could be involved in generating oncogenic translocations. Lastly, we also analyzed recombination junctions from I-SceI–infected ΔSμΔSγ1/I-SceI^a B cell or hybridoma populations, and all fell within or in close proximity to I-SceI sites (Fig. 1B and figs. S9 and S11), confirming that I-SceI–dependent switching on ΔSμΔSγ1/I-SceI^a alleles involved cutting and joining of I-SceI sequences.

We sought to approximate the impact of distance on ability of two separate I-SceI–mediated breaks to be joined. To do this, we assessed the frequency of short-range I-SceI–dependent deletions resulting from joining DSBs at the two I-SceI sites that flank the 500-bp *XPF* intron cassette of ΔSμΔSγ1/I-SceI^a B cell hy-

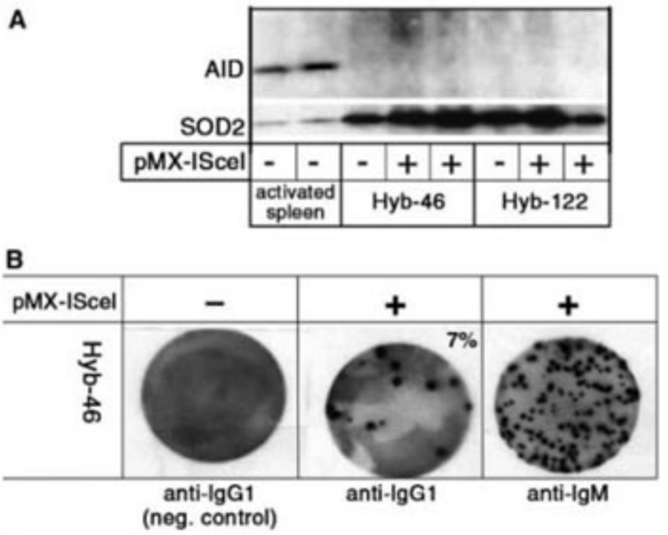

C

	Class switching %		
	Un-infected	pMX-vector	pMX-ISceI
Exp-1	0	ND	7
Exp-2	0	0	6
Exp-3	0	0	8

Fig. 3. Frequency of class switching in IgM^a-producing hybridomas derived from ΔSμΔSγ1/I-SceI^a B cells. (**A**) Western blot analyses of AID expression in two IgM^a-producing hybridomas derived from the ΔSμΔSγ1/I-SceI^a heterozygous B cells. Extracts from activated splenic B cells, noninfected pMX–I-SceI–infected hybridomas, or pMX–I-SceI–infected hybridomas (two independent experiments) were probed with antibodies against AID. Anti-SOD2 (Mn superoxide dismutase) was used as a loading control. (**B**) ELISpot assay done after 6 days after infection of IgM^a-producing hybridoma-46 with pMX–I-SceI. Hybridoma cells were infected with pMX vector or pMX–I-SceI, plated at different densities, and probed with antibodies against κλ, IgM, or IgG$_1$ (additional results are in fig. S7). (**C**) The results obtained from three independent experiments with hybridoma 46 cells uninfected, infected with control pMX vector, or infected with pMX–I-SceI. ND, not determined.

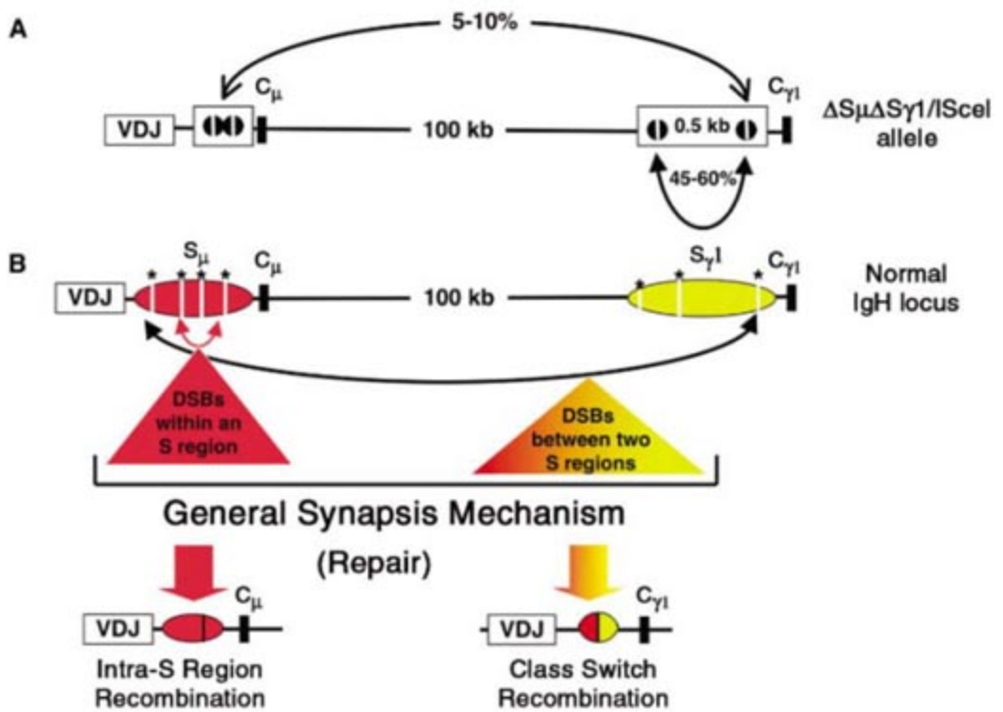

Fig. 4. A general mechanism may mediate high-frequency long-range chromosomal joins and CSR. (**A**) A schematic of joining events on the ΔSμΔSγ1/I-SceI allele. The two sets of I-SceI sites that replace Sμ and Sγ1 are indicated as solid circles in open boxes with splits in the dots representing potential DSBs. Short-range (500-bp) deletions between the two I-SceI sites that replace Sγ1 in ΔSμΔSγ1/I-SceI IgM^a-producing hybridomas (indicated by double arrow connecting DSBs) after infection with pMX–I-SceI was estimated to occur in 45 to 60% of the cells (fig. S10). Long-range deletions leading to class switching in the same infected hybridoma populations was estimated to occur in 5 to 10% of the cells (Fig. 3, B and C, and fig. S7). (**B**) A model for synapsis of AID-generated DSBs between two S regions during CSR that relies on a general DNA synapsis mechanism that leads to a high relative frequency of long-range (up to 200 kb) versus short-range joining or rejoining of DSBs within a chromosome.

bridomas. For this purpose, IgM^a-expressing ΔSμΔSγ1/I-SceI^a hybridomas were infected with pMX–I-SceI retrovirus and, after 5 days, subcloned by serial dilution; short-range deletions were assessed by Southern blotting and PCR. After pMX–I-SceI infection, about 45 to 60% of ΔSμΔSγ1/I-SceI^a hybridoma subclones contained short-range deletions within the ΔSγ1/I-SceI^a cassette, with most breakpoints occurring at or near the two I-SceI sites (Fig. 4A and figs. S10 and S11). This result confirms that I-SceI cuts efficiently, because both I-SceI sites had to be cut simultaneously to form short-range joins. Assuming that all inserted I-SceI sites are similarly cut, these findings also indicate that long-range joins of I-SceI DSBs at the location of Sμ to I-SceI DSBs 100 kb downstream at Sγ1 [which occurred in 5 to 10% of these hybridoma clones (Fig. 3C and figs. S10 and S11)] occur at about 10 to 20% of the frequency of short-range joins between the I-SceI DSBs flanking the 500-bp spacer.

We find that AID-initiated DSBs within Sμ- or I-SceI–mediated breaks at the site of Sμ frequently locate and join to I-SceI–generated DSBs 100 kb downstream at the normal Sγ1 site. Frequencies of resultant I-Sce-I–mediated switching to IgG$_1$ were at least 5 to 10% of bona fide IgG$_1$ switching mediated by full-length Sμ and Sγ1. In activated B cells, CSR frequency to IgG$_1$ is proportional to length of the repetitive Sγ1 sequence (*23*). In this regard, I-SceI sites inserted in place of Sμ and Sγ1 mediate switching to IgG$_1$ at about the frequency of an allele containing a full-length (4.6-kb) Sμ and a 1-kb Sγ1 (*23*). This frequency of switching approaches that of normal CSR to some other IgG isotypes, which ranges from 20 to 50% that of IgG$_1$ (*3*). Moreover, the frequency of long-range joins between two I-SceI DSBs in the IgH locus is three to four orders of magnitude greater than that for joining I-SceI DSBs on different chromosomes (*19*, *21*). Therefore, our studies reveal an unanticipated process that leads to frequent joining of widely separated IgH locus DSBs. Although we do not rule out roles for AID or normal S regions in enhancing joining of AID-initiated DSBs, we conclude that substantial IgH class switching resulting from joining two widely separated I-SceI DSBs requires neither AID nor S regions.

What processes promote synapsis of widely separated IgH locus DSBs? One candidate is B cell–specific higher-order IgH locus structural features, perhaps related to germline C_H transcription, that could influence interactions of DSBs in certain locations (*1*, *7*). However, we find similar amounts of I-SceI–dependent switching to IgG$_1$ in LPS-activated B cells and IgM-producing hybridomas that have not up-regulated transcription of or CSR to the Cγ1 locus. This finding indicates that synapsis of I-SceI DSBs does not require the processes that direct CSR to a particular C_H gene and suggests a potential role for more general mechanisms. In yeast and

mammalian cells, widely separated DSBs can be brought together before repair (*24*, *25*). In this regard, activated DSB response proteins, such as γ-H2AX, form foci that spread over chromatin regions up to a megabase flanking DSBs (*26*), and these proteins have been implicated in S region synapsis (*14*). Therefore, an attractive possibility is that simultaneous DSBs within the several-hundred-kb C_H portion of the IgH locus might generate overlapping domains of activated DSB response factors that promote synapsis and long-range joining, potentially as a by-product of a general mechanism that evolved to prevent translocations (*13*). Such a mechanism might also contribute to the propensity of certain chromosomal regions to undergo deletions (*27*).

In our model system, retrovirally introduced I-SceI frequently generates multiple DSBs within the IgH locus in activated B cells, which results either in rejoining of a DSB at a given I-SceI site, short-range deletions from joining DSBs at two proximal I-SceI sites (e.g., inserted in place of Sγ1), or long-range deletions from joining a DSB at an I-SceI site that replaced Sμ with a DSB at an I-SceI site that replaced Sγ1 (Fig. 4A). This pattern is reminiscent of the fate of the multiple AID-induced DSBs in S regions (*12*, *28*–*30*) (Fig. 4B). Moreover, long-range deletions occurred at an apparent frequency that was roughly 10 to 20% that of short-range deletions (Fig. 4A). Although I-SceI– and AID-generated breaks are not necessarily equivalent, these findings suggest an unanticipated aspect of the IgH CSR synapsis and joining mechanism. Specifically, we propose that the CSR evolved to ensure that the number of AID-dependent DSBs introduced into two participating S regions during the course of a given B cell's activation (3 to 4 days) is sufficiently high to yield physiological cellular amounts of CSR on the basis of a general mechanism that promotes an unexpectedly high relative proportion of long-range joining versus short-range joining or rejoining events (Fig. 4B).

References and Notes

1. D. D. Dudley, J. Chaudhuri, C. H. Bassing, F. W. Alt, *Adv. Immunol.* **86**, 43 (2005).
2. T. M. Luby, C. E. Schrader, J. Stavnezer, E. Selsing, *J. Exp. Med.* **193**, 159 (2001).
3. A. A. Khamlichi *et al.*, *Blood* **103**, 3828 (2004).
4. R. Shinkura *et al.*, *Nat. Immunol.* **4**, 435 (2003).
5. A. A. Zarrin *et al.*, *Nat. Immunol.* **5**, 1275 (2004).
6. M. Muramatsu *et al.*, *Cell* **102**, 553 (2000).
7. J. P. Manis, M. Tian, F. W. Alt, *Trends Immunol.* **23**, 31 (2002).
8. C. Rada, J. M. Di Noia, M. S. Neuberger, *Mol. Cell* **16**, 163 (2004).
9. R. A. Wuerffel, J. Du, R. J. Thompson, A. L. Kenter, *J. Immunol.* **159**, 4139 (1997).
10. J. S. Rush, S. D. Fugmann, D. G. Schatz, *Int. Immunol.* **16**, 549 (2004).
11. C. E. Schrader, E. K. Linehan, S. N. Mochegova, R. T. Woodland, J. Stavnezer, *J. Exp. Med.* **202**, 561 (2005).
12. D. D. Dudley *et al.*, *Proc. Natl. Acad. Sci. U.S.A.* **99**, 9984 (2002).
13. S. Franco *et al.*, *Mol. Cell* **21**, 201 (2006).
14. B. Reina-San-Martin *et al.*, *J. Exp. Med.* **197**, 1767 (2003).
15. B. Reina-San-Martin, H. T. Chen, A. Nussenzweig, M. C. Nussenzweig, *J. Exp. Med.* **200**, 1103 (2004).
16. E. D. Larson, M. L. Duquette, W. J. Cummings, R. J. Streiff, N. Maizels, *Curr. Biol.* **15**, 470 (2005).
17. V. Barreto, B. Reina-San-Martin, A. R. Ramiro, K. M. McBride, M. C. Nussenzweig, *Mol. Cell* **12**, 501 (2003).
18. A. Jacquier, B. Dujon, *Cell* **41**, 383 (1985).
19. C. Richardson, M. Jasin, *Nature* **405**, 697 (2000).
20. J. Chen, R. Lansford, V. Stewart, F. Young, F. W. Alt, *Proc. Natl. Acad. Sci. U.S.A.* **90**, 4528 (1993).
21. B. Elliott, C. Richardson, M. Jasin, *Mol. Cell* **17**, 885 (2005).
22. H. Nagaoka, M. Muramatsu, N. Yamamura, K. Kinoshita, T. Honjo, *J. Exp. Med.* **195**, 529 (2002).
23. A. A. Zarrin, M. Tian, J. Wang, T. Borjeson, F. W. Alt, *Proc. Natl. Acad. Sci. U.S.A.* **102**, 2466 (2005).
24. J. A. Aten *et al.*, *Science* **303**, 92 (2004).
25. M. Lisby, U. H. Mortensen, R. Rothstein, *Nat. Cell Biol.* **5**, 572 (2003).
26. E. P. Rogakou, C. Boon, C. Redon, W. M. Bonner, *J. Cell Biol.* **146**, 905 (1999).
27. L. Toffolatti *et al.*, *Genomics* **80**, 523 (2002).
28. H. Gu, Y. R. Zou, K. Rajewsky, *Cell* **73**, 1155 (1993).
29. C. E. Schrader *et al.*, *EMBO J.* **22**, 5893 (2003).
30. G. D. Yancopoulos *et al.*, *EMBO J.* **5**, 3259 (1986).

31. We thank Y. Fujiwara, T. Borjeson, and A. Riley for performing ES cell injections; Alt's laboratory members for their input; J. Manis, and K. Mills for their critical comments; A. A. Khamlichi and M. Cogne for providing the Sμ targeting construct and probe; J. Walsh and R. Mulligan for providing I-SceI vector; T. Honjo for P-MX retroviral vector; and J. Seagal and K. Rajewsky for providing technical advice on ELISpot. This work was supported by NIH grants PO1CA092625-05 and 2PO1AI031541-15 (to F.W.A.). F.W.A. is an investigator of Howard Hughes Medical Institute.

Supporting Online Material

www.sciencemag.org/cgi/content/full/1136386/DC1
Material and Methods
SOM Text
Figs. S1 to S11
References

16 October 2006; accepted 23 November 2006
Published online 14 December 2006;
10.1126/science.1136386
Include this information when citing this paper.

Farmland Biodiversity and the Footprint of Agriculture

S. J. Butler,[1]* J. A. Vickery,[2] K. Norris[1]

Sustainable development requires the reconciliation of demands for biodiversity conservation and increased agricultural production. Assessing the impact of novel farming practices on biodiversity and ecosystem services is fundamental to this process. Using farmland birds as a model system, we present a generic risk assessment framework that accurately predicts each species' current conservation status and population growth rate associated with past changes in agriculture. We demonstrate its value by assessing the potential impact on biodiversity of two controversial land uses, genetically modified herbicide-tolerant crops and agri-environment schemes. This framework can be used to guide policy and land management decisions and to assess progress toward sustainability targets.

Biodiversity and ecosystem function are inextricably linked. The case for biodiversity conservation can be argued on economic, sociocultural, and aesthetic grounds (*1*–*3*). Although biodiversity loss has occurred across all terrestrial ecosystems, many of its drivers are associated with the intensification of agriculture (*4*, *5*). Agricultural production is set to double again by 2050 (*6*). Unless the footprint of agriculture is carefully managed through sustainable development, both agricultural systems and remaining natural ecosystems will suffer further degradation, increasing the proportion of the world's species threatened with extinction and further limiting the ecosystem services they are capable of providing (*7*, *8*).

Managing the environmental effects of agriculture requires an assessment of biodiversity risks and benefits for all new agricultural practices (*4*, *9*). An appreciation of the ecological mechanisms that affect extinction risk is fundamental to the development of risk assessment protocols. One key factor appears to be the degree of specialization shown by a species (*10*, *11*). Specialists have narrower niche requirements and are disproportionately affected by reduced niche availability; the corollary is that generalist species are likely to be more resilient to environmental perturbation (*12*).

We have developed a trait-based risk assessment framework capable of predicting the impact of environmental change on biodiversity and ecosystem services. We used farmland birds as a model system to which to apply this framework. In the United Kingdom, birds have already been adopted as a focus for biodiversity conservation, with an index of wild bird population trends included as one of the government's 15 headline indicators of sustainable development. This indicator, presented as the overall proportional change since 1970, can be partitioned by habitat to reveal underlying trends (*13*). The farmland bird index (FBI) component shows that farmland bird populations have almost halved since 1970, and it is widely ac-

[1]Centre for Agri-Environment Research, School of Agriculture, Policy, and Development, University of Reading, Reading RG6 6AR, UK. [2]British Trust for Ornithology, The Nunnery, Nunnery Place, Thetford, Norfolk IP24 2PU, UK.

*To whom correspondence should be addressed. E-mail: s.j.butler@reading.ac.uk

cepted that these declines have been driven by agricultural intensification (*14*, *15*). The UK government has set a public service agreement (PSA) target to reverse this long-term decline in farmland bird populations by 2020.

Our framework draws on a matrix of species' ecological requirements covering components of diet, foraging habitat, and nesting habitat. The framework assumes that an agricultural change will affect a species if it leads to a change in food abundance and/or a change in nesting success. Food abundance can be altered by changes in foraging habitat availability and/or changes in food abundance in existing foraging habitats. Nesting success can be altered by changes in nesting habitat availability and/or changes in nest success in existing nesting habitats. Risk score calculation has its basis in the assumption that species with broader niches will be less vulnerable to the effects of agricultural change than species with narrower niches. Niche breadth is reflected in a species' risk score by calculating and summing the proportion of diet, foraging habitat, and nesting habitat components used by the species that are affected by an agricultural change. Higher scores are attributed to species demonstrating a greater proportion of affected requirements (*16*).

To validate our framework, we assessed the environmental effects of six key components of agricultural intensification in the United Kingdom over the past 4 decades: the switch from spring to autumn sowing, increased agrochemical inputs, loss of noncropped habitats (i.e., land not used for growing crops), increased land drainage, the switch from hay to silage, and the increased intensity of grassland management (*14*, *15*). We determined from the available literature whether these components had led to a reduction in the abundance or availability of each diet, foraging habitat, and nesting habitat component included in our matrix of ecological requirements. By using this matrix, we identified every species likely to have been adversely affected by any such reduction and calculated a risk score for each species. When summed across all six changes, the overall risk score for each species reflects the degree to which agricultural intensification has affected the species' ecological requirements (*16*).

Each of these agricultural changes has occurred at a national scale, and any detrimental environmental effects are likely to have caused population-scale responses in vulnerable species. We predicted that the risk score for each species should be significantly related to its conservation status and population growth rate over the period of recent agricultural change. The conservation status of UK birds is listed as red (most threatened), amber, and green (least threatened) and is assigned according to a range of criteria covering breeding range and population trends (*17*). We found that risk score was significantly related to the probability of being listed in these conservation status categories (Fig. 1A) (mean score ± 1 SE for species on the red list was 6.6 ± 0.8; for the amber list, 4.9 ± 0.8; and for the green list, 2.2 ± 0.4; ordinal logistic regression, $\chi^2 = 25.4$, $P < 0.001$). We also found that the risk score was significantly related to the annual rate of population growth (Fig. 1B) (*16*): Higher risk assessment scores were associated with species with negative population growth rates and therefore experiencing population decline [$F(1, 49) = 11.3$, $P = 0.002$]. The predicted FBI, based on population changes from 1970–2001 and calculated by using a bootstrapping procedure on population growth rates generated from jack-knife analyses (*16*), is 0.59 (0.42 to 0.85 are 95% confidence limits), compared to the actual FBI of 0.54.

Our risk-scoring system assumes equal weighting for each source of risk in terms of its relation to conservation status and population growth and assumes that different risk sources have an additive effect. To critically assess these assumptions, we constructed a series of more-complex alternative models that decomposed the total risk score into various component parts, allowing the weighting of different sources of risk to vary. We also created a set of models that assumed multiplicative rather than additive effects (tables S6 and S7). This analysis showed that our assumptions were reasonable: The most parsimonious models of conservation status and population growth rate only included total risk score. However, two alternative models for predicting population growth rates, one specifying additive effects of risk score decomposed into diet-related and nest-related components and the other specifying multiplicative effects of these two variables, also received support.

Parameter estimates from these regression models can be used to predict the likely impact of new agricultural practices on farmland bird populations. We demonstrate this process by applying our risk assessment framework to two controversial land uses, genetically modified herbicide-tolerant (GMHT) crops and agri-environment schemes, which have generated debate over their possible contributions to sustainable development and their impacts on biodiversity (*18*–*22*). Species scores from these risk assessments were combined with their scores from the validation process, which characterize responses to current landscape conditions, to predict population growth rates and conservation status in the resultant landscapes (*16*).

The Farm Scale Evaluation project investigated the effects of GMHT crop management on UK farmland wildlife. Its results suggested that introduction of GMHT sugar beet and oilseed rape is likely to cause a long-term reduction in above-ground invertebrates and weeds in the cropped area of fields (*23*). Thirty-nine farmland bird species have ecological requirements that make them susceptible to such changes. Each of these species would therefore

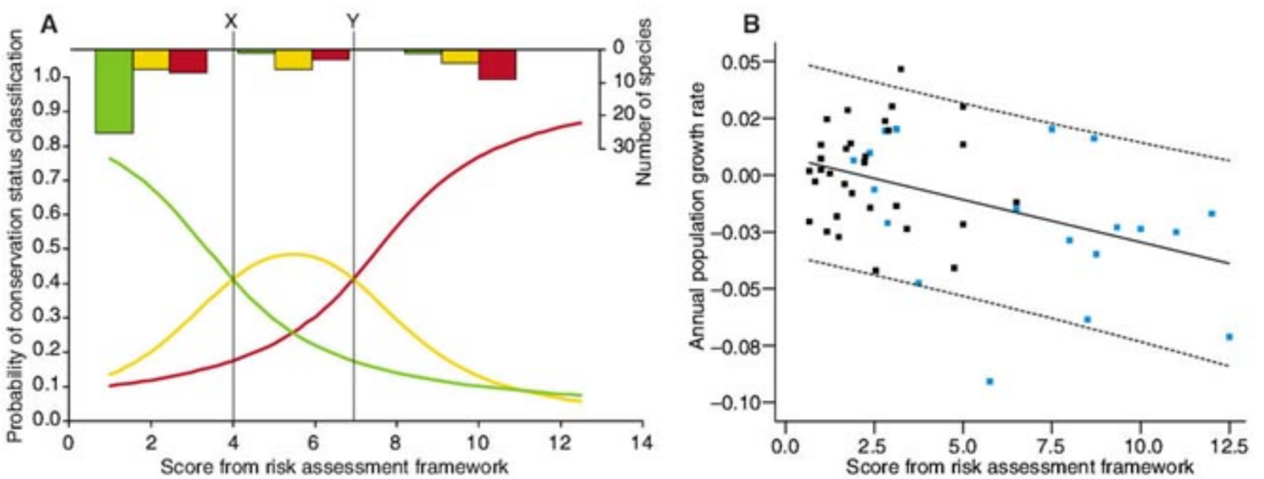

Fig. 1. Relationships between total risk score and (A) conservation status category and (B) annual population growth rate. (**A**) Probability of conservation status category classification derived from parameter estimates of the ordinal logistic regression model (*16*). Colors represent UK conservation status categories (*17*). Below a risk score of 4 (to the left of line X), the probability of being green-listed is highest. Between risk scores of 4 and 6.9 (between lines X and Y), the probability of being amber-listed is highest. Above a risk score of 6.9 (to the right of line Y), the probability of being red-listed is highest. Bar charts show the distribution of actual species status within these risk score boundaries. Cross-tabulation of predicted versus actual classification shows strong symmetry (Somer's $d = 0.50$, $P < 0.001$). (**B**) Annual population growth rate declines with increasing score from risk assessment of recent agricultural intensification (*16*). Data for species included in FBI are shown in blue. Solid black line shows fitted model for all species ($y = 0.0079 - 0.0037x$, $r^2 = 0.19$); dashed lines show 95% confidence limits.

be expected to experience reduced population growth rates following nationwide GMHT crop introduction. However, we predict that just one species, meadow pipit (*Anthus pratensis*), would be reclassified to a less-favorable conservation status as a consequence (changing from amber- to red-listed). Overall, it appears that replacing equivalent conventional crops in the current agricultural landscape with GMHT crops would only have a limited effect on the FBI (Table 1 and Fig. 2).

Agri-environment schemes are designed to mitigate the detrimental impacts of agriculture and increase the value of the landscape to biodiversity. Clearly these schemes will be most effective if they target the main drivers of biodiversity decline. Our validation results suggest these key drivers have been the loss of food and nesting habitats in the cropped areas of the agricultural landscape (table S8).

An example scheme, entry-level stewardship (ELS), was launched in England in 2005, offering a range of management options for all farming types. Over 13,000 agreements, covering 1.5 million hectares, have already been implemented, with payments totalling £47 million in the first year (*24*). However, analyses of option objectives and initial uptake rates (*16*, *25*, *26*) show that the main emphasis of current agreements is on hedgerow and margin management rather than improving the environmental value of the cropped area (table S8). This disparity between the causes of farmland bird population decline and the uptake of mitigation measures, rather than scheme design per se, suggests that the ELS may not deliver its biodiversity objectives. Even if all causes of decline associated with margin and hedgerow habitats in the current agricultural landscape are countered by management agreements under ELS, our analyses suggest that the FBI will continue to decline, driven by the detrimental conditions persisting in the cropped area (Table 1 and Fig. 2). More importantly, the three models predict that the percentage of FBI species with annual population growth rates of zero or above will lie between only 37% and 53% [8/19, 10/19, and 7/19 of FBI species (table S9)]. Furthermore, several red-list species, such as skylark (*Alauda arvensis*) and corn bunting (*Miliaria calandra*), which rely solely on the cropped area of fields, are likely to continue declining at their current rate (Fig. 2). Unless greater emphasis is placed on improving the value of the cropped area for biodiversity, progress toward reversing the long-term declines in farmland birds is liable to fall short of the UK government's PSA target.

This trait-based approach could have a broad range of applications in agricultural ecosystems and beyond. For example, it could be used to assess the risk of agricultural changes to pollinating insect populations and therefore pollination services. The necessary data for developing an ecological requirements matrix for many of these species, particularly in the United Kingdom and Western Europe, are readily attainable (*27*). Pollinator diversity is essential for sustaining this highly valued service, estimated to be worth S14 ha^{-1} $year^{-1}$ (*28*), but agricultural intensification has reduced both the diversity and the abundance of native insect pollinators (*27*). By assessing the impact on key ecological requirements, our framework could be used to predict the response of pollinating insect populations to any proposed change and therefore facilitate the effective management of pollination services in the agricultural landscape. Our framework provides a robust basis for assessing risk, and its application to GMHT crops and agri-environmental management has important implications for policy- and decision-makers. We believe our framework can also contribute greatly to the economic evaluation of proposed agricultural changes that alter the functioning of ecosystem services through their impact on biodiversity.

Table 1. Predicted FBI in 2020 derived from risk scores associated with continued current management, the introduction of GMHT crops in 2005, or the introduction of the ELS scheme in 2005. Mean predicted FBI values and 95% confidence limits (in parentheses) were generated from three alternative models of population growth rate (*16*). Predicted FBI for 2001 generated from the three alternative models are also shown. For comparison, the FBI in 2001 calculated from actual population growth rates was 0.54.

Model structure	Predicted FBI in 2001	Predicted FBI in 2020		
		Current management continued	GMHT crops introduced in 2005	ELS introduced in 2005
Total risk	0.59 (0.42–0.85)	0.42 (0.26–0.65)	0.40 (0.25–0.62)	0.47 (0.31–0.71)
Diet-related risk plus nest-related risk	0.59 (0.38–0.86)	0.42 (0.27–0.62)	0.41 (0.26–0.62)	0.47 (0.30–0.70)
Diet-related risk multiplied by nest-related risk	0.62 (0.41–0.94)	0.47 (0.30–0.71)	0.45 (0.28–0.67)	0.52 (0.34–0.77)

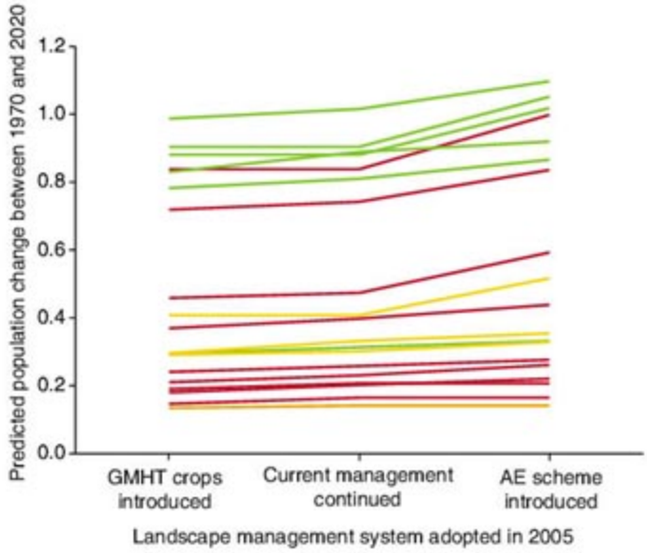

Fig. 2. Predicted proportional changes in the populations of the 19 FBI species between 1970 and 2020 under three land management scenarios (*16*). Line colors represent current UK conservation status categories (*17*). Population growth rates estimated from parameter estimates were derived from the model of total risk score used to illustrate predicted responses.

References and Notes

1. A. Balmford *et al.*, *Science* **297**, 950 (2002).
2. M. Loreau *et al.*, *Science* **294**, 804 (2001).
3. W. M. Adams *et al.*, *Science* **306**, 1146 (2004).
4. R. S. Hails, *Nature* **418**, 685 (2002).
5. R. E. Green, S. J. Cornell, J. P. Scharlemann, A. Balmford, *Science* **307**, 550 (2005); published online 23 December 2004 (10.1126/science.1106049).
6. D. Tilman, *Proc. Natl. Acad. Sci. U.S.A.* **96**, 5995 (1999).
7. F. S. Chapin III *et al.*, *Nature* **405**, 234 (2000).
8. D. Tilman *et al.*, *Science* **292**, 281 (2001).
9. Advisory Committee on Releases to the Environment (ACRE), *Managing the Footprint of Agriculture: Towards a Comparative Assessment of Risks and Benefits for Novel Agricultural Systems* [Department for Environment, Food, and Rural Affairs (Defra), London, 2006]; available at www.defra.gov.uk/environment/acre/fsewiderissues/acre-fse-060317draft.pdf.
10. I. P. F. Owens, P. M. Bennett, *Proc. Natl. Acad. Sci. U.S.A.* **97**, 12144 (2000).
11. K. Norris, N. Harper, *Proc. R. Soc. London Ser. B* **271**, 123 (2004).
12. G. M. Siriwardena *et al.*, *J. Appl. Ecol.* **35**, 24 (1998).
13. R. D. Gregory *et al.*, *Ornis Hung* **12–13**, 11 (2003).
14. J. R. Krebs, J. D. Wilson, R. B. Bradbury, G. M. Siriwardena, *Nature* **400**, 611 (1999).
15. I. Newton, *Ibis* **146**, 579 (2004).
16. Detailed materials and methods are available as supporting material on *Science* Online.
17. R. D. Gregory *et al.*, *Br. Birds* **95**, 410 (2002).
18. R. P. Freckleton, P. A. Stephens, W. J. Sutherland, A. R. Watkinson, *Proc. R. Soc. London Ser. B* **271**, 325 (2004).
19. J. N. Perry *et al.*, *Nature* **428**, 313 (2004).
20. D. Kleijn, F. Berendense, R. Smit, N. Gilissen, *Nature* **413**, 723 (2001).
21. D. Kleijn, W. J. Sutherland, *J. Appl. Ecol.* **40**, 947 (2003).

22. J. Whitfield, *Nature* **439**, 908 (2006).
23. S. Zeki, *Philos. Trans. R. Soc. Lond. Ser. B* **358**, 1775 (2003).
24. Defra, press release (8 February 2006); available at www.defra.gov.uk/news/2006/060208a.htm.
25. Defra, *Entry Level Stewardship Handbook* (Defra, London, 2005); available at www.defra.gov.uk/erdp/pdfs/es/els-handbook.pdf.
26. Rural Development Service (Strategic Delivery Team), *ES Option Uptake Report* (Defra, London, 2006).
27. J. C. Biesmeijer *et al.*, *Science* **313**, 351 (2006).
28. R. Costanza *et al.*, *Nature* **387**, 253 (1997).
29. We thank R. Bradbury, J. Quinn, R. Green, and three anonymous referees for helpful comments and discussion. This work was funded by Defra under project code AR0317.

Supporting Online Material
www.sciencemag.org/cgi/content/full/315/5810/381/DC1
Materials and Methods
Tables S1 to S9
References

23 October 2006; accepted 21 November 2006
10.1126/science.1136607

Control of *Drosophila* Gastrulation by Apical Localization of Adherens Junctions and RhoGEF2

Verena Kölsch,[1]* Thomas Seher,[1] Gregorio J. Fernandez-Ballester,[2] Luis Serrano,[3]† Maria Leptin[1]‡

A hallmark of epithelial invagination is the constriction of cells on their apical sides. During *Drosophila* gastrulation, apical constrictions under the control of the transcription factor Twist lead to the invagination of the mesoderm. Twist-controlled G protein signaling is involved in mediating the invagination but is not sufficient to account for the full activity of Twist. We identified a Twist target, the transmembrane protein T48, which acts in conjunction with G protein signaling to orchestrate shape changes. Together with G protein signaling, T48 recruits adherens junctions and the cytoskeletal regulator RhoGEF2 to the sites of apical constriction, ensuring rapid and intense changes in cell shape.

Apical constriction of cells can contribute to the invagination of epithelia, such as during gastrulation or organogenesis, and the closure of wounds. In the *Drosophila* embryo, apical constrictions occur along the ventral side of the blastoderm epithelium, leading to the formation of the ventral furrow and the invagination of the mesoderm (*1*). Proteins necessary for the mechanics of these cell shape changes include the Rho guanosine 5′-triphosphate–exchange factor RhoGEF2 (*2*, *3*) and a heterotrimeric G protein. Whereas RhoGEF2 is essential for furrow formation, disruption of the heterotrimeric G protein, such as by loss of its α subunit Concertina (Cta), leads to a delay but no lasting defects in mesoderm morphogenesis (*4*, *5*). These maternally supplied proteins must be activated under the control of the zygotic genome in the embryo.

Twist is the zygotic transcriptional activator that is essential for the cell shape changes that produce the ventral furrow. One of its targets is the transcriptional repressor Snail, which is also essential for mesodermal morphogenesis (*6*). However, the cell biological events responsible for the cell shape changes must ultimately be regulated by targets that are not transcription factors. Of the known Twist targets, only one, *folded gastrulation* (*fog*), is involved in mediating shape changes. Mutants in *fog*, which codes for a secreted peptide (*7*, *8*), show the same defects as embryos lacking Cta. Fog is therefore thought to act in the same pathway as Cta, which we refer to as Fog/Cta signaling.

Fog/Cta signaling is thought to cause changes in the actin cytoskeleton in conjunction with RhoGEF2. Recruitment of myosin from basal to apical in constricting ventral cells is partly dependent on Fog/Cta and absolutely dependent on RhoGEF2 (*8*, *9*). Furthermore, the mammalian homologs of RhoGEF2 and Cta interact (*10*). Finally, binding of *Drosophila* RhoGEF2 to microtubules by means of EB1 is disrupted by activated Cta (*11*). Given that myosin recruitment and apical constriction are reduced but not abolished in the absence of Fog/Cta (*8*), there must be other factors regulated by Twist that explain its effects on apical constriction.

In a screen for genes that mediate the zygotic control of gastrulation (*12*), we found the re-

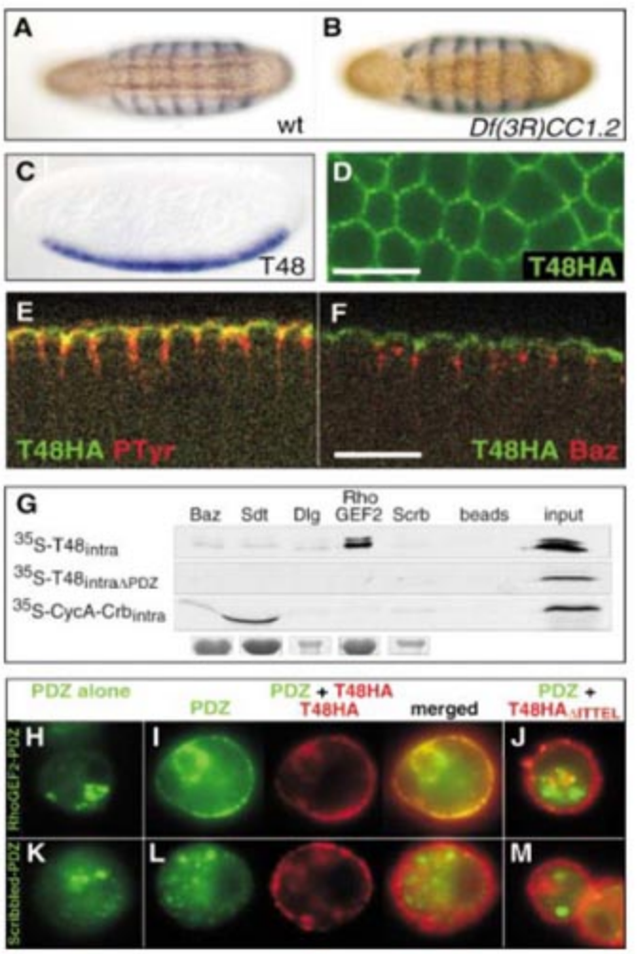

Fig. 1. Characterization of T48. (**A** and **B**) Wild-type and age-matched *Df(3R)CC1.2* (*T48*$^{-}$) embryos stained for Twist (brown) and Even-skipped (blue). For statistical evaluation, see figs. S2 and S3. (**C**) *T48* RNA expression at blastoderm stage. (**D** to **F**) T48HA localization. (D) Surface view of stage 5 embryo; staining is at the cellular interfaces. [(E) and (F)] Optical sections through the blastoderm epithelium, apical is up. T48 is at the apical cell membranes, overlapping phospho-tyrosine (PTyr) staining, but not Bazooka (Baz). Scale bars, 10 μm. (**G**) Coimmunoprecipitates of ^{35}S-labeled T48 and Crb with glutathione *S*-transferase fusions of PDZ domains (*17*). Coomassie-stained SDS–polyacrylamide gel electrophoresis bands of the PDZ-construct input shown below. (**H** to **M**) Colocalization of PDZ domains with T48HA. S2 cells transfected with GFP-tagged RhoGEF2-PDZ [(H) to (J)] or Scribbled-PDZ [(K) to (M)] alone or in combination with T48HA or T48HA$_{\Delta ITTEL}$. (See figs. S4 and S5 for statistical and graphic evaluation.)

[1]Institute of Genetics, University of Cologne, Zülpicher Strasse 47, 50674 Cologne, Germany. [2]Instituto de Biología Molecular y Celular, Universidad Miguel Hernández, Edificio Torregaitán, Avenida de la Universidad, 03202 Elche, Spain. [3]European Molecular Biology Laboratory, Meyerhofstrasse 1, 69012 Heidelberg, Germany.

*Present address: Section of Cell and Developmental Biology, Division of Biological Sciences and Center for Molecular Genetics, University of California, San Diego, La Jolla, CA 92093, USA.
†Present address: Centre de Regulació Genòmica, 08003 Barcelona, Spain.
‡To whom correspondence should be addressed. E-mail: mleptin@uni-koeln.de

gion uncovered by the chromosomal deficiency *Df(3R)Tl*^{P} to be necessary for the proper formation of the ventral furrow (fig. S1). Phenotypic analysis and molecular mapping of a set of overlapping deficiencies (table S1) identified the gene *T48* as being responsible for the defects seen in *Df(3R)Tl*^{P} [supporting online material (SOM) text and Fig. 1, A and B]. T48 is expressed in the mesoderm (Fig. 1C) under control of Twist (*13*, *14*). It codes for a predicted protein with a signal peptide and a potential transmembrane domain. When an internally hemagglutinin-tagged T48 protein (T48HA) was expressed in embryos, it localized at the peripheries of blastoderm cells, consistent with a close association with or insertion into the plasma membrane (Fig. 1D). Optical cross-sections showed that T48HA is targeted to the apical membrane (Fig. 1, E and F).

No other structural motifs are recognizable in the protein. However, the C-terminal amino acid sequence –Ile-Thr-Thr-Glu-Leu (-ITTEL) conforms to the class I consensus for peptides that interact with PDZ domains. T48 has no obvious human ortholog but shows some similarity to the intracellular part of Fras1 (*15*), which also has a PDZ-binding motif. To find candidates for PDZ domains that might interact with T48, we analyzed the putative PDZ-binding sequence with an algorithm designed to determine the PDZ domains that show the optimal fit for any given peptide (*16*, *17*). Of the predicted interactors (table S2), RhoGEF2 was particularly interesting in view of its role in ventral furrow formation (*2*, *3*). Furthermore, the mammalian ortholog of RhoGEF2 has been shown to bind to Plexin-B1 by means of a PDZ-binding motif (–Val-Thr-Asp-Leu) very similar to that of T48 (*18*).

We tested whether the C terminus of T48 is indeed able to interact with RhoGEF2. A ^{35}S-labeled C-terminal peptide of T48 preferentially coprecipitated with the PDZ domain of RhoGEF2 rather than those of other PDZ domain–containing proteins, in contrast to Crumbs, which was used as a control and which preferentially coprecipitated with PDZ domains from its physiological interaction partner Stardust, as well as Bazooka (Fig. 1G). In Schneider S2 cells, a green fluorescent protein (GFP)–tagged RhoGEF2 PDZ domain or full-length RhoGEF2 was localized in the cytoplasm or formed intracellular aggregates (Fig. 1H) when expressed alone, but localized to the plasma membrane when coexpressed with T48 (Fig. 1I and figs. S4 and S5). In both assays, the interaction required the presence of the -ITTEL motif and was not seen with other PDZ domains (Fig. 1, J to M). Thus, T48 interacts with RhoGEF2 by means of its PDZ-binding motif and is able to enrich RhoGEF2 to the plasma membrane.

To understand the function of T48 during gastrulation, we studied the subcellular localization of RhoGEF2 and its dependence on T48 in the developing embryo. Before gastrulation, the apical surfaces of the blastoderm epithelium are dome shaped and the developing adherens junctions are located subapically. RhoGEF2 is associated with the basally located furrow canals, whereas Armadillo is found just below this site and at a subapical position of the lateral cell membranes (Fig. 2, A to C) (*19*, *20*).

After cellularization was completed, these distributions changed specifically in ventral cells (Fig. 2, B to E). Even before morphological changes occurred, RhoGEF2 and Armadillo disappeared from the basal ends (Fig. 2, A to C and F). Subsequently, Armadillo disappeared from its subapical site and accumulated apically (*8*) (Fig. 2, D and G). A weak association of RhoGEF2 with the apical plasma membrane was seen at this stage (Fig. 2, E and G).

As cells began to flatten apically, high levels of both RhoGEF2 and Armadillo accumulated apically (*8*, *20*) (Fig. 2, H to L). Although they concentrated in the same region of the cell, Armadillo was restricted to the cell junctions, whereas RhoGEF2 was often more enriched between these sites (Fig. 2J). Notably, movement of the adherens junctions occurred not only in constricting cells but also in the more lateral mesodermal cells that flattened and became stretched on their apical sides (Fig. 2K).

To examine whether these processes depend on T48, we stained stage-selected *T48* mutant embryos (*17*). Loss of RhoGEF2 and Armadillo from the basal side was unaffected in these

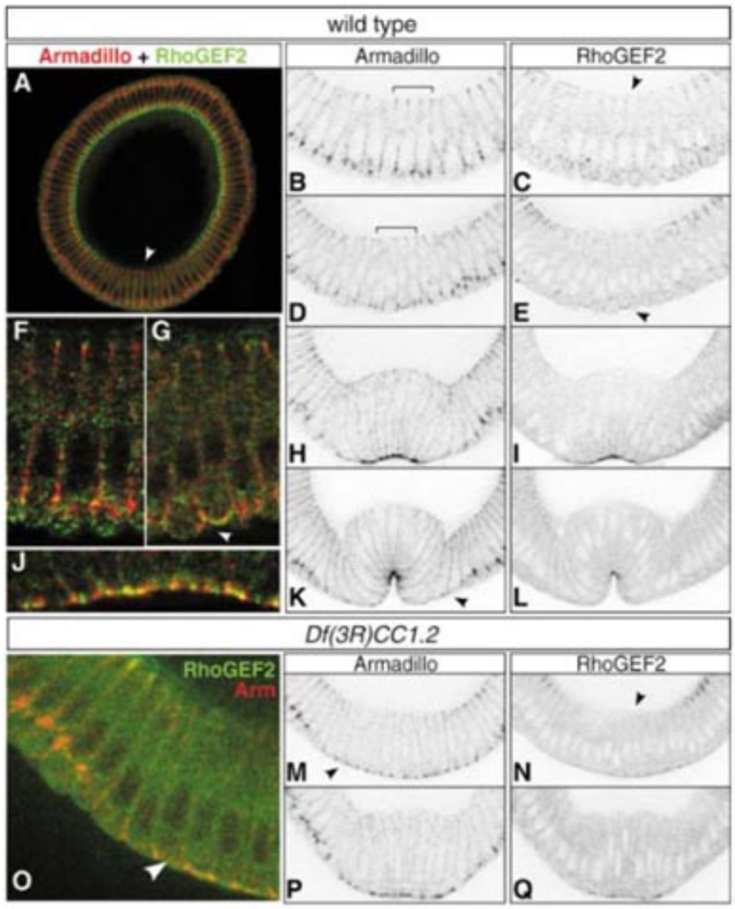

Fig. 2. Redistribution of RhoGEF2 and Armadillo. Sections of wild-type [(A) to (L)] and *T48*$^{-}$ embryos [(M) to (Q)] stained for RhoGEF2 and Armadillo as indicated. (**A** to **C** and **F**) Stage 5 wild-type embryos; RhoGEF2 and Armadillo are lost from the basal end in ventral cells (arrowhead). (**D**, **E**, and **G**) Late stage 5: Disappearance of subapical Armadillo in ventral cells and first signs of apical localization of RhoGEF2 in cells with still-rounded surfaces [arrowheads in (E) and (G)]. [(F) and (G)] Details of embryos shown in (B) and (C) and in (D) and (E), respectively [marked by brackets in (B) and (D)]. (**H** to **L**) Stage 6: Strong apical localization of RhoGEF2 and Armadillo in constricting cells. (J) Detail of (H) and (I): Nonoverlapping localization of Armadillo (concentrated at cell junctions) and RhoGEF2 (apical surface). [(K) and (L)] Adherens junctions are apical throughout the mesoderm, including nonconstricting cells (arrowhead). (**M** to **Q**) Stage 6 *T48*$^{-}$ mutant embryos (*17*) show reduced apical localization of RhoGEF2 [(N) and (Q)]. Armadillo relocalization and apical flattening occur [(O), arrowhead], but apical constriction is delayed. Black-and-white fluorescence images were color-inverted in Photoshop.

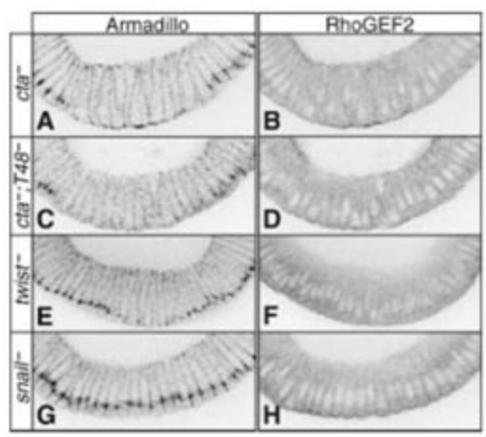

Fig. 3. Effect of Cta, Twist, and Snail on RhoGEF2 and Armadillo. Sections of stage 6 mutant embryos. (**A** and **B**) Embryos derived from homozygous *concertina*^{R10} mothers. (**C** and **D**) Homozygous *T48*$^{-}$ embryos derived from homozygous *concertina* mutant mothers. See fig. S6 for a more extensive documentation of the *cta;T48* mutant phenotype. (**E** and **F**) Homozygous *twist*^{EY53R1} mutant embryos. (**G** and **H**) Homozygous *snail* mutant embryos (*Df(2L)TE116GW11*). Fluorescent pictures were inverted.

embryos (Fig. 2, M and N), as was the apical concentration of Armadillo. The cells flattened apically (Fig. 2O) and lengthened, but the absence of constrictions resulted in a thick placode rather than an indentation (Fig. 2, P and Q). Localization of RhoGEF2 to the apical membrane was slightly delayed and possibly reduced (Fig. 2, N and Q). T48 therefore contributes to but is not essential for the recruitment of RhoGEF2 to the apical membrane. This is consistent with the observation that furrow formation is not completely abolished, but only delayed or weakened. We therefore examined other mechanisms that might participate in RhoGEF2 localization.

As in the case of T48, mutations in the Fog/Cta pathway delay but do not abolish apical constriction and furrow formation (*4*, *7*). We therefore considered whether Fog/Cta signaling might cooperate with T48 to recruit RhoGEF2. In embryos lacking Cta, the recruitment of RhoGEF2 was weakened (Fig. 3B). Combining mutations in *cta* and *T48* resulted in much more notable effects (Fig. 3D). These *cta,T48* embryos failed to make a furrow; the lack of apical constrictions was mirrored by a failure to accumulate RhoGEF2 apically (Fig. 3 and fig. S6). Thus, T48 and Fog/Cta signaling act in parallel to concentrate RhoGEF2 apically.

We also observed severe defects in the behavior of the adherens junctions in the double-mutant embryos. Armadillo staining disappeared from its tight subapical localization but did not reaccumulate apically (Fig. 3C and fig. S6). Thus, movement of the junctions is not simply mediated by a tensile force from the constricting actin cytoskeleton—an independent step of at least partial disassembly must occur. We speculated that this might be controlled by Snail, which regulates the disassembly of cell junctions in vertebrates. We found that the disassembly of Armadillo from the subapical position was indeed blocked in *snail* (but not in *twist*) mutant embryos (Fig. 3, E and G). Thus, Snail acts in parallel to Twist to direct the disassembly of subapical junctions, a process to which currently unknown Twist targets may also contribute (SOM text).

Having observed that T48 and Fog/Cta activation are required for the apical localization of RhoGEF2 and Armadillo, we tested whether T48, like Fog/Cta signaling, was able to trigger their relocalization in other cells. Ubiquitous expression of T48 in the embryo led to a concentration of RhoGEF2 at the apical membranes of lateral cells (compare Fig. 4, A and B; fig. S7). Armadillo localization in ectodermal cells was no longer restricted to a distinct subapical domain but extended to the apical end of the lateral membranes in many cells. When T48 was coexpressed with activated Cta, this effect was slightly enhanced, and some embryos showed morphological defects (fig. S7).

With T48, we found a missing factor in the control cascade from transcriptional regulation by Twist to the cell biological mediators of furrow morphogenesis (Fig. 4, C and D). Two Twist targets, Fog and T48, appear to act in separate pathways that converge on RhoGEF2, which integrates the signal to activate myosin and modify the actin cytoskeleton (*8*, *9*). Our model shows the maternally supplied RhoGEF2 as largely attached to microtubules by means of EB1 (*11*). The onset of Twist expression has two effects. Fog is synthesized, which triggers the activation of Cta. This in turn releases RhoGEF2 from the microtubules that, by analogy to its vertebrate homologs, may bind to Cta through its RGS domain (*10*), allowing some myosin activation and constriction. In parallel, T48 is synthesized and targeted to the apical membrane, where it acts to concentrate RhoGEF2 through its PDZ-binding motif. In the absence of Fog-mediated displacement of RhoGEF2 from EB1, T48 can probably still recruit sufficient freely diffusible RhoGEF2 to allow slow constriction. Only when both mechanisms fail are the downstream events of constriction and junction reassembly abolished completely.

The utilization of Gα12/13 proteins and a microtubule-bound RhoGEF have also been reported in vertebrate gastrulation (*21*, *22*). The absence of an obvious homolog of *T48* in vertebrates might suggest that this element of the control mechanism is unique to *Drosophila* gastrulation. However, the PDZ-binding motif in Plexin-B1 is similar to that of T48 and acts during neuronal growth cone remodeling by recruiting PDZ-RhoGEF (*18*). Therefore, this mechanism of controlling cell shape may operate in a variety of systems.

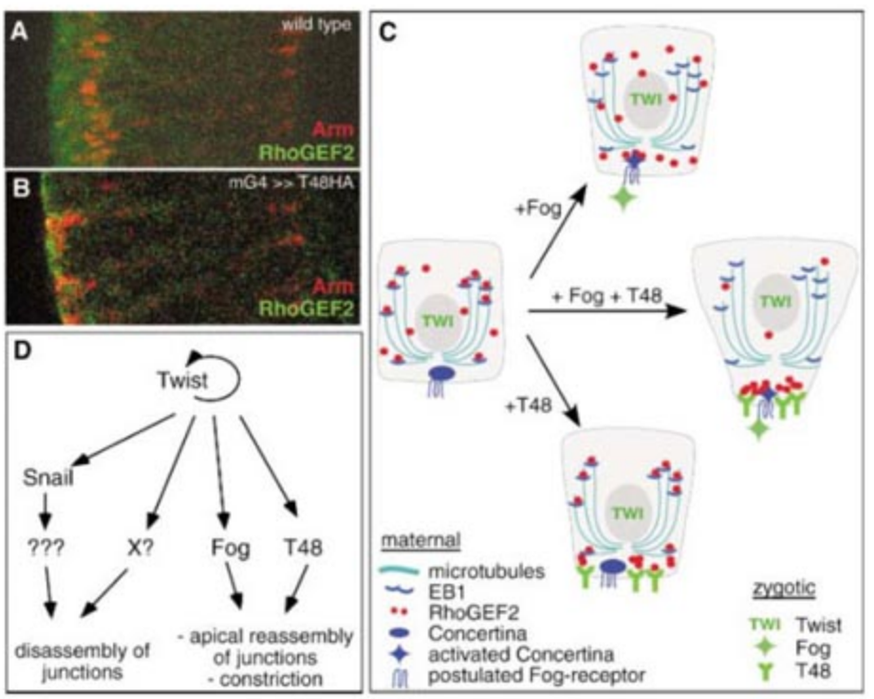

Fig. 4. Induced relocalization of RhoGEF2 and Armadillo, and a model for the control of furrow formation. (**A** and **B**) Details of sections of the wild-type (A) and T48-overexpressing (B) embryos shown in fig. S7. (**C**) Model for T48 and Fog/Cta function during gastrulation. (**D**) Genetic hierarchy of the genes acting downstream of Twist in regulating adherens junctions and cytoskeletal rearrangements.

References and Notes

1. D. Sweeton, S. Parks, M. Costa, E. Wieschaus, *Development* **112**, 775 (1991).
2. U. Häcker, N. Perrimon, *Genes Dev.* **12**, 274 (1998).
3. K. Barrett, M. Leptin, J. Settleman, *Cell* **91**, 905 (1997).
4. S. Parks, E. Wieschaus, *Cell* **64**, 447 (1991).
5. Y. Izumi, N. Ohta, A. Itoh-Furuya, N. Fuse, F. Matsuzaki, *J. Cell Biol.* **164**, 729 (2004).
6. M. Leptin, B. Grunewald, *Development* **110**, 73 (1990).
7. M. Costa, E. T. Wilson, E. Wieschaus, *Cell* **76**, 1075 (1994).
8. R. E. Dawes-Hoang *et al.*, *Development* **132**, 4165 (2005).
9. K. K. Nikolaidou, K. Barrett, *Curr. Biol.* **14**, 1822 (2004).
10. M. J. Hart *et al.*, *Science* **280**, 2112 (1998).
11. S. L. Rogers, U. Wiedemann, U. Häcker, C. Turck, R. D. Vale, *Curr. Biol.* **14**, 1827 (2004).
12. T. C. Seher, M. Leptin, *Curr. Biol.* **10**, 623 (2000).
13. M. Leptin, *Genes Dev.* **5**, 1568 (1991).
14. D. I. Strutt, R. A. White, *Mech. Dev.* **46**, 27 (1994).
15. L. McGregor *et al.*, *Nat. Genet.* **34**, 203 (2003).
16. J. Reina *et al.*, *Nat. Struct. Biol.* **9**, 621 (2002).
17. Materials and methods are available as supporting material on *Science* Online.
18. J. M. Swiercz, R. Kuner, J. Behrens, S. Offermanns, *Neuron* **35**, 51 (2002).
19. M. Padash Barmchi, S. Rogers, U. Häcker, *J. Cell Biol.* **168**, 575 (2005).
20. J. Grosshans *et al.*, *Development* **132**, 1009 (2005).
21. K. M. Kwan, M. W. Kirschner, *Development* **132**, 4599 (2005).
22. F. Lin *et al.*, *J. Cell Biol.* **169**, 777 (2005).

23. We thank J. Grosshans, R. White, K. Barrett, K. Anderson, T. Lecuit, H. A. Müller, E. Wieschaus, K. Johnson, R. Wilson, M. Rembold, and J. Hancke for reagents, assistance, and discussions. We are especially grateful to C. Gonzales for suggesting the bioinformatic approach for identifying T48 interactors. Financial support was from the Deutsche Forschungsgemeinschaft (SFB572 and LE546/2) and EU (LSHG-CT-2005-512028 and LSHG-CT-2004-503567).

Supporting Online Material

www.sciencemag.org/cgi/content/full/315/5810/384/DC1
Materials and Methods
SOM Text
Figs. S1 to S7
Tables S1 to S3
References

7 September 2006; accepted 6 December 2006
10.1126/science.1134833

High-Throughput Identification of Catalytic Redox-Active Cysteine Residues

Dmitri E. Fomenko,[1] Weibing Xing,[2] Blakely M. Adair,[3] David J. Thomas,[3] Vadim N. Gladyshev[1]*

Cysteine (Cys) residues often play critical roles in proteins; however, identification of their specific functions has been limited to case-by-case experimental approaches. We developed a procedure for high-throughput identification of catalytic redox-active Cys in proteins by searching for sporadic selenocysteine-Cys pairs in sequence databases. This method is independent of protein family, structure, and taxon. We used it to selectively detect the majority of known proteins with redox-active Cys and to make additional predictions, one of which was verified. Rapid accumulation of sequence information from genomic and metagenomic projects should allow detection of many additional oxidoreductase families as well as identification of redox-active Cys in these proteins.

Relative to other amino acids in proteins, cysteine (Cys) residues are often conserved and functionally important. Cys residues critical to protein function are frequently used at enzyme active sites; they may bind metals such as iron, zinc, and copper; and they may be subjected to posttranslational modifications that regulate protein function or target proteins to a particular cellular location. A Cys pair may form a disulfide bond that stabilizes protein structure (*1*), and numerous additional roles of Cys have been described.

However, the presence of Cys in a protein sequence per se does not mean that this residue has a critical function, nor does it establish what that function might be. Analyses of Cys conservation may help identify catalytic Cys, but only for proteins with already known function (*2*–*4*). Cys is chemically similar to selenocysteine (Sec), a rare but widely distributed amino acid encoded by UGA and known as the 21st amino acid in the genetic code (*5*–*9*). In functionally characterized selenoprotein families, Sec is located in enzyme active sites and serves various redox functions. In addition, most selenoproteins have close homologs in which Sec is replaced by Cys.

Selenoproteins are found in all three domains of life, but a given organism contains a relatively small number of these proteins. A core of about 20 selenoproteins is widespread; however, many organisms also evolved rare or lineage-specific selenoproteins. For example, methionine-*S*-sulfoxide reductase (MsrA) occurs as a selenoprotein in green algae and a Cys-containing form in most other species (*9*), whereas the Cys-containing methionine-*R*-sulfoxide reductase (MsrB) evolved into a selenoprotein in vertebrates (*10*). Although Sec occurs only in several MsrA and MsrB sequences, it aligns with the catalytic Cys in other members of these protein families. Only the catalytic Cys aligns with Sec, whereas other Cys residues, such as the conserved Cys that serve as resolving residues or coordinate zinc, do not have Sec pairs. Thus, identification of rare Sec-containing forms of MsrA and MsrB indicates the thiol-based redox function of these proteins. Moreover, it pinpoints the location of catalytic Cys in these protein families. Similarly, the occurrence of rare Sec-containing forms of other protein families containing conserved Cys may be indicative of redox functions of these families.

We used this property of homologous Cys-Sec pairs to develop a procedure for large-scale identification of catalytic redox-active Cys in proteins. To identify Cys-Sec pairs, we analyzed, with tblastn (*11*), all Cys-containing proteins in National Center for Biotechnology Information (NCBI) databases against NCBI nucleotide sequences to identify pairs of homologous protein sequences, in which one sequence was a Cys-containing protein and the other was a candidate selenoprotein derived from a nucleotide sequence translated in all six open reading frames (ORFs) (i.e., Cys in a protein sequence aligned to TGA in a translated nucleotide sequence) (Fig. 1A). Using this procedure, we screened major nucleotide sequence databases, including completed genomes as well as environmental, whole-genome shotgun (WGS), and expressed sequence tag (EST) sequences. Independently, blastp (*11*) searches were carried out to identify Cys-containing homologs of a manually compiled set of previously identified selenoproteins. The two data sets were then combined and clustered into protein families, and a nonredundant set of Cys proteins in which each protein contained a predicted catalytic redox-active Cys was developed.

[1]Department of Biochemistry, University of Nebraska, Lincoln, NE 68588, USA. [2]Curriculum in Toxicology, University of North Carolina, Chapel Hill, NC 27599, USA. [3]Experimental Toxicology Division, National Health and Environmental Effects Research Laboratory, U.S. Environmental Protection Agency, Research Triangle Park, NC 27709, USA.

*To whom correspondence should be addressed. E-mail: vgladyshev1@unl.edu

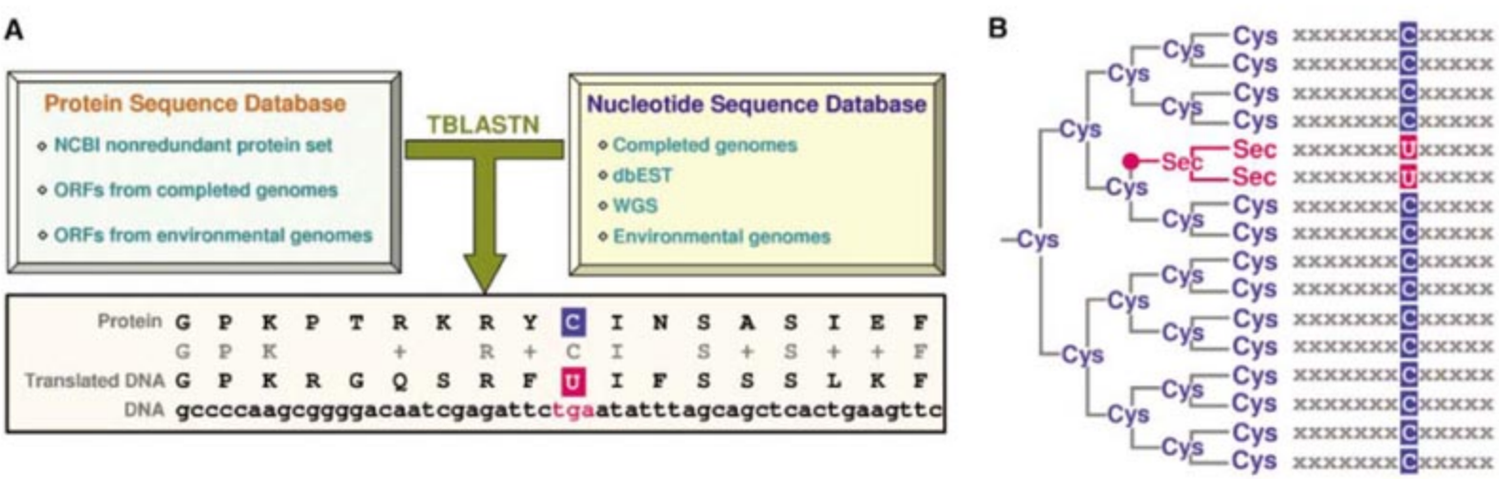

Fig. 1. High-throughout prediction of redox-active cysteine residues. (**A**) Scheme illustrating the method used for prediction of redox-active Cys residues by homology to sporadic selenoproteins [(*12*); U denotes selenocysteine]. MsrB is used as an example that illustrates the Cys-Sec pairs. (**B**) Model of evolution of proteins containing catalytic redox-active Cys. Redox-active Cys residues are conserved during evolution. In some organisms, these proteins may evolve into selenoproteins such that Sec replaces the catalytic Cys. Detection of such Cys-Sec pairs could reveal redox function for the entire protein family (or subfamily) and indicate location of the redox-active Cys.

The set of proteins containing predicted redox-active Cys had 10,412 unique sequences, which were organized into 40 protein families and superfamilies (Table 1 and table S1). Each sequence had a conserved Cys that corresponded to Sec in at least one homolog found in any of the analyzed sequence databases. The functional diversity of the identified proteins exceeded the 40 families, as some proteins with distinct functions belonged to the same family. For example, thioredoxins, protein disulfide isomerases, DsbA, DsbC, and DsbG were present in one cluster, although each of these proteins has a distinct function. The 10,412 Cys-containing sequences accounted for ~0.5% of the initial set of tested proteins and represented all completely sequenced genomes. The number of proteins found in a particular genome generally correlated with the size of the proteome, although archaea had fewer such proteins than other organisms (figs. S1 and S2).

We divided proteins represented by Cys-Sec pairs into functionally characterized proteins and proteins of unknown function. Most functionally characterized proteins detected in our search were those that used redox-active Cys in the active site for thiol-based redox catalysis, including the well-known oxidoreductases thioredoxin (fig. S3), glutaredoxin (fig. S4), peroxiredoxin (fig. S5), and glutathione peroxidase (fig. S6). Many contained a CxxC motif (two Cys separated by two residues) or motifs derived from it [e.g., CxxS in arsenate reductase (fig. S7), TxxC in peroxiredoxin, and CxxT in glutathione peroxidase] (*12*). A common property of the detected proteins was the use of a conserved nucleophilic redox-active Cys residue. During catalysis, this Cys changes redox state to a disulfide (e.g., in thioredoxin, glutaredoxin, and AhpD) or a sulfenic acid intermediate (e.g., in glutathione peroxidase, peroxiredoxin, MsrA, and MsrB). These observations suggested that the remaining Cys-containing proteins detected in the search may also be redox proteins that use redox-active Cys residues.

Conserved Cys residues are frequently used to coordinate metal ions (most often zinc, iron, and copper). However, such Cys were not present in our data set. Likewise, the data set had no proteins in which catalytic Cys residues carried out nonredox functions or were involved in posttranslational modifications or structural disulfides. Further analysis (table S1) revealed that the identified proteins represented

Table 1. Proteins identified in the searches for Cys-Sec pairs in homologous sequences. Each cell shows numbers of detected redox-active Cys–containing sequences (left) and numbers of Sec-containing sequences that support predictions of redox-active Cys residues (right). See also table S1.

Proteins	Bacterial Cys-Sec sequences	Archaeal Cys-Sec sequences	Eukaryotic Cys-Sec sequences
Functionally characterized proteins containing catalytic redox-active Cys	6222/363	257/21	1514/194
Proteins with predicted redox function and catalytic redox-active Cys	2045/256	59/9	315/360
Total	8267/619	316/30	1829/554

Fig. 2. Arsenic methyltransferases. (**A**) Amino acid sequence alignment of arsenic methyltransferases (*12*). The alignment is limited to the region that corresponds to the active site and its flanking sequences. GenBank accession numbers of sequences and organisms from which these sequences are derived are shown at the left. Predicted Sec are shaded in red, the corresponding catalytic Cys in blue, and the resolving Cys in green; conserved residues are in gray. (**B**) Domain structure of mouse AS3MT. The methyltransferase domain contains a resolving Cys, whereas the redox-active Cys-Sec is located downstream of this domain. (**C**) Activity of mouse AS3MT and its Cys^{157} → Ser and Cys^{207} → Ser mutants. AS3MT catalyzes AdoMet-dependent methylation of inorganic arsenicals (iAs) to its methylated forms. MAs, monomethylated arsenicals; DMAs, dimethylated arsenicals; TMAs, trimethylated arsenicals. (**D**) Structural model of mouse AS3MT. Cys^{207} and Cys^{157} are shown as ball-and-stick models.

essentially all known families of oxidoreductases that carry out thiol-based catalysis. For example, both protein families that reduce methionine sulfoxides (MsrA and MsrB) were detected, as were all known thiol peroxidase families. The data are consistent with the idea that the presence of Sec in a protein family, even if represented by only one or a few selenoprotein sequences, can indicate a redox function for the entire protein family and the location of redox-active Cys in proteins in this family. Several detected proteins had multiple conserved Cys. For example, thioredoxin, glutaredoxin, and AhpD contained conserved Cys in the form of CxxC motifs, whereas peroxiredoxin, MsrA, and MsrB had conserved Cys that were separated by variable distances. However, only those Cys that carried out catalytic functions (e.g., attacking nucleophiles) were identified by the Cys-Sec pairs, whereas Cys that served supporting functions (e.g., resolving Cys) were not detected. We further discuss several protein families predicted to use catalytic redox-active Cys.

A Cys-Sec pair represented by five Sec-containing sequences and numerous Cys-containing homologs revealed a redox-active Cys in *S*-adenosylmethionine (AdoMet)–dependent methyltransferases (Fig. 2A). However, only some members of this superfamily had Cys in this position. We constructed a phylogenetic tree and found that the methyltransferases containing the predicted redox-active Cys clustered and were present in both prokaryotes and eukaryotes. Thus, a protein family within a superfamily of AdoMet-dependent methyltransferases contained a catalytic redox-active Cys. Analysis of gene neighborhoods of bacterial methyltransferase genes revealed a functional link to arsenic detoxification.

In the detected methyltransferases, the predicted redox-active Cys was located in a C-terminal portion of the protein downstream of the common methyltransferase domain (Fig. 2B). In addition, these enzymes had a second conserved Cys residue. The common mammalian homolog of the detected methyltransferases is known as arsenic (+3 oxidation state) methyltransferase (AS3MT) (*13*, *14*). The production of methylated arsenicals in reactions catalyzed by AS3MT requires a reductant (*15*). Earlier studies with recombinant rat AS3MT found that the replacement of Cys^{156} with Ser led to a loss of catalytic activity (*16*). However, the Cys-Sec pair predicted that a different Cys donates the reducing equivalents to arsenic during the methylation reaction. We cloned the mouse AS3MT homolog and prepared $Cys^{157} \rightarrow$ Ser (corresponding to rat Cys^{156}) and $Cys^{207} \rightarrow$ Ser mutants. Both proteins were completely inactive, whereas the wild-type form efficiently converted inorganic arsenicals to monomethylated, dimethylated, and trimethylated forms (Fig. 2C). These data verified the function of the predicted redox-active Cys in arsenic methylation. We modeled the structure of mouse AS3MT (Fig. 2D). In the model, the active-site Cys was surface-exposed and protein topology supported the formation of an intramolecular disulfide during the catalytic cycle.

Predicted redox-active Cys were also found in other protein families, such as HesB-like (fig. S8), whose homologs participate in the biosynthesis of iron-sulfur proteins (*17*); DsrE (fig. S9), a small soluble protein first identified as part of the bacterial dsrABEFHCMK gene cluster (*18*); a subfamily of glutathione-*S*-transferases (*19*) (fig. S10); four families within the superfamily of rhodanese-like sulfurtransferases (*20*) (fig. S11); MoeB (fig. S12), which is thought to regenerate a thiocarboxylate group at the C terminus of MoaD in the molybdopterin synthase complex (*21*); heterodisulfide reductases (*22*) (fig. S13); and other proteins (figs. S14 to S19).

We examined the sequences that flank Cys-Sec pairs and found that a second Cys is often present in the vicinity of the redox-active Cys (fig. S20). In particular, a CxxC motif was abundant in the data set. Either the first or second Cys in this motif could serve as a redox-active residue. In addition, an increased frequency of glycine residues was found both upstream and downstream of the redox-active Cys. By contrast, negatively charged residues were extremely rare around the redox-active Cys and were absent in positions –3, +1, and +2 relative to the Cys. Analysis of secondary structures, either for the entire set of proteins or for non–thioredoxin-fold proteins (because thioredoxin-fold was the dominant fold in the data set), revealed a high frequency of β strands upstream and α helices downstream of the redox-active Cys. The Cys itself was most often present in loops (fig. S21). This distribution held for both thioredoxin-fold and non–thioredoxin-fold proteins.

It is remarkable that the searches for Cys-Sec pairs in homologous sequences could so selectively identify proteins with catalytic redox-active residues and filter out not only nonfunctional Cys but also conserved Cys that do not serve a catalytic redox function. Although this procedure selected only 0.5% of the initial sequences, it identified the majority of known families that use catalytic redox-active Cys. Our search strategy was not limited to organisms that contained selenoproteins. Moreover, it was sufficient to identify a single selenoprotein sequence (even if it was present as a hypothetical sequence from an unknown source, such as a metagenomics project) to predict a redox function for the entire family of proteins homologous to this selenoprotein. Arsenic methyltransferase provides a good illustration of this idea. Its Sec-containing sequences were detected in environmental soil sequences from a Minnesota farm (*23*), yet predictions of occurrence and location of redox-active Cys could be made for the entire protein family, which occurs in organisms from bacteria to mammals.

Our view on the evolution of Cys-Sec pairs is illustrated in Fig. 1B. In this model, most selenoproteins evolve from their redox-active Cys–containing homologs. To be selected during evolution, Sec must provide substantial advantages, as its use also results in disadvantages (slow Sec insertion, dependence on selenium, sensitivity to oxidation reactivity, and side reactions of Sec) (*10*). Thus, the Cys-to-Sec changes occur only in situations in which the catalytic properties of Sec are maximized, as is the case in redox proteins.

The major advantages of our method are its simplicity and strong predictive power. Redox-active Cys appears to be unique in that it could be so selectively identified, whereas other Cys (such as those involved in nonredox catalysis, structural disulfides, posttranslational modifications, and metal binding) could be filtered out. The set of predicted redox proteins described here should form the basis for further experimental verification. Increased availability of sequences, particularly from completed genomes and environmental projects, should further increase the predictive power of our method and lead to the identification of additional redox-active Cys.

References and Notes

1. M. Beeby *et al.*, *PLoS Biol.* **3**, e309 (2005).
2. D. E. Fomenko, V. N. Gladyshev, *Biochemistry* **42**, 11214 (2003).
3. J. S. Fetrow *et al.*, *Protein Sci.* **10**, 1005 (2001).
4. L. I. Leichert, U. Jakob, *PLoS Biol.* **2**, e333 (2004).
5. G. V. Kryukov *et al.*, *Science* **300**, 1439 (2003).
6. D. L. Hatfield, M. J. Berry, V. N. Gladyshev, *Selenium: Its Molecular Biology and Role in Human Health* (Springer, New York, 2006).
7. R. M. Tujebajeva *et al.*, *EMBO Rep.* **1**, 158 (2000).
8. P. R. Copeland, V. A. Stepanik, D. M. Driscoll, *Mol. Cell. Biol.* **21**, 1491 (2001).
9. S. V. Novoselov *et al.*, *EMBO J.* **21**, 3681 (2002).
10. H. Y. Kim, V. N. Gladyshev, *PLoS Biol.* **3**, e375 (2005).
11. S. F. Altschul *et al.*, *Nucleic Acids Res.* **25**, 3389 (1997).
12. Single-letter abbreviations for amino acid residues: A, Ala; C, Cys; D, Asp; E, Glu; F, Phe; G, Gly; H, His; I, Ile; K, Lys; L, Leu; M, Met; N, Asn; P, Pro; Q, Gln; R, Arg; S, Ser; T, Thr; V, Val; W, Trp; Y, Tyr.
13. B. P. Rosen, *FEBS Lett.* **529**, 86 (2002).
14. B. M. Adair *et al.*, *Environ. Chem.* **2**, 161 (2005).
15. S. B. Waters, M. Styblo, D. J. Thomas, *Chem. Res. Toxicol.* **17**, 404 (2004).
16. J. Li *et al.*, *Toxicol. Appl. Pharmacol.* **204**, 164 (2005).
17. J. R. Cupp-Vickery, J. J. Silberg, D. T. Ta, L. E. Vickery, *J. Mol. Biol.* **338**, 127 (2004).
18. C. Dahl *et al.*, *J. Bacteriol.* **187**, 1392 (2005).
19. J. D. Hayes, J. U. Flanagan, I. R. Jowsey, *Annu. Rev. Pharmacol. Toxicol.* **45**, 51 (2005).
20. D. Bordo, P. Bork, *EMBO Rep.* **3**, 741 (2002).
21. S. Leimkuhler, M. M. Wuebbens, K. V. Rajagopalan, *J. Biol. Chem.* **276**, 34695 (2001).
22. S. Madadi-Kahkesh *et al.*, *Eur. J. Biochem.* **268**, 2566 (2001).
23. S. G. Tringe *et al.*, *Science* **308**, 554 (2005).

24. Supported by NIH grants GM061603 and AG021518 (V.N.G.) and by U.S. Environmental Protection Agency–University of North Carolina Toxicology Research Program training grant T901915 (W.X.).

Supporting Online Material

www.sciencemag.org/cgi/content/full/315/5810/387/DC1
Materials and Methods
SOM Text
Figs. S1 to S21
Table S1
References

27 July 2006; accepted 4 December 2006
10.1126/science.1133114

Balanced Inhibition and Excitation Drive Spike Activity in Spinal Half-Centers

Rune W. Berg,[1] Aidas Alaburda,[2] Jørn Hounsgaard[1]*

Many limb movements are composed of alternating flexions and extensions. However, the underlying spinal network mechanisms remain poorly defined. Here, we show that the intensity of synaptic excitation and inhibition in limb motoneurons varies in phase rather than out of phase during rhythmic scratchlike network activity in the turtle. Inhibition and excitation peak with the total neuron conductance during the depolarizing waves of scratch episodes. Furthermore, spike activity is driven by depolarizing synaptic transients rather than pacemaker properties. These findings show that balanced excitation and inhibition and irregular firing are fundamental motifs in certain spinal network functions.

The prevailing half-center model for rhythm-generating motor circuits in the spinal cord proposes that excitatory interneurons in each half-center drive agonist motoneurons and interneurons, which in turn inhibit motoneurons and interneurons in the antagonist half-center (*1*–*5*). This reciprocal arrangement predicts half-center neurons to be excited and inhibited in alternation during rhythmic network activity. Temporally segregated excitation and inhibition would permit spinal motor networks to operate at low intensity of synaptic activity (fig. S1). Low conductance would facilitate the contribution of the intrinsic response properties of postsynaptic neurons to cell and network dynamics (*6*–*9*). We tested these predictions directly by intracellular recordings from motoneurons during scratchlike network activity in an isolated carapace–spinal cord preparation from adult turtles.

Stereotypical episodes of scratchlike network activity can be evoked by mechanical sensory stimulation in the isolated carapace–spinal cord preparation from adult turtles (*10*–*12*). To probe the neuronal organization of functional network activity, we first examined the origin of the periodic high-conductance state reported in motoneurons during scratch episodes (*12*). The periodic nerve activity recorded in parallel from the ipsilateral hip flexor nerve (Fig. 1A) served

[1]Department of Neuroscience and Pharmacology, Panum Institute, University of Copenhagen DK 2200 Copenhagen N, Denmark. [2]Department of Biochemistry and Biophysics, Faculty of Natural Sciences, Vilnius University, Ciurlionio 21/27, 03101 Vilnius, Lithuania.

*To whom correspondence should be addressed. E-mail: j.hounsgaard@mfi.ku.dk

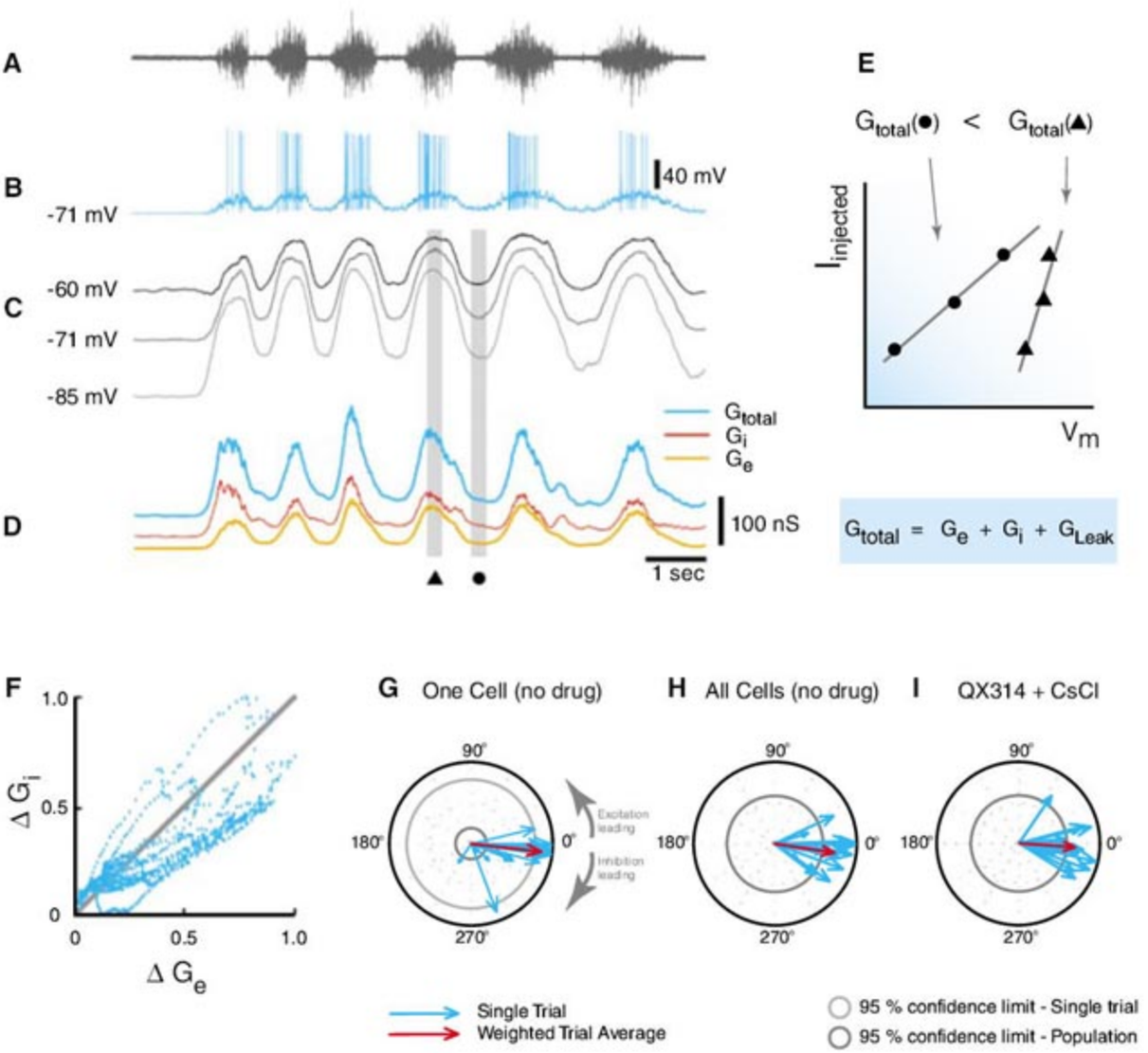

Fig. 1. Inhibition and excitation covary in motoneurons during scratching. (**A**) Hip flexor nerve activity and (**B**) intracellular recording from a motoneuron during scratch episode. (**C**) The smoothed traces of three consecutive trials at three different levels of constant holding current (from top: +1.0, 0.0, and −1.0 nA). (**D**) The mean total conductance (G_{total}) in blue was estimated from the records in (C) as the slope of the current-voltage plot at different times, as illustrated in (**E**). G_i and G_e were extracted from the equation (blue box) and from Ohm's law (*13*), as shown in (E) for the two time points marked in (D) with a circle and a triangle, respectively. (**F**) Relation between normalized increase in inhibitory and excitatory conductance (ΔG_e and ΔG_i) during scratch episodes in (D). (**G** to **I**) Population data of coherence between inhibition and excitation. Blue arrows represent single trials, and red arrows the trial average, for a single cell (G), weighted average for all cells (H), and weighted average for cells in which voltage-sensitive conductances were reduced by QX314 and Cs^+ in recording electrodes (I).

as reference for optimal temporal alignment of scratch episodes (*13*). The membrane potential V_m was recorded intracellularly from motoneurons (Fig. 1B) at different levels of holding current during successive scratch episodes (shown smoothed in Fig. 1C). With the simplifying assumptions proposed by Borg-Graham *et al.* (*14*), the average total conductance (G_{total}) and the underlying average excitatory and inhibitory conductances (G_e and G_i) were estimated from smoothened, aligned records as illustrated in Fig. 1E [see (*13*–*16*)]. In the cell illustrated and in all cells examined ($n = 16$), not only G_{total} but also G_e and G_i peaked with each depolarizing wave during scratch episodes (Fig. 1, C and D). The increases in normalized inhibitory and excitatory conductances were closely correlated ($R = 0.86$, $P << 0.05$) (Fig. 1F). Polar plots of the vectorial expression of the coherence between G_e and G_i during cyclic depolarizations clustered near a 0° phase lag for successive episodes (Fig. 1G for the cell in Fig. 1, A to D, and Fig. 1H for all 157 episodes in 16 cells). Nonsynaptic K^+ conductance recruited during depolarizing waves would contribute to the increased G_i (*16*, *17*). This was not a major factor, however, because high-conductance states and the coherence between G_e and G_i remained in 13 additional motoneurons in which spiking was eliminated and K^+ conductance was reduced by using recording electrodes containing QX314 and CsCl (Fig. 1I and fig. S2). The remaining explanation is that there is strong inhibitory synaptic activity during the depolarizing phase of the scratch.

To investigate this possibility, local inhibition was reduced pharmacologically (Fig. 2). Both amplitude and duration of the depolarizing waves increased when inhibitory synaptic input to the recorded motoneuron was reduced by addition of the glycine receptor blocker strychnine (0.1 mM) to the superfusate (Fig. 2) ($n = 5$). This shows that the depolarizing waves during scratching are limited by ongoing synaptic inhibition.

Balanced increase in excitation and inhibition perturbs the regular firing mediated by intrinsic response properties (*18*, *19*). We therefore investigated the relative role of synaptic and intrinsic conductances on the firing pattern during depolarizing waves of scratching. First, the regular firing in motoneurons, induced by a steady depolarizing current in the absence of network activity (purple in Fig. 3A), is largely determined by the intrinsic response properties. Successive action potentials (APs) are connected by the smooth voltage trajectory produced by spike after-hyperpolarizations (*20*). In contrast, firing is highly irregular during the depolarizing waves of scratch episodes (Fig. 3A, blue trace; coefficient of variation range, 0.43 to 1.2, $n = 6$), and the membrane potential undergoes rapid fluctuations between spikes (blue trace in Fig. 3A; see also Fig. 4 and fig. S3). Spike-triggered averaging revealed that APs during irregular firing are preceded by a brief depolarizing transient arising from a flat average voltage trajectory (Fig. 3B, blue; $n = 7$; see also fig. S3) in contrast to the smoothly depolarizing pacemaker potential during regular firing (purple). Thus, irregular firing is induced by depolarizing synaptic transients in the high-conductance state during network activity. A possible source of these transients is a high incidence of uncorrelated excitatory and inhibitory synaptic events (*19*, *21*). We tested the sensitivity of irregular firing during scratch episodes to successive reductions in synaptic inhibition and synaptic excitation (Fig. 3, C to E). During scratch in control conditions (Fig. 3C), irregular firing (left and middle) was revealed by the lack of correlation between the nth interspike interval (ISI) plotted against the $(n + 1)$th ISI (right) ($R < 0.2$, $n = 6$) (*22*). Reduced local inhibition (0.1 mM strychnine) rendered firing less irregular (Fig. 3D). Finally, regular firing with highly correlated ISIs was induced by a combined local reduction of inhibition and excitation (0.1 mM strychnine and 25 μM 6-cyano-7-nitroquinoxaline-2,3-dione) (Fig. 3E, bottom) [spiking during the low-amplitude depolarizing waves aided by 1.0 nA depolarizing holding current ($R = 0.56$, $p << 0.05$)]. These conditions also reduced the amplitude of the rapid synaptic fluctuations in membrane potential to a minimum. We assume that the remaining low-amplitude depolarizing waves reflect the attenuated synaptic projections from network neurons located far enough below the cut surface to be unaffected by the receptor antagonists.

Our conclusion, that motoneurons are driven by a balanced increase in excitatory and inhibitory synaptic activity, is supported by previous theoretical and experimental findings in other systems. The balanced state hampers regular firing by increasing conductance and promotes irregular firing by increasing fluctuations in membrane potential (*21*, *23*–*25*). In turtle motoneurons, regular firing driven by intrinsic response properties is severely obstructed by a conductance increase of the magnitude observed during the depolarizing waves of scratch episodes (*12*). At the same time, however, the 2- to 5-fold increase in conductance that brings the membrane potential near threshold for action potentials is associated with a parallel increase in the amplitude and frequency of voltage fluctuations and a more than 20-fold increase in integrated power spectrum in the 25- 80-Hz band (Fig. 4) (*26*). The broad spectral content associated with the rhythmic activity is fully in line with predictions for a state of intense and balanced inhibitory and excitatory synaptic activity (*16*, *19*, *21*, *24*) and orders of magnitude higher than expected for channel noise (*27*). The parallel increase in conductance and fluctuations in membrane potential during depolarizing waves, observed in all experiments analyzed ($n = 5$), is incompatible with high-conductance states mediated by a slow intrinsic conductance change.

The spinal network studied here shares several properties with the balanced state in mathematical models of large-scale random networks of inhibitory and excitatory neurons (*28*, *29*). Although the overall motor nerve activity showed little variation in successive scratch episodes, the pattern of impulse activity in individual motoneurons did (fig. S5) ($n = 10$). The raster plots of the spikes generated in a motoneuron during seven consecutive trials showed no relation between number and timing of APs during depolarizing waves within the same trial or between successive trials (Fano factor ~ 1) (see fig. S5). This suggests that the scratch network in the spinal cord produces stereotypical mo-

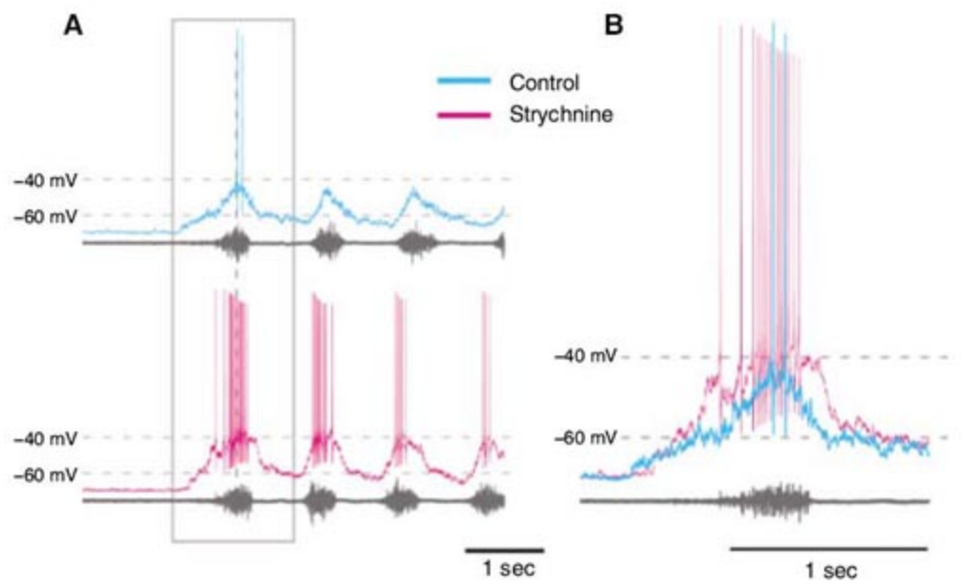

Fig. 2. Depolarizing waves enhanced by local reduction in inhibition. (**A**) Depolarizing waves in motoneuron (blue) enhanced by reduced inhibition during superfusion with strychnine (red). (**B**) Single wave highlighted.

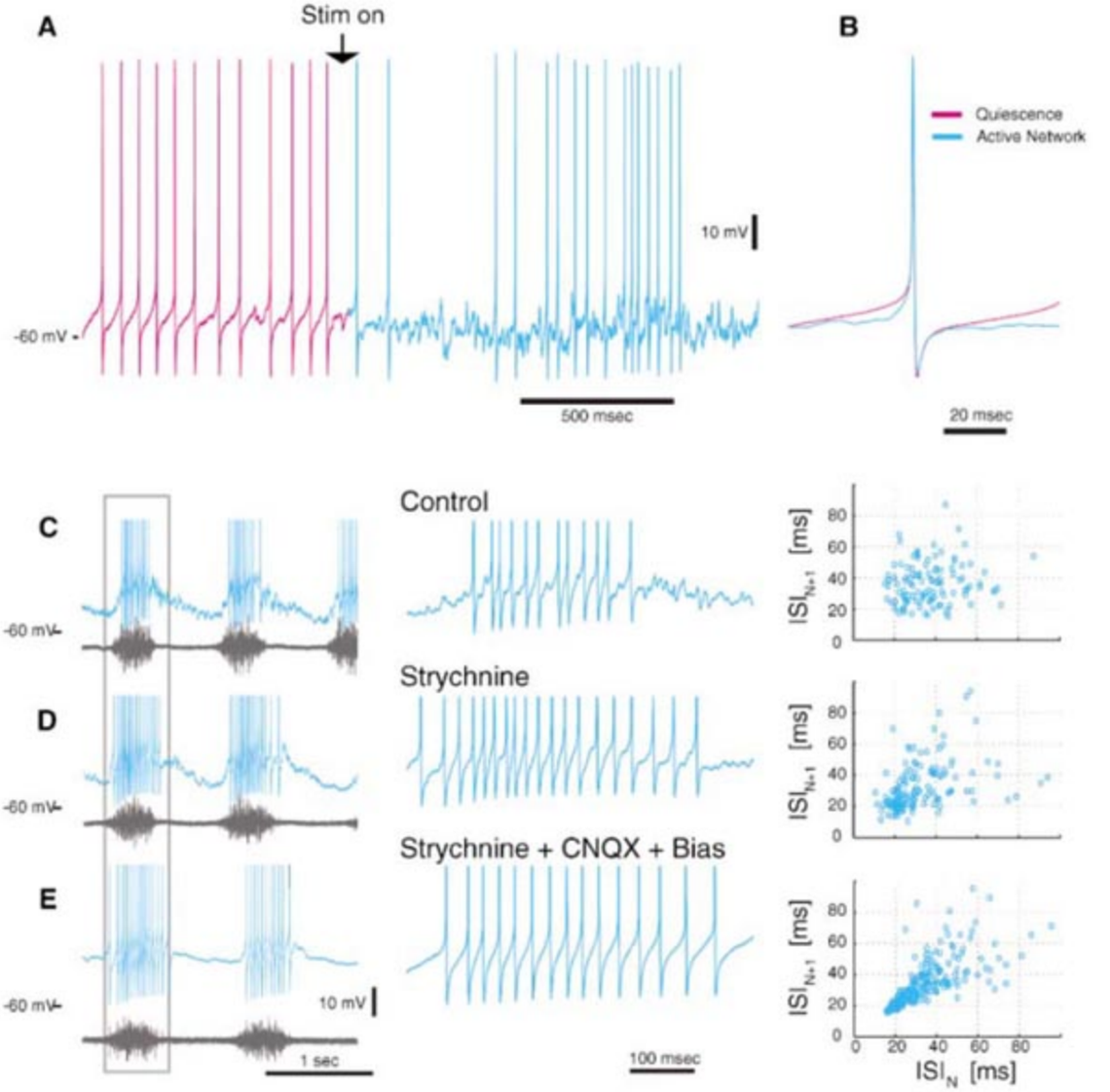

Fig. 3. Regular firing by intrinsic properties at rest, irregular firing by synaptic transients during network activity. **(A)** Regular firing in motoneuron at rest (purple) replaced by irregular firing during network activity (blue) induced at the onset of mechanical stimulus (vertical arrow). **(B)** Spikes triggered by pacemaker potential at rest and by depolarizing transient during network activity. Spike triggered averaged spikes with ~50 ms ISIs at rest (n = 50, purple) and during network activity (n = 30, blue). **(C** to **E)** Increasingly regular firing (left) and correlated ISIs (right) during scratch in control (C), reduced inhibition (D), and reduced inhibition and excitation (E). Aligned recordings from hip flexor nerve (black) and motoneuron (blue) during scratch episodes (left). Highlighted depolarizing wave (middle). Relation between successive ISIs [(n + 1)th versus nth ISI] during depolarizing waves (right).

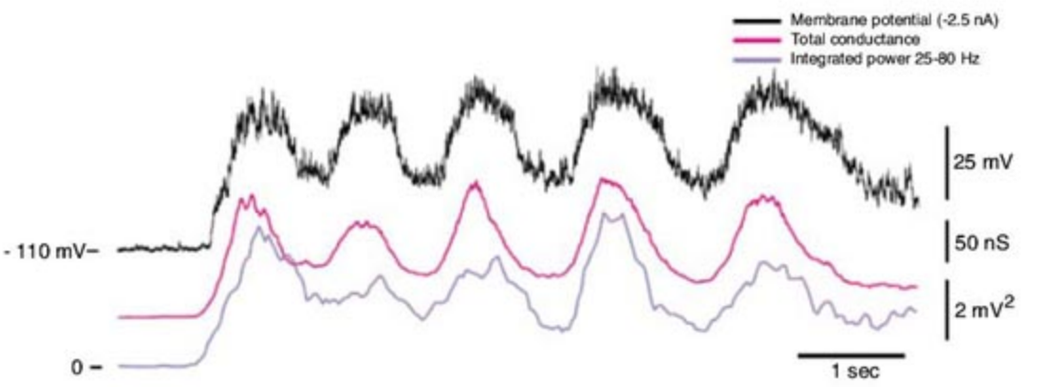

Fig. 4. The intensity of synaptic fluctuations covaries with conductance and depolarizing waves during scratching. (Upper trace) Sample intracellular recording obtained with −2.5 nA holding current. (Middle trace) G_{total} obtained as in Fig. 1C. (Lower trace) The integrated 25- to 80-Hz band power spectrum of the subthreshold membrane potential.

tor episodes in a nondeterministic way without repeating the spike patterns of individual neurons. This is in agreement with the chaotic nature of the balanced state in mathematically modeled networks in which the activity of individual neurons is stochastic and highly sensitive to initial conditions (*29*). Adopting a half-center model with balanced inhibition and excitation may help us to understand the robustness of the spinal scratch generator, its sensitivity to external input, and its ability to self organize in response to transient sensory stimuli. The high-conductance state, however, sacrifices the temporal dynamics offered by models based on weakly coupled neurons with oscillatory intrinsic properties (*6*, *7*). It remains to be seen whether high-conductance states occur throughout the scratch network or only in the motoneurons and large interneurons (*12*).

Our study suggests that balanced states of inhibitory and excitatory synaptic activity did not evolve with higher brain function (*14*, *19*, *23*, *24*, *30*) but were already present with functional motor networks in the spinal cord. The straightforward functional correlate and absence of anesthetics and other drugs makes our experimental model appealing in the search for computational advantages that balanced inhibition and excitation may provide in large-scale neural networks in general.

References and Notes

1. C. Sherrington, *The Integrative Action of the Nervous System* (Cambridge Univ. Press, Cambridge, 1947).
2. T. Graham Brown, *Proc. R. Soc. London B. Biol. Sci.* **84**, 308 (1911).

3. S. Grillner, in *Handbook of Physiology, Sect. 1: The Nervous System*, vol. 2, *Motor Control*, V. B. Brooks, Ed. (American Physiological Society, Bethesda, MD, 1981), pp. 1179–1236.
4. E. Jankowska, M. G. Jukes, S. Lund, A. Lundberg, *Nature* **206**, 198 (1965).
5. P. S. Stein, *J. Comp. Physiol. A* **191**, 213 (2005).
6. E. Marder, R. L. Calabrese, *Physiol. Rev.* **76**, 687 (1996).
7. S. Grillner, *Nat. Rev. Neurosci.* **4**, 573 (2003).
8. O. Kiehn, O. Kjaerulff, M. C. Tresch, R. M. Harris-Warrick, *Brain Res. Bull.* **53**, 649 (2000).
9. R. Delgado-Lezama, J. Hounsgaard, *Prog. Brain Res.* **123**, 57 (1999).
10. J. Keifer, P. S. Stein, *Brain Res.* **266**, 148 (1983).
11. A. Alaburda, J. Hounsgaard, *J. Neurosci.* **23**, 8625 (2003).
12. A. Alaburda, R. Russo, N. MacAulay, J. Hounsgaard, *J. Neurosci.* **25**, 6316 (2005).
13. Materials and methods are available as supporting material on *Science* Online.
14. L. J. Borg-Graham, C. Monier, Y. Fregnac, *Nature* **393**, 369 (1998).
15. J. S. Anderson, M. Carandini, D. Ferster, *J. Neurophysiol.* **84**, 909 (2000).
16. Y. Shu, A. Hasenstaub, D. A. McCormick, *Nature* **423**, 288 (2003).
17. E. A. Stern, A. E. Kincaid, C. J. Wilson, *J. Neurophysiol.* **77**, 1697 (1997).
18. W. R. Softky, C. Koch, *J. Neurosci.* **13**, 334 (1993).
19. M. N. Shadlen, W. T. Newsome, *J. Neurosci.* **18**, 3870 (1998).
20. J. Hounsgaard, O. Kiehn, I. Mintz, *J. Physiol.* **398**, 575 (1988).
21. G. L. Gerstein, B. Mandelbrot, *Biophys. J.* **4**, 41 (1964).
22. W. H. Calvin, C. F. Stevens, *J. Neurophysiol.* **31**, 574 (1968).
23. A. Destexhe, M. Rudolph, D. Pare, *Nat. Rev. Neurosci.* **4**, 739 (2003).
24. F. S. Chance, L. F. Abbott, A. D. Reyes, *Neuron* **35**, 773 (2002).
25. E. Salinas, T. J. Sejnowski, *J. Neurosci.* **20**, 6193 (2000).
26. B. Haider, A. Duque, A. R. Hasenstaub, D. A. McCormick, *J. Neurosci.* **26**, 4535 (2006).
27. K. Diba, H. A. Lester, C. Koch, *J. Neurosci.* **24**, 9723 (2004).
28. C. van Vreeswijk, H. Sompolinsky, *Neur. Comput.* **10**, 1321 (1998).
29. C. van Vreeswijk, H. Sompolinsky, *Science* **274**, 1724 (1996).
30. J. Marino *et al.*, *Nat. Neurosci.* **8**, 194 (2005).

31. This study was supported by grants from the Danish Research Council and the Lundbeck Foundation (J.H.) and a NATO Reintegration Grant (A.A.). We thank J. F. Perrier for critically reading the manuscript. Thanks to D. Kleinfeld and lab members for helpful discussions (R.B.).

Supporting Online Material

www.sciencemag.org/cgi/content/full/315/5810/390/DC1
Materials and Methods
Figs. S1 to S5
References

11 September 2006; accepted 23 November 2006
10.1126/science.1134960

Wandering Minds: The Default Network and Stimulus-Independent Thought

Malia F. Mason,[1]*§ Michael I. Norton,[2] John D. Van Horn,[1]† Daniel M. Wegner,[3] Scott T. Grafton,[1]‡ C. Neil Macrae[4]

Despite evidence pointing to a ubiquitous tendency of human minds to wander, little is known about the neural operations that support this core component of human cognition. Using both thought sampling and brain imaging, the current investigation demonstrated that mind-wandering is associated with activity in a default network of cortical regions that are active when the brain is "at rest." In addition, individuals' reports of the tendency of their minds to wander were correlated with activity in this network.

What does the mind do in the absence of external demands for thought? Is it essentially blank, springing into action only when some task requires attention? Everyday experience challenges this account of mental life. In the absence of a task that requires deliberative processing, the mind generally tends to wander, flitting from one thought to the next with fluidity and ease (*1*, *2*). Given the ubiquitous nature of this phenomenon (*3*), it has been suggested that mind-wandering constitutes a psychological baseline from which people depart when attention is required elsewhere and to which they return when tasks no longer require conscious supervision (*4*, *5*). But how does the brain spontaneously produce the images, voices, thoughts, and feelings that constitute stimulus-independent thought (SIT)?

We investigated whether the default network—brain regions that remain active during rest periods in functional imaging experiments (*6*)—is implicated in mind-wandering (*7*). The default network is minimally disrupted during passive sensory processing and attenuates when people engage in tasks with high central executive demand (*8*, *9*), which matches precisely the moments when the mind is most and least likely to wander (*2*, *4*, *5*). We thus trained individuals to become proficient on tasks (*10*) so that their minds could wander when they performed practiced versus novel task sequences (*11*). Although previous research has compared brain activity during rest to that during engagement in a task (*12*), the present investigation assesses directly both the production of SIT and activity in the default network during tasks that allow for varying degrees of mind-wandering.

Despite its regular occurrence, not all minds wander to the same degree; individuals exhibit stable differences in their propensity to produce SIT (*1*, *3*). If regions of the default network underpin the mind's wandering, then the magnitude of neural activity in these regions should track with people's proclivity to generate SIT. Specifically, individuals who report frequent mind-wandering should exhibit greater recruitment of the default network when performing tasks that are associated with a high incidence of SIT.

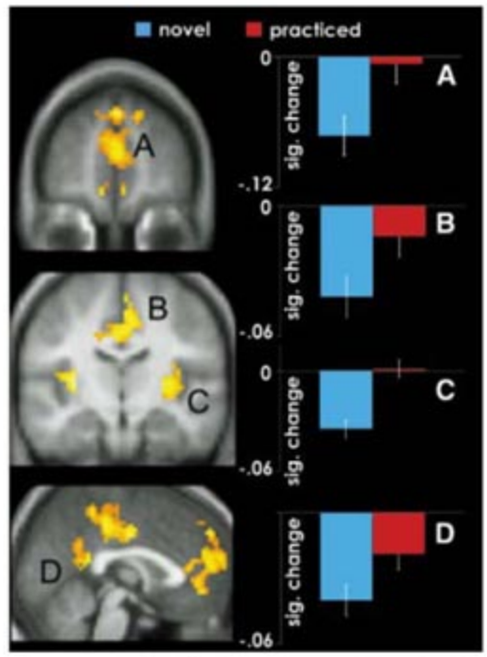

Fig. 1. Graphs depict regions of the default network exhibiting significantly greater activity during practiced blocks (red) relative to novel blocks (blue) at a threshold of $P < 0.001$, number of voxels (k) = 10. Mean activity was computed for each participant by averaging the signal in regions within 10 mm of the peak, across the duration of the entire block. Graphs depict the mean signal change across all participants. (**A**) Left (L.) mPFC (BA 9; −6, 54, 22); (**B**) Bilateral (B.) cingulate (BA 24; 0, −7, 36); (**C**) Right (R.) insula (45, −26, 4); and (**D**) L. posterior cingulate (BA 23/31; −9, −39, 27). Activity is plotted on the average high-resolution anatomical image and displayed in neurological convention (left hemisphere is depicted on the left).

[1]Department of Psychological and Brain Sciences, Dartmouth College, Hanover, NH 03755, USA. [2]Harvard Business School, Harvard University, Boston, MA 02163, USA. [3]Department of Psychology, Harvard University, Cambridge, MA 02138, USA. [4]School of Psychology, University of Aberdeen, Aberdeen AB24 2UB, Scotland.

*Present address: Martinos Center for Biomedical Imaging, MGH, Charlestown, MA 02129, USA.
†Present address: Department of Neurology, University of California, Los Angeles, CA 90095, USA.
‡Present address: Department of Psychology, University of California, Santa Barbara, CA 93106, USA.
§To whom correspondence should be addressed. E-mail: malia@nmr.mgh.harvard.edu

To investigate the relation between default network activity and mind-wandering, we first established high-incidence mind-wandering periods by training participants on blocks of verbal and visuospatial working-memory tasks (days 1 to 4), then verified that these frequent mind-wandering periods were associated with increased default network recruitment as seen with functional magnetic resonance imaging (fMRI) on day 5. Finally, we related participants' patterning of default network activity to their self-reported propensity to generate SITs (*13*).

On day 4, the proportion of sampled thoughts participants classified as SIT varied by block type (baseline, practiced, or novel), $F(2, 34) = 81.49$, $P < 0.01$. Participants reported a greater proportion of SIT during the baseline blocks (mean = 0.93; SD = 0.16) than during both practiced blocks (mean = 0.32, SD = 0.20), $t(17) = 9.22$, $P < 0.01$, and novel blocks (mean = 0.22, SD = 0.18), $t(17) = 10.96$, $P < 0.01$. Participants reported a significantly greater proportion of SIT during the practiced blocks than during the novel blocks, $t(17) = 2.11$, $P < 0.05$, despite the fact that the tasks were identical. Thus, periods of reduced central executive demand were associated with a greater incidence of mind-wandering.

On day 5, we performed functional imaging. We first functionally defined the default network by comparing the BOLD response associated with baseline (i.e., fixation) to the response associated with task periods (i.e., novel and practiced working-memory tasks). This comparison revealed significantly greater recruitment at rest in a distributed network of regions that included aspects of the posterior cingulate and the precuneus [Brodmann areas (BAs) 23 and 31], the posterior lateral cortices (BAs 40 and 39), the insular cortices, the cingulate (BA 24), and aspects of both ventral and dorsal medial prefrontal cortex (mPFC) [BAs 6, premotor and supplementary motor cortex; 8, including frontal eye field; 9, dorsolateral prefrontal cortex; and 10, frontopolar area (most rostral part of superior and middle frontal gyri)] (*8*, *9*) [table S1 (*13*)].

To determine whether a relation exists between the default network and mind-wandering, we investigated how BOLD activity within this functionally defined network changed as a function of block type, by comparing activity when participants performed practiced (i.e., high-incidence SIT periods) blocks to activity during novel (i.e., low-incidence SIT periods) blocks (*13*). Default network recruitment was greater during high-incidence SIT periods. Regions of the default network that exhibited greater activity during these periods included bilateral aspects of the mPFC (BAs 6, 8, 9, and 10); bilateral superior frontal gyri (SFG; BAs 8 and 9); the anterior cingulate (BA 10); bilateral aspects of the posterior cingulate (BAs 29 and 30) and precuneus (BAs 7 and 31); the left angular gyrus (BA 39); bilateral aspects of the insula (BA 13); the left superior temporal (BA 22), the right superior temporal (BA 41) and the left middle temporal gyri (BA 19) (Fig. 1 and table S2) (*13*). No single default network region exhibited greater activity during low-incidence SIT periods. These findings are consistent with the hypothesis that the tonic activity observed in the default network during conscious resting states is associated with mind-wandering.

If recruitment of the default network during tasks with low processing demands reflects mind-wandering (rather than some other psychological process), changes in default network BOLD activity during practiced relative to novel blocks should be related to individuals' minds propensity to wander. Voxel-wise correlations were conducted on participants' standardized score on the daydream frequency scale of the Imaginal Processes Inventory (IPI) (*14*) and their practiced relative to novel contrast images [threshold at $r(14) > 0.50$, $P < 0.05$] (table S3). Results revealed a significant positive relation between the frequency of mind-wandering and the change in BOLD signal observed when participants performed "practiced" relative to "novel" blocks in several regions, including the right SFG (BA 8; 12, 48, 36), the mPFC, bilaterally (BA 10; –6, 51, –9), bilateral aspects of the cingulate (BA 31; 7, –21, 51) and neighboring precuneus (BA 31/7; 3, –45, 37), and the left (BA 13; –36, –16, 17) and right insula (BA 13; 47, 0, 4) (Fig. 2). No region of the default network exhibited a significant negative correlation with daydream frequency scores at this threshold.

We proposed that mind-wandering constitutes a psychological baseline that emerges when the brain is otherwise unoccupied, supported by activity in a default network of cortical regions. Results demonstrated that reductions in processing demands, that is, performing practiced versus novel sequences of otherwise identical tasks, were accompanied by increases in both the generation of SIT and activity in the default network. Furthermore, the magnitude of BOLD increases that participants exhibited as they were able to generate increasing levels of SIT was positively correlated with their self-reported daydreaming propensities. Other research provides further evidence for default

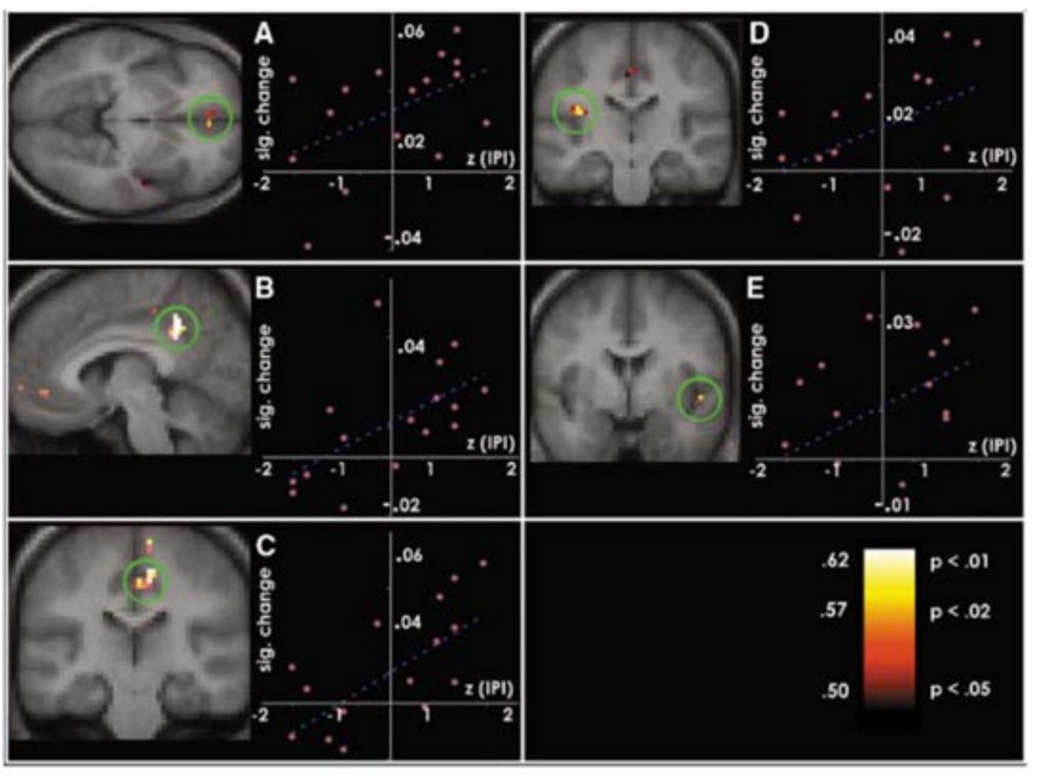

Fig. 2. Graphs depict regions that exhibited a significant positive relation, $r(14) > 0.50$, $P < 0.05$, between the frequency of mind-wandering and the change in BOLD signal observed when people performed practiced relative to novel blocks. Participants' BOLD difference scores (practiced – novel) are plotted against their standardized IPI daydreaming score. BOLD signal values for the two blocks were computed for each participant by averaging the signal in regions within 10 mm of the peak, from 4 TRs (10 s) until 10 TRs (22.5 s) after the block onset. (**A**) B. mPFC (BA 10; –6, 51, –9; $k = 25$). (**B**) B. precuneus and p. cingulate (BA 31, 7; –3, –45, 37; $k = 72$). (**C**) R. cingulate (BA 31; 7, –21, 51; $k = 73$). (**D**) L. insula (BA 13; –36, –16, 17; $k = 10$). (**E**) R. insula (BA 13; 47, 0, 4; $k = 13$). Activity is plotted on the average high-resolution anatomical image and displayed in neurological convention (left hemisphere is depicted on the left).

network involvement in the production of SIT. First, damage to parts of the network (e.g., mPFC) is associated with "mental emptiness" and an absence of spontaneous speech and thought (*15*). Second, aging is associated with the development of plaques in default network regions and a corresponding reduction in SIT (*16*, *17*). Taken together, these findings provide converging evidence for the role of the default network in mind-wandering.

Of course, mind-wandering is not the only cognitive process that ensues when tasks cease to require conscious supervision. Reductions in task difficulty are also likely accompanied by qualitative changes in attention and, perhaps, the implementation of general "housekeeping" functions (*18*). It is likely that activity in the default network is associated with a range of cognitive functions. For example, although we interpret results from our correlational analyses as evidence that cortical regions in the default network play a general role in the production of SIT, it is possible that some of these regions mediate the meta-awareness of SIT (*19*), such as the insular cortices, which subserve interoception and self-awareness (*20*, *21*), and regions of the mPFC, which are involved in self-referential mental activity (*22*, *23*). In light of behavioral evidence suggesting that people are frequently unaware that their mind is wandering (*19*, *24*), it may be the case that the daydream frequency scale (*14*) used in the current investigation assesses people's awareness of their mind's wandering rather than their propensity to engage in SIT.

The purpose of the current inquiry was to explore how and when the mind generates SIT. A more intractable question, however, is why these thoughts emerge at all. What is the functional significance of a system that wanders from its current goals (*25*)? One possibility is that SIT enables individuals to maintain an optimal level of arousal, thereby facilitating performance on mundane tasks (*4*). A second possibility is that SIT—as a kind of spontaneous mental time travel—lends a sense of coherence to one's past, present, and future experiences (*26*–*29*). Finally, the mind may generate SIT not to attain some extrinsic goal (e.g., staying alert) but simply because it evolved a general ability to divide attention and to manage concurrent mental tasks. Although the thoughts the mind produces when wandering are at times useful, such instances do not prove that the mind wanders because these thoughts are adaptive; on the contrary the mind may wander simply because it can.

References and Notes

1. J. L. Singer, *Daydreaming* (Plenum Press, New York, 1966).
2. J. S. Antrobus, J. L. Singer, S. Greenberg, *Percept. Mot. Skills* **23**, 399 (1966).
3. J. L. Singer, V. McRaven, *Int. J. Soc. Psychiatry* **8**, 272 (1962).
4. E. Klinger, *Structure and Functions of Fantasy* (Wiley, New York, 1971).
5. J. Smallwood, J. W. Schooler, *Psychol. Bull.* **132**, 946 (2006).
6. fMRI evidence suggests that, when deprived of variable sensory input, the mind recruits a discrete network of brain regions that includes the medial posterior cingulate (BAs 30 and 31); the precuneus (BA 7); paracentral lobule (BA 5); inferior parietal regions (BAs 40, 39, and 7); the angular gyri (BAs 19 and 39); the inferior frontal cortices (BAs 10, 47); superior and middle frontal gyri (BAs 8, 9, and 10); and a cluster spanning dorsal medial frontal regions (BAs 8, 9, 10, and 32) (*8*). These distributed foci have temporal coherence and constitute a tightly coupled, organized neural network.
7. P. K. McGuire, E. Paulesu, R. S. Frackowiak, C. D. Frith, *Neuroreport* **7**, 2095 (1996).
8. D. A. Gusnard, M. E. Raichle, *Nat. Rev. Neurosci.* **2**, 685 (2001).
9. K. A. McKiernan, J. N. Kaufman, J. Kucera-Thompson, J. R. Binder, *J. Cognit. Neurosci.* **15**, 394 (2003).
10. J. D. Teasdale *et al.*, *Mem. Cognit.* **23**, 551 (1995).
11. R. M. Shiffrin, W. Schneider, *Psychol. Rev.* **84**, 127 (1977).
12. K. Christoff, J. M. Ream, J. D. E. Gabrieli, *Cortex* **40**, 623 (2004).
13. Materials and methods are available as supporting material on *Science* Online.
14. J. L. Singer, J. S. Antrobus, in *The Function and Nature of Imagery*, P. Sheehan, Ed. (Academic Press, New York, 1972), pp. 175–202.
15. A. Damasio, G. Van Hoesen in *Neuropsychology of Human Emotion*, K. Heilman, P. Satz, Eds. (Guilford, New York, 1983), pp. 85–110.
16. L. M. Giambra, *Psychol. Aging* **4**, 136 (1989).
17. R. L. Buckner *et al.*, *J. Neurosci.* **25**, 7709 (2005).
18. M. E. Raichle *et al.*, *Proc. Natl. Acad. Sci. U.S.A.* **98**, 676 (2001).
19. J. W. Schooler, *Trends Cognit. Sci.* **6**, 339 (2002).
20. A. D. Craig, *Curr. Opin. Neurobiol.* **13**, 500 (2003).
21. A. R. Damasio *et al.*, *Nat. Neurosci.* **3**, 1049 (2000).
22. D. A. Gusnard *et al.*, *Proc. Natl. Acad. Sci. U.S.A.* **98**, 4259 (2001).
23. W. M. Kelley *et al.*, *J. Cognit. Neurosci.* **14**, 785 (2002).
24. J. W. Schooler, E. D. Reichle, D. V. Halpern, in *Thinking and Seeing: Visual Metacognition in Adults and Children*, D. T. Levin, Ed. (MIT Press, Cambridge, MA, 2004), pp. 203–226.
25. D. M. Wegner, in *Scientific Approaches to Consciousness*, J. Cohen, J. Schooler, Eds. (Lawrence Erlbaum, Hillsdale, NJ, 1997), pp. 295–316.
26. E. Tulving, *Can. Psychol.* **26**, 1 (1985).
27. E. A. Maguire *et al.*, *Philos. Trans. R. Soc. Lond. B Biol. Sci.* **356**, 1441 (2001).
28. R. Cabeza *et al.*, *J. Cognit. Neurosci.* **16**, 1583 (2004).
29. J. L. Vincent *et al.*, *J. Neurophysiol.* **96**, 3517 (2006).

30. This research was based on M.F.M.'s doctoral dissertation, which was completed at Dartmouth College. The authors thank H. Gordon, D. Turk, J. Smallwood, T. Heatherton, M. Bar, J. Fugelsang, and three anonymous reviewers for their advice and assistance. C.N.M. was supported by a Royal Society–Wolfson Fellowship; M.F.M. by NIH grant R01 NS050614; and D.M.W. by NIH grant MH49127.

Supporting Online Material

www.sciencemag.org/cgi/content/full/315/5810/393/DC1
Materials and Methods
SOM Text
Figs. S1 to S7
Tables S1 to S3
References

14 June 2006; accepted 1 December 2006
10.1126/science.1131295

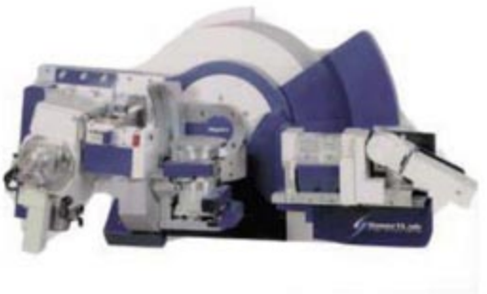

X-Ray Diffraction System

The SmartLab NANO-Extreme is an advanced automated x-ray diffraction system designed for nanomaterials research. Combining a horizontal sample mount with unique patented Cross Beam Optic technology, and equipped with proprietary software, the instrument offers nanomaterials researchers the full range of x-ray diffraction measurements in one automated instrument. The NANO-Extreme provides flexibility and performance for applications including powder diffraction for bulk nanomaterial identification, glancing incidence diffraction for the analysis of deposited structures, small angle x-ray scattering for determination of general morphology and particle size distributions in both liquids and solids, and in-plane diffraction for surface orientation and analysis of ultra-thin layers.

Rigaku For information 281-362-2300 www.Rigaku.com

Macrophage Transfection Reagent

A powerful polyethylenimine-derived transfection reagent optimized for the delivery of DNA to primary macrophages and macrophage-derived cells is available. Compatible with serum and antibiotics, jetPEI-Macrophage DNA transfection reagent is extremely easy to use and requires no media changes or washes. Protein expression is determined 24 to 72 hours post-transfection.

Polyplus-transfection For information 760-481-4918 www.polyplus-transfection.com

Glycoprotein Enrichment

The ClinProt MB-LAC LCA (lectin affinity chromatograph—lens culinaris agglutinin) glycoprotein kit is based on magnetic beads. The LCA magnetic beads complement the portfolio of ClinProt glycobeads, which are functionalized with either concanavalin A, wheat germ agglutinin, or boronic acid. The combination of optimized beads enables protein scientists to follow intelligent enrichment strategies for glycosylated peptides and proteins prior to mass spectometric analysis.

Bruker Daltonics For information 978-667-9580 www.bdal.com

Solvent Removal

The Auto-Defrost and Drain is a new option to improve the efficiency and drying effectiveness of the Genevac HT-4X, HT-8, HT-12, and HT-24 centrifugal evaporation systems. The option enables the evaporators to automatically drain the condenser of volatile solvents between stages in a method, and at the end of a method to fully defrost and drain the system with no user intervention. In this way, volatile solvents that boil off first and are collected in the condenser can be simply removed. To then remove solvents that boil at higher temperatures, evaporators with the option can quickly lower the pressures required without the traditional problem of volatile solvent boiling out of the condenser and spoiling the vacuum. The option avoids the current practice of manually draining the condenser after the volatile solvents have been removed. The option enables applications requiring the removal of mixed solvents with differing boiling points, such as lyophilization or evaporation of high-performance liquid chromatography fractions, to be carried out automatically.

Genevac For information 845-267-2211 www.genevac.co.uk

Fume Hoods

The DWS Downflow Workstations are fume hoods that provide protection for operators using hazardous substances. The workstations provide a small bench-mounted unit with unrestricted access for operations that are difficult to perform in a conventional fume hood. They feature high-quality pre-filters and carbon filters with efficiencies better than 99.6%, a unique downflow air pattern, no ducting or installation costs, a stainless steel working tray, and alarms that monitor filter, airflow, and filter lifetime.

Air Science USA For information 800-306-0656 www.air-science.com

Dynamic Light Scattering Instrument

The Model 802 Dynamic Light Scattering (DLS) instrument contains innovations to overcome the limitations of traditional light scattering instruments in terms of sensitivity and resolution. An option for the new generation system, Dual Attenuation Technology (DAT), is a unique technique that controls the level of light entering the sample as well as controlling scattered light going to the detector. This enables researchers to work at the optimum conditions for the laser and detector irrespective of sample type. The system automatically adjusts to optimum settings sample by sample, from 100% transmission for maximum sensitivity down to 0.0001% transmission for concentrated samples. Other innovations include a 544-channel correlator for improved resolution and distribution accuracy. In addition to operating at up to 90° C, the new instrument incorporates digital sensors that provide automatic environmental control as well as real-time humidity and dew point information. Model 802 DLS is designed for laboratories that need a complete understanding of how their protein, biopolymer, or nanoparticulate material behaves in solution.

Viscotek Europe For information +44 1344 467180 www.viscotek.com

Newly offered instrumentation, apparatus, and laboratory materials of interest to researchers in all disciplines in academic, industrial, and government organizations are featured in this space. Emphasis is given to purpose, chief characteristics, and availability of products and materials. Endorsement by *Science* or AAAS of any products or materials mentioned is not implied. Additional information may be obtained from the manufacturer or supplier by visiting www.science.labvelocity.com on the Web, where you can request that the information be sent to you by e-mail, fax, mail, or telephone.

POSITIONS OPEN

HUMAN MOLECULAR GENETICS FACULTY POSITIONS
Human Molecular Genetics Program
Children's Memorial Research Center (CMRC) and Northwestern University, Chicago, Illinois

The Human Molecular Genetics Program at Children's Memorial Research Center is expanding and seeks applications for new faculty positions. Research in all areas of human genetics including the regulation of gene expression will be considered. Applicants must have an interest in translational research. Candidates with quality postdoctoral experience, a strong publication record, and potential to attract nationally competitive research funds are encouraged to apply. New laboratory space, state-of-the-art equipment and generous startup packages are available. Successful applicants will be eligible for tenure-track faculty positions in the Department of Pediatrics, Feinberg Medical School, Northwestern University.

For further details of the program see **website: http://www.childrensmrc.org/human_molecular_genetics.**

Please send applications/letters of interest including full curriculum vitae, an outline of research interests, the names and contact details of three references, and PDF files of three recent publications to: **Chris Pomeroy, Program Assistant, Human Molecular Genetics Program, Children's Memorial Research Center, 2430 N. Halsted Street (211), Chicago, IL 60614-4314 U.S.A. E-mail: c-pomeroy@northwestern.edu.** Review of applications will start immediately and continue until the positions are filled.

An Equal Opportunity/Affirmative Action Employer. Women and minority candidates are strongly encouraged to apply.

ASSISTANT OR ASSOCIATE PROFESSOR INFECTIOUS DISEASES FACULTY POSITION

The Epidemiology Research Unit of the Division of Infectious Diseases, Department of Medicine, University of Pittsburgh, is recruiting research faculty with expertise in bacterial genomics or molecular pathogenesis of bacterial infections to complement existing programs in epidemiology and molecular epidemiology of drug-resistant, vaccine-preventable, foodborne, or nosocomial bacterial diseases. Experience in whole genomic sequencing and analysis desirable. Laboratory space, salary support, and startup funds are available. Candidates should have a doctoral degree (M.D. and/or Ph.D.) and at least three years of postdoctoral experience with a demonstrated record of recent research accomplishments and sufficient evidence to establish an independent, funded research program. Academic rank will be commensurate with experience. Interested candidates should send their curriculum vitae, statement of research interests, and the names of three references to: **Lee H. Harrison, M.D., University of Pittsburgh, 521 Parran Hall, 130 DeSoto Street, Pittsburgh, PA 15261; e-mail: lharriso@edc.pitt.edu.**

The University of Pittsburgh is an Affirmative Action/Equal Opportunity Employer.

GENOME SCIENCE
Vanderbilt University School of Medicine

Vanderbilt University School of Medicine has established translational and personalized medicine as institutional research priorities and seeks new faculty expert in genome sciences that can be applied to these areas. This will include investigators with a record of research accomplishment in areas such as comparative genomics, technology development, or computational genomics. New laboratory space will be available for the successful candidate to establish a research program that complements existing strengths at the School; candidates with expertise in pharmacogenomics are especially encouraged. Faculty will be appointed at the level of **ASSISTANT, ASSOCIATE,** or **FULL PROFESSOR.** Send letters of interest with curriculum vitae to: **Dan M. Roden, Assistant Vice Chancellor for Personalized Medicine, 1285B MRB4, Vanderbilt University Medical Center, Nashville, TN 37232-0575.** *Vanderbilt is an Equal Opportunity/Affirmative Action Employer.*

POSITIONS OPEN

BASIC SCIENTISTS
Duke University Eye Center
A Service of Duke University Health System

The Department of Ophthalmology, Duke University School of Medicine (DUSM), seeks applications for one or two faculty positions at **ASSOCIATE or FULL PROFESSOR** levels to join our dynamically growing group at the new Albert Eye Research Institute **(website: http://www.dukeeye.org/research/).** We are looking for mid-career investigators with an outstanding record of accomplishment in eye research and an established funding record. Within this broad scope, research areas including but not limited to the following are of special interest: ocular electrophysiology, application of modern imaging techniques to studying cell biology, and neuroprotective mechanisms in the retina ganglion cell.

Applicants should send curriculum vitae, names of four references, and a brief letter of career and programmatic interests to: **David L. Epstein, M.D., Chairman, c/o Wendy Morris, Duke University Eye Center, P.O. Box 3802, Durham, NC 27710,** or by **e-mail: morri019@mc.duke.edu.** *Duke University is an Affirmative Action, Equal Opportunity Employer.*

MEDICAL ONCOLOGIST WITH EXPERTISE IN NOVEL COMPOUNDS WITH ANTI-CANCER ACTIVITY ASSISTANT/ASSOCIATE PROFESSOR
Department of Medicine
Division of Hematology, Oncology, and Transplantation

The Division of Hematology, Oncology, and Transplantation at the University of Minnesota Medical School seeks a Physician Scientist, tenure track, with a career interest in clinical medical oncology and laboratory-based drug discovery. This individual will establish an independently funded laboratory focused on the discovery and scale up of novel compounds with anti-tumor activity. This individual will also engage in clinical outpatient and inpatient medical oncology activity including participation in phase I-II cancer clinical trials. The successful candidate will have an M.D. and will be Board-certified or eligible in internal medicine and medical oncology. He/she will also have a demonstrable track record in laboratory-based anti-cancer drug discovery. In particular, this individual should have a background in development of peptide- based small molecule therapy. Academic appointment will be at the Assistant or Associate Professor level (tenure-track/tenured), and compensation will be commensurate with experience. Applicants should submit a letter of intent, description of their research background, current curriculum vitae, and names of three individuals who will serve as professional references. Please apply online at **website: http://www.employment.umn.edu** (requisition 145672 for tenure-track Assistant Professor, or 145673 for tenured Associate Professor) and address cover letter to:

Philip McGlave, M.D.
Director of Division of Hematology, Oncology, and Transplantation
University of Minnesota Medical School
E-mail: mcgla001@umn.edu

The University of Minnesota is an Equal Opportunity Employer and Educator.

POSTDOCTORAL POSITIONS available to study antigen presentation and to develop novel immunotherapy and vaccines against tumors. Experience in gene transfer and immunology, especially dendritic cells biology, mouse models, and Adv vector is preferred. Send curriculum vitae and three references to: **Dr. Xue F. Huang (e-mail: xhuang@bcm.edu), Center for Cell and Gene Therapy, Baylor College of Medicine, Houston, TX 77030.**

Baylor College of Medicine is an Equal Opportunity/Affirmative Action/Equal Access Employer.

Positions @ NIH

THE NATIONAL INSTITUTES OF HEALTH

Health Scientist Administrator
National Institute of Dental and Craniofacial Research (NIDCR)

The National Institute of Dental and Craniofacial Research (NIDCR), National Institutes of Health (NIH), Department of Health & Human Services (DHHS) is seeking applicants for a supervisory Health Scientist Administrator position in the Center for Integrative Biology and Infectious Diseases (CIBID). The position advertised is for the Chief of the Translational Genomics Research Branch. The Branch coordinates the development and implementation of the NIDCR extramural basic and translational genomics research program related to NIDCR-relevant human and microbial genetics and genomics. To this end, areas of basic and applied research in the NIDCR mission include: infectious diseases such as dental caries and periodontal diseases, microbiology, molecular and cellular neuroscience, developmental biology, mineralized tissue and salivary gland physiology, immunology and immunotherapy, epithelial cell regulation and transformation, as well as biomaterials, biomimetics and tissue engineering, and behavior, health promotion and environment. In addition, there are cross-cutting programs involving clinical trials and comprehensive centers of discovery.

The incumbent will direct and oversee the administration of a portfolio of research projects employing translational genetics and genomics research strategies targeted to NIDCR-relevant diseases and will stimulate interest in and provide advice to the extramural community regarding the respective research portfolio. In addition, the incumbent will participate in funding decisions, policy development, as well as implementation and coordination with other programs both within and outside of the NIDCR.

The salary range for this position is $107,521 to $139,774 per annum, commensurate with qualifications and professional experience. A full benefits package is available, which includes retirement, Thrift Savings Plan participation, health, life and long-term care insurance.

Applications will be accepted through **February 15, 2007**. For qualifications required, evaluation criteria, and application instructions, view the vacancy announcements at: **http://jobsearch.usajobs.opm.gov/a9nih.asp** . Refer to announcement **# NIDCR-07-162498-DE or NIDCR-07-162738-MP.** Please contact **Elan Ey at 301-594-2320 or eye@mail.nih.gov** if you have questions.

TENURE TRACK POSITION
LABORATORY OF CELLULAR AND MOLECULAR BIOLOGY

The Laboratory of Cellular and Molecular Biology (LCMB), Center for Cancer Research, of the National Cancer Institute, National Institutes of Health (http://ccr.cancer.gov/labs/lab.asp?labid=64) has a long tradition of excellence in the investigation of signal transduction pathways involved in both normal cellular function and malignant transformation. The Laboratory now invites applications for a tenure track investigator to develop an independent basic research program in cellular and molecular biology with emphasis on understanding basic signal transduction processes. Areas of potential interest include but are not restricted to the role of signaling pathways in stem cell biology, inflammation and cancer, or malignant transformation. The applicant should hold a Ph.D, M.D., or M.D., Ph.D. degrees. Salary is commensurate with education and experience. This position is supported by the intramural Center for Cancer Research of the National Cancer Institute. A two-page statement of research interests and goals should be submitted in addition to three letters of recommendation and a curriculum vitae by March 9, 2007 to: Mrs. Erin M. Breedlove, Executive Secretary, Laboratory of Cellular and Molecular Biology, CCR, NCI, Building 37, Room 2066, Bethesda, MD 20892-4256; phone: 301-496-9683. Fax: 301-496-8479, email: breedlovee@mail.nih.gov. Candidates must be U.S. citizens or permanent residents. NIH Tenure track investigators with educational debts may be eligible for the NIH Loan Repayment Program. The NCI is an Equal Opportunity Employer.

Fellow in Translational Chemistry and Genomics

The Oncogenomics Section of the Pediatric Oncology Branch, at the Center for Cancer Research, National Cancer Institute, National Institutes of Health, has a Research Fellow position in Chemistry available immediately. The NCI in collaboration with the University of Maryland College Park, and NASA Goddard Space Flight Center, have recently launched an interdisciplinary NanoBioSensor Initiative to develop electronic sensors to detect nucleic acids, biomolecules and chemicals. The candidate should hold a Ph.D. and have experience in oligonucelotide chemistry and synthesis as well as considerable interest in molecular and cellular biology. The position involves 50% service and 50% research components. The successful applicant would be expected to interact with biologists, physicists and engineers and thus, excellent oral and written communications skills are required. Correspondence, names of references and CV should be sent to:

Dr. Javed Khan, Advanced Technology Center, National Cancer Institute, Room 134E, 8717 Grovemont Circle, Bethesda, MD 20892, Tel: 301-435-2937 or via email at khanjav@mail.nih.gov.

WWW.NIH.GOV

Tenure-Track and Tenured Investigator Positions in Systems Immunology and Infectious Disease Modeling

The National Institute of Allergy and Infectious Diseases (NIAID), Division of Intramural Research (DIR) is seeking several outstanding individuals for its new Program in Systems Immunology and Infectious Disease Modeling (PSIIM).

Modern technology allows the analysis of immune responses and host-pathogen interactions at multiple levels—from intracellular signaling networks, to individual cell behavior, to the functioning of a tissue, organ, or even whole organism. The challenge is not only to collect large amounts of data, but also to organize it in a manner that enhances our understanding of how the immune system operates or how pathogens affect their hosts. To do this, we need to develop detailed quantitative models that can be used to predict the behavior of a complex biological system. These models can help to explain the mechanisms underlying physiological and pathological responses to infection or vaccination, which can then be exploited to design better therapies or vaccines.

Achieving this goal requires an interdisciplinary effort and to this end the PSIIM will be organized as an integrated team of scientists and support staff with expertise in computational biology, bioinformatics, proteomics, cell biology, immunology, and infectious diseases, rather than as a group of independent laboratories. These teams will have access to the latest technology for gene-expression profiling, high-content screening of RNAi libraries for the discovery of pathway components, imaging tools, cores for the genetic manipulation of animals and for proteomic analysis, and a substantial computer infrastructure. BSL-3 facilities for working with high priority pathogens will also be available.

Although the PSIIM has been established within NIAID and has an immune system/infectious disease focus, we expect it to foster the growth of systems biology efforts at other NIH Institutes, primarily through the development of new software tools for complex systems modeling and methods for high-throughput screening. Thus, PSIIM team members are expected to interact extensively with other NIH scientists and with extramural groups in the U.S. and abroad who share our interest in a systems approach to biology.

The PSIIM is now recruiting for tenure-track or tenure level team leader appointments in three key areas:

Computational Biology: The incumbent will lead a group focused on the development and improvement of software tools for multiscale modeling and simulation that can be used by the PSIIM as well as by biologists interested in subjects other than immunity or infectious diseases. The ideal candidate will have a strong background in mathematics, physics, and computer programming, and a clear desire and ability to interact with and support the efforts of biologists. A demonstrated ability to generate computer software tools for biological modeling will be a strong plus.

Molecular/Cell Biology: The incumbent will lead a group involved in the design, implementation, and interpretation of screening efforts to identify and determine the interactions among the components in signaling networks that could then be modeled using the software generated by the computational biology team or obtained from other sources. Discovery tools such as gene arrays, high-content image-based screens using RNAi methods, various protein-protein hybrid screening methodologies, and optical imaging are expected to be key elements in the efforts of this group. A strong background in basic cell biology and molecular biology with experience in analysis of protein-protein interactions, signaling, and/or gene regulation is required. Expertise in large-scale screening is highly desirable.

Infectious Diseases: The incumbent will be responsible for developing novel approaches to systems-wide analysis of the interaction of infectious agents and their hosts. These may include the use of gene-expression signatures, the production of gene-modified animals, the development of methods for in vivo testing of the predictions of models, and the use of sophisticated imaging and other tools for probing the interaction of pathogens and host cells in vitro. A strong background in viral and/or bacterial infectious diseases and cell and molecular biology are necessary; training in the immunology of infectious diseases and substantial bioinformatics experience are highly desirable.

These positions and the research activities they conduct are fully funded by the intramural research program of NIH. Each team leader is expected to build a working group consisting of postdoctoral fellows, staff scientists, technicians, and students. The team leaders will work with the program director to help set the goals for the PSIIM and to determine how best to reach these goals as an integrated group. To ensure appropriate career trajectories for those joining the PSIIM team, the NIH has modified its tenure decision policies to encourage and account for contributions made in such a team science setting. Applicants should be seeking a difficult challenge in which creativity, technical expertise, and a strong desire to achieve in a team environment are critical for success.

Interested candidates may contact **Dr. Ronald Germain, Program Director, PSIIM, DIR, NIAID at 301-496-1904 or rgermain@niaid.nih.gov** for additional information about these positions.

To apply, submit your curriculum vita, bibliography, and detailed statement of how you can contribute to the success of the PSIIM program to **Felicia Braunstein at braunsteinf@niaid.nih.gov**. In addition, three letters of reference must be sent directly from the referee to **Dr. Robert Hohman, Chair, NIAID Search Committee, c/o Ms. Felicia Braunstein, DIR Committee Management Team Lead, 10 Center Drive, MSC 1356, Building 10, Room 4A31, Bethesda, Maryland 20892-1356**. Completed applications **MUST** be received by **February 16, 2007** for computational biology, and **March 16, 2007** for Molecular/Cell Biology as well as for infectious diseases. Please refer to ad **#012 for computational biology, #013 for molecular/cell biology, and #014 for infectious diseases** on all correspondence. Further information on these positions and guidance on submitting your application are available at **http://healthresearch.niaid.nih.gov**. For more information about the NIAID systems biology program, please visit **http://www.nih.gov/catalyst/2006/06.09.01/page1.html**

香 港 大 學

THE UNIVERSITY OF HONG KONG

Centenary Recruitment Plan

Founded in 1911, The University of Hong Kong is committed to the highest international standards of excellence in teaching and research, and has been at the international forefront of academic scholarship for many years. Of a number of recent indicators of the University's performance, one is its ranking at 33 among the top 200 universities in the world by the UK's Times Higher Education Supplement. The University has a comprehensive range of study programmes and research disciplines, with 20,000 undergraduate and postgraduate students from 50 countries, and a complement of 1,200 academic members of staff, many of whom are internationally renowned.

As the University approaches its 100th anniversary, a major human resource expansion plan has been launched to provide 200 new academic positions. The purpose of this **Centenary Recruitment Plan** is to enhance our research competitiveness and to facilitate the introduction and delivery of a new four-year undergraduate curriculum from 2012.

Building on Hong Kong's international status and its mission to serve China, the University offers an intellectually-stimulating and culturally-rich academic environment, with attractive remuneration packages. The University is now seeking strong candidates in the following ten faculties:

- **Architecture**
- **Arts**
- **Business and Economics**
- **Dentistry**
- **Education**
- **Engineering**
- **Law**
- **Medicine**
- **Science**
- **Social Sciences**

An artist's impression of the Centennial Campus

More details can be viewed at **https://www.hku.hk/apptunit/**. Further announcements about these positions will be made shortly. Enquiries can be addressed to the respective Faculty Dean or Department Head.

The University is an equal opportunity employer and is committed to a No-Smoking Policy

---

URBAN ENVIRONMENT FACULTY POSITION

YALE UNIVERSITY
School of Forestry & Environmental Studies

Yale University's School of Forestry and Environmental Studies (FES) seeks to fill a junior- or senior-level faculty position focused on the urban environment. We seek an individual who takes a quantitative systems approach to urban areas, particularly with a spatial geographical focus. We are particularly interested in an individual concerned with the interface between manmade and environmental systems. Research topics of interest include, but are not limited to, urban land use and land cover; urban modeling, and urban development as they relate to the environment. Interest and experience in international urban systems is desirable. The successful candidate will have an earned doctorate and an active research program that complements those of existing faculty in FES. She or he will demonstrate capacity for excellence in teaching at the graduate level, and will advise Master's and Doctoral students. Teaching might include courses that address the environmental aspects of urban land use planning, GIS modeling, transportation analysis and planning, and international urban development. We prefer a candidate with formal training in a relevant discipline such as geography, urban studies, or allied fields. Understanding of key underlying environmental sciences such as ecology or Earth science is desirable.

Applicants should send a c.v., a statement of research and teaching interests, two reprints or other professional publications, and a list of three references to: **Assistant Dean Jane Coppock, Urban Environment Search Committee, School of Forestry and Environmental Studies, Yale University, 205 Prospect St., New Haven, CT 06511, USA**. The deadline for applications is **March 2, 2007**.

Yale University is an Affirmative Action/Equal Opportunity Employer. Men and women of diverse racial/ethnic backgrounds and cultures are encouraged to apply. Women and minority candidates, as well as candidates from developing countries, are particularly urged to apply.

DIVISION OF PRIMARY ORAL HEALTH CARE
(Oral Microbiology and Biofilms)

The School of Dentistry at the University of Southern California invites applications and nominations from qualified candidates for a tenure-track or tenured position within the Division of Primary Oral Health Care, at the level of **Assistant, Associate** or **Full Professor**, in the area of oral microbiology and biofilms.

Successful applicants should have a PhD and/or DDS degree. Preference will be given to candidates who have a proven record of publication and research support in the study of oral pathogens, an interest in the structure and function of microbial biofilm communities in the oral environment, and a proven record in implementation of cutting-edge techniques to the study of oral and medical pathogenic biofilms.

Involvement with cross-discipline interactions with Medicine, Engineering, Cell science and Bioinformatics is expected. Candidates with experience working in large interactive multidisciplinary team environments are encouraged to apply.

Interested applicants should send a cover letter, complete curriculum vitae, selected recent publications, statement of current and future research plans, and at least three letters of recommendation to: **Dean Harold Slavkin, USC School of Dentistry, 925 W. 34th Street, DEN 203, Los Angeles, CA 90089-0641**.

Review of applications will begin immediately and will continue until the position is filled.

The University of Southern California values diversity and is committed to Equal Opportunity in Employment.

Research Opportunities

Virginia Bioinformatics Institute

Assistant, Associate and Full Professorships at the Virginia Bioinformatics Institute: Laboratory-Centered and Computationally-Centered

State-of-the-art facilities. The Virginia Bioinformatics Institute (VBI) at Virginia Tech has faculty openings for assistant, associate and full professorship levels. VBI is a world-class research institute in the life sciences, integrating theory, modeling, simulation and wet laboratories in a transdisciplinary, team research model. Areas of strength among the 18 research groups at VBI include infectious diseases, ranging from the molecular to the population scale, systems biology approaches to study stress response in several organisms, modeling and simulation of biological networks, functional genomics, metabolomics, proteomics and bioinformatics/computational/synthetic biology. Successful candidates at all levels are expected to have an established research program and a strong track record of substantial extramural research funding.

About VBI. Established in 2000 by the Commonwealth of Virginia, the Institute is a part of Virginia Tech (VT) and has its own 130,000 sq ft research facility with state-of-the-art core laboratory and computational facilities as well as new facilities in the Washington, D.C. area (in Alexandria, VA). VBI strongly emphasizes team science and organizes research outside of boundaries of academic disciplines. Research programs represented at VBI assemble to meet the specific needs of those programs; it is a flexible environment that rewards the notion of a problem-solving capability on the move. Extensive national and international collaborations complement the expertise of the faculty, including strong interactions with several biomedical research centers. Faculty entrepreneurial activities are strongly encouraged and the university provides support for the establishment of commercial ventures.

VBI's facility in Alexandria is an integral part of Virginia Tech's expansion into that region. Faculty members whose programs will not require proximity to their own laboratory facilities will have the option of basing their primary research efforts there while still accessing VBI's state-of-the-art wet laboratory facilities in Blacksburg. VBI strongly encourages candidates requiring wet-laboratory facilities to apply. Exceptional new faculty may also have the option of joint affiliations with other departments at Virginia Tech and two prominent medical schools on the East Coast. Reference posting 061384.

Along with a strong research environment, the Institute actively participates in "Genetics, Bioinformatics, and Computational Biology" (GBCB), an interdepartmental Ph.D. program that emphasizes both computational and experimental sciences, and which attracts outstanding students from diverse disciplinary backgrounds.

Other Research Opportunities at VBI:

- Genetical Genomics Analyst, posting 060988
- Micro- and Molecular Biologist, posting 061418
- Postdoctoral Associate: Nucleotide Metabolism Modeler, posting 061331
- Systems Administrator (multiple openings), posting 060434
- Training, Education and Outreach Program Manager, posting 061188
- Whole Genome Sequencer, posting 061332

For more Information:

To apply, visit www.jobs.vt.edu and search by posting number.
To learn more about VBI and our research, please visit us at www.vbi.vt.edu

To learn more about the Interdisciplinary PhD program in Genetics, Bioinformatics, and Computational Biology (GBCB), visit http://www.grads.vt.edu/academics/programs/gbcb/index.html

VBI
VirginiaTech
Invent the Future

FACULTY POSITIONS

PROGRAM IN DEVELOPMENTAL NEUROSCIENCE
CHILD HEALTH INSTITUTE OF NEW JERSEY

The newly established Child Health Institute of New Jersey (CHINJ) at the Robert Wood Johnson Medical School (RWJMS) is launching a major research initiative in vertebrate developmental biology to gain fundamental insights into congenital malformations and developmental disabilities. As part of this effort, CHINJ is seeking outstanding individuals with emerging or established research programs in **Developmental Neuroscience** to join a core group of investigators studying the basic principles of nervous system development. We are particularly interested in neuroscientists who use mouse models to elucidate mechanisms relevant to developmental disorders of the nervous system at the molecular, cellular, physiological, or systems level.

Qualified candidates must have a Ph.D., M.D. or equivalent graduate degree and outstanding academic credentials. We particularly encourage applications at the rank of **assistant professor**, but appointments at the **associate** and **full professor** levels will also be considered. Successful recruits will receive competitive start-up packages commensurate with prior training and experience, and will have faculty appointments at RWJMS with full access to graduate training programs and resources. Faculty in the **Program in Developmental Neuroscience** at the CHINJ will join a strong and growing community of Neuroscientists at RWJMS and Rutgers University (RU). They will also have the opportunity of interacting with colleagues at the neighboring Cancer Institute of New Jersey and soon-to-be-built Stem Cell Institute of New Jersey. Successful candidates will be expected to develop strong, externally funded research programs, and participate in collaborative projects with other Departments and Institutes at RWJMS and RU.

For more information visit our website at http://www2.umdnj.edu/chinjweb/. Interested applicants should send their CV, a brief description of their research interests (including past achievements and future plans), and arrange to have three letters of recommendation sent VIA email, addressed to: **Francesco Ramirez, Ph.D. Chair, CHINJ Search Committee, UMDNJ-RWJMS CHINJ, 89 French Street, New Brunswick, NJ 08901, neurodev@umdnj.edu. Completed applications should be received by April 15, 2007.** Appointments are expected to begin in September 2007. The University of Medicine & Dentistry of New Jersey is an equal opportunity/affirmative action employer.

UMDNJ
ROBERT WOOD JOHNSON MEDICAL SCHOOL
University of Medicine & Dentistry of New Jersey

Top 100 Hospital expanding in Central Texas

Endowed Chair in Pediatric Research
Scott & White Health System
Texas A&M System Health Science Center College of Medicine

The Children's Hospital at Scott & White and The Texas A&M System Health Science Center College of Medicine are seeking a nationally recognized research scientist as the first holder of the Josephine Ballard Endowed Chair in pediatric research. Applicants should be accomplished investigators (Ph.D., M.D. or M.D./Ph.D.) at the associate or professor level with current federal grants and a proven track record in basic, clinical, and/or translational research. The successful candidate will join an expanding faculty within a large academic healthcare system. The chair holder will play a critical role in directing and expanding research activities in pediatric disease, in close collaboration with investigators in local, national and international experts in cell biology, genomics and proteomics.

The Children's Hospital at Scott & White serves a large clinical base throughout Central Texas. There are outstanding clinical practice and laboratory facilities on campus that perform state of the art molecular and cellular biology techniques, flow cytometry, proteomics and genomics as well as biostatistical support services. Animal laboratory facilities include areas to perform medical and surgical procedures. Laboratory space and an appropriate start-up package for the chair holder will be provided. The Scott & White Healthcare system is one of the largest multi-specialty integrated delivery systems in the nation. Scott & White is the primary clinical and hospital teaching campus for the College of Medicine. Academic appointments at the associate and professor level through the College of Medicine are commensurate with qualifications and experience.

Interested candidates should send a copy of their curriculum vitae, letter addressing their qualifications and a list of 3 individuals who can provide references to: **Don P. Wilson, M.D., Chair, Search Committee for Josephine Ballard Centennial Chair in Pediatric Research; Chairman, Department of Pediatrics, 2401 South 31st Street, Temple, Texas 76508, 254-724-4363, fax 254-724-1938, email: dwilson@swmail.sw.org.**

Scott & White is an equal opportunity employer. For more information regarding Scott & White and The Texas A&M System Health Science Center College of Medicine, please log onto: www.tamu.edu and www.sw.org.

The Children's Hospital at SCOTT & WHITE

TEXAS A&M HEALTH SCIENCE CENTER COLLEGE OF MEDICINE

香港城市大學
City University of Hong Kong

The University invites applications for the following posts. Candidates with applied research achievements will receive very positive consideration. Relevant experience in business and industry will be a definite asset.

Professor/Associate Professor/Assistant Professor
Department of Physics and Materials Science *[Ref. A/484/49]*

Applications are invited from outstanding candidates for Assistant Professor and higher positions. The University endeavours to be internationally recognized as a leading university in the Asia-Pacific region. The Department of Physics and Materials Science was formed in 1993 as the first of its kind in Hong Kong, and already excels in several fields.

The Department seeks strong candidates in emerging fields that strengthen and expand its existing areas of focus. Particularly strong candidates are welcome in any field.

Requirements: A PhD in a closely related discipline with a promising research record and a strong teaching ability. The successful candidates are expected to develop new research directions and courses.

Salary and Conditions of Service
Salary offered will be highly competitive and commensurate with qualifications and experience. Appointment will be on a fixed-term gratuity-bearing contract. Fringe benefits include annual leave, medical and dental schemes, and housing benefits where applicable.

Application and Information
Information concerning the posts and the University is available at http://www.cityu.edu.hk or from the Human Resources Office, City University of Hong Kong, Tat Chee Avenue, Kowloon, Hong Kong [Fax : (852) 2788 1154 or (852) 2788 9334/email : hrojob@cityu.edu.hk]. Additional information about the Department is available at http://www.ap.cityu.edu.hk/. Please send an application letter enclosing i) a current CV with evidence of teaching ability in English; ii) a concise (up to 1 page) statement of research interests and teaching philosophy; iii) names and addresses of four referees to the Human Resources Office. **Applications will be considered until positions are filled.** Please quote the reference of the post in the application and on the envelope. The University reserves the right to consider late applications and nominations, and to fill or not to fill the positions.

JOHANN WOLFGANG GOETHE
UNIVERSITÄT
FRANKFURT AM MAIN

Johann Wolfgang Goethe University at Frankfurt

Cluster of Excellence "Macromolecular Complexes"

The newly founded Cluster of Excellence "Macromolecular Complexes" at Frankfurt University is seeking to appoint outstanding scientists in the following subject areas:

P1: Associate Professor (W2) in Mitochondrial Biology

The successful candidate should have a strong research profile in mitochondrial cell biology and/or pathobiochemistry and should be willing to collaborate with other groups within the cluster to elucidate the molecular details of the protein networks and macromolecular complexes of mitochondria. The candidate's research group will be located on the Medical Campus of Frankfurt University.

P2: Full Professor (W3) in Molecular Membrane Biology

We are looking for an outstanding individual to develop a strong research program on the structure and function of transport complexes, membrane-associated macromolecular assemblies and/or organelle biogenesis. The group will be integrated into the Department of Biochemistry, Chemistry and Pharmacy.

P3: Associate Professor (W2) in Large Synaptic Complexes

The successful candidate will develop a competitive research programme in molecular neurobiology to elucidate the temporal and spatial sequence of transient protein-protein interactions and their functional implications at the synapse. The new research group will be in the Department of Biosciences at the Biocentre on the Riedberg campus.

P4: Associate Professor (W2) in Quantitative Biology of Signalosomes

The successful candidate is expected to develop a competitive research program in the field of signalling complexes, covering quantitative aspects of macromolecular assemblies, structure and function analyses of signalosomes, post-translational modifications and/or their recognition by specific domains, with special emphasis on the integration of quantitative biology with bioinformatics or systems biology. The new research group will be located at the Biocentre or on the Medical Campus.

P5: Assistant Professor (W2) in Research on Nuclear Complexes

The successful candidate should develop a strong research programme on epigenetic processes, and should complement ongoing research on the biology and pathology of leukemias and lymphomas. We expect a strong background in molecular biology, cell biology and/or biochemistry. The new group will be integrated into the Department of Biochemistry, Chemistry and Pharmacy.

P6: Assistant Professor (W2) in X-ray Crystallography of RNA-protein Complexes

The research of the new professor should focus on RNA and RNA-protein structure determination by X-ray crystallography. Relevant postdoctoral research experience and a proven track record as a research group leader are expected. The new group will be housed in the Institute of Organic Chemistry and Chemical Biology.

P7: Associate Professor (W2) in Chemical Biology and Medicinal Chemistry

We are seeking to appoint a highly qualified junior scientist with a strong research profile in target- and diversity-oriented synthesis strategies and/or synthesis of small biomolecules and investigations into the chemical and biological mechanisms of miRNA and rRNA, TLR signalling and/or lipidomics. The research group will be at the interface of the Institutes of Organic Chemistry and Chemical Biology, and of Pharmaceutical Chemistry.

P8: Full Professor (W3) in Electron Cryo-Microscopy of Large Macromolecular Complexes

The scientific interests of the new professor should reinforce and complement ongoing research in the Cluster of Excellence into the structure and molecular mechanisms of membrane proteins, transport machineries, RNA-protein complexes, or related areas. The candidate's research group will be located in the University Physics Department, adjacent to the Max Planck Institute of Biophysics, and will have access to excellent facilities and infrastructure.

P9: Full Professor (W3) in Advanced Light Microscopy

We are seeking an outstanding individual with a strong research interest in applying advanced light microscopy to cellular neuroscience. Studies on single particle movement, organelle trafficking, assembly of macromolecular complexes, development of methods with increased resolution or in fluorescence microscopy will all be considered. The candidate's research group will be integrated into the Department of Biosciences.

P10: Assistant Professor (W2) in Mass Spectrometry

We seek to establish a junior research group headed by an Assistant Professor devoted to the analysis of multiprotein complexes by mass spectrometry and proteomics. The group will be housed by the Institute of Pharmaceutical Chemistry at the Biocentre and will have full access to its instrumentation.

P11: Associate Professor (W2) in Single Molecule Spectroscopy

The successful candidate will have a strong track record in single molecule spectroscopy, and should have an interest in developing new methods and applying them to macromolecular systems in biology. The research group will be in the Institute of Physical Chemistry.

P12: Associate Professor (W2) in Developmental Biology

We are looking for an outstanding junior scientist with a research focus in developmental genetics and cell biology of higher eukaryotic model organisms. The research efforts should complement the eukaryotic model systems (S. cerevisiae, C. elegans and mouse) that are already established in the Cluster and target the functional analysis of macromolecular complexes. The group will be integrated into the Department of Biosciences.

* * *

The Cluster of Excellence comprises leading research groups in the Departments of Biosciences, Biochemistry, Chemistry and Pharmacy, Physics, the Max Planck Institute of Biophysics and the Frankfurt Institute of Advanced Studies (FIAS) on the new Riedberg Science Campus, and the Department of Medicine, the Max Planck Institute of Brain Research and the Georg Speyer Haus on the Niederrad Medical Campus of Frankfurt University. Excellent, state-of-the-art core facilities, including imaging, proteomics, genomics, and bioinformatics will be available to all groups in the Cluster.

Start-up funds as well as substantial resources for personnel and running costs are available to all new groups from the Cluster and from Frankfurt University. Participation in new or existing DFG-funded Collaborative Research Centres (SFBs) in Frankfurt is expected. Successful candidates will be required to teach at both Bachelor's and Master's degree level.

The designated salary for the position is W2 (tenure track; initially for 5 years) or W3 (tenured) on the German university scale. For details, see http://www.uni-frankfurt.de/aktuelles/ausschreibung/ professuren/nichtfb.html. The Goethe University Frankfurt is committed to equal opportunity in science and a lively campus community.

Applications including a curriculum vitae, pdf.files of 5 key publications, statements of research achievements (one page) and future plans (3 pages), and the names and addresses of 5 academic referees should be sent via Email by **February 10, 2007** to:

Director, Cluster of Excellence Macromolecular Complexes
Goethe University Frankfurt
E-mail office@biochem2.de

Hier wird Wissen Wirklichkeit

www.uni-frankfurt.de

Morgridge Institute for Research

Executive Director
The Morgridge Institute for Research
At the University of Wisconsin-Madison

The Morgridge Institute for Research at the University of Wisconsin seeks nominations and applications for the position of Executive Director. The Morgridge Institute for Research (MIR) is a new private, not-for-profit research institute whose core mission is to bring together scientists from a range of disciplines to advance the study of human biology and biomedical science. The work will be conducted in collaboration with various centers on campus, as well as with industry partners and others to translate new knowledge and discoveries into real-world applications. The Morgridge Institute for Research seeks an outstanding scientist and accomplished research leader to assume the position of Executive Director; he/she will play a significant role in crystallizing the vision and strategy for the Institute.

The Executive Director will be the Chief Executive Officer, with overall responsibility for the scientific and financial success of the institute. He/she will create an organization that has the agility, character and staff to ensure the Institute has an organizational structure and culture that will foster successful interdisciplinary work. The Executive Director also has responsibility for guiding the institutional advancement program to build the MIR endowment and, where appropriate, fund ongoing research and operations. Technology transfer activities, government grants, private philanthropy, and the establishment of alliances and partnerships with venture firms and pharmaceutical companies will be part of the institutional advancement initiatives.

The successful candidate for this position will have an established record of achievement in building and leading scientific enterprises in the public and/or private sector. He/she must be a high-energy leader with finely tuned political, team building and organizational developmental skills, and must be eager to mentor the next generation of scientists.

The Executive Director will have an advanced degree in biology, medicine, engineering, genetics, bioinformatics or related scientific field. He/she will have engaged in scientific work with a priority on interdisciplinary collaboration. Credibility in the scientific and academic community to establish MIR as a highly sought-after scholarly opportunity will also be important. The successful candidate will also have a commitment to education as well as research; evidence of success in establishing collaborations with industry; a deep appreciation of and respect for academic values and culture, and an understanding of the critical role that basic and translational research serves in sustaining and broadening the intellectual rigor of an elite research university.

Nominations and applications should be sent to: **Nicholas Brill, Brill Neumann Associates, Inc., 312 Stuart Street, Boston, MA 02116; morgridge@brillneumann.com.**

The Morgridge Institute for Research is an Equal Opportunity Employer.

Woods Hole Oceanographic Institution

Marine Microbial Biogeochemistry

Assistant/Associate Scientists

The Departments of Biology and Marine Chemistry & Geochemistry with the Woods Hole Oceanographic Institution invite applications for one or more tenure-track positions at the Assistant or Associate Scientist level in the area of marine microbial biogeochemistry, physiology, or genomics. We seek investigators using biogeochemical or molecular biological techniques (e.g. isotopic tracers, molecular probes, whole genome analyses, microarrays or proteomics) to investigate biogeochemical transformations, elemental cycles, physiology, ecology, and the forces acting on the selection of marine prokaryotes (Bacteria and Archaea). Areas of interest include, but are not limited to, planktonic phototrophs and heterotrophs, vent/seep and deep biosphere microbes.

The successful applicants are expected to have a strong interest in collaborative research, seek funding to establish a productive research program, hold a Ph.D. and contribute to graduate teaching in the MIT/WHOI Joint Program in Biological or Chemical Oceanography.

For a full job description log on to **http://jobs.whoi.edu** and follow the steps to apply. Candidate should submit a current CV, Research Statement, and names of potential references along with their on line application.

To be considered, complete application materials should be received by February 2007.

Women and Minorities are encouraged to apply.
M/F/D/V/EOE

Chair - Department of Molecular Biology and Microbiology

TUFTS UNIVERSITY SCHOOL OF MEDICINE

Tufts University School of Medicine invites applications for Professor and Chair of the Department of Molecular Biology and Microbiology. The candidate should have a Ph.D. or an M.D. and be an internationally recognized scientist in microbiology with an outstanding and well-funded research program. The candidate should also have a track record of institutional service and participation in the mentorship of junior faculty.

Tufts University School of Medicine has a distinguished record of training some of the leading physicians and scientists in the U.S. The Department of Molecular Biology and Microbiology has a particularly outstanding and distinguished history of excellence in research and training. The faculty is well funded by both federal and private sources of support, including Gates Foundation awards as well as Howard Hughes Medical Institute Investigatorships. The Department occupies the 4th floor of the recently built Jaharis Family Center for Biomedical and Nutrition Research as well as adjoining buildings of the M&V Research Complex. A notable strength of the Department is the atmosphere of cooperation and collegiality that prevails at all levels. A variety of available core facilities in the Medical School serve to greatly enhance the research environment. The Molecular Microbiology Graduate Program based in the Department is vigorous and is funded by two training grants. This Chair position provides an exciting opportunity to lead and further build an already distinguished department.

Please send a curriculum vitae, statement of research funding, and the names of at least three references by March 9, 2007 to:

Henry H. Wortis M.D., Chair, Molecular Biology and Microbiology Search Committee c/o Mary Broderick, Medical Deans Office, Sackler 8, Tufts University School of Medicine, 136 Harrison Avenue, Boston, MA 02111

Tufts University School of Medicine is an AA/EO employer and actively seeks candidates from diverse backgrounds.

Tufts UNIVERSITY

FACULTY POSITION
Reproductive Biology & Development
BAKER INSTITUTE FOR ANIMAL HEALTH

Located in Ithaca, N.Y., Cornell University is a bold, innovative, inclusive and dynamic teaching and research university where staff, faculty, and students alike are challenged to make an enduring contribution to the betterment of humanity.

The Baker Institute for Animal Health at Cornell University seeks outstanding candidates for a tenure-track faculty position. Preferred candidates must have a Ph.D. and/or D.V.M. or equivalent, and will use cutting-edge experimental approaches to investigate important questions in reproductive biology and development. The Institute has a distinguished record of discovery in areas benefiting both companion animal and human health. It supports an interdisciplinary research environment with studies in rodent, small animal, and large animal systems, ranging from immunology and infectious diseases to the inheritance of complex traits. In this search, priority will be given to scientists who complement or strengthen current Institute research, with particular interest in candidates with active programs in germ cell / stem cell biology, fetal / placental development, epigenetics, or genomics. The recruited faculty will join an appropriate department in the College of Veterinary Medicine and will have opportunities to participate in the University's campus-wide Life Sciences Initiative and the Center for Vertebrate Genomics.

Successful candidates will be expected to have, or to develop, extramurally funded research programs and to contribute to professional (DVM) and graduate education. The Institute offers competitive start-up packages and new laboratory facilities in a supportive, interactive research environment. The position is offered at the Assistant Professor level, with revision appropriate to the successful applicant's qualifications.

For more information, go to: **http://bakerinstitute.vet.cornell.edu/**. Applicants should submit a cover letter, curriculum vitae, statement of research plans, and contact information for three references together in a single PDF file to: **bakersearch@cornell.edu.**

Review of applications will begin on February 15, 2007 and will continue until the position is filled.

Cornell University

Cornell University is an Affirmative Action, Equal Opportunity Employer and Educator.

http://chronicle.com/jobs/profiles/2377.htm

The European Commission

The European Commission, Directorate General Joint Research Centre (JRC), is seeking to recruit (m/f):

DIRECTOR

INSTITUTE FOR PROTECTION AND SECURITY OF THE CITIZEN IN ISPRA (JRC.G - IPSC) (COM/2007/10039)

DIRECTOR

INSTITUTE FOR ENERGY IN PETTEN (JRC.F - IE) (COM/2007/10040)

Official Journal n° C 7 A – 12 January 2007

We are the Joint Research Centre. Our mission is to provide customer-driven scientific and technical support for the conception, development, implementation and monitoring of EU policies. JRC comprises 7 research institutes spread across 5 sites in Europe. We have a staff of 2,650 and an operating budget of € 300M per annum. Our core competence areas are food, chemical products and health, environment and sustainability, nuclear safety and security, and horizontal activities such as reference materials and measurements, techno-economic foresight, public security and anti-fraud.

We propose:

- **A post of Director of the Institute for the Protection and Security of the Citizen (JRC.G - IPSC - ISPRA) (COM/2007/10039)**

The mission of the Institute is to provide research-based, systems-oriented support to EU policies so as to protect the citizens against economic and technological risks. It has some 430 staff and a budget of ca. € 45M. The Director will in addition be expected to provide strategic orientation for and coordination of activities across the whole of the JRC related to internal/external security, anti-fraud and development aid research and services.

- **A post of Director of the Institute for Energy (JRC.F - IE - PETTEN) (COM/2007/10040)**

The Institute provides scientific and technical support to community policies related to energy. It has a staff of about 200 and a yearly budget of ca. € 30 M. The Director will in addition be expected to provide strategic orientation for and coordination of energy-related research and services across the whole of the JRC.

The Directors are responsible for the overall management of their Institute and have delegated financial and recruitment responsibilities for the complete budget and staff of their Institute. They are members of the JRC senior management team and contribute to the overall development and implementation of the JRC mission.

Applicants must: • be a national of one of the European Union Member States; • hold a university degree that gives access to undertake doctoral studies; • have at least 15 years' postgraduate professional experience at a level to which the qualifications referred to above given admission; at least 5 years of that professional experience must have been gained at senior management level; • have a thorough knowledge of one of the EU official languages and an adequate knowledge of another of these languages. Candidates should note that the selection procedures will be carried out in English, French and German only.

The Directors will be selected and appointed by the Commission according to its selection and recruitment procedures. Salaries and conditions of employment are those laid down in the Staff Regulations for AD 14 grade officials of the European Communities. The Commission applies an equal opportunities policy. Full job description, selection criteria and application details can be found at ***http://ec.europa.eu/dgs/personnel_administration/working_senior_mgt_en.htm****.*
The link to the on-line application is: ***http://ec.europa.eu/dgs/personnel_administration/seniormanagementvacancies/index_en.html****.*
If you encounter technical problems, please send an e-mail to:
ADMIN-MANAGEMENT-ONLINE@ec.europa.eu.

The closing date for registration is 12 February 2007*.*
On-line registration will not be possible after 12.00 noon Brussels time.

Smithsonian

Dean of Academic Programs

The Smithsonian Tropical Research Institute (STRI) invites applications for a new position, Dean of Academic Programs. STRI, a bureau of the Smithsonian Institution, and a world leader in tropical research, maintains a series of research facilities to support marine and terrestrial research in the Republic of Panama. Each year our scientists, superb field and laboratory facilities, and the unique geography of the Isthmus of Panama attract hundreds of students and fellows at the undergraduate, pre- and post-doctoral levels from more than 40 nations. Fellows are supported by a combination of STRI, university, national and international fellowships. STRI also maintains formal arrangements with universities in the US and Canada that use STRI facilities to present semesters abroad, as well as a university-based graduate program offering advanced degrees in tropical science.

STRI's Dean of Academic Programs will provide leadership, oversight and evaluation of academic programs, as well as develop new initiatives and strategic alliances that provide off campus educational opportunities at STRI. The position will be based at the Institute's headquarters in the Republic of Panama.

The successful applicant will likely have the following qualifications: a Ph.D. degree, a research background in an area of STRI expertise (see **www.stri.org**), experience in administration at the college or university level, and demonstrated ability to work in an international context.

Applications should be submitted electronically to the **Director of STRI, c/o Ms. Luz Latorraca, Office of Human Resources**, at: **latorral@si.edu**. Please include a complete curriculum vitae with a summary of research, teaching and administrative experience, a statement of interest in the present position, and the names and contact information of three potential references. We will accept applications until the position is filled, and review of applications will begin in **March 2007**.

STRI is an Equal Opportunity Employer and appointments can be made regardless of nationality.

Uniformed Services University of the Health Sciences

Chair of Department of Pharmacology

The Uniformed Services University seeks applications for the position of Chair of the Department of Pharmacology, a tenured position within the F. Edward Herbert School of Medicine in Bethesda, Maryland. Candidates, who must be U.S. citizens or permanent residents, should have an outstanding record of accomplishments, including an internationally recognized research program in pharmacology or a related discipline, and leadership skills to oversee the research programs and faculty in the department and to direct the pharmacology teaching in the School of Medicine. Current department strengths include neuropharmacology and molecular mechanisms of signal transduction. Salary and benefits will be based on Federal pay ranges for senior scientists. Further information on the position may be obtained from the Search Committee; the department web site can be found at **http://www.usuhs.mil/pha**. Nominations of qualified persons are welcomed.

REQUIREMENTS: Selected candidates will be subject to a favorable security background investigation for employment.

Applications should be sent to:

David S. Krantz, Ph.D.
Chair, Pharmacology Search Committee
Department of Medical and Clinical Psychology
Uniformed Services University of the Health Sciences
4301 Jones Bridge Road
Bethesda MD 20814-4799
dskrantz@usuhs.mil

The University is an Equal Opportunity Employer committed to excellence through diversity.

UTMB

The University of Texas Medical Branch

Breast Cancer Research Faculty Position

A tenure-track faculty position is currently available at the assistant professor level in the research area of molecular and cellular biology of breast cancer at the Sealy Center for Cancer Cell Biology and Center for Interdisciplinary Research in Women's Health at UTMB. Preference will be given to candidates interested in working in a highly collaborative, interdisciplinary environment with interests in breast cancer etiology, progression or treatment. We are particularly interested in recruiting candidates with scientific backgrounds in inflammatory mechanisms of cancer, stromal interactions with cancers, novel animal models of cancer, or discovery of novel chemotherapeutic agents.

The recruited candidate will be provided with a generous start-up package, competitive compensation and benefits, modern laboratory space within the center, and access to state-of-the-art core facilities. The faculty member will be expected to establish and maintain independent, externally funded research programs. Diversity is one of UTMB's core values, and we look for diversity in our applicant pools, including ethnic, cultural, gender and research interests. Applicants should have at least two years, but no more than five years, of post-doctoral or equivalent experience and a strong publication record. Please send an electronic curriculum vitae, statement of research interests and goals, and the names of three references to:

Abbey B. Berenson, M.D.
Route 0587
The University of Texas Medical Branch
Galveston, Texas
or email: **abberens@utmb.edu**

UTMB is an Equal Opportunity Affirmative Action Institution that proudly values diversity. Candidates of all backgrounds are encouraged to apply.

JAIST
JAPAN ADVANCED INSTITUTE OF SCIENCE AND TECHNOLOGY
1990

JAPAN ADVANCED INSTITUTE OF SCIENCE AND TECHNOLOGY (JAIST)

Invites applications for a professorship (or associate professorship depending on experience) for training in English Technical Communication. This position is not for research. The appointment starts after April 1, 2007.

JAIST is a national graduate university that has Schools of Knowledge Science, Information Science, and Materials Science. Before graduation the students are required to have abilities to read, write, and orally present technical papers in English. JAIST is located near the city of Kanazawa, which is known as "Little kyoto," rich with traditional Japanese art and culture.

- **Area of specialty:** Education in English Technical Communication
- **Job description:** Teaching of technical English classes; Tutoring in technical paper writing; Correcting scientific papers; Planning of curriculum for English Technical Communication
- **Qualifications:** A successful candidate should have a Ph. D. or M. S. in Science or Engineering, and should have demonstrated ability to write technical papers. We are looking for teachers with enthusiasm for training graduate students.
- **The applicant should submit the following information:** Resume, Publication list, Summary of previous experience in education and research (up to 1000 words), Future plans as an educator (up to 1000 words), Names of three professional references including e-mail addresses
- **Deadline:** Application must be received by March 20, 2007.

Please send your application to: **Prof. Takuya Honda, JAIST, 1-1 Asahidai, Nomi, Ishikawa, 923-1292, JAPAN; Tel:+81-761-51-1750; Fax: +81-761-51-1149; t-honda@jaist.ac.jp**. For inquiries contact **Ms. Michi Kashida** at **+81-761-51-1937; michi-k@jaist.ac.jp**. Institute website is at **http://www.jaist.ac.jp/index-e.html**.

VICE PRESIDENT FOR RESEARCH
University of North Texas

Founded in 1890, the University of North Texas at Denton is the largest and most comprehensive student-centered public research university in the Dallas/Fort Worth metroplex. As the state's fourth largest university and one of the fastest growing in the country, UNT services more than 33,500 students offering 93 bachelor, 111 master and 50 doctoral degrees.

DUTIES AND RESPONSIBILITIES: The Vice President for Research reports directly to the University President. This position provides leadership for the development and implementation of a campus-wide strategic and operational plan for research, sponsored projects and activities across all academic disciplines for the purpose of securing increased levels of external support from federal, state, and private sources; oversees all policies, procedures and support services dedicated to research and technology transfer and all research regulatory requirements; works closely with researchers to develop research and sponsored program activity in support of UNT's research mission; is responsible for promoting interdisciplinary and inter-institutional collaboration and enhancing relationships with sponsoring agencies; and represents UNT's research, scholarship, and creative activity with appropriate state and federal offices.

This position also carries the management and continued development responsibilities of the recently acquired 550,000 sq. ft., 200 acre Research Park which houses the College of Engineering and the newly created interdisciplinary Center for Advanced Research and Technology (CART).

QUALIFICATIONS: Qualified candidates should possess the following:

- Earned doctorate or terminal degree
- An extensive research record within an academic or related setting
- Service on state and federal review committees, advisory boards, or policy and planning committees
- Proven record of increasing institutional research funding
- A demonstrated record of effective leadership in research administration with increasingly responsible positions in higher education, corporate or non-profit organizational environments
- Working knowledge of major functional areas, especially federal funding agencies, technology transfer, intellectual property issues, and compliance
- Understanding of national trends affecting academic research and the ability to develop a strategic research plan for elevating the national and international research prominence of UNT
- Successful experience in policy and procedural development in all facets of research and research administration.
- An understanding of higher education and the academic environment, both at the undergraduate and graduate levels with experience in the establishment and development of comprehensive training programs supporting research
- A demonstrated commitment to diversity and the ability to work with diverse constituencies
- Proven interpersonal skills to interact and lead people at all levels of the organization
- Excellent written and oral communication skills

APPLICATION AND NOMINATION PROCEDURE: Interested applicants should submit a resume; a letter of application that highlights qualifications for the position and management philosophy of a research enterprise; and the names, addresses, telephone numbers and e-mail addresses of five professional references. Review of applications will begin **January 16, 2007**, and will continue until the position is filled. Nominations and applications should be directed to:

Valerie Green
University of North Texas
PO Box 311010
Denton, TX 76203

https://jobs.unt.edu

References will be contacted only after permission from the applicant is obtained. For information on UNT, please consult the web site at **www.unt.edu**.

The University of North Texas is an ADA/Affirmative Action/ Equal Opportunity Employer.

Fulfill your hunger to improve life

The Applied Biosystems postdoctoral fellowship program offers candidates the chance to gain skills that would be difficult to acquire in other environments while at the same time encouraging them to present their work at open scientific meetings and publish in peer-reviewed journals. Competitive salary and benefits will be offered.

Genetic Analysis, Molecular and Cell Biology, Foster City, CA

Contribute to a research program involving novel applications of next generation, ultra-high-throughput, sequencing technologies. The list of potential topics includes analyses of the utility of ultra-high-throughput sequencing in whole-genome resequencing, digital gene expression, digital karyotyping, rare biomarker detection, *de novo* assembly and whole-genome methylation analysis.

Qualifications Required

Ph.D. in computational biology, statistics, computer science, genetics, or a related field. The candidate should have experience with developing novel bioinformatics algorithms, preferably in the areas of sequence alignment and assembly and/or pattern classification, and experience with statistical modeling and simulation.

Protein Engineering, Advanced Research and Technology, Foster City, CA

Work on novel technologies to engineer protein-based fluorescent biosensors. Projects will focus on protein molecular evolution and design, library construction, high-throughput screening, as well as biochemical characterization of fluorescent biosensors.

Qualifications Required

The successful candidate will have a Ph.D. degree with backgrounds in molecular biology, protein design and directed evolution. Experience with protein purification and characterization and real-time PCR is desirable.

Research and Development, Protein and Small Molecules, Framingham, MA

Design, synthesize and develop chemistries targeted towards metabolite classes for high-throughput metabolite profiling and quantization using mass spectrometry.

Qualifications Required

Ph.D. in organic or bio-organic chemistry with extensive knowledge of chemical transformations and bioconjugation. Knowledge of mass spectrometry with a biology background is highly desirable.

For more information about these opportunities, please visit our website at **www.appliedbiosystems.com**.
If interested, send your resume in confidence to **barrink1@appliedbiosystems.com** with Postdoc Genetic Analysis, Protein Engineering or Protein and Small Molecule in the subject heading.

Our diverse life science contributions are a proud reflection of the diversity of our workforce.

25 YEARS ADVANCING SCIENCE

Applied Biosystems

Department of Biochemistry and Molecular Biology Tenure Track Faculty Positions

The Department of Biochemistry and Molecular Biology at the University of Maryland School of Medicine, chaired by **Richard L. Eckert, Ph.D.**, is initiating a major expansion (**http://medschool.umaryland.edu/biochemistry/**). Highly qualified individuals will be considered at the **Assistant, Associate** and **Full Professor** levels. The department has significant strengths in muscle biology, cell signaling, cancer biology, structural biology and imaging, and a highly successful graduate training program. The initial expansion will include positions in surface epithelial biology with a focus on investigators utilizing biochemical, cellular and animal model approaches to understand protein and cell function in normal, diseased and cancerous tissue. Successful candidates are expected to establish and maintain active research programs, and participate in department teaching and service opportunities. The Medical School and the Department are highly ranked with respect to NIH funding. The Department provides excellent laboratory facilities, competitive salaries and startup packages, and access to numerous core facilities. Applicants should hold a Ph.D. or M.D., have substantial research experience, and a strong desire to participate in an interactive, multidisciplinary research environment.

Interested applicants are invited to submit a letter of interest and curriculum vitae by e-mail and have three letters of reference sent by e-mail to **biochem@umaryland.edu**. Mail applications can be sent to: **Biochemistry Search Committee, Department of Biochemistry, University of Maryland, School of Medicine, 108 N. Greene Street, Baltimore, MD 21201**.

The University of Maryland, Baltimore is an Equal Opportunity, Affirmative Action Employer.

Cleveland State University

- ***Temporary Post-Doctoral Fellow (BGES)***

A temporary Post-doctoral Fellow position is available immediately in the Biological, Geological & Environmental Sciences Department at Cleveland State University to conduct laboratory research on RNA processing. Develop, optimize and implement specialized techniques in molecular and cellular biology. Establish tumor cell lines as experimental model systems for cancer research. Participate in preparing publications and grant proposals. Mentor and train graduate and undergraduate students in laboratory studies. Interact professionally with all internal and external customers using strong interpersonal skills.

Minimum qualifications are a Ph.D. in Molecular and Cellular Biology, Biochemistry, or related field. Skilled in molecular and cellular biology and in molecular cloning techniques. Experience in mammalian cell culture. Preferred qualifications are knowledge of nuclear pre-mRNA splicing, microRNA, and cancer genetics. Strong skills in mammalian cell culture.

Send curriculum vitae along with three names and contact information of references to Dr. Girish Shukla, Chair, Search Committee, Cleveland State University, 2121 Euclid Avenue, SI 219, Cleveland, OH 44115. Position open until filled. Salary commensurate with experience.

CSU is an AA/EOE institution committed to non-discrimination in employment and education. M/F/D/V encouraged.

UK UNIVERSITY OF KENTUCKY

Department of Microbiology, Immunology and Molecular Genetics Two Positions at the Assistant/Associate Professor Level

The Department of Microbiology, Immunology and Molecular Genetics, College of Medicine, University of Kentucky, seeks two tenure track **IMMUNOLOGISTS/MICROBIOLOGISTS** at the Assistant or Associate Professor level. We are interested in faculty whose research bridges the disciplines of immunology, microbiology and/or molecular genetics/genomics/bioinformatics. Examples of research include immunoregulation, genetics of the immune system, molecular immunology, autoimmunity, host response to microbial pathogens, genetic basis of resistance to microbial infection, innate defenses against infection, viral immunology, immunoparasitology, and vaccines. Applicants should have a Ph.D. and/or M.D., or equivalent degree, and postdoctoral experience. Successful candidates are expected to develop/maintain an innovative, externally funded research program as well as participate in graduate and medical student teaching. This is an excellent opportunity to join a department with strong predoctoral and postdoctoral training programs, and research programs in microbial pathogenesis, eukaryotic molecular biology, molecular and cellular immunology, and molecular virology. Excellent start-up funds, state-funded salary commensurate with experience and modern research facilities will be provided.

Applications should include curriculum vitae, representative reprints, a summary of past experience, a statement regarding research interests and future plans, as well as three letters of recommendation. All material should be sent to: **Chair, Faculty Search Committee, Department of Microbiology and Immunology and Molecular Genetics, MS409, Medical Center, University of Kentucky, Lexington, KY 40536-0298; Telephone: 800-462-5257; FAX: 859-257-8994; kfres1@pop.uky.edu**.

The University of Kentucky is an Equal Opportunity/Affirmative Action Employer and has an affirmative duty to reasonably accommodate otherwise qualified individuals with a disability.

Molecular FOUNDRY

A USER FACILITY FOR NANOSTRUCTURED MATERIALS

Biological Nanostructures Staff Scientist

Lawrence Berkeley National Laboratory (LBNL) is a world leader in science and engineering research, with 11 Nobel Prize recipients over the past 75 years, and 59 present members of the National Academy of Sciences. LBNL conducts unclassified research across a wide range of scientific disciplines and hosts four national user facilities, including the Molecular Foundry.

The Molecular Foundry is a national user facility for the design, synthesis, and characterization of materials with nanometer dimensions [**http://foundry.lbl.gov**]. This position is located within the Foundry's Biological Nanostructures Facility, which provides instruments and techniques for users pursuing integration of biological components into functional nanoscale materials and mimicry of biological architectures. Learn more at **http://foundry.lbl.gov/facilities/bionano.htm**.

The successful candidate will design and lead a vigorous individual research program at the interface of biomaterials and nanoscience. He/she will also provide scientific support and collaborate on research projects brought to the Molecular Foundry by its users.

Apply at **http://jobs.lbl.gov/LBNLCareers/details.asp?jid=20026&p=1**. Please submit a single attachment including your CV, one or more research proposals that involve aspects of nanoscience and biology, list of references, and cover letter. Reference "Science Magazine" as your source.

LBNL is an AA/EEO employer committed to the development of a safe and diverse workforce.

MARTIN-LUTHER-UNIVERSITÄT
HALLE-WITTENBERG

Institute for Biotechnology at the Martin-Luther-University Halle-Wittenberg

Independent junior research group leader fellowship
4 post-doctoral research fellowships
4 PhD-fellowships

The Institute for Biotechnology at the Martin-Luther University Halle-Wittenberg has been awarded funding for a junior research group in context of the "InnoProfile" program by the German ministry of research and education (BMBF). The research group will focus on the development of new methods for the generation of artificial binding proteins for pharmaceutical and industrial applications (see Hey et al., Trends Biotechnol. 23, 514-522 (2005)). This includes the development of phage display and ribosomal display methods as well as the design and evaluation of highly stable scaffold proteins. The junior research group will operate in close contact with the protein technology group (Rainer Rudolph), with local biotech companies as well as local collaborative research centers (see http://www.exzellenznetzwerk-biowissenschaften.uni-halle.de).

The candidates should have documented experience (group leader, postdoc) or interests in the generation of artificial binding proteins using phage display, ribosomal display, or other display technologies. Furthermore, competence in molecular biology as well as protein chemistry and biophysics is expected

The Institute offers high end infrastructure for the production of recombinant proteins and their biophysical characterization (X-ray, NMR, fluorescence, CD, DSC, ITC and dedicated equipment for the analysis of protein-/protein interactions).

Appointments will be made at the level of E 15 (group leader), of up to E 14 (postdoctoral fellows) for a period up to October 2011. Applicants with a proven publication record in quality journals should send their CV, publication list and reprints of the three most important publications to stating registration number D 19/2006 Abteilung 3 **- Personalamt der Martin-Luther-Universität Halle-Wittenberg, D-06099 Halle (Saale).** The Martin-Luther-University Halle-Wittenberg is an affirmative action employer. Female scientists are specifically encouraged to apply for this position. Suitably qualified disabled candidates will the treated preferentially.

Closing date for applications 05.02.2007

FACULTY POSITION IN APPLIED PHYSICS

The Applied Physics Program at Caltech invites applications for one tenure track position as assistant professor. We are seeking highly qualified candidates who are committed to a career in research and teaching. Exceptionally well-qualified candidates may be considered at the associate or full professor level. In addition to applicants from traditional areas including device and/or materials physics we are interested in applicants with interdisciplinary backgrounds spanning these and other areas such as biology and chemistry.

Interested applicants should submit an electronic application by visiting **http://www.eas.caltech.edu/search/aph**. You will be asked to upload the following pdf documents: CV, research statement, three publications, and the names and contact information for three references.

The term of the initial appointment is normally four years, and appointment is contingent upon completion of all the requirements for a Ph.D.

CALIFORNIA INSTITUTE OF TECHNOLOGY
Division of Engineering and Applied Science
Caltech is an Equal-Opportunity/Affirmative-Action Employer.
Women, minorities, veterans, and disabled persons are encouraged to apply.

IMMUNOLOGY
Faculty-Level Positions

Roswell Park Cancer Institute

Under the leadership of a newly appointed department chair, Roswell Park Cancer Institute is committed to the expansion of its Immunology program. The Department of Immunology invites applications for positions equivalent to the Associate Professor (Associate Member) level. Candidates must have a strong Immunology background with special interest in Tumor Immunology, to complement and broaden the expertise of existing faculty in the department and strengthen the mission of the Institute as an NCI designated Comprehensive Cancer Center.

Selection will be based on excellence in research, current peer-reviewed funding and potential to maintain an outstanding independent research program. The new recruits will have the opportunity to contribute to the graduate education program at the Institute and to administrative responsibilities of the department. We encourage applicants who desire an environment that fosters interaction with a diverse group of scientists and clinicians both within the Institute and the State University of New York at Buffalo.

Laboratory space in a newly opened 300,000 sq ft. Buffalo Life Sciences Complex provides a highly multidisciplinary environment, access to state-of-the-art core facilities, and the opportunity to interact with both research scientists and research-oriented clinicians from several departments.

Applicants should send their CV, description of research accomplishments and future research objectives and the names and addresses of three references to: **Dr. Yasmin Thanavala, Search Committee Chair, Department of Immunology, Roswell Park Cancer Institute, Elm & Carlton Streets, Buffalo, NY 14263.**

RPCI is an Equal Opportunity and Affirmative Action Employer.

ROSWELL PARK CANCER INSTITUTE

Molecular Therapeutics of Cancer
Tenure Track Faculty Position
Dartmouth Medical School
Norris Cotton Cancer Center, New Hampshire

Dartmouth's Norris Cotton Cancer Center invites candidate applications for a tenure track faculty position to join our expanding Molecular Therapeutics Program. This Program comprises leading basic science, translational, and clinical researchers focused on the development of novel therapeutic strategies for cancer.

We are seeking an individual with a strong record of academic productivity and the potential to establish or bring an independent program focused on the development of novel, targeted therapeutic agents for cancer. Preference for this position will be given to investigators with laboratory-based research programs that are at the preclinical or early clinical stage of development.

In addition to an appointment in the Cancer Center, the recruited faculty member will receive primary appointment in an appropriate basic science department of Dartmouth Medical School, and will have teaching, clinical, and administrative opportunities and responsibilities that reflect their interests and institutional needs. Applicants with PhD, MD, or MD/PhD degrees will be considered for appointment at the assistant, associate, or full professor level.

Submissions should include a letter of intent, a curriculum vitae, names and contact information for three references, and a brief description of prior research accomplishments and future goals. Application materials may mailed to: **Christopher H. Lowrey, MD, Chair, Molecular Therapeutics Search Committee, c/o Ms. Brenda Berube, Norris Cotton Cancer Center, HB 7920, One Medical Center Drive, Lebanon, NH, 03756.** OR **E-mailed to: Brenda.K.T.Berube@Dartmouth.edu (Note in subject line: Mol Tx #12979A).** Review of applications will commence on **February 1, 2007** and will continue until the position is filled.

Dartmouth Medical School is an Affirmative Action/Equal Opportunity Employer and encourages women and minority candidates to apply.

Max-Planck-Institut für Meteorologie

Max Planck Institute for Meteorology

The Institute with its three Departments *(The Atmosphere in the Earth System, The Land in the Earth System, The Ocean in the Earth System)* is committed to basic research on climate and Earth system science (http://www.mpimet.mpg.de). The Institute has an opening for the position of

Director and Head

of the Department ***The Atmosphere in the Earth System*** to succeed Professor Guy Brasseur. The position is equivalent to a tenured full professorship at a German university. There are no teaching obligations; however, the Institute participates in various teaching activities at the University of Hamburg and jointly with the University of Hamburg runs a Ph.D. program, the *International Max Planck Research School on Earth System Modelling.*

In this context, the Max Planck Institute for Meteorology organizes a symposium

Atmospheric Processes in Earth System Dynamics

in Hamburg on 23-24 April, 2007.

The Max Planck Society is an equal opportunity employer and specifically welcomes applications of female scientists. The Max Planck Society is committed to employing more handicapped individuals and especially encourages them to apply.

Scientists interested in this position and in participating in the symposium are requested to submit the title and abstract of a possible presentation, a summary of their research plans, a CV, and the list of publications before **28 February, 2007,** to

Max Planck Institute for Meteorology
Prof. Dr. Martin Claussen
Bundesstrasse 53
20146 Hamburg, Germany
martin.claussen@zmaw.de

Participants in the symposium will be notified before **31 March, 2007.**

MAX-PLANCK-GESELLSCHAFT

RUTGERS

THE STATE UNIVERSITY OF NEW JERSEY

DIRECTOR, INSTITUTE OF MARINE AND COASTAL SCIENCES

Rutgers, The State University of New Jersey, seeks an imaginative and distinguished scientist with strong leadership skills for the position of Director of the Institute of Marine and Coastal Sciences (IMCS).

The Director will develop a vision and strategic plan for the Institute that will not only advance its current leadership role in marine and coastal sciences worldwide, but will also enhance the international prominence of the entire spectrum of allied fields at Rutgers, including earth, ocean, atmospheric, and environmental sciences. The Director will promote an integrated program of research, education, and service in the Institute.

Rutgers, New Jersey's comprehensive public research university and member of the Association of American Universities (AAU), is one of the nation's oldest and largest institutions of higher education. IMCS is a multi-disciplinary research institute with distinguished faculty from a variety of departments, a substantial professional staff, and a demonstrated record of acquiring competitive external funding. It has a strong academic reputation and fosters one of the top-ranked marine science programs in the country. Present research strengths include ocean ecology/evolution, biogeochemistry, ocean observatories, ocean modeling, and climate change. The Institute maintains a facility in New Brunswick, close to New York City and New Jersey's natural areas, and supports several field stations along the coast and in the Pine Barrens. Rutgers' vision for this collaborative, multi-disciplinary program includes a strong commitment of significant new resources, including additional faculty and a new building.

The salary range for this senior tenured faculty position is competitive, commensurate with experience and qualifications. Candidates are expected to provide evidence of exceptional scholarly accomplishments in research and teaching, administrative achievement, and demonstrated leadership ability at the local, national, and international level. Nominations are welcome. To ensure full consideration, a nomination or a letter of interest and current vitae should be sent to the address below by March 15, 2007. Review of nominations and applications will begin immediately and will continue until the position is filled. All correspondence will be held in confidence.

Professor Fred Roberts, Chair, IMCS Search Committee
c/o Diane Carlino
Institute of Marine and Coastal Sciences
71 Dudley Road, New Brunswick, NJ 08901
E-mail: imcsdirector@aesop.rutgers.edu Phone: 732-932-6555, x511

For more information, go to **http://marine.rutgers.edu**. An Affirmative Action/Equal Opportunity Employer

CENTER FOR BIOSYSTEMS RESEARCH

Nanoscale Biosciences and Engineering Tenure-Track Faculty Position

The University of Maryland Biotechnology Institute (UMBI) and University of Maryland College Park (UMCP) invite applications for a tenure track position at the level of **Assistant Professor.** UMBI and UMCP have initiated a new multi-disciplinary program that brings together Biosciences and Engineering Faculty from the Center for Biosystems Research (CBR; **http://www.umbi.umd.edu/~cbr**) and the Fischell Department of Bioengineering (UMCP-BioE, **http://www.bioe.umd.edu**) to address emerging topics in nanotechnology. This position will be located in UMBI-CBR with a joint appointment in UMCP-BioE. The successful applicant will benefit from existing strengths in biomolecular and metabolic engineering, pathobiology and genome sciences at UMBI-CBR and biomaterials/BioMEMS, cellular and tissue engineering, biomechanics and drug delivery at UMCP-BioE.

A Ph.D. in the general area of nanobiotechnology is required. The successful applicant will have demonstrated exceptional accomplishments and promise in a research and teaching area that integrates nanoscale engineering with biological sciences. Examples include but are not limited to the interfacing of nanodevices with biomolecules for detection, development of nano-bio-molecules for use in imaging and drug delivery in living systems, the use of biological systems or components for the harvesting of solar or chemical energy, and the engineering of self-assembling bio-composite materials with novel nanostructures and functions.

The investigator is expected to build a competitively funded research group within the setting of an interdisciplinary research institute located on a large university campus in the Washington, D.C./Baltimore metropolitan area. For full consideration, submit a letter of application, curriculum vitae, a description of research and teaching interest, copies of pertinent reprints and three letters of reference by **February 23, 2007** to:

Faculty Search Committee – Position # 300893
cbrsrch@umbi.umd.edu

UMBI is committed to Affirmative Action and Equal Opportunity Employment. As required by the 1986 Immigration Act, applicants should be prepared to present acceptable documentation showing their identities, their U.S. citizenship or alien status, and their authorization to work in the United States

UCIrvine
University of California, Irvine

Assistant/Associate Professor Microbiology and Molecular Genetics

The Department of Microbiology and Molecular Genetics at the University of California, Irvine is seeking applicants for a faculty position at the Assistant or Associate Professor level, depending upon qualifications. We seek applicants with Ph.D., M.D. or M.D./Ph.D. degrees, significant postdoctoral experience, and an established record of accomplishment in research demonstrated by excellent peer-reviewed publications. A strong commitment to the development of a vigorous and innovative independent research program supported with extramural funds, the rigorous training of graduate students and instruction of graduate and medical students is essential. We are especially interested in two broad areas of research focus: **(1) gene expression studies in systems ranging from prokaryotes through mammals,** including transcriptional and/or post-transcriptional regulation; small RNA biology, or molecular genetics/genomics; and **(2) molecular biology of infectious diseases,** including molecular genetics of bacterial, viral, fungal or parasitic infections; molecular and cell biology of host-pathogen interactions and host response to infection.

Please send curriculum vitae, summary of research interests, and names of three references to: **Dr. Bert L. Semler, Faculty Search Committee Chair, Department of Microbiology and Molecular Genetics, School of Medicine, University of California, Irvine, CA 92697-4025.**

University of California, Irvine has an active career partner program and an NSF ADVANCE Program for Gender Equity and is an Equal Opportunity Employer committed to excellence through diversity. All qualified candidates, including women and minorities are encouraged to apply.

POSITIONS OPEN

NEUROBIOLOGY FACULTY POSITIONS
University of Maryland School of Medicine
Baltimore, Maryland

The Department of Anatomy and Neurobiology **(website: http://neurobiology.umaryland.edu)** is recruiting established investigators with active, funded research programs in neuroscience. We are interested in candidates who use multidisciplinary approaches to understand the function or plasticity of the nervous system. Of particular interest are candidates that complement existing strengths in the Department, including motivated behavior and addiction, sensory, systems, molecular and developmental neuroscience.

The Department contains new, state-of-the-art laboratories and core facilities. We offer an outstanding intellectual and collaborative environment with highly competitive salary and recruitment packages. All Department faculty are members of the Graduate Program in Life Sciences and the interdisciplinary Program in Neuroscience **(website: http://neuroscience.umaryland.edu).**

Applications received posted by March 15, 2007, will receive strongest consideration. Candidates should submit the following as PDF files to **e-mail: facsearch@umaryland.edu:** (1) detailed curriculum vitae, (2) statement of research interests and goals, and (3) names and contact information for three to five references. Applications should be addressed to the attention of: **Drs. Steven D. Munger, Ph.D. and Patricio O'Donnell, Co-Chairs, Faculty Search Committee.**

NEUROIMAGING FACULTY
Department of Neurosciences
College of Medicine
Medical University of South Carolina, Charleston

The Department of Neurosciences at the Medical University of South Carolina (MUSC) invites applications for a tenure-track faculty position in the general area of human brain imaging. This position offers a competitive and generous startup package and provides a unique opportunity to use the basic and clinical imaging resources at MUSC to grow an area of advanced interdisciplinary research based on human brain imaging. The faculty member **(ASSISTANT, ASSOCIATE, OR FULL PROFESSOR)** will closely collaborate with basic and clinical neuroscientists, other MUSC researchers from the Center for Advanced Imaging Research (CAIR) and imaging researchers through the statewide Brain Imaging Center of Excellence. The position requires an M.D. and/or Ph.D., a record of extramural grant funding in the area of human brain imaging, and a demonstrated ability to work with an interdisciplinary research team. Depending on the candidate's interests and qualifications, the successful candidate may also assume the position of CAIR Director and/or occupy an endowed Chair.

Review of applications will begin on February 1, 2007, and continue until the position is filled. Applicants must apply online at **website: http://www.musc.edu/hrm/careers/faculty.htm** (position/requisition number 041747). Your online application for this position should also include curriculum vitae, the names and contact information of at least three references, and a cover letter expressing your qualifications and statement of research interests addressed to: **Mark S. George, M.D., Chair, Neuroscience Imaging Search Committee, Department of Neurosciences, Medical University of South Carolina, 173 Ashley Avenue, BSB 403, Charleston, SC 29425.**

Nominations of qualified individuals are also welcome. The nominee's curriculum vitae should be sent via e-mail to: **Mark George, M.D., Chair Neuroscience Imaging Search Committee, c/o Cheri Kubalak** at **e-mail: kubalakc@musc.edu.**

MUSC is an Equal Employment Opportunity/Affirmative Action Employer.

POSITIONS OPEN

PROFESSOR AND CHIEF, ANATOMIC PATHOLOGY
University of California, Irvine
Department of Pathology and Laboratory Medicine

The University of California (UC), Irvine, Department of Pathology and Laboratory Medicine, **website: http://www.ucihs.uci.edu/som/pathology** invites applicants for the position of Chief of the Division of Anatomic Pathology.

The successful applicant will be an accomplished, American Board of Pathology-certified Surgical Pathologist and/or Cytopathologist who must hold or be eligible for a medical license in the state of California. Applicants should possess demonstrated leadership skills for guiding an academic anatomic pathology group that currently includes eleven faculty operating in a generalist/specialist hybrid model. It is anticipated that this appointment will be at the **FULL PROFESSOR** level. Appointment will be in the professorial track (i.e., Tenured; Professor of Clinical Pathology; or Clinical Professor) that best matches the qualifications of the successful candidate.

The appointee will join a state-of-the-art Department with diverse diagnostic services, teaching and basic/clinical research activities. UC Irvine Medical Center is a tertiary hospital and the only academic medical center in Orange County. The Department provides diagnostic services to UC Irvine Health System patients, including those of the UC Irvine Children's Hospital and the Chao Family Cancer Center (an NCI designated comprehensive cancer center), and also provides referral services to more than 70 regional hospitals. The Department hosts an Accreditation Council for Graduate Medical Education-accredited residency training program in anatomic and clinical pathology, with established fellowships in surgical pathology and cytopathology. The Department encourages scholarly development of physicians-in-training.

Candidates are invited to submit their curriculum vitae and names of four references to:

Anatomic Pathology Chief Search Committee
c/o Julienne Jose (e-mail: josejm@uci.edu)
Department of Pathology and Laboratory Medicine
D440 Med Sci 1
University of California, Irvine
Irvine, CA 92697-4800

The University of California, Irvine, has an active career partner program and an NSF ADVANCE Program for Gender Equity and is an Equal Opportunity Employer committed to excellence through diversity.

POSTDOCTORAL FELLOW IN VASCULAR DEVELOPMENT AND FUNCTION
University of Cincinnati
Department of Molecular Genetics, Biochemistry, and Microbiology

A Postdoctoral position is available in the area of vascular development and function. A major focus in our laboratory centers around the transcription factor KLF2 which is involved in the function of multiple tissues including the vascular system. This transcription factor is induced by shear stress and appears to protect against lesion formation. We have developed both standard and conditional knockouts for studying the role of KLF2. The training environment within the Department is outstanding with 24 faculty, 45 graduate students, and approximately equal number of postdoctoral fellows. Interested candidates should send their resume to: **Jerry B Lingrel, Ph.D., Professor and Chair, at the Department of Molecular Genetics, Biochemistry and Microbiology, University of Cincinnati College of Medicine, 231 Albert Sabin Way, Cincinnati, OH 45267-0524** or **e-mail: jerry.lingrel@uc.edu.**

POSITIONS OPEN

MILLER SCHOOL OF MEDICINE
UNIVERSITY OF MIAMI

FACULTY POSITION
Molecular and Cellular Pharmacology

The Department of Molecular and Cellular Pharmacology at the University of Miami Miller School of Medicine is seeking applications for a tenure-track **FACULTY POSITION** (rank open). Candidates must have a Ph.D. and/or M.D. degree and have an established record of research excellence. Applicants from all areas of molecular/cellular biology and biomedical research are welcome. The new faculty member will complement existing research efforts in the Department. Rank and salary will be commensurate with experience. Generous laboratory space and startup funds are available.

Applicants should send electronic and hard copies of their curriculum vitae, statement of research interests and direction, and contact information for three references, to **e-mail: elalor@med.miami.edu** (e-copies) and to: **Dr. James D. Potter, Search Committee Chair, Department of Molecular and Cellular Pharmacology, University of Miami Miller School of Medicine, P.O. Box 016189, Miami, FL 33101.**

An Equal Opportunity/Affirmative Action Employer.

FACULTY POSITIONS AT THE UNIVERSITY OF VIRGINIA

A newly established Center for Molecular Design, emphasizing the identification and usage of new chemical tools, together with the Department of Pharmacology, seek to fill two faculty positions (open rank). Individuals conducting research in the broad areas of chemical biology and drug discovery of nuclear receptors or other drug targets are encouraged to apply. Ph.D. required in pharmacology, chemistry, biochemistry, or related discipline. The successful applicant will be provided with an attractive startup package, including laboratory space within Pharmacology **(website: http://www.healthsystem.virginia.edu/internet/pharmacology/)** and access to core facilities. To apply send curriculum vitae, research plan with names and addresses of at least three references (including e-mail address and telephone number) to: **Pharmacology Search Committee, Department of Pharmacology, University of Virginia, P.O. Box 800735, Charlottesville, VA 22908-0735 (e-mail: pharmsearch@virginia.edu).** Review of applications will begin January 15, 2007; however, the position will remain open until filled. *The University of Virginia is an Equal Opportunity/Affirmative Action Employer.*

ASSISTANT PROFESSOR OF BIOLOGY, VISITING TWO-YEAR POSITION, Lawrence University, an undergraduate liberal arts college, seeks applicants for a full-time, two-year Visiting Assistant Professor in biology to begin September 2007. Teaching responsibilities include general zoology and upper level courses which might include vertebrate morphology, developmental biology, genetics, evolutionary biology, or an appropriate course in the candidate's area of expertise. Most courses have both lecture and laboratory components; teaching load is one laboratory course per term (three terms per year). The successful candidate will have access to a well-equipped laboratory space and funding for research involving undergraduate biology majors. Lawrence offers a competitive salary and benefits. Application deadline is February 15, 2007. To apply, send curriculum vitae, statements of teaching philosophy and research interests, undergraduate and graduate transcripts, and three letters of reference to: **Brad Rence, Chair, Biology Department, Lawrence University, Appleton, WI 54912. E-mail: renceb@lawrence.edu.** *Affirmative Action/Equal Opportunity Employer.*

Ajinomoto Co., Inc. is pleased to announce the recipients of the 3ARP grant 2006.

Ajinomoto Co., Inc. appreciate the interest and participation of a large number of scientists. We received over 150 high-quality proposals from around the world for this program in 2006. After extensive review and deliberation, the following 6 proposals were selected for funding.

Exploratory Category

Tao Pan, Ph.D. (The University of Chicago)
Amino Acids as Sensors and Regulators of Global Metabolic State

Pengxiang She, Ph.D. (Pennsylvania State University)
Mechanisms by Which Mice Lacking BCAA Catabolism Improve Glucose Homeostasis

Robert A. Harris, Ph.D. (Indiana University)
Exploratory Study on the Metabolic and Neurological Defects Induced by Chronically Reduced BCAA Levels.

Focused Category

Charles C. Horn, Ph.D. (Monell Chemical Senses Center)
Mechanisms for Detection of Amino Acids by Sensory Nerve Fibers of the Gut

Teresa A. Davis, Ph.D. (Baylor College of Medicine)
Parenteral and Enteral Leucine as a Nutrient Signal to Stimulate Protein Synthesis in Neonates

Scot R. Kimball, Ph.D. (Pennsylvania State University)
Leucine-Induced Assembly of an Activated Subcellular mTOR Signaling Complex

POSITIONS OPEN

ASSISTANT/ASSOCIATE PROFESSOR
Neurophysiology/Neuropharmacology
The University of Montana

Applications are invited for a tenure-track faculty position at the **ASSISTANT** or **ASSOCIATE PROFESSOR** level in the Department of Biomedical and Pharmaceutical Sciences to strengthen research and graduate education in central nervous system (CNS) physiology and pharmacology as part of an NIH-funded Center for Biomedical Research Excellence (COBRE) in Structural and Functional Neuroscience (CSFN). Research strengths in the Center include CNS protein structure/function, synthetic chemistry, neurotransmitter transport, membrane protein biophysics and optics, and neuropathology. Successful candidates will be expected to establish a vigorous externally funded research program in the area of CNS physiology and/or pharmacology, supervise graduate students, and be committed to teaching excellence at the graduate and undergraduate levels. Applicants must have a doctoral degree and relevant postdoctoral research experience. A competitive startup package is available. Applications received by April 15, 2007, will receive full consideration; review will continue until the position is filled. More detailed information about research in the CSFN may be obtained from **website: http://www.umt.edu/csfn.**

The Skaggs School of Pharmacy, which will complete a new 60,000 square-feet research facility in 2007, is ranked sixth in NIH-funded research amongst U.S. schools of pharmacy and is part of the University of Montana campus in Missoula. This cosmopolitan Rocky Mountain community of 70,000 has been singled out in national publications for its high quality of life. Abundant recreational opportunities in surrounding state and national forests including Yellowstone and Glacier National Parks complement a thriving intellectual atmosphere.

Applicants should send a letter of application including curriculum vitae, a statement of research plans and teaching interests, and contact information for three references to: **Michael Kavanaugh, Ph.D., Chair, Center for Structural and Functional Neuroscience Search, Department of Biomedical and Pharmaceutical Sciences, The University of Montana, Missoula, MT 59812-1552.**

The University of Montana is the recipient of an NSF ADVANCE award focused on increasing the presence of women in science. *Equal Opportunity/Affirmative Action Employer.*

BIOMEDICAL IMAGING FACULTY CLUSTER. The University of Wisconsin, Milwaukee (UWM), invites applications for **TENURED** or **TENURE-TRACK FACULTY** positions at open rank as part of an interdisciplinary cluster in biomedical imaging. UWM expects to hire four to six Biomedical Imaging Faculty within two years. Applicants with expertise in all areas of biomedical imaging are welcome; medical image analysis, molecular, emerging, and hybrid imaging techniques are of particular interest. Candidates must have completed a Ph.D. and/or M.D. degree in an appropriate field of study, and will be expected to establish an independent, extramurally funded research program. For senior candidates, a strong track record of scientific publication and extramural funding is expected. Successful candidates will join appropriate science and engineering departments; joint appointments are feasible. Candidates should submit curriculum vitae, a brief research plan, and names of at least three references electronically to **e-mail: bio-medimaging@uwm.edu** or mail hard copies to: **Chair, Biomedical Imaging Search Committee, University of Wisconsin-Milwaukee, Department of Physics, P.O. Box 413, Milwaukee, WI 53201.** Application reviews will begin on February 15, 2007, and continue until all positions are filled. UWM offers competitive salary and startup packages, commensurate with experience. Further information about UWM may be found at **website: http://www.uwm.edu.** *UWM is an Equal Opportunity/Affirmative Action Employer.*

POSITIONS OPEN

USDA ARS Agricultural Research Service
www.ars.usda.gov

RESEARCH LEADER INTERDISCIPLINARY: SUPERVISORY RESEARCH PLANT PATHOLOGIST/PLANT PHYSIOLOGIST/GENETICIST (GS-14/15)
Salary Range of $87,533 to $133,850

The Grain Legume Genetics and Physiology Research Unit, Pullman, Washington, is seeking a permanent full-time Research Leader. The successful candidate will provide scientific leadership and operational management for the research unit and conduct personal research on physiology, pathology, and/or genetics and breeding of cool season food legumes contributing to the development of improved germplasm and cultivars. For details and application directions, see announcement number ARS-X7W-0077 at **website: http://www.afm.ars.usda.gov/divisions/hrd/index.html.** To have a printed copy mailed, call **telephone: 509-335-8663.** *U.S. citizenship is required.* Announcement closes March 5, 2007. Applications must be received by the closing date of the announcement. *USDA/Agricultural Research Service is an Equal Opportunity Employer and Provider.*

BIOINFORMATICS CORE DIRECTOR POSITION
Available at the University of Vermont
Department of Biology

Available now: faculty-level appointment as a **RESEARCH ASSISTANT PROFESSOR** in bioinformatics at the University of Vermont through the Vermont Genetics Network (VGN) **(website: http://www.uvm.edu/~vgn/.)** VGN is an NIH-funded state program for building biomedical research infrastructure. The successful candidate will oversee and participate in the data analysis of the Bioinformatics Core, which assists faculty from across the state with microarray, genomics, and proteomic mass spectrometry data analysis. The Director will work with UVM and baccalaureate institution faculty, a staff systems analyst, proteomics and microarray facility managers, and an educational program coordinator, who assists undergraduates with microarray, bioinformatics, and proteomics experiments.

Requirements include a Ph.D. in bioinformatics, proteomics, molecular biology, or a related field with background and interest in genomics and proteomics.

Candidates should apply online at **website: http://www.uvmjobs.com** under requisition number 031737 and include a cover letter highlighting key qualifications and interests, curriculum vitae, and a list of three references.

The University of Vermont is an Affirmative Action/Equal Opportunity Employer. The Department is committed to increasing faculty diversity and welcomes applications from women and underrepresented ethnic, racial, and cultural groups and from people with disabilities.

POSTDOCTORAL POSITION. A Postdoctoral position funded by the National Institutes of Health is available, to study the roles of insulin, nitric oxide, and protein tyrosine phosphatases in regulation of vascular smooth muscle cell signaling and neointima formation in vascular injury. Our projects address important basic science questions and also have relevance to clinical problems. Experience in molecular biology and/or rat and mouse surgery is essential. Competitive salary is offered.

Please send curriculum vitae and the names of three references to: **Dr. Aviv Hassid, Department of Physiology, University of Tennessee, 894 Union Avenue, Memphis TN 38163. E-mail: ahassid@tennessee.edu, fax: 901-448-7126.** *The University of Tennessee is an Equal Employment Opportunity/Affirmative Action/Title VI/Title IX/Section 504/ADA/ADEA Institution in the provision of its education and employment programs and services.*

POSITIONS OPEN

ASSISTANT/ASSOCIATE/FULL PROFESSOR
Baruch College/City University of New York

The Department of Natural Sciences at Baruch College/City University of New York seeks a scientist (rank and science discipline open) with a global perspective to develop courses in environmental sustainability that will broaden the education of students in the arts and sciences, business law, and public affairs. Areas of expertise might include global climate, water resources, ecosystem management, environmental threats to human health, clean technologies, alternative energy, integrated pest management, and green architecture. The candidate must also establish a vigorous research program and mentor undergraduates.

Salary: competitive and commensurate with qualifications and experience.

Doctorate in an appropriate discipline required. Candidates should offer evidence of excellence in undergraduate teaching and research; strong leadership skills. Experience obtaining funding from government and private sources a plus. Practical experience in the United States and abroad highly desirable.

Please send curriculum vitae and three letters of recommendation, by February 28, 2007, to:

Professor John H. Wahlert, Chair
Department of Natural Sciences
Baruch College/City University of New York
One Bernard Baruch Way, Box A-0506
New York, NY 10010

An Affirmative Action/Equal Opportunity/Americans with Disabilities Act Employer.

POSTDOCTORAL FELLOWSHIP AT WELLESLEY COLLEGE

Wellesley College invites applications for a two-year **POSTDOCTORAL RESEARCH/TEACHING FELLOWSHIP,** sponsored by a grant from the Howard Hughes Medical Institute Undergraduate Biological Sciences Education Program. The Fellow will work with an interdisciplinary team of faculty members (biology and computer science) and our undergradute students on a project applying bioinformatics techniques toward understanding gene regulation in bacteria. Bacteriology experience is expected. Teaching (25 percent of time) will be either in molecular biology or bioinformatics. Applications, including curriculum vitae, statement of research interests and experience, and three letters of recommendation should be sent to: **Brian Tjaden, Computer Science Department, Wellesley College, Wellesley, MA 02481,** or **e-mail: btjaden@wellesley.edu** prior to April 1, 2007.

Wellesley College is an Equal Opportunity/Affirmative Action Educational Institution and Employer. The College is committed to increasing the diversity of the college community and the curriculum. Candidates who believe they will contribute to that goal are encouraged to apply.

ASSISTANT PROFESSOR IN BIOLOGICAL ENGINEERING
Purdue University

The successful candidate will establish a renowned research program focusing on integration of biological sciences into engineering. A full job announcement and application requirements are available at **website: http://www.purdue.edu/ABE/.** Review of applications will begin February 16, 2007. For questions, **e-mail: bioengr@purdue.edu.**

GRANTS

FARAN LABORATORIES S.A., completing 50 years of innovations in the pharmaceutical industry is announcing a grant for funding in the area of prostate cancer prevention using natural products. It is anticipated that a two-year grant will be awarded for a maximum amount of $100,000, of which no more than 10 percent can be used for indirect costs. The second year of funding will be based upon successful completion of measurable goals in the first year of study. For more details visit **website: http://www.faran.gr.**

It's a new day in miRNA detection when you can do it in one day.

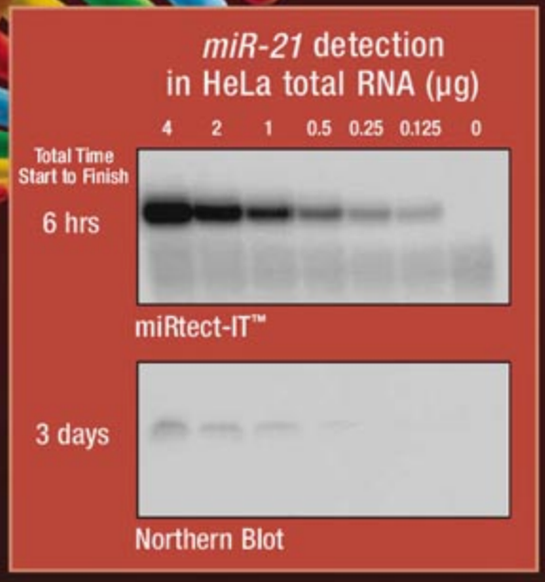

Announcing USB's new miRtect-IT™ miRNA Labeling and Detection Kit. This highly sensitive, novel method is fast and easy, allowing you to achieve direct labeling and quantitative measurement of miRNAs in less than one day. So don't waste another 3 days using the old Northern Blot method—go to our website today to learn more.

miRtect-IT™ miRNA Labeling and Detection Kit

- Based on splinted-ligation technology — A bridge oligo hybridizes to a specific miRNA and a labeled detection oligo
- miRNA becomes directly labeled by ligation, then visualized

Benefits

- ***Speed*** - capture and label miRNA in just over 2 hours
- ***Sensitivity*** - detect miRNA in as little as 50 ng or less of total RNA
- ***Quantitative Results*** - accurate miRNA measurement in 6 hours

For more information on miRtect-IT™
call 800.321.9322 or visit www.usbweb.com/mirtect-it
In Europe: +49(0)76 33-933 40 0 or visit www.usbweb.de/mirtect-it

usb
Fueling Innovation in Life Science™